

ISSN 2310-6697

toiser—open transactions on independent scientific-engineering research

FUNKTECHNIKPLUS # JOURNAL

Théorie—Expérimentation—Métrologie—Logiciel—Applications

VOLUME 1 – WEDNESDAY 2 DECEMBER 2015 – YEARS 1 & YEAR 2

Page PDF

1 Contents

2 About

3 Editorial Team – Technical Support

4 Information for Authors

6 Electronic Publishing – Submissions – Internet Addresses

7 ISSUE 1 – MONDAY 30 SEPTEMBER 2013 – YEAR 1 – PILOT ISSUE

39 ISSUE 2 – SUNDAY 17 NOVEMBER 2013 – YEAR 1 – EXTRA ISSUE

91 ISSUE 3 – FRIDAY 31 JANUARY 2014 – YEAR 1

119 ISSUE 4 – SATURDAY 31 MAY 2014 – YEAR 1

187 ISSUE 5 – TUESDAY 30 SEPTEMBER 2014 – YEAR 2

235 ISSUE 6 – SATURDAY 31 JANUARY 2015 – YEAR 2

279 ISSUE 7 – SUNDAY 31 MAY 2015 – YEAR 2



*This small European Journal is
In the Defense of Honesty in Science and Ethics in Engineering*

Publisher – otoiser—open transactions on independent scientific engineering research, www.otoiser.org—info@otoiser.org : Hauptstraße 52, 2831 Scheiblingkirchen, Austria

Language – We emphasize the origins of the Journal by using English, German and French, as well as, a Hellenic vignette in the cover page. However, since we recognize the dominance of US English in the technical literature, we adopted it as the Journal's language, although it is not our native language.

Focus – We consider Radio–FUNK, which still creates a vivid impression of the untouchable, and its Technology–TECHNIK, from an Advanced–PLUS point of view, Plus–PLUS Telecommunications Engineering, Electrical Engineering and Computer Science, that is, we dynamically focus at any related scientific-engineering research regarding Théorie, Expérimentation, Métrologie, Logiciel, ou Applications.

Scope – We emphasize this scope broadness by extending the title of the Journal with a Doppelkreuz-Zeichen # which we use as a placeholder for substitution of our Editorial Team disciplines: # Telecommunications etc. as above, or # High Voltage, # Software Engineering, # Simulation etc. as below.

Frequency – We publish 3 issues per year: on 31st of January, on 31st of May, and on 30th of September, as well as, an extra issue every 3 papers and a volume every 2 years.

Editions – We increase the edition number of an issue only when is needed to reform one or more of its papers—thus to increase their version numbers—but we keep unchanged its 1st edition date shown on its front page and we number its pages sequentially from 1. We count the editions of *About* separately.

Format – We use a fixed-space font, hyphenation, justification, unfixed word spacing, and the uncommon for Journals **A5** (half A4) page size to achieve WYSIWYG printing and clear reading of 2 to 4 side-by-side pages on wide-screen displays.

Printing-on-Demand – We can email gratis PDF files at 300-4000 dpi in booklet page scaling of brochure and book type.

Copyright – We publish under a Creative Commons Attribution, CC-BY 3.0 Unported or CC-BY 4.0 International, License only.

Please download the latest *About* edition from
www.about.ftpj.otoiser.org

Editorial Team

Electrical Engineering

Professor Michael Danikas, mdanikas@ee.duth.gr
EECE, Democritus University of Thrace, Greece

High Voltage Engineering # Insulating Materials

Assistant Professor Athanasios Karlis, akarlis@ee.duth.gr
EECE, Democritus University of Thrace, Greece

Electrical Machines # Renewable Energies # Electric Vehicles

Computer Science

Professor Vasilis Katos, vkatos@bournemouth.ac.uk
Head of Computer and Informatics Dept, Bournemouth Univ, UK

Computer Engineering # Software Engineering # Cyber Security

Lecturer Sotirios Kontogiannis, skontog@gmail.com
Business Administration Dept, TEI, Western Macedonia, Greece

Internet Engineering # Learning Management Systems

Dr. Apostolos Syropoulos, asyropoulos@yahoo.com
BSc-Physics, MSc-Computer Science, PhD-Computer Science
Independent Researcher, Xanthi, Greece

Hypercomputation # Fuzzy Computation # Digital Typography

Telecommunications Engineering

Dr. Nikolaos Berketis, nberketis@gmail.com
BSc-Mathematics, MSc-Applied Maths, PhD-Applied Mathematics
Independent Researcher, Athens, Greece

Applied EM Electromagnetics # Applied Mathematics

Dr. Nikolitsa Yannopoulou, yin@arg.op4.eu [*]
Diploma Eng-EE, MEng-Telecom-EECE, PhD-Eng-Antennas-EECE
Independent Researcher, Scheiblingkirchen, Austria

Dr. Petros Zimourtopoulos, pez@arg.op4.eu [*]
BSc-Physics, MSc-Radio-Electronics, PhD-Antennas-EE
Independent Researcher, Scheiblingkirchen, Austria

Antennas # Metrology # EM Software # Simulation # Virtual Labs

Applied EM # Education # FLOSS # Amateur Radio # Electronics

* Copy and Layout Editing, Proof Reading, Issue and Website
Management, Paper and About Reprints, Volumes and Web Pages

Technical Support

Konstantinos Kondylis, kkondylis@gmail.com
Diploma Eng-EECE, MEng-Telecom-EECE, Doha, Qatar

Christos Koutsos, ckoutsos@gmail.com
Diploma Eng-EECE, MEng-Telecom-EECE, Bratislava, SK

Information for Authors

This is a small, but independent, low profile Journal, in which we are all—Authors, Reviewers, Readers, and Editors—free at last to be Peers in Knowledge, without suffering from Journal roles or positions, Professional—Amateur—Academic statuses, or established "impact factorizations", under the following guiding principles:

Authors – We know what Work means, we respect the Work of the Independent Researcher in Science and Engineering and we want to exhibit his Work. Thus, we decided to found this Free and Open Access Journal in which to publish this Work. Furthermore, as we care indeed for the Work of the technical author—especially a young or a beginner one—we strongly support the publication of his Work, as follows:

- 1 We do not demand from the author to transfer his own copyright to us. Instead, we only consider papers resulting from original research work only, and only if the author can assure us that he owns the copyright of his own paper as well as that he submits to the Journal either an original copy or a revised version of his own paper, for possible publication after review—or even for immediate republication, if this paper has already been published after review—but, in any case under a Creative Commons Attribution, CC-BY 3 Unported or CC-BY 4 International, License, only.
- 2 We encourage the author to submit his own paper written just in Basic English plus Technical Terminology.
- 3 We encourage the author even to select a pen name, which may drop it at any time to reveal his identity.
- 4 We encourage the author to submit an accepted for publication paper, which he was forced to decline that publication because it would be based on a review with unacceptable evaluation or derogatory comments.
- 5 We encourage the author to submit any paper that was rejected after a poor, impotent, inadequate, unreasonable, irresponsible, incompetent, or "just ticking" review.
- 6 We encourage the author to submit an unreviewed paper of his own that he uploaded on some Open Access repository.
- 7 We encourage the author to upload his published paper in our Journal to at least one Truly Free Open Repository, e.g. such as <http://viXra.org> and <https://archive.org>.

About

- 8 We provide the author with the ability to update, at any time, the reference links of his paper.
- 9 We provide the author with a decent, express, peer review process, of up to just 4 weeks, by at least 2, either anonymous or onymous, reviewers.
- 10 We provide the author with the option to choose from 2 review processes: the traditional, anonymous, close one, as well as, a contemporary, onymous, open review in our private mailing list for Peer Discussion.
- 11 Under the Clause 1 : We immediately accept for publication a research paper directly resulting from a Project Report, or a Diploma-, Master-, or PhD-thesis, which already the author has successfully defended before a committee of experts, as long as he can mention 2 members of this committee who approved his Work.
- 12 Under the Clause 1 : We immediately accept for publication any paper which is not Openly Accessible on the Internet.
- 13 We immediately publish online a paper, as soon as it is accepted for publication in the Journal.
- 14 We quickly publish an extra issue—that is in excess of the 3 issues we publish a year—as soon as the review process of 3 papers is completed.

Reviewers – Every peer may voluntarily become a reviewer of the Journal in his skillfulness for as long as he wishes. In addition, each author of the Journal must review one paper in his expertness for each one of his published papers.

Readers – Every reader is a potential post-reviewer: we welcome comments and post-reviews in our private mailing list for Peer Discussion.

Editors – Every editor owns a PhD degree—to objectively prove that he really has the working experience of passing through the dominant publishing system. An editor pre-reviews a paper in order to check its compliance to our guiding principles and to select the appropriate reviewers of it. We can accept for consideration papers only in the expertise areas currently shown in the Editorial Team page, above. However, since we are very willing to amplify and extend the Scope of the Journal, we welcome the volunteer expert, in any related subject, who wants to join the Editorial Team as long as he unreservedly accepts our guiding principles.

Electronic Publishing

We regularly use the Free Libre Open Source Software Libre Office with the Free Liberation Mono font and the Freewares PDFCreator and PDF-Xchange Viewer. We also use, with some basic html code of ours: the Free Open Source Software Open Journal System OJS by the Public Knowledge Project PKP installed in our website, and the Free Open Digital Library of Internet Archive website, where we upload the FTP#J Collection of Issues, Paper reprints, *About* documents, and Volumes, in both portrait and landscape orientations, for download or very clear online reading with the Free Open Source BookReader.

Submissions

We can only consider papers written in the preferable and recommended odt format of LibreOffice, or even a paper in the MS Office with MathType doc format, if it would be proved that it is fully compatible with LibreOffice indeed.

Legal Notice – It is taken for granted that the submitter–correspondent author accepts, without any reservation, the totality of our publication conditions as they are analytically detailed here, in this *About*, as well as, that he also carries, in the case of a paper by multiple authors, the independent will of each one of his co-authors to unreservedly accept all the aforementioned conditions for their paper.

Internet Addresses

Submissions : sub@ftpj.otoiser.org
Send Updates : updates@ftpj.otoiser.org
Printing-on-Demand : pod@ftpj.otoiser.org
Technical Support TS : technical-support@ftpj.otoiser.org
Principal Contact : principal-contact@ftpj.otoiser.org
Peer Discussion List : www.peers.ftpj.otoiser.org
Editorial Team & TS List : www.etts.ftpj.otoiser.org
The FTP#J Collection at Internet Archive Digital Library :
<https://archive.org/details/@funktechnikplusjournal>
Sample Paper Templates : www.template.ftpj.otoiser.org
Reference Link Updates : www.updates.ftpj.otoiser.org
Internet Publishing : www.ftpj.otoiser.org

This document is licensed under a Creative Commons Attribution 4.0 International License – <https://creativecommons.org/licenses/by/4.0>

ISSN 2310-6697

toiser—open transactions on independent scientific-engineering research

FUNKTECHNIKPLUS # JOURNAL

Théorie—Expérimentation—Métrologie—Logiciel—Applications

ISSUE 1 – MONDAY 30 SEPTEMBER 2013 – YEAR 1

- 1 Contents
- 2 About
- 3 Editorial Board – Technical Support
- 4 Information for Peers – Guiding Principles
- # Telecommunications Engineering – Applications
- 7 All-Band 2G+3G Radial Disc-Cone Antennas:
Design, Construction, and Measurements
N.I. Yannopoulou, P.E. Zimourtopoulos, E.T. Sarris
- # Telecommunications Engineering – Métrologie
- 17 Measurement Uncertainty in Network Analyzers:
Differential Error Analysis of Error Models Part 1:
Full One-Port Calibration
N.I. Yannopoulou, P.E. Zimourtopoulos
- 23 Measurement Uncertainty in Network Analyzers:
Differential Error Analysis of Error Models Part 2:
Full Two-Port Calibration
N.I. Yannopoulou, P.E. Zimourtopoulos



About

This European Journal defends
honesty in science and ethics in engineering

Publisher – **otoiser** open transactions on independent scientific-engineering research – **ARG NP UoP** Antennas Research Group Non Profit Union of Persons – Hauptstraße 52, 2831 Scheiblingkirchen, Austria – **www.otoiser.org** – **www.antennas.gr**

Language – We declare the origins of the Journal by using English, German and French, as well as, a Hellenic vignette, in the cover page. However, since we recognize the dominance of USA English in technical literature, we adopted it as the Journal's language, although it is not our native language.

Focus – We consider Radio-FUNK, which still creates a vivid impression of the untouchable, and its Technology-TECHNIK, from an Advanced-PLUS point of view. That is, we dynamically focus at any scientific-engineering discipline producing FUNKTECHNIKPLUS Théorie, Expérimentation, Métrologie, Logiciel, ou Applications.

Scope – We emphasize this scope broadness by extending the title of the Journal with a Doppelkreuz-Zeichen #, which we use as a placeholder for the disciplines of Editorial Board:

Electrical – # Electronics – # Computer – # Telecommunications – Engineering # Computer Science # Applied Mathematics, etc.

Frequency – We regularly publish 3 issues per year on January, May, and September as well as an issue every 3 papers.

Editions – We follow the arXiv.org system, that is the 1st edition date of every issue is on the cover page and any update date is on the odd pages with its version on all pages.

Format – We use the uncommon for Journals A5 paper size and the much readable Liberation Mono fixed-space font, with hyphenation, justification, and unfixed word spacing, to display 2 pages side-by-side on widescreen monitors with WYSIWYG printout. We can consider only papers in ODF odt or MS doc format written in LibreOffice or MS Office with MathType. We use PDFCreator and PDF-Xchange to produce pdf and export to images for printing on demand and electronic publishing.

License – We use the free Open Journal System OJS from the PKP Public Knowledge Project for internet publication

Copyright – Creative Commons Attribution 3 Unported CC-BY 3

Please download the latest *About* edition from
about.ftpj.otoiser.org

Editorial Board

Electrical Engineering

High Voltage Engineering # Insulating Materials

Professor Michael Danikas

EECE, Democritus University of Thrace, mdanikas@ee.duth.gr

Electrical Machines and Drives # Renewable Energies

Electric Vehicles

Assistant Professor Athanasios Karlis

EECE, Democritus University of Thrace, akarlis@ee.duth.gr

Computer Engineering # Software Engineering

Cyber Security

Associate Professor Vasileios Katos

EECE, Democritus University of Thrace, vkatos@ee.duth.gr

Internet Engineering # Computer Science

Simulation # Applied Education # Learning Management Systems

Lecturer Sotirios Kontogiannis

BA, TE Institute of Western Macedonia, skontog@gmail.com

Applied Mathematics # Functional and Numerical Analysis

Applied Electromagnetics # Control Theory

Dr. Nikolaos Berketis, Athens, Greece

BS-Math, MSc-Appl.Math, PhD-Appl.Math, nberketis@gmail.com

Telecommunications Engineering

Applied Electromagnetics # Metrology # Applied Education

Simulation # Virtual Reality # Amateur Radio # FLOSS

Applied Physics # Electronics Engineering

Dr. Nikolitsa Yannopoulou, Scheiblingkirchen, Austria

Diploma Eng-EE, MEng-EECE, PhD-EECE, yin@arg-at.eu

Assistant Professor Petros Zimourtopoulos

EECE, Democritus University of Thrace, pez@ee.duth.gr

Technical Support

Konstantinos Kondylis, Doha, Qatar

Diploma Eng-EECE, MEng-EECE, k8k@arg-at.eu

Christos Koutsos, Bratislava, Slovakia

Diploma Eng-EECE, MEng-EECE, cak@arg-at.eu

Information for Peers Guiding Principles

This is a small, but independent, low profile Journal, in which we are all – Authors – Reviewers – Readers – Editors – free at last to be Peers in Knowledge, without suffering from either:

- Journal roles or positions,
- Professional, amateur, or academic statuses, or
- Established impact factorizations,

but with the following Guiding Principles:

Authors – We do know what work means; and we do respect the research work of the scientist – engineer; and we do want to highlight this work; and we do decided to found this Journal; and we do publish this work openly; and furthermore, we do care for the work of the technical author, especially the beginner one, whom we do support strongly as follows:

- 1 We encourage the author to submit his own paper written just in Basic English plus Technical Terminology.
- 2 We encourage the author even to select a pen name, which may drop it at any time to reveal his identity.
- 3 We encourage the author to submit an accepted for publication paper, which he was forced to decline that publication because it would be based on a review with unacceptable evaluation or comments.
- 4 We encourage the author to resubmit a non accepted for publication paper that was rejected after a poor, inadequate, unreasonable, irresponsible, incompetent, or ticking only, review.
- 5 We encourage the author to submit a paper that he already self-archived on some open repository, such as arXiv.org.
- 6 We encourage the author to self-archive all of the preprint and postprint versions of his paper.
- 7 We provide the author with a decent, express review process of up to just 4 weeks, by at least 2 peers, never have been co-authors with him.
- 8 We provide the author with a selection of review process between: a traditional, anonymous, peer review decision, and an immediate online pre-publication of his paper followed by an open discussion with at least 2 reviewers.

About

- 9 We immediately accept for publication a research paper directly resulting from a Project Report, Diploma-, Master-, or PhD-thesis, which the author already has successfully defended before a committee of experts and he can mention 2 members of it, who reviewed and approved his work.
- 10 We immediately publish online a paper, as soon as, it is accepted for publication in the Journal.
- 11 We quickly print-on-demand an issue every 3 papers, in excess of the 3 issues we regularly publish 3 times a year.
- 12 We do not demand from the author to transfer his own copyright to us.
- 13 Nevertheless, we publish only an original research work paper and only if the author does assure us that he owns the copyright of his own paper and submit this paper or a revised version of it to the Journal for publication or even for republication under the Creative Commons–Attribution 3.0 Unported License, CC-BY 3.

Reviewers – Any peer may voluntarily become a reviewer of the Journal in his expertise for as long as he wishes. Each author of the Journal has to support the peer-to-peer review process by reviewing one paper, written by non co-author(s) of him, for every one of his papers published in the Journal.

Readers – Any reader is a potential reviewer. We welcome online comments and post-reviews by the readers.

Editors – Any editor holds a PhD degree, to objectively prove that he really has the working experience of passing through the established publishing system. An editor pre-reviews a paper in order to check its compliance to the Guiding Principles and to select the appropriate reviewers of the Journal. We can only accept for consideration papers in the expertise areas currently shown in the Editorial Board page. However, since we are willing to amplify and extend the Scope of the Journal, we welcome the volunteer expert, in any subject included into it, who wants to join the Board, if he unreservedly accepts our Guiding Principles.

Antennas Research Group – Non-Profit 12(3) * Union of Persons

* The Constitution of Greece, Article: 12(3) 2008:
www.hellenicparliament.gr/en/Vouli-ton-Ellinon/To-Politevma

* The Hellenic Supreme Court of Civil and Penal Law:
www.areiospagos.gr/en/ – Court Rulings:Civil|A1|511|2008

Submissions

sub@ftpj.otoiser.org

Electronic Publishing

www.ftpj.otoiser.org

Printing-on-Demand

pod@ftpj.otoiser.org

Directly:

Georgios Tontrias, msn.expresscopy.xan@hotmail.com
ExpressCopy, V.Sofias 8, 671 00, Xanthi, Greece

More – Detailed information will be available soon at:
www.ftpj.otoiser.org/gp

All-Band 2G+3G Radial Disc-Cone Antennas: Design, Construction and Measurements

N.I. Yannopoulou, P.E. Zimourtopoulos, E.T. Sarris *

Antennas Research Group, Austria – Hellas [1, 2]
EECE Dept, Democritus University of Thrace, Hellas [2 and 3]

Abstract

We define as "All-Band 2G+3G" any band that includes all frequencies allocated to both 2G and 3G services. We define as "Radial Disc-Cone Antenna RDCA" any discone antenna with a structure of radial wires. The RDCA was theoretically analyzed and software simulated with the purpose of computationally design a broadband model of it. As an application, a broadband RDCA for operation from 800 to 3,000 MHz, which include all 2G and 3G frequencies, was designed and an experimental model was constructed and tested. In order to evaluate the agreement between theory and practice, mathematically expressed measurement error bounds were computed.

Introduction

In 1945, Kandoian invented the well-known discone antenna, that is a dipole made of a disc above a cone [1]. In 1953, Nail gave experimentally two naive relations for the discone dimensions [2].

In 1987, Rappaport designed discones using an N-type connector feed [3]. In 1993, Cooke studied a discone with a structure of radial wires [4]. In 2005, Kim et al. presented a double radial discone antenna for Ultra Wide-Band applications [5].

In this short paper we present an All-Band 2G+3G RDCA fed by an N-type/Female/50-Ohm connector.

Research

The RDCA was theoretically analyzed as a group of identical filamentary V-dipoles with unequal arms connected in parallel. The dipoles recline on equiangular vertical ϕ -planes around z-axis to form a disconical array. Fig.1A shows two such coplanar dipoles conformed with the apex angle α . Each V-dipole has a total length L equal to the sum of arm lengths r and s plus the gap g between its terminals.

The simulation was based on a suite of developed visual tools which are supported by a fully analyzed, corrected and redeveloped edi-

tion of the original thin-wire computer program by J.H. Richmond [6].

Two arithmetic criteria were adopted for the broadband characterization of a model:

- (1) 50-Ohm VSWR lower than 2
- (2) Normalized radiation intensity U/U_{max} lower than 3 dB on the horizontal plane.

A visual application program was specifically developed to design a broadband radial discone with bare wires of diameter d embedded in free space when the wire conductivity, the type of feeding connector and the frequency band are given.

The program uses the model of a radial discone fed by an N-type connector shown in Fig.2. Starting with an appropriate combination of the relations given by [2]-[4] the program computes by iteration in terms of wavelength λ , the geometric characteristics r , s , g , a , just when the criteria are satisfied.

Fig.1B shows a Ground Plane Antenna GPA that was designed for reference and consists of equal number of cone radials s and a vertical monopole with height r .

As a practical application of the broadband design, the 2G+3G band from 800 to 2,500

MHz was selected to begin with and an experimental radial discone of copper wire fed by N-type connector was built, as shown in Fig.3.

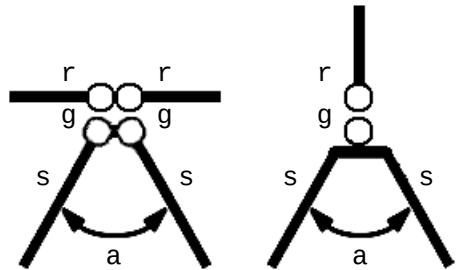


Fig.1: A - RDCA, B - GPA

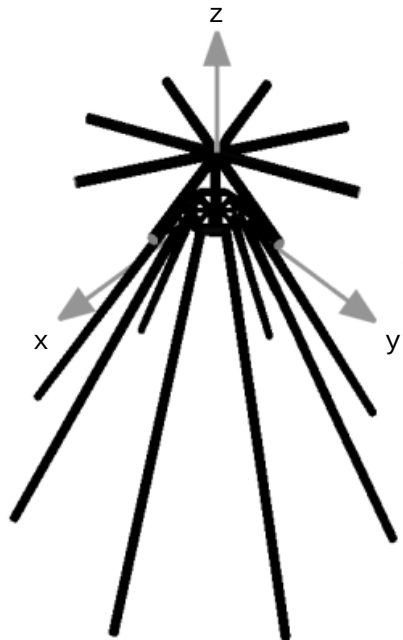


Fig.2: RDCA - Designed Model

In order to demonstrate the particular behavior of the experimental model, the 2G+3G band was divided as follows:

2G+3G Sub-Bands
800 MHz – 2,500 MHz

Sub-Band	MHz
I	806 – 960
II	1,429 – 1,513
III	1,710 – 1,900
IV	1,910 – 2,025
V	2,110 – 2,170
VI	2,400 – 2,499

Our measurement system consists of an EM anechoic chamber, a network analyzer, a number of support instruments, a set of standard loads of factory accuracy and a constructed antenna rotation mechanism with a built hardware control unit of its step motor. The combined characteristics of system parts specify a measurement band from 600 to 1300 MHz, which overlaps with the 2G/3G band. Developed control software synchronizes the system and collects data using the IEEE-488 protocol.

A developed general mathematical method expresses the measurement error bounds. Another set of developed software applications processes the collected data and computes the error bounds.

Results

The consideration of radial discone as an array of at least eight 8 V-dipoles produces a theta-polarized vector radiation pattern with magnitude a surface almost by revolution around z-axis. So the radial discone has indeed on the horizontal plane xOy the basic properties of a vertically polarized almost omni-directional antenna, that is a fact that encouraged the design of a broadband model by using simulation.

The application of the broadband criteria to 2G/3G band resulted to the design of a RDCA with the following geometrical characteristics:

All-Band 2G+3G RDCA
800 MHz – 3,000 MHz

Geometry		Units
d	1.5	[mm]
r	44	[mm]
g	6	[mm]
s	125	[mm]
a	60	[°]

The RDCA operates from 800 to 3,000 MHz, which exceeds that of 2G+3G band. The accordingly constructed experimental radial discone of Fig.3 should be implied with a constructional tolerance of ±0.5 mm and ±0.5°.

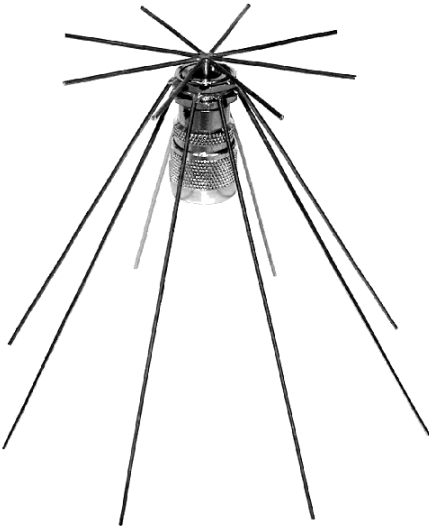


Fig.3: RDCA experimental model

The broadband model has a directivity from about -0.5 to 2.9 dBd with slope angle between -65° and $+58^\circ$, but the directivity gain on horizontal plane stays very close to the desirable value of 0 dBi, since it changes from -1 to $+1.7$ dBi only. Fig.4 shows that the predicted horizontal normalized radiation intensity remains below 3 dB indeed, while it stays above 0 dB relative to the reference antenna in all 2G+3G subbands indicated by the vertical gray strips, when both are fed by the same $50\text{-}\Omega$ source.

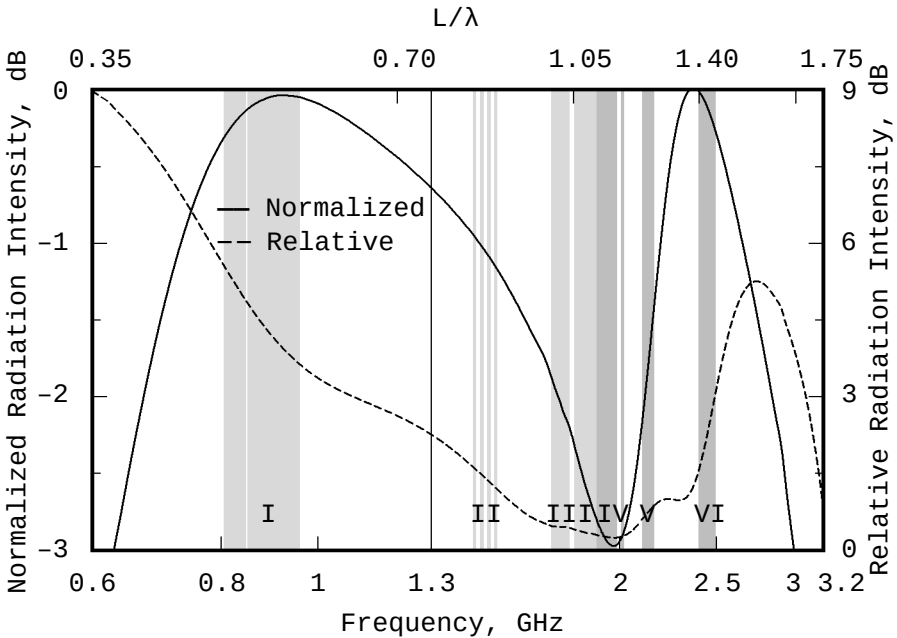


Fig.4: Predicted radiation intensity on horizontal plane.

Fig.5A shows the predicted normalized radiation patterns in dB at the center of each sub-band, which confirms the horizontal omni-directional radiation properties of the broadband model.

At the center frequency of 950 MHz of the measurement band, the predicted and measured radiation intensity on the three main cuts of the radiation pattern are in good

agreement, as shown in Fig. 5B.

This is made clearer by the measurement error bounds on a vertical plane as shown in Fig.6.

Fig.7 shows that the 50-Ohm VSWR predicted results for the broadband disccone are below 2 indeed and almost covered by the error bounds in the measurement band.

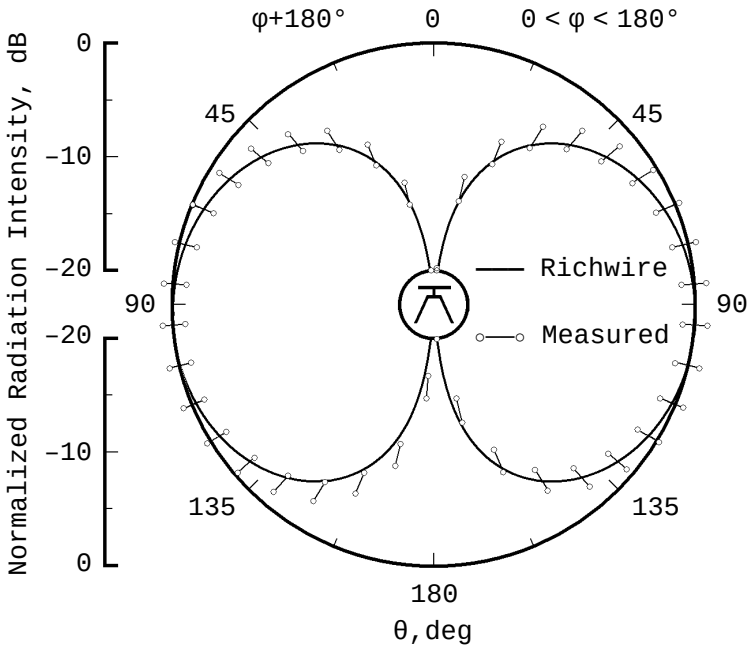


Fig.6: Measurement error bounds on a vertical plane

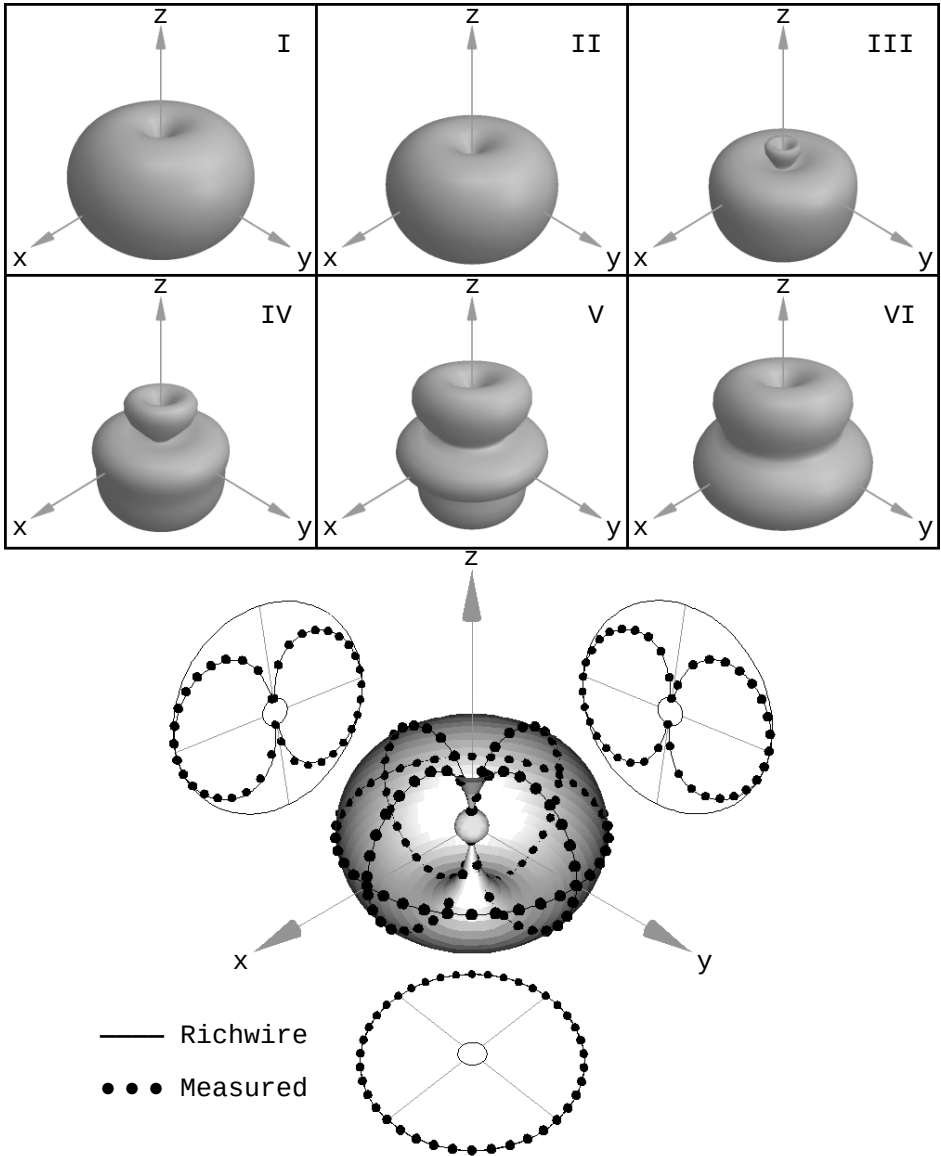


Fig.5: A (Up) Predicted normalized radiation intensity patterns at the center of each 2G+3G sub-band – B (Down) Normalized radiation intensity pattern at the center of measurements band

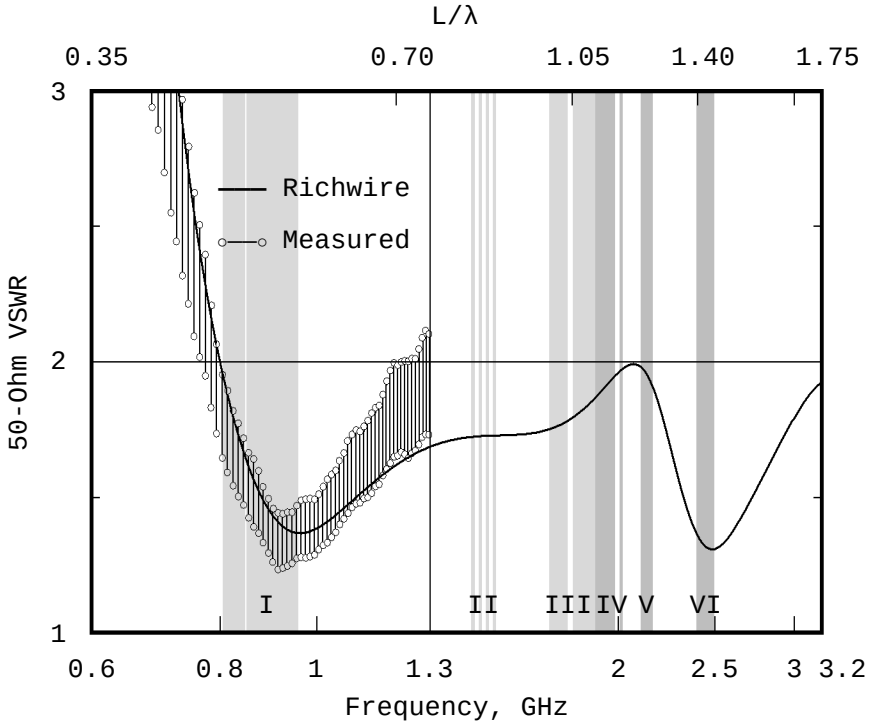


Fig.7: Standing wave ratio against frequency or ratio of total length to wavelength

Conclusion

Prediction and experimentation in the measurement band 600 MHz to 1,300 MHz proposes a successfully de-

signed, constructed, and measured Radial Disk Cone Antenna RDCA capable to serve All-Band 2G+3G applications from 800 MHz to 3,000 MHz.

Credits

The authors acknowledge Adamantios Diamantidis, SV7FSF, a former member of Computer Center – Network Administration Center at Democritus University of Thrace, now Systems Engineer, Systems Administrator (honorary), Berlin, Germany, who motivated the study of Discone Antennas on behalf of FSF Free Software Foundation followers on the purpose to be openly supported in their Wi-Fi activities.

References

- [1] Kandoian A.G., "Three New Antenna Types and Their Applications", Proceedings of IRE, Vol. 34, February 1946, pp. 70W-75W
- [2] Nail J.J., "Designing Discone Antennas", Electronics, August 1953, pp. 167-169
- [3] Rappaport T.S., "Discone Design Using N-Connector Feed", IEEE Antennas and Propagation Society Newsletter, Vol. 30, February 1988, pp. 12-14
- [4] Cooke D.W., "The Skeleton Discone", The ARRL Antenna Compendium, Vol. 3, 1993, pp. 140-143
- [5] Kim K.H., Kim J.U. and Park S.O.: "An Ultrawide-Band Double Discone Antenna With the Tapered Cylindrical Wires", IEEE Transactions on Antennas and Propagation, Vol. 53, No. 10, October 2005, pp. 3403-3406
- [6] Richmond J.H., "Radiation and scattering by thin-wire structures in a homogeneous conducting medium", IEEE Transactions on Antennas and Propagation, Vol. 22, Issue 2, March 1974, p.365

Preprint Versions

Broadband radial discone antenna:
Design, application and measurements
N. I. Yannopoulou, P. E. Zimourtopoulos, E. T. Sarris
"<http://arxiv.org/abs/physics/0612043>"

Follow-Up Research Paper

Not until now

Previous Publication in FUNKTECHNIKPLUS # JOURNAL

None

* About The Authors

Nikolitsa Yannopoulou, SV7DMC, was born in Chania, Crete, Greece in 1969. She graduated in 1992 from Electrical Engineering at Democritus University of Thrace, Xanthi, Greece and since then she is with the Antennas Research Group (1992). She received the MEng degree with full marks in Microwaves in 2003 and her PhD degree in Antennas, in 2008 at Democritus University. Her research interests are in antenna theory, software, simulation, built, measurements and virtual laboratories.

yin@arg-at.eu – www.arg-at.eu

Petros Zimourtopoulos, SV7BAX, was born in Thessaloniki, Greece in 1950. 1976: Physics degree, 1978: Electronic Physics (*Radio-Electrology*) MSc and four courses to Mathematics degree, from Aristotle University of Thessaloniki. 1985: PhD in Antennas, from Electrical Engineering Department at Democritus University of Thrace. 1986: Lecturer; 1992: Assistant Professor; and since 1994, in permanent position, at Electrical Engineering and Computer Engineering Department of Democritus University. In 1985, he founded, and since then he leads, the independent Antennas Research Group.

pez@arg-at.eu – www.arg-at.eu

Emmanuel Sarris was born in Athens, Greece, 1945. Diploma of Physics, University of Athens, 1967. PhD in Space Physics (with J.A.Van Allen), University of Iowa, 1973. Post Doctoral Fellow, Applied Physics Laboratory of the Johns Hopkins University, 1974-76. Research Scientist, Max-Planck Institut, 1976-77. Professor of Electrodynamics at the Department of Electrical Engineering of the University of Thrace and Director of the Space Research Laboratory, 1977-2012. Experience: Space Plasma Electrodynamics; Design, Construction and Testing of Space Instruments and Systems; Satellite Communications; Satellite Remote Sensing. Co-I or P-I in the International Space Missions: Ulysses, Geotail, Interball-Aurora, Interball-Tail, Cluster, Spektr-R. Over 300 refereed publications and 1700 citations. COSPAR Plenary Council. Corresponding Member of the Academy of Athens, 2003. ESA and/or NASA Awards for outstanding contributions to the Ulysses, Geotail and Cluster Missions.

This paper is licensed under a Creative Commons Attribution 4.0 International License – <https://creativecommons.org/licenses/by/4.0/>

[This Page Intentionally Left Blank]

Measurement Uncertainty in Network Analyzers: Differential Error Analysis of Error Models Part 1: Full One-Port Calibration

N.I. Yannopoulou, P.E. Zimourtopoulos *

Antennas Research Group, Austria – Hellas [1, 2]
EECE Dept, Democritus University of Thrace, Hellas [2]

Abstract

An analytical method was developed to estimate errors in quantities depended on full one-port vector network analyzer (VNA) measurements using differentials and a complex differential error region (DER) was defined. To evaluate the method, differences instead of differentials were placed over a DER which was then analyzed and compared with another commonly used estimated error. Two real differential error intervals (DEIs) were defined by the greatest lower and least upper bounds of DER projections. To demonstrate the method, a typical device under test (DUT) was built and tested against frequency. Practically, a DER and its DEIs are solely based on manufacturer's data for standard loads and their uncertainties, measured values and their inaccuracies.

Introduction

In full one-port measurements with a VNA of real characteristic impedance Z_0 , a DUT with impedance Z has a reflection coefficient ρ defined by

$$\rho = (Z - Z_0)/(Z + Z_0)$$

and related to its measured value m by the bilinear transformation

$$\rho = (m - D)/[M(m - D) + R]$$

in terms of errors D , M and R [1]. This transformation can be uniquely determined from given distinct ρ_n , $n = 1, 2, 3$ and respectively known m_k , $k = n$ [2].

Research

We considered ρ_n , m_k as the elements of given ordered triples (A, B, C) , (a, b, c) , solved the resulting system and appropriately expressed its solution by

$$F = \sum cC(B - A)$$

$$D = \sum abC(A - B)/F$$

$$M = \sum c(B - A)/F$$

$$R = [\prod (A - B)(a - b)]/F^2$$

where \sum and \prod produce two more terms from the one shown, by rotation of the ordered triple elements. These errors were then considered

as depended on the independent variables ρ_n, m_k . Therefore, their differentials were expressed in the same manner by

$$dD = [\prod (a - b) \sum (B - C)BC \, da + \sum (b - c)^2(B - A)(C - A)BC \, da]/F^2$$

$$dM = [\sum (a - b)(c - a)(B - C)^2 \, da - \prod (A - B) \sum (b - c) \, da]/F^2$$

$$dR = \{ \sum [F + 2(a - b)B(A - C)] [(B - C)^2 \, da \prod (a - b) - (b - c)^2 \, da \prod (A - B)] \} / F^3$$

After that, the differential of ρ was expressed by

$$d\rho = [-RdD - (m - D)^2 dM - (m - D)dR + Rdm] / [M(m - D) + R]^2$$

and was considered depended, through dD, dM and dR , on $L = 7$ independent variables and their independent differentials: $\rho_n, n = 1, 2, 3$ and $m_k, k = n$ or $k = 0$ with $m_0 = m$.

The developed expressions were mechanically verified using a developed software program for symbolic computations.

Manufacturer's data for standard loads used in full-one port VNA measurements are substituted in ρ_n , and for their uncertainties in $d\rho_n$. Since Z_0 is real, the domain of each ρ_n is the closed unit circle [3]. For $|\rho_n| = 0$ or 1, care must be exercised to restrict its differential value onto its domain. The VNA mea-

surements have specified bounded ranges for their modulus and argument, so that the domain of each m_k is a bounded circular annular with its center at the origin O of the complex plane. Measurement data are substituted in m_k and manufacturer's data for measurement inaccuracy in dm_k . Uncertainty and inaccuracy data outline domains for $d\rho_n$ and dm_k . If $z = |r|e^{j\varphi}$, stands for any of the independent variables and dz for its differential then the contribution of dz to $d\rho$ is a summation term of the form Wdz , with $W = |U|e^{jV}$, so that

$$Wdz = |U|e^{j(V + \varphi)} d|r| + |U|e^{j(V + \varphi + \pi/2)} |r| d\varphi$$

where W is in fact a known value of the respective partial derivative and $d|r|, d\varphi$ are the independent real differentials of the complex dz in polar form. Each expression Wdz outlines a contour for a partial DER around O . If $z \neq 0$, the partial DER is a parallelogram with perpendicular sides $d|r|$ and $|r|d\varphi$, stretched or contracted by $|U|$ and rotated by $(V + \varphi)$ around O . If $z = \rho_n = 0$, the partial DER is a circle with radius $|U|d|r|$. Accordingly, a DER is the sum of either L parallelograms or $(L - 1)$ parallelograms and 1 circle. DER is

then a convex set with contour either a polygonal line with 4L vertices at most, or a piecewise curve composed of $4(L - 1)$ line segments and $4(L - 1)$ circular arcs at most. The greatest lower and least upper differential error bounds are the end-points of DEIs for the real and imaginary parts of ρ and result from the projections of DER for ρ on the coordinate axes. These conclusions can be generalized for any other quantity directly or indirectly depended on all, some or just one of the above independent variables and their differentials. Thus, the quantity has an L-term DER, where $7 \geq L \geq 1$. For example, the impedance Z of a DUT has the 7-term DER:

$$dZ = 2Z_0 dp / (1 - \rho)^2$$

Results

All of the following data are specified by manufacturers of the parts for our measurement system. This system operates from 1 to 1300 MHz with 100 Hz PLL stability and consists of a type-N $Z_0 = 50 \Omega$ network analyzer, a number of support instruments and a set of standard loads. The standards are: a short circuit A, a matching load B with reflection coefficient 0.029 and an open circuit C with reflection coefficient 0.99 and phase accuracy $\pm 2^\circ$. In the absence of manufacturer's

data for A we considered its uncertainty equal to that of C. So, the following values were substituted in the developed expressions:

$$A = -1, \quad 0 \leq d|A| \leq 0.01, \quad -180^\circ \leq d\varphi_A \leq -178^\circ \text{ or } 178^\circ \leq d\varphi_A \leq 180^\circ,$$

$$B = 0, \quad |dB| = 0.029,$$

$$C = 1, \quad -0.01 \leq d|C| \leq 0, \quad -2^\circ \leq d\varphi_C \leq +2^\circ$$

The annular domain for m_k of VNA is specified from 0 to -70 db in modulus and ± 180 degrees in argument. Measurements m_k result with a decimal floating point precision of 4 digits, for both modulus and argument. We consider the modulus and argument of dm_k equal to $\pm 1/2$ of the unit in the last place of the corresponding mantissa in modulus and argument of m_k . Consequently, our system produces a DER, either for ρ or Z, as a sum of $(L - 1) = 6$ parallelograms and 1 circle, with a contour of $(4L + 4L) = 48$ vertices at most.

A suite of developed software applications: (i) controls the system and collects the data in terms of frequency using the IEEE-488 protocol, (ii) processes the collected data and computes the vertices of DER and the end-points of its DEIs (iii) sketches pictures of DER for ρ and Z in terms of the frequency steps and make a film using them as frames.

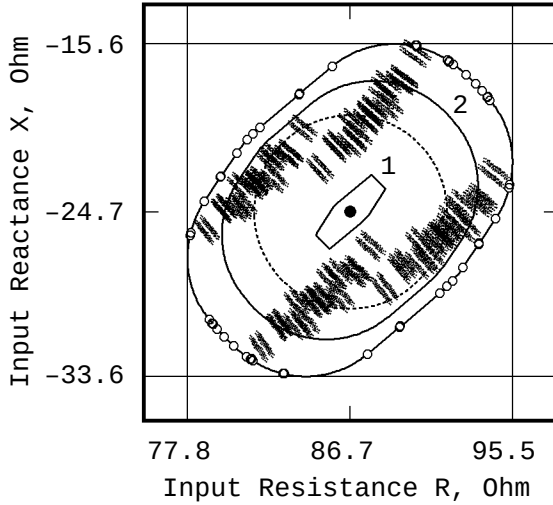


Fig.1: A typical DER for the impedance Z

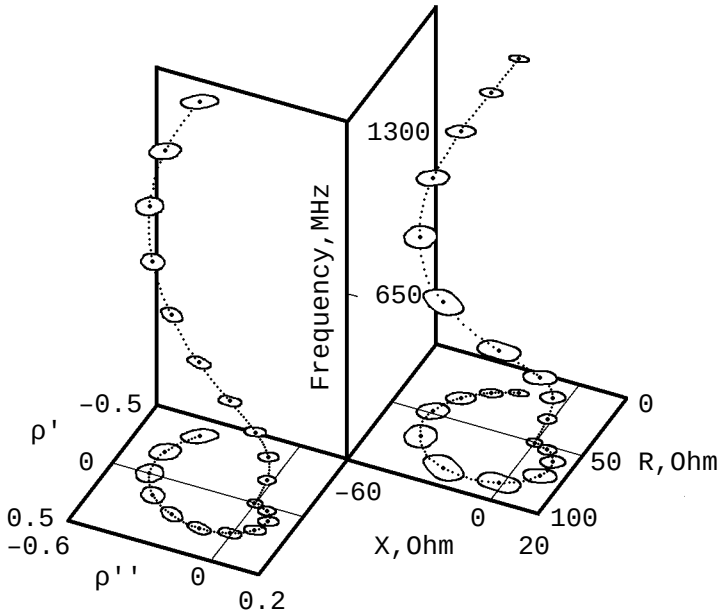


Fig.2: DER for the reflection coefficient ρ and for its associated impedance Z against frequency

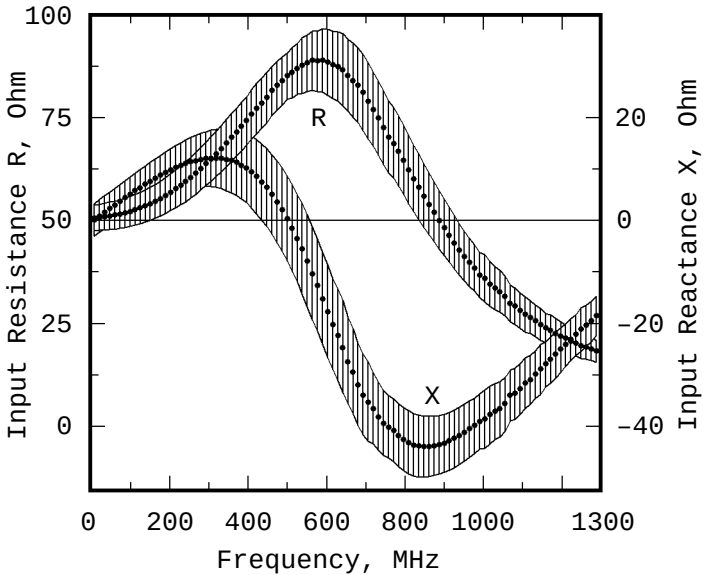


Fig.3: Greatest lower and least upper differential error bounds for resistance R and reactance X against frequency

A typical resistor with a nominal DC impedance of 50Ω $\pm 20\%$ tolerance was soldered on a type-N base connector and enclosed in an aluminium box to serve as a simple DUT for testing its Z from 2 to 1289 MHz in 13 MHz steps. The center frequency $f_c = 639$ MHz was chosen to reveal the details of the proposed method in Fig.1, where the contour of a typical DER for Z is outlined with small circles as its vertices. This contour surrounds that of the 4-terms DER due to inaccuracy of measurements (1) and that of 3-

terms DER for the uncertainty of loads (2). A properly circumscribed rectangle of DER shows graphically how the DEIs for R and X result. The commonly used error from the matching load only is shown as a dotted circle. This is in fact a 1-term DER which is surrounded from the contour of the DER by a factor of about 125% to 185% in all directions. Finally, in the same figure, $2^{7 \times 2}$ differences ΔZ resulting from the same $d\rho_n$ and dm_k , dense enough to appear as stripes, were placed over DER to compare

them with differential dZ values. Notably, almost all of ΔZ values are belong to DER while the computation time for these ΔZ exceeds that for DER by more than one order of magnitude. To demonstrate the method, a set of selected DER frames for ρ and Z are shown in Fig.2, as beads on space curved filaments against frequency.

Finally, the computed DEIs for R and X are shown in Fig.3 against frequency.

Conclusion

The proposed method may be efficiently used in the same way, to successfully estimate errors in any quantity depended on full one-port vector network analyzer measurements.

References

- [1] Fitzpatrick J., "Error Models for Systems Measurement", Microwave Journal, 21, May 1978, pp. 63-66
- [2] Spiegel M.R., "Complex Variables with an introduction to Conformal Mapping and its applications", McGraw-Hill, 1974, p.203
- [3] Chipman R.A., "Transmission Lines", McGraw-Hill, 1968, p.137

Preprint Versions

Differential Error Region of a Quantity Dependent on Full One-Port Network Analyser Measurements
N. I. Yannopoulou, P. E. Zimourtopoulos
"http://arxiv.org/abs/physics/0612049"

Follow-Up Research Paper

Total Differential Errors in One-Port Network Analyzer Measurements with Application to Antenna Impedance
N. Yannopoulou, P. Zimourtopoulos
Radioengineering, June 2007, Volume 16, Number 2
www.radioeng.cz/papers/2007-2.htm
www.radioeng.cz/fulltexts/2008/08_01_01_08.pdf

Previous Publication in FUNKTECHNIKPLUS # JOURNAL

"All-Band 2G+3G Radial Disc-Cone Antennas: Design, Construction and Measurements", Issue 1, pp. 7-15

This paper is licensed under a Creative Commons Attribution 4.0 International License – <https://creativecommons.org/licenses/by/4.0/>

Measurement Uncertainty in Network Analyzers: Differential Error Analysis of Error Models Part 2: Full Two-Port Calibration

N.I. Yannopoulou, P.E. Zimourtopoulos *

Antennas Research Group, Austria – Hellas [1, 2]
EECE Dept, Democritus University of Thrace, Hellas [2]

Abstract

Since S-parameter measurements without uncertainty cannot claim any credibility, the uncertainties in full two-port Vector Network Analyzer (VNA) measurements were estimated using total complex differentials (Total Differential Errors). To express precisely a comparison relation between complex differential errors, their differential error regions (DERs) were used. To demonstrate the method in the most accurate case of a direct zero-length thru, practical results are presented for commonly used Z-parameters of a simple, two-port, DC resistive T-network, which was built and tested against frequency with a VNA measurement system extended by two lengthy transmission lines.

Introduction

It is well known that in full two-port VNA measurements the S-parameters for a two-port Device Under Test (DUT) are given in terms of their 4 measurements m_{ij} , $i=1, 2$, $j=1, 2$ by

$$S_{11} = \{[(m_{11} - D)/R][1 + (m_{22} - D')M'/R'] - L(m_{21} - X)(m_{12} - X')\}/(TT')\}/H \quad (1)$$

$$S_{21} = \{[1 + (m_{22} - D')(M' - L)/R'] (m_{21} - X)/T\}/H \quad (2)$$

$$H = [1 + (m_{11} - D)M/R][1 + (m_{22} - D')M'/R'] - LL'(m_{21} - X)(m_{12} - X')\}/(TT') \quad (3)$$

S_{22} , S_{12} have expressions that result from (1)-(2) by substituting i, j with j, i and D, M, R, L, T, X with D', M', R', T', L', X' and vice-versa [1]. These 12 quantities have been defined as system errors [2]. Stumper gave non-generalized expressions for the partial deviations of S-parameters due to calibration standard uncertainties, in 2003 [3]. Furthermore, the developed total differential errors for full one-port VNA measurements [4] are also not generalized in the two-port case. To the

best of the authors' knowledge, there are no analytical expressions for total differential errors in full two-port VNA measurements.

Research

Since S-parameters are functions of 16 complex variables, their total differential errors were initially expressed as

$$\begin{aligned}
 dS_{11} = & \{ T T' (1 - MS_{11}) [R' + M' (m_{22} - D')] \} (dm_{11} - dD) \\
 & - RR' L (1 - L' S_{11}) [(m_{21} - X) (dm_{12} - dX') + (m_{12} - X') (dm_{21} - dX)] \\
 & + M' T T' [(m_{11} - D) (1 - MS_{11}) - RS_{11}] (dm_{22} - dD') \\
 & - T T' S_{11} (m_{11} - D) [R' + M' (m_{22} - D')] dM \\
 & + T T' (m_{22} - D') [(m_{11} - D) (1 - MS_{11}) - RS_{11}] dM' \\
 & - (R' L (1 - L' S_{11}) (m_{12} - X') (m_{21} - X) + \\
 & + T T' S_{11} [R' + M' (m_{22} - D')]) dR \\
 & - (RL (1 - L' S_{11}) (m_{12} - X') (m_{21} - X) \\
 & - T T' [(m_{11} - D) (1 - MS_{11}) - RS_{11}]) dR' \\
 & - RR' (m_{12} - X') (m_{21} - X) [(1 - L' S_{11}) dL - LS_{11} dL'] \\
 & + [(m_{11} - D) (1 - MS_{11}) - RS_{11}] [R' + M' (m_{22} - D')] \\
 & (T' dT + T dT') \} / P
 \end{aligned} \tag{4}$$

$$\begin{aligned}
 dS_{21} = & \{ -MT T' S_{21} [R' + M' (m_{22} - D')] \} (dm_{11} - dD) \\
 & + RR' LL' S_{21} (m_{21} - X) (dm_{12} - dX') \\
 & + R \{ T' [R' + (m_{22} - D') (M' - L)] + R' LL' S_{21} (m_{12} - X') \} (dm_{21} - dX) \\
 & + T' (R (m_{21} - X) (M' - L) - M' TS_{21} [R + M (m_{11} - D)]) (dm_{22} - dD') \\
 & - T T' S_{21} (m_{11} - D) [R' + M' (m_{22} - D')] dM \\
 & + T' (m_{22} - D') (R (m_{21} - X) - TS_{21} [R + M (m_{11} - D)]) dM' \\
 & + \{ (m_{21} - X) (T' (m_{22} - D') (M' - L) + R' [T' + LL' S_{21} (m_{12} - X')]) \\
 & - T T' S_{21} [R' + M' (m_{22} - D')] \} dR \\
 & + (R (m_{21} - X) [T' + LL' S_{21} (m_{12} - X')]) \\
 & - T T' S_{21} [R + M (m_{11} - D)]) dR' \\
 & + R (m_{21} - X) [R' L' S_{21} (m_{12} - X') - T' (m_{22} - D')] dL \\
 & + RR' LS_{21} (m_{12} - X') (m_{21} - X) dL' \\
 & - T' S_{21} [R + M (m_{11} - D)] [R' + M' (m_{22} - D')] dT \\
 & + (R (m_{21} - X) [R' + (m_{22} - D') (M' - L)] \\
 & - TS_{21} [R + M (m_{11} - D)] [R' + M' (m_{22} - D')]) dT' \} / P
 \end{aligned} \tag{5}$$

$$P = T T' [R' + M' (m_{22} - D')] [R + M (m_{11} - D)] - R R' L L' (m_{12} - X') (m_{21} - X) \quad (6)$$

dS_{22} and dS_{12} resulted from (4), (5) with the mentioned substitutions. X, X' errors stand for crosstalk measurements. $D, M, R (D', M', R')$ errors are uniquely determined in terms of 3 standard loads $A, B, C (A', B', C')$ and their 3 measurements $a, b, c (a', b', c')$, by full one-port VNA measurements, so the number of independent complex variables increases from 16 to 22. $L, T (L', T')$ errors are accurately determined after the replacement of DUT with a direct thru (or approximately, if an adapter is used instead) in terms of new measurements $t_{11}, t_{21} (t_{22}, t_{12})$ and of previously found quantities. Their expressions were appropriately stated as

$$L = [\sum (ab + ct_{11})C(B - A)]/E \quad (7)$$

$$T = (t_{21} - X) [\prod (A - B)(a - b)] / (E [\sum cC(B - A)]) \quad (8)$$

$$E = \sum (ab + ct_{11})(B - A) \quad (9)$$

where \sum and \prod produce two more terms, from the given one, by cyclic rotation of the letters $a, b, c (a', b', c')$ or $A, B, C (A', B', C')$. In this way, each S-parameter has as total differential error dS , a sum of 22 differential terms:

16 due to measurement inaccuracies $dm_{ij}, dX, dX', dt_{ij}, da, db, dc, da', db', dc'$ and 6 due to standard uncertainties given by their manufacturer $dA, dB, dC, dA', dB', dC'$. The expressions for $dD, dM, dR (dD', dM', dR')$ are known [4]. The expressions for the rest of differential errors were developed as

$$dL = \{ \sum (B - C)(b - t_{11})(c - t_{11}) [(B - C)(b - a)(c - a)dA - (b - c)(B - A)(C - A)da] + [\prod (A - B)(a - b)] dt_{11} \} / E^2 \quad (10)$$

$$dT = \{ \sum (t_{21} - X)(b - c)(B - C) [(t_{11} - c)(b - a)^2 B(A^2 + C^2) + (b - t_{11})(c - a)^2 C(A^2 + B^2) - 2ABC(b - c)(t_{11}(b + c - 2a) - bc + a^2)] [(B - C)(b - a)(c - a)dA - (b - c)(B - A)(C - A)da] \} / (E^2 [\sum cC(B - A)]^2) + [\prod (A - B)(a - b)] \{ [(t_{21} - X) \sum a(B - C)/E] dt_{11} + dt_{21} - dX \} / (E [\sum cC(B - A)]) \quad (11)$$

Each complex differential error defines a Differential Error Region (DER) on the complex plane with projections to coordinate axes the Differential Error Intervals (DEIs) [4]. Obviously, any

quantity differentially dependent on the above variables has also a DER. For example, after another correction to the given S to Z-parameters relations [5], the Z-DERs are resulted from

$$dZ_{11} = 2Z_0[(1 - S_{22})^2 dS_{11} + (1 - S_{22})S_{21} dS_{12} + (1 - S_{22})S_{12} dS_{21} + S_{12}S_{21} dS_{22}] / [(1 - S_{11})(1 - S_{22}) - S_{12}S_{21}]^2 \quad (12)$$

$$dZ_{21} = 2Z_0[(1 - S_{22})S_{21} dS_{11} + S_{21}^2 dS_{12} + (1 - S_{11})(1 - S_{22}) dS_{21} + (1 - S_{11})S_{21} dS_{22}] / [(1 - S_{11})(1 - S_{22}) - S_{12}S_{21}]^2 \quad (13)$$

while dZ_{22} , dZ_{12} result from (12), (13) by application of the mentioned substitutions.

S-DER is a sum of 20 parallelograms and 2 circles, with a contour of 160 vertices at most [4].

Results

Six calibration standards, in pairs of opposite sex, were used and their manufacturers' data were substituted in the developed expressions:

$$A = -1 = A', \quad 0 \leq d|A| = d|A'| \leq 0.01, \quad -180^\circ \leq d\varphi_A = d\varphi_{A'} \leq -178^\circ \text{ or } 178^\circ \leq d\varphi_A = d\varphi_{A'} \leq 180^\circ,$$

$$B = 0 = B', \quad |dB| = 0.029 = |dB'|,$$

$$C = 1 = C', \quad -0.01 \leq d|C| = d|C'| \leq 0 \text{ and } -2^\circ \leq d\varphi_C = d\varphi_{C'} \leq +2^\circ.$$

The inaccuracy of any VNA measurement was conservatively considered as a symmetric interval defined by just 1 unit in the last place of the corresponding mantissa, both in modulus and argument. Consequently, each

To demonstrate the method, a typical T-network of common resistors with nominal DC values $Z_1 = 24.2 \Omega$, $Z_2 = 120 \Omega$ for the horizontal arms and $Z_{12} = 1.1 \Omega$ for the vertical arm, were soldered on type-N base connectors of opposite sex and enclosed in an aluminium box, to form a two-port DUT.

The VNA measurement system was extended by two transmission lines of 3.66 m and 14 m, respectively, up to the DUT. The DUT was tested from 2 to 1289 MHz in 13 MHz steps. The frequency 1003 MHz was selected to illustrate the proposed method for S-DERs shown in Fig. 1.

To study the total differential error, dS was expressed as $dU + dI$, where dU is due to the uncertainty of 6 standards and dI to the inaccuracy of 16 measurements. The contribution of these, conservatively considered measurement inaccuracies to the total differential error is as much significant as the uncertainties of standard loads are. For example, computations for S_{12} over the whole measurement band show that $\max|dU|$ and $\max|dI|$ contribute ~35%-80% and ~25%-70% to $\max|dS_{12}|$, respectively. In addition, Fig. 1 shows how the projections of each S-DER result its real and imaginary DEI. To display the variation of S-DER against frequency, a number of selected S-DER frames are shown in Fig. 2 as beads on a space-curved filament. It is worth mentioning that S_{11} -DER (S_{22} -DER) was greater than it resulted from appropriately organized full one-port measurements, as it was expected. Finally, the computed Z-DEIs are shown in Fig. 3, along with their LF Z-values.

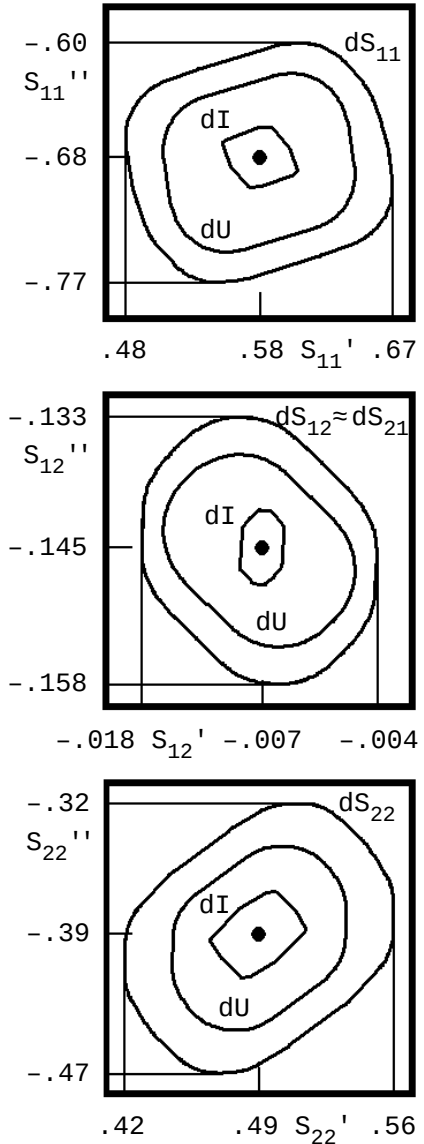


Fig.1: S-DERs at 1003 MHz

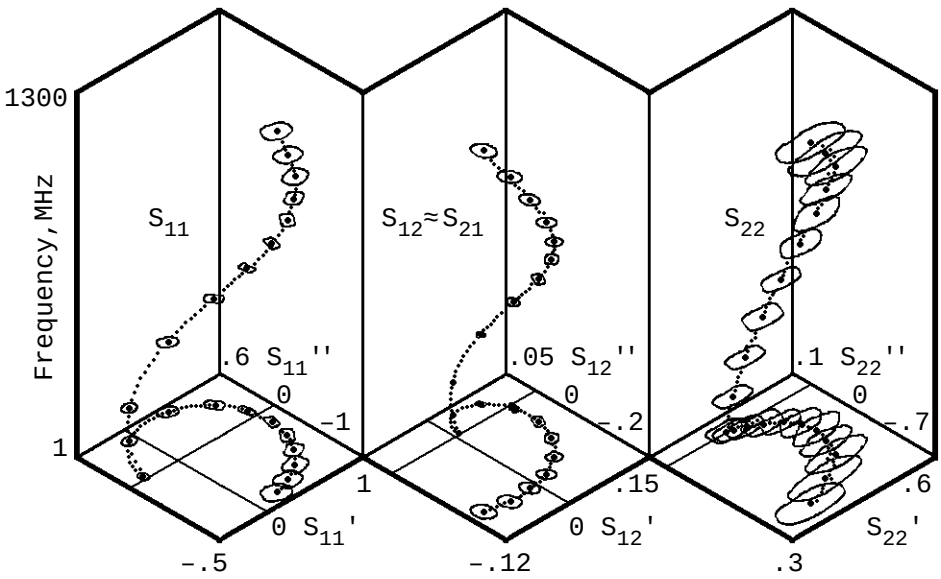


Fig.2: S-DERs against frequency

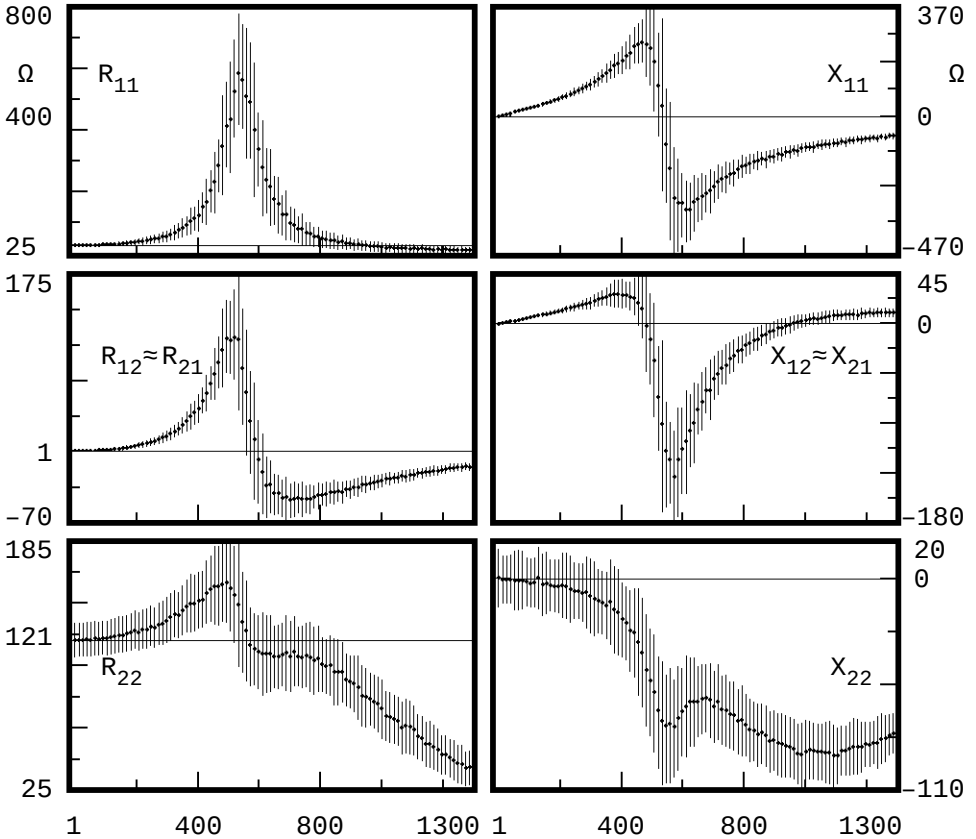


Fig.3: Z-DEIs against frequency

Conclusion

The proposed method may be efficiently used to estimate

uncertainties in any case where the process equations (1), (2) and (4), (5) can find application.

References

- [1] Ballo D., "Network Analyzer Basics", Hewlett-Packard Company, 1998, p. 58
- [2] Fitzpatrick J., "Error Models for Systems Measurement", Microwave Journal, 21, May 1978, pp. 63-66
- [3] Stumper U., "Influence of TMS0 calibration standards uncertainties on VNA S-parameters measurements", IEEE Transactions on Instrumentation and Measurements, Vol. 52, No. 2, April 2003, pp. 311-315
- [4] Yannopoulou N., Zimourtopoulos P., "Total Differential Errors in One-Port Network Analyzer Measurements with Application to Antenna Impedance", arXiv:physics/0703204, Radioengineering, Vol. 16, No. 2, June 2007, pp. 1-8
- [5] Beatty R.W., Kerns D.M., "Relationships between Different Kinds of Network Parameters, Not Assuming Reciprocity or Equality of the Waveguide or Transmission Line Characteristic Impedances", Proceedings of the IEEE, Vol. 52, Issue 1, January 1964, p. 84

Preprint Versions

Total Differential Errors in One-Port Network Analyzer Measurements with Application to Antenna Impedance
Nikolitsa Yannopoulou, Petros Zimourtopoulos
"http://arxiv.org/abs/physics/0703204"

Follow-Up Research Paper

S-Parameter Uncertainties in Network Analyzer Measurements with Application to Antenna Patterns
N. Yannopoulou, P. Zimourtopoulos
Radioengineering, April 2008, Volume 17, Number 1
www.radioeng.cz/papers/2008-1.htm
www.radioeng.cz/fulltexts/2008/08_01_01_08.pdf

Previous Publication in FUNKTECHNIKPLUS # JOURNAL

"Measurement Uncertainty in Network Analyzers: Differential Error Analysis of Error Models Part 1: Full One-Port Calibration", Issue 1, pp. 17-22

This paper is licensed under a Creative Commons Attribution 4.0 International License – <https://creativecommons.org/licenses/by/4.0/>

[This Page Intentionally Left Blank]

In case of any doubt,
download the genuine papers from
genuine.ftpj.otoiser.org

FRONT COVER VIGNETTE

A faded synthesis of an anthemion rooted in a meandros

The thirteen-leaf is a symbol for a life tree leaf.
"Herakles and Kerberos", ca. 530–500 BC,
by Paseas, the Kerberos Painter,
Museum of Fine Arts, Boston.

www.mfa.org/collections/object/plate-153852

The simple meandros is a symbol for eternal immortality.
"Warrior with a phiale", ca. 480–460 BC,
by Berliner Maler,
Museo Archeologico Regionale "Antonio Salinas" di Palermo.

commons.wikimedia.org/wiki/File:Warrior_MAR_Palermo_NI2134.jpg

ISSN 2310-6697

toiser—open transactions on independent scientific-engineering research

FUNKTECHNIKPLUS # JOURNAL

Théorie—Expérimentation—Métrologie—Logiciel—Applications

ISSUE 2 – SUNDAY 17 NOVEMBER 2013 – YEAR 1

- 1 Contents
- 2 About
- 3 Editorial Board – Technical Support
- 4 Information for Peers – Guiding Principles
- # Applied Electromagnetics – Théorie
- 7 Direct and Related Far-Field Inverse Scattering Problems for Spherical Electromagnetic Waves in Chiral Media
Nikolaos M. Berketis
- # Electrical Engineering – Expérimentation
- 19 Experimental Results on the Behavior of Water Droplets on Polymeric Surfaces Under the Influence of Electric Fields: the Case of an Inclined Test Arrangement for PVC, Rubber and Silicone Rubber
M.G. Danikas, P. Ramnalis, R. Sarathi
- # Telecommunications Engineering – Métrologie
- 41 Measurement Uncertainty in Network Analyzers: Differential Error Analysis of Error Models Part 3: Short One-Port Calibration – Comparison
N.I. Yannopoulou, P.E. Zimourtopoulos



About

This European Journal defends
honesty in science and ethics in engineering

Publisher – **otoiser** open transactions on independent scientific-engineering research – **ARG NP UoP** Antennas Research Group Non Profit Union of Persons – Hauptstraße 52, 2831 Scheiblingkirchen, Austria – **www.otoiser.org** – **www.antennas.gr**

Language – We declare the origins of the Journal by using English, German and French, as well as, a Hellenic vignette, in the cover page. However, since we recognize the dominance of USA English in technical literature, we adopted it as the Journal's language, although it is not our native language.

Focus – We consider Radio-FUNK, which still creates a vivid impression of the untouchable, and its Technology-TECHNIK, from an Advanced-PLUS point of view. That is, we dynamically focus at any scientific-engineering discipline producing FUNKTECHNIKPLUS Théorie, Expérimentation, Métrologie, Logiciel, ou Applications.

Scope – We emphasize this scope broadness by extending the title of the Journal with a Doppelkreuz-Zeichen #, which we use as a placeholder for the disciplines of Editorial Board:

Electrical – # Electronics – # Computer – # Telecommunications – Engineering # Computer Science # Applied Mathematics, etc.

Frequency – We regularly publish 3 issues per year on January, May, and September as well as an issue every 3 papers.

Editions – We follow the arXiv.org system, that is the 1st edition date of every issue is on the cover page and any update date is on the odd pages with its version on all pages.

Format – We use the uncommon for Journals A5 paper size and the much readable Liberation Mono fixed-space font, with hyphenation, justification, and unfixed word spacing, to display 2 pages side-by-side on widescreen monitors with WYSIWYG printout. We can consider only papers in ODF odt or MS doc format written in LibreOffice or MS Office with MathType. We use PDFCreator and PDF-Xchange to produce pdf and export to images for printing on demand and electronic publishing.

License – We use the free Open Journal System OJS from the PKP Public Knowledge Project for internet publication

Copyright – Creative Commons Attribution 3 Unported CC-BY 3

Please download the latest *About* edition from
about.ftpj.otoiser.org

Editorial Board

Electrical Engineering

High Voltage Engineering # Insulating Materials

Professor Michael Danikas

EECE, Democritus University of Thrace, mdanikas@ee.duth.gr

Electrical Machines and Drives # Renewable Energies

Electric Vehicles

Assistant Professor Athanasios Karlis

EECE, Democritus University of Thrace, akarlis@ee.duth.gr

Computer Engineering # Software Engineering

Cyber Security

Associate Professor Vasileios Katos

EECE, Democritus University of Thrace, vkatos@ee.duth.gr

Internet Engineering # Computer Science

Simulation # Applied Education # Learning Management Systems

Lecturer Sotirios Kontogiannis

BA, TE Institute of Western Macedonia, skontog@gmail.com

Applied Mathematics # Applied Functional & Numerical Analysis

Applied Electromagnetics # Control Theory

Dr. Nikolaos Berketis, Athens, Greece

BS-Math, MSc-Appl.Math, PhD-Appl.Math, nberketis@gmail.com

Telecommunications Engineering # Applied Electromagnetics

Antennas # RF & Microwave Metrology # Software Applications

Simulation # Virtual Reality # Amateur Radio # FLOSS

Applied Education # Applied Physics # Electronics Engineering

Dr. Nikolitsa Yannopoulou, Scheiblingkirchen, Austria

Diploma Eng-EE, MEng-EECE, PhD-EECE, yin@arg-at.eu

Assistant Professor Petros Zimourtopoulos

EECE, Democritus University of Thrace, pez@ee.duth.gr

Technical Support

Konstantinos Kondylis, Doha, Qatar

Diploma Eng-EECE, MEng-EECE, k8k@arg-at.eu

Christos Koutsos, Bratislava, Slovakia

Diploma Eng-EECE, MEng-EECE, cak@arg-at.eu

Information for Peers Guiding Principles

This is a small, but independent, low profile Journal, in which we are all – Authors – Reviewers – Readers – Editors – free at last to be Peers in Knowledge, without suffering from either:

- Journal roles or positions,
- Professional, amateur, or academic statuses, or
- Established impact factorizations,

but with the following Guiding Principles:

Authors – We do know what work means; and we do respect the research work of the scientist – engineer; and we do want to highlight this work; and we do decided to found this Journal; and we do publish this work openly; and furthermore, we do care for the work of the technical author, especially the beginner one, whom we do support strongly as follows:

- 1 We encourage the author to submit his own paper written just in Basic English plus Technical Terminology.
- 2 We encourage the author even to select a pen name, which may drop it at any time to reveal his identity.
- 3 We encourage the author to submit an accepted for publication paper, which he was forced to decline that publication because it would be based on a review with unacceptable evaluation or comments.
- 4 We encourage the author to resubmit a non accepted for publication paper that was rejected after a poor, inadequate, unreasonable, irresponsible, incompetent, or ticking only, review.
- 5 We encourage the author to submit a paper that he already self-archived on some open repository, such as arXiv.org.
- 6 We encourage the author to self-archive all of the preprint and postprint versions of his paper.
- 7 We provide the author with a decent, express review process of up to just 4 weeks, by at least 2 peers, never have been co-authors with him.
- 8 We provide the author with a selection of review process between: a traditional, anonymous, peer review decision, and an immediate online pre-publication of his paper followed by an open discussion with at least 2 reviewers.

About

- 9 We immediately accept for publication a research paper directly resulting from a Project Report, Diploma-, Master-, or PhD-thesis, which the author already has successfully defended before a committee of experts and he can mention 2 members of it, who reviewed and approved his work.
- 10 We immediately publish online a paper, as soon as, it is accepted for publication in the Journal.
- 11 We quickly print-on-demand an issue every 3 papers, in excess of the 3 issues we regularly publish 3 times a year.
- 12 We do not demand from the author to transfer his own copyright to us.
- 13 Nevertheless, we publish only an original research work paper and only if the author does assure us that he owns the copyright of his own paper and submit this paper or a revised version of it to the Journal for publication or even for republication under the Creative Commons–Attribution 3.0 Unported License, CC-BY 3.

Reviewers – Any peer may voluntarily become a reviewer of the Journal in his expertise for as long as he wishes. Each author of the Journal has to support the peer-to-peer review process by reviewing one paper, written by non co-author(s) of him, for every one of his papers published in the Journal.

Readers – Any reader is a potential reviewer. We welcome online comments and post-reviews by the readers.

Editors – Any editor holds a PhD degree, to objectively prove that he really has the working experience of passing through the established publishing system. An editor pre-reviews a paper in order to check its compliance to the Guiding Principles and to select the appropriate reviewers of the Journal. We can only accept for consideration papers in the expertise areas currently shown in the Editorial Board page. However, since we are willing to amplify and extend the Scope of the Journal, we welcome the volunteer expert, in any subject included into it, who wants to join the Board, if he unreservedly accepts our Guiding Principles.

Antennas Research Group – Non-Profit 12(3) * Union of Persons

* The Constitution of Greece, Article: 12(3) 2008:

www.hellenicparliament.gr/en/Vouli-ton-Ellinon/To-Politevma

* The Hellenic Supreme Court of Civil and Penal Law:

www.areiospagos.gr/en/ – Court Rulings:Civil|A1|511|2008

Submissions

sub@ftpj.otoiser.org

Electronic Publishing

www.ftpj.otoiser.org

Printing-on-Demand

pod@ftpj.otoiser.org

Directly:

Georgios Tontrias, msn.expresscopy.xan@hotmail.com

ExpressCopy, V.Sofias 8, 671 00, Xanthi, Greece

More – Detailed information will be available soon at:

www.ftpj.otoiser.org/gp

Direct and Related Far-Field Inverse Scattering Problems for Spherical Electromagnetic Waves in Chiral Media

N.M. Berketis *

Independent Researcher, Athens, Greece

Abstract

This paper studies the direct and inverse scattering problem when the incident electromagnetic field is a time harmonic point - generated wave in a chiral media and the scatterer is a perfectly conducting sphere. The exact Green's function and the electric far-field patterns of the scattering problem are constructed. For a small sphere, a closed-form approximation of the scattered wave field at the source of the incident spherical wave is obtained. Also treats the same inverse problem using far-field results via the leading order term in the low-frequency asymptotic expansion of the scattering cross-section.

Introduction

In a homogeneous isotropic chiral media the electromagnetic fields are composed of left - circularly polarized (LCP) and right - circularly polarized (RCP) components, which have different wave numbers and independent directions of propagation.

The LCP and RCP components are assumed to be spherical Beltrami fields since in practice such wave fields are more readily realized.

In this work, the author has studied the electromagnetic waves in chiral media produced by a point source in the vicinity of the scat-

terer. In particular, in [1], [2], reciprocity, optical and general scattering theorems for stimulation of point-source asymmetric media have been demonstrated. This paper studies the inverse problem of far field [2]. Specifically, we measure the scattering cross-section for a five-point source area.

In the second Section, considering Bohren decomposition into suitable Beltrami fields, we formulate the direct scattering problem of a spherical electromagnetic wave by a perfectly conducting obstacle. This problem is well posed, the existence and

uniqueness has been proved in [1], [3].

In the third Section, after expanding the incident field in terms of spherical wave functions, we obtain the exact solution of the scattering problem as well as an expansion for the electric far-field pattern [2].

Finally in the fourth Section, we consider either LCP or RCP incidence and we obtain an approximation of the scattering cross-section. For the far-field experiments, we measure the scattering cross-section for various point source locations [2].

Statement of the problem

Our goal is to study the direct and inverse scattering problems when the incident electromagnetic field is a time harmonic point - generated wave in a chiral medium and the scatterer is a perfectly conducting sphere of radius a centered at the origin. The exterior space ($r = |\mathbf{r}| > a$) is an infinite homogeneous isotropic chiral medium with chirality measure β , electric permittivity ϵ and magnetic permeability μ .

We consider a time harmonic spherical electromagnetic wave due to a point source at P_0 with position

vector \mathbf{r}_0 with respect to an origin O in the vicinity of the scatterer. In order to define spherical electromagnetic fields $\mathbf{E}_{\mathbf{r}_0}$, $\mathbf{H}_{\mathbf{r}_0}$, we make use of the Bohren decomposition into Beltrami fields $\mathbf{Q}_{L,\mathbf{r}_0}$ and $\mathbf{Q}_{R,\mathbf{r}_0}$, as follows

$$\begin{aligned} \mathbf{E}_{\mathbf{r}_0} &= \mathbf{Q}_{L,\mathbf{r}_0} + \mathbf{Q}_{R,\mathbf{r}_0} \\ \mathbf{H}_{\mathbf{r}_0} &= \frac{1}{i\eta} (\mathbf{Q}_{L,\mathbf{r}_0} - \mathbf{Q}_{R,\mathbf{r}_0}) \end{aligned} \quad (1)$$

where $\eta = (\mu/\epsilon)^{1/2}$ is the intrinsic impedance of the chiral medium. The Beltrami fields satisfy the equations [4], [5],

$$\begin{aligned} \nabla \times \mathbf{Q}_{L,\mathbf{r}_0} &= \gamma_L \mathbf{Q}_{L,\mathbf{r}_0} \\ \nabla \times \mathbf{Q}_{R,\mathbf{r}_0} &= -\gamma_R \mathbf{Q}_{R,\mathbf{r}_0} \end{aligned} \quad (2)$$

where γ_L and γ_R are wave numbers given by,

$$\gamma_L = \frac{k}{1 - k\beta}, \quad \gamma_R = \frac{k}{1 + k\beta} \quad (3)$$

with $k = \omega(\epsilon\mu)^{1/2}$, ω being the angular frequency. The indices L and R denote the LCP and RCP fields respectively. The spherical incident Beltrami fields with suitable normalization have the form [1], [2],

$$\begin{aligned}
 \mathbf{Q}_{L,r_0}^{inc}(\mathbf{r} | \hat{\mathbf{p}}_L) &= \frac{1}{2} \left(\tilde{\mathbf{I}} + \frac{1}{Y_L^2} \nabla \nabla + \frac{1}{Y_L} \nabla \times \tilde{\mathbf{I}} \right) \left(\frac{h_0(Y_L |\mathbf{r} - \mathbf{r}_0|)}{h_0(Y_L r_0)} \right) \cdot \hat{\mathbf{p}}_L = \\
 &= \frac{2\pi r_0 e^{-iY_L r_0}}{Y_L} [Y_L \tilde{\mathbf{G}}_{fs}(\mathbf{r}, \mathbf{r}_0) + \nabla \times \tilde{\mathbf{G}}_{fs}(\mathbf{r}, \mathbf{r}_0)] \cdot \hat{\mathbf{p}}_L
 \end{aligned} \tag{4}$$

$$\begin{aligned}
 \mathbf{Q}_{R,r_0}^{inc}(\mathbf{r} | \hat{\mathbf{p}}_R) &= \frac{1}{2} \left(\tilde{\mathbf{I}} + \frac{1}{Y_R^2} \nabla \nabla - \frac{1}{Y_R} \nabla \times \tilde{\mathbf{I}} \right) \left(\frac{h_0(Y_R |\mathbf{r} - \mathbf{r}_0|)}{h_0(Y_R r_0)} \right) \cdot \hat{\mathbf{p}}_R = \\
 &= \frac{2\pi r_0 e^{-iY_R r_0}}{Y_R} [Y_R \tilde{\mathbf{G}}_{fs}(\mathbf{r}, \mathbf{r}_0) - \nabla \times \tilde{\mathbf{G}}_{fs}(\mathbf{r}, \mathbf{r}_0)] \cdot \hat{\mathbf{p}}_R
 \end{aligned} \tag{5}$$

where $h_0(x) = h_0^1(x) = e^{ix}/(ix)$ is the zeroth-order spherical Hankel function of first kind, $\tilde{\mathbf{I}} = \hat{\mathbf{x}}\hat{\mathbf{x}} + \hat{\mathbf{y}}\hat{\mathbf{y}} + \hat{\mathbf{z}}\hat{\mathbf{z}}$ is the identity dyadic, $r_0 = |\mathbf{r}_0|$ and $\tilde{\mathbf{G}}_{fs}(\mathbf{r}, \mathbf{r}_0)$ is the free space dyadic Green function [4]. The constant unit vectors $\hat{\mathbf{p}}_L$ and $\hat{\mathbf{p}}_R$ satisfy the relations

$$\begin{aligned}
 \hat{\mathbf{r}}_\theta \cdot \hat{\mathbf{p}}_L &= \hat{\mathbf{r}}_\theta \cdot \hat{\mathbf{p}}_R = 0 \\
 \hat{\mathbf{r}}_\theta \times \hat{\mathbf{p}}_L &= i\hat{\mathbf{p}}_L \\
 \hat{\mathbf{r}}_\theta \times \hat{\mathbf{p}}_R &= -i\hat{\mathbf{p}}_R
 \end{aligned} \tag{6}$$

We note that when $r_0 \rightarrow \infty$, the incident electric field

$$\begin{aligned}
 \mathbf{E}_{r_0}^{inc}(\mathbf{r} | \hat{\mathbf{p}}_L, \hat{\mathbf{p}}_R) &= \\
 &= \mathbf{Q}_{L,r_0}^{inc}(\mathbf{r} | \hat{\mathbf{p}}_L) + \mathbf{Q}_{R,r_0}^{inc}(\mathbf{r} | \hat{\mathbf{p}}_R)
 \end{aligned} \tag{7}$$

reduces to plane electric wave with direction of propagation $-\hat{\mathbf{r}}_\theta$ and polarizations $\hat{\mathbf{p}}_L, \hat{\mathbf{p}}_R$, since

$$\begin{aligned}
 \lim_{r_0 \rightarrow \infty} \mathbf{Q}_{L,r_0}^{inc}(\mathbf{r} | \hat{\mathbf{p}}_L) &= e^{-iY_L \hat{\mathbf{r}}_\theta \cdot \mathbf{r}} \hat{\mathbf{p}}_L = \\
 &= \mathbf{Q}_L^{inc}(\mathbf{r}; -\hat{\mathbf{r}}_\theta, \hat{\mathbf{p}}_L)
 \end{aligned} \tag{8}$$

$$\begin{aligned}
 \lim_{r_0 \rightarrow \infty} \mathbf{Q}_{R,r_0}^{inc}(\mathbf{r} | \hat{\mathbf{p}}_R) &= e^{-iY_R \hat{\mathbf{r}}_\theta \cdot \mathbf{r}} \hat{\mathbf{p}}_R = \\
 &= \mathbf{Q}_R^{inc}(\mathbf{r}; -\hat{\mathbf{r}}_\theta, \hat{\mathbf{p}}_R)
 \end{aligned} \tag{9}$$

We consider $\mathbf{E}_{r_0}^{inc}$ is incident upon a perfectly conducting sphere of radius a . Then, we want to calculate the scattered electric field $\mathbf{E}_{r_0}^{sc}$, which is the unique solution of the following exterior boundary value problem

$$\nabla \times \nabla \times \mathbf{E}_{r_0}^{sc}(\mathbf{r}) - 2\gamma^2 \beta \nabla \times \mathbf{E}_{r_0}^{sc}(\mathbf{r}) - \gamma^2 \mathbf{E}_{r_0}^{sc}(\mathbf{r}) = \mathbf{0}, \quad r > a \quad (10)$$

$$\hat{\mathbf{n}} \times \mathbf{E}_{r_0}^{sc}(\mathbf{r}) = -\hat{\mathbf{n}} \times \mathbf{E}_{r_0}^{inc}(\mathbf{r}), \quad r = a \quad (11)$$

The Silver-Müller radiation condition is modified as follows

$$\hat{\mathbf{r}} \times \nabla \times \mathbf{E}_{r_0}^{sc}(\mathbf{r}) - \beta \gamma^2 \hat{\mathbf{r}} \times \mathbf{E}_{r_0}^{sc}(\mathbf{r}) + \frac{i\gamma^2}{k} \mathbf{E}_{r_0}^{sc}(\mathbf{r}) = o\left(\frac{1}{r}\right), \quad r \rightarrow \infty \quad (12)$$

uniformly in all directions $\hat{\mathbf{r}} \in S^2$, where S^2 is the unit sphere in \mathbb{R}^3 , $\hat{\mathbf{n}}$ is the outward normal unit vector on the scatterer and $\gamma^2 = \gamma_L \gamma_R$. The scattered electric field will be depended on the polarizations $\hat{\mathbf{p}}_L$, $\hat{\mathbf{p}}_R$ and will have the decomposition

$$\mathbf{E}_{r_0}^{sc}(\mathbf{r} | \hat{\mathbf{p}}_L, \hat{\mathbf{p}}_R) = \mathbf{Q}_{L,r_0}^{sc}(\mathbf{r} | \hat{\mathbf{p}}_L, \hat{\mathbf{p}}_R) + \mathbf{Q}_{R,r_0}^{sc}(\mathbf{r} | \hat{\mathbf{p}}_L, \hat{\mathbf{p}}_R) \quad (13)$$

where $\mathbf{Q}_{L,r_0}^{sc}(\mathbf{r} | \hat{\mathbf{p}}_L, \hat{\mathbf{p}}_R)$ and

$\mathbf{Q}_{R,r_0}^{sc}(\mathbf{r} | \hat{\mathbf{p}}_L, \hat{\mathbf{p}}_R)$ are the corresponding scattered Beltrami fields which have the following behavior, when $r \rightarrow \infty$

$$\mathbf{Q}_{L,r_0}^{sc}(\mathbf{r} | \hat{\mathbf{p}}_L, \hat{\mathbf{p}}_R) = h_0(\gamma_L r) \cdot \mathbf{g}_{L,r_0}(\hat{\mathbf{r}} | \hat{\mathbf{p}}_L, \hat{\mathbf{p}}_R) + o\left(\frac{1}{r^2}\right) \quad (14)$$

$$\mathbf{Q}_{R,r_0}^{sc}(\mathbf{r} | \hat{\mathbf{p}}_L, \hat{\mathbf{p}}_R) = h_0(\gamma_R r) \cdot \mathbf{g}_{R,r_0}(\hat{\mathbf{r}} | \hat{\mathbf{p}}_L, \hat{\mathbf{p}}_R) + o\left(\frac{1}{r^2}\right) \quad (15)$$

The functions \mathbf{g}_{L,r_0} and \mathbf{g}_{R,r_0} are the LCP and RCP far-field patterns respectively [4], [6].

If either a LCP or a RCP spherical electric wave $\mathbf{E}_{r_0}^{inc}(\mathbf{r} | \hat{\mathbf{p}}_A)$, $A = L, R$, is incident upon the scatterer, then the scattering cross-section, is given by [6],

$$\sigma_{A,r_0}^{sc} = \int_{S^2} \left[\frac{1}{\gamma_L^2} \left| \mathbf{g}_{L,r_0}(\hat{\mathbf{r}} | \hat{\mathbf{p}}_A) \right|^2 + \frac{1}{\gamma_R^2} \left| \mathbf{g}_{R,r_0}(\hat{\mathbf{r}} | \hat{\mathbf{p}}_A) \right|^2 \right] ds(\hat{\mathbf{r}}) \quad (16)$$

Exact Green's function

We take spherical coordinates (r, θ, φ) where $\theta \in [0, \pi]$ and $\varphi \in [0, 2\pi)$, with the origin at the center of the spherical scatterer, so that the point source is at $r = r_0$, $\theta = 0$.

Thus, $\mathbf{r}_0 = r_0 \hat{\mathbf{z}}$, $\hat{\mathbf{p}}_L = \frac{1}{\sqrt{2}}(\hat{\mathbf{x}} - i\hat{\mathbf{y}})$

and $\hat{\mathbf{p}}_R = \frac{1}{\sqrt{2}}(\hat{\mathbf{x}} + i\hat{\mathbf{y}})$, where $\hat{\mathbf{x}}$, $\hat{\mathbf{y}}$ and $\hat{\mathbf{z}}$ are unit vectors in

the x, ψ and z directions, respectively. Using spherical vector wave functions, [4], [5], [7], and taking into account (4), and (5), we obtain [2],

$$\mathbf{Q}_{L,r_0}^{inc}(\mathbf{r} | \hat{\mathbf{p}}_L) = \sum_{n=1}^{\infty} B_n^L \{ \mathbf{L}_{o1n}^{(1)}(\mathbf{y}_L \mathbf{r}) + \mathbf{iL}_{e1n}^{(1)}(\mathbf{y}_L \mathbf{r}) \} \quad (17)$$

or

$$\mathbf{Q}_{R,r_0}^{inc}(\mathbf{r} | \hat{\mathbf{p}}_R) = \sum_{n=1}^{\infty} B_n^R \{ \mathbf{R}_{o1n}^{(1)}(\mathbf{y}_R \mathbf{r}) - \mathbf{iR}_{e1n}^{(1)}(\mathbf{y}_R \mathbf{r}) \} \quad (18)$$

where, for $r < r_0$

$$B_n^A = \frac{1}{2\sqrt{2}h_0(\mathbf{y}_A r_0)} \frac{2n+1}{n(n+1)} H_n(\mathbf{y}_A r_0) \quad (19)$$

$$H_n(\mathbf{y}_A r_0) = h_n(\mathbf{y}_A r_0) - \mathbf{i}\tilde{h}_n(\mathbf{y}_A r_0)$$

with $A = L, R$. The h_n is a spherical Hankel function of first kind of order n ,

$$\tilde{h}(x) = x^{-1}h_n(x) + h'_n(x),$$

$\mathbf{L}_{s1n}^{(\rho)}$ and $\mathbf{R}_{s1n}^{(\rho)}$, with $s = e, o$ (even or odd) are the spherical functions [4], [5],

$$\mathbf{L}_{s1n}^{(\rho)}(\mathbf{y}_L \mathbf{r}) = \mathbf{M}_{s1n}^{(\rho)}(\mathbf{y}_L \mathbf{r}) + \mathbf{N}_{s1n}^{(\rho)}(\mathbf{y}_L \mathbf{r}) \quad (20)$$

$$\mathbf{R}_{s1n}^{(\rho)}(\mathbf{y}_R \mathbf{r}) = \mathbf{M}_{s1n}^{(\rho)}(\mathbf{y}_R \mathbf{r}) - \mathbf{N}_{s1n}^{(\rho)}(\mathbf{y}_R \mathbf{r})$$

where $\rho = 1, 3$, the $\mathbf{M}_{s1n}^{(\rho)}$ and $\mathbf{N}_{s1n}^{(\rho)}$ are known spherical vector function [7]. The scattered electric field that comes from a LCP incident field or a RCP incident field has a similar expansion to (17) or to (18)

$$\begin{aligned} \mathbf{E}_{r_0}^{SC}(\mathbf{r} | \hat{\mathbf{p}}_L) &= \mathbf{Q}_{L,r_0}^{SC}(\mathbf{r} | \hat{\mathbf{p}}_L) + \mathbf{Q}_{R,r_0}^{SC}(\mathbf{r} | \hat{\mathbf{p}}_L) = \\ &= \sum_{n=1}^{\infty} B_n^L a_n^L \{ \mathbf{L}_{o1n}^{(3)}(\mathbf{y}_L \mathbf{r}) + \mathbf{iL}_{e1n}^{(3)}(\mathbf{y}_L \mathbf{r}) \} + \sum_{n=1}^{\infty} B_n^L a_n^R \{ \mathbf{R}_{o1n}^{(3)}(\mathbf{y}_R \mathbf{r}) + \mathbf{iR}_{e1n}^{(3)}(\mathbf{y}_R \mathbf{r}) \} \end{aligned} \quad (21)$$

or

$$\begin{aligned} \mathbf{E}_{r_0}^{SC}(\mathbf{r} | \hat{\mathbf{p}}_R) &= \mathbf{Q}_{L,r_0}^{SC}(\mathbf{r} | \hat{\mathbf{p}}_R) + \mathbf{Q}_{R,r_0}^{SC}(\mathbf{r} | \hat{\mathbf{p}}_R) + \\ &= \sum_{n=1}^{\infty} B_n^R b_n^L \{ \mathbf{L}_{o1n}^{(3)}(\mathbf{y}_L \mathbf{r}) - \mathbf{iL}_{e1n}^{(3)}(\mathbf{y}_L \mathbf{r}) \} + \sum_{n=1}^{\infty} B_n^R b_n^R \{ \mathbf{R}_{o1n}^{(3)}(\mathbf{y}_R \mathbf{r}) - \mathbf{iR}_{e1n}^{(3)}(\mathbf{y}_R \mathbf{r}) \} \end{aligned} \quad (22)$$

Using the boundary condition (11) on $r = a$, we obtain [2],

$$a_n^L = -\frac{j_n(\gamma_L a) \tilde{h}_n(\gamma_R a) + \tilde{j}_n(\gamma_L a) h_n(\gamma_R a)}{h_n(\gamma_L a) \tilde{h}_n(\gamma_R a) + \tilde{h}_n(\gamma_L a) h_n(\gamma_R a)} \quad (23)$$

and

$$a_n^R = -\frac{j_n(\gamma_L a) \tilde{h}_n(\gamma_L a) - \tilde{j}_n(\gamma_L a) h_n(\gamma_L a)}{h_n(\gamma_L a) \tilde{h}_n(\gamma_R a) + \tilde{h}_n(\gamma_L a) h_n(\gamma_R a)} \quad (24)$$

or

$$b_n^L = -\frac{j_n(\gamma_R a) \tilde{h}_n(\gamma_R a) - \tilde{j}_n(\gamma_R a) h_n(\gamma_R a)}{h_n(\gamma_L a) \tilde{h}_n(\gamma_R a) + \tilde{h}_n(\gamma_L a) h_n(\gamma_R a)} \quad (25)$$

and

$$b_n^R = -\frac{j_n(\gamma_R a) \tilde{h}_n(\gamma_L a) + \tilde{j}_n(\gamma_R a) h_n(\gamma_L a)}{h_n(\gamma_L a) \tilde{h}_n(\gamma_R a) + \tilde{h}_n(\gamma_L a) h_n(\gamma_R a)} \quad (26)$$

Using the asymptotic forms [4], [7],

$$\mathbf{L}_{s1n}^{(3)}(\gamma_L \mathbf{r}) \sim \sqrt{n(n+1)}(-i)^n h_\theta(\gamma_L r) \mathbf{f}_{s1n}^L(\hat{\mathbf{r}}) \quad (27)$$

$$\mathbf{R}_{s1n}^{(3)}(\gamma_R \mathbf{r}) \sim \sqrt{n(n+1)}(-i)^n h_\theta(\gamma_R r) \mathbf{f}_{s1n}^R(\hat{\mathbf{r}}) \quad (28)$$

where let us introduce LCP Beltrami angular $\mathbf{f}_{s1n}^L(\hat{\mathbf{r}})$, and RCP Beltrami angular $\mathbf{f}_{s1n}^R(\hat{\mathbf{r}})$ [4], satisfy by relations,

$$\mathbf{f}_{s1n}^L(\hat{\mathbf{r}}) = \mathbf{C}_{s1n}(\hat{\mathbf{r}}) + i\mathbf{B}_{s1n}(\hat{\mathbf{r}}), \quad \mathbf{f}_{s1n}^R(\hat{\mathbf{r}}) = \mathbf{C}_{s1n}(\hat{\mathbf{r}}) - i\mathbf{B}_{s1n}(\hat{\mathbf{r}}) \quad (29)$$

we calculate the electric far-field patterns [2],

$$\mathbf{g}_{A,r_\theta}^{sc}(\hat{\mathbf{r}} | \hat{\mathbf{p}}_L) = \sum_{n=1}^{\infty} \frac{(2n+1)(-i)^{n-1}}{2\sqrt{2n(n+1)}} \frac{H_n(\gamma_L r_\theta)}{h_\theta(\gamma_L r_\theta)} a_n^A \{ \mathbf{f}_{e1n}^A(\hat{\mathbf{r}}) - i\mathbf{f}_{o1n}^A(\hat{\mathbf{r}}) \} \quad (30)$$

or

$$\mathbf{g}_{A,r_\theta}^{sc}(\hat{\mathbf{r}} | \hat{\mathbf{p}}_R) = \sum_{n=1}^{\infty} \frac{(2n+1)(-i)^{n-1}}{2\sqrt{2n(n+1)}} \frac{H_n(\gamma_R r_\theta)}{h_\theta(\gamma_R r_\theta)} b_n^A \{ -\mathbf{f}_{e1n}^A(\hat{\mathbf{r}}) - i\mathbf{f}_{o1n}^A(\hat{\mathbf{r}}) \} \quad (31)$$

A far-field inverse problem

So far, all of our formulas are exact. In the asymptotic results to follow, there are three parameters $y_A a$, with $A=L, R$ and $\tau = a/r_0$. We note that the geometrical parameter τ must satisfy $0 < \tau < 1$ because the point source is outside of the sphere.

We assume that $|y_A a| \ll 1$, as well; that is we make the so-called low-frequency assumption. From (23), (24), (26), (27), we obtain [2],

$$\begin{aligned} a_n^L &\sim \frac{1 + \beta k}{2i\zeta_n^2(2n+1)} (y_L a)^{2n+1} \\ a_n^R &\sim -\frac{i}{2n\zeta_n^2} \frac{(1 - \beta k)^{n+2}}{(1 + \beta k)^{n+1}} (y_L a)^{2n+1} \\ y_L a &\rightarrow 0 \end{aligned} \quad (32)$$

or

$$\begin{aligned} b_n^L &\sim -\frac{i}{2n\zeta_n^2} \frac{(1 + \beta k)^{n+2}}{(1 - \beta k)^{n+1}} (y_R a)^{2n+1} \\ b_n^R &\sim -\frac{i(1 - \beta k)}{2\zeta_n^2(2n+1)} (y_R a)^{2n+1} \\ y_R a &\rightarrow 0 \end{aligned} \quad (33)$$

where

$$\zeta_n = 1 \cdot 3 \cdot 5 \cdots (2n-1) = (2n)! / (2^n n!).$$

In particular,

$$\begin{cases} a_1^L = -i \frac{1 + \beta k}{6} (y_L a)^3 + o((y_L a)^5) \\ a_2^L = -i \frac{1 + \beta k}{90} (y_L a)^5 + o((y_L a)^7) \end{cases} \\ y_L a \rightarrow 0 \quad (34)$$

$$\begin{cases} a_1^R = -\frac{i(1 - \beta k)^3}{2(1 + \beta k)^2} (y_L a)^3 + o((y_L a)^5) \\ a_2^R = -\frac{i(1 - \beta k)^4}{36(1 + \beta k)^3} (y_L a)^5 + o((y_L a)^7) \end{cases} \\ y_L a \rightarrow 0 \quad (35)$$

or

$$\begin{cases} b_1^L = -\frac{i(1 + \beta k)^3}{2(1 - \beta k)^2} (y_R a)^3 + o((y_L a)^5) \\ b_2^L = -\frac{i(1 + \beta k)^4}{36(1 - \beta k)^3} (y_R a)^5 + o((y_L a)^7) \end{cases} \\ y_R a \rightarrow 0 \quad (36)$$

$$\begin{cases} b_1^R = -\frac{i(1 - \beta k)}{6} (y_R a)^3 + o((y_R a)^5) \\ b_2^R = -\frac{i(1 - \beta k)}{90} (y_R a)^5 + o((y_R a)^7) \end{cases} \\ y_R a \rightarrow 0 \quad (37)$$

In order to calculate \mathbf{g}_{A, r_0}^{SC} with an error of $O((y_A a)^4)$ we only need the following [4]

$$\mathbf{C}_{o11}(\hat{\mathbf{r}}) = \frac{1}{\sqrt{2}} (\cos\varphi \hat{\boldsymbol{\theta}} - \cos\theta \sin\varphi \hat{\boldsymbol{\phi}}) \quad \mathbf{C}_{o12}(\hat{\mathbf{r}}) = (3/2)^{1/2} \cdot (\cos\theta \cos\varphi \hat{\boldsymbol{\theta}} - \cos 2\theta \sin\varphi \hat{\boldsymbol{\phi}}) \quad (40)$$

$$\mathbf{B}_{o11}(\hat{\mathbf{r}}) = -\frac{1}{\sqrt{2}} (\cos\theta \sin\varphi \hat{\boldsymbol{\theta}} + \cos\varphi \hat{\boldsymbol{\phi}}) \quad \mathbf{B}_{e12}(\hat{\mathbf{r}}) = (3/2)^{1/2} \cdot (\cos 2\theta \cos\varphi \hat{\boldsymbol{\theta}} - \cos\theta \sin\varphi \hat{\boldsymbol{\phi}}) \quad (41)$$

$$\mathbf{B}_{e11}(\hat{\mathbf{r}}) = \frac{1}{\sqrt{2}} (\cos\theta \sin\varphi \hat{\boldsymbol{\theta}} - \sin\varphi \hat{\boldsymbol{\phi}}) \quad \mathbf{B}_{o12}(\hat{\mathbf{r}}) = (3/2)^{1/2} \cdot (\cos 2\theta \sin\varphi \hat{\boldsymbol{\theta}} + \cos\theta \cos\varphi \hat{\boldsymbol{\phi}}) \quad (42)$$

$$\mathbf{C}_{e11}(\hat{\mathbf{r}}) = \frac{1}{\sqrt{2}} (-\sin\varphi \hat{\boldsymbol{\theta}} - \cos\theta \cos\varphi \hat{\boldsymbol{\phi}}) \quad \hat{\mathbf{C}}_{e12}(\hat{\mathbf{r}}) = (3/2)^{1/2} \cdot (-\cos\theta \sin\varphi \hat{\boldsymbol{\theta}} - \cos 2\theta \cos\varphi \hat{\boldsymbol{\phi}}) \quad (43)$$

So from (30) and (31), we finally obtain [2],

$$\begin{aligned} \mathbf{g}_{A, \mathbf{r}_0}^{\text{sc}}(\hat{\mathbf{r}} | \hat{\mathbf{p}}_A) &= \varpi_A \frac{(1 - \varpi_A \beta k)}{8} [- (\gamma_A a) \tau^2 [\mathbf{f}_{e11}^A(\hat{\mathbf{r}}) + \varpi_A \mathbf{i} \mathbf{f}_{o11}^A(\hat{\mathbf{r}})] + \\ &+ (\gamma_A a)^2 \{ 2\mathbf{i} \tau [\mathbf{f}_{e11}^A(\hat{\mathbf{r}}) + \varpi_A \mathbf{i} \mathbf{f}_{o11}^A(\hat{\mathbf{r}})] + \frac{\mathbf{i}}{\sqrt{3}} \tau^3 [\mathbf{f}_{e12}^A(\hat{\mathbf{r}}) + \varpi_A \mathbf{i} \mathbf{f}_{o12}^A(\hat{\mathbf{r}})] \} + \\ &+ (\gamma_A a)^3 \{ 2[\mathbf{f}_{e11}^A(\hat{\mathbf{r}}) + \varpi_A \mathbf{i} \mathbf{f}_{o11}^A(\hat{\mathbf{r}})] + \frac{4}{3\sqrt{3}} \tau^2 [\mathbf{f}_{e12}^A(\hat{\mathbf{r}}) + \varpi_A \mathbf{i} \mathbf{f}_{o12}^A(\hat{\mathbf{r}})] \} + \\ &+ O((\gamma_A a)^4) \end{aligned} \quad (44)$$

and

$$\begin{aligned} \mathbf{g}_{A, \mathbf{r}_0}^{\text{sc}}(\hat{\mathbf{r}} | \hat{\mathbf{p}}_{A^c}) &= \varpi_A \frac{3(1 - \varpi_A \beta k)^2}{8(1 + \varpi_A \beta k)} (\gamma_A a) \tau^2 [\mathbf{f}_{e11}^A(\hat{\mathbf{r}}) - \varpi_A \mathbf{i} \mathbf{f}_{o11}^A(\hat{\mathbf{r}})] + \\ &+ (\gamma_A a)^2 \{ -\varpi_A \frac{3\mathbf{i}(1 - \varpi_A \beta k)}{4} \tau [\mathbf{f}_{e11}^A(\hat{\mathbf{r}}) - \varpi_A \mathbf{i} \mathbf{f}_{o11}^A(\hat{\mathbf{r}})] - \\ &- \varpi_A \frac{5\mathbf{i}}{16\sqrt{3}} \frac{(1 - \varpi_A \beta k)^2}{1 + \varpi_A \beta k} \tau^3 [\mathbf{f}_{e12}^A(\hat{\mathbf{r}}) - \varpi_A \mathbf{i} \mathbf{f}_{o12}^A(\hat{\mathbf{r}})] \} + \\ &+ (\gamma_A a)^3 \{ -\varpi_A \frac{3(1 + \varpi_A \beta k)}{4} [\mathbf{f}_{e11}^A(\hat{\mathbf{r}}) - \varpi_A \mathbf{i} \mathbf{f}_{o11}^A(\hat{\mathbf{r}})] - \end{aligned} \quad (45)$$

$$- \varpi_A \frac{5(1 - \varpi_A \beta k)}{12\sqrt{3}} \tau^2 [\mathbf{f}_{e12}^A(\hat{\mathbf{r}}) - \varpi_A \mathbf{i} \mathbf{f}_{012}^A(\hat{\mathbf{r}})] + O((\gamma_A a)^4)$$

where $\varpi_A = \begin{cases} -1, & A = L \\ 1, & A = R \end{cases}$ and if $A = L, R$ at that case $A^c = R, L$.

Now the scattering cross-section, by LCP or RCP spherical Beltrami fields, from (16), is given by the relations [2],

$$\begin{aligned} \sigma_{L, r_0}^{sc} &= \int_{S^2} \left[\frac{1}{\gamma_L^2} |\mathbf{g}_{L, r_0}^{sc}(\hat{\mathbf{r}} | \hat{\mathbf{p}}_L)|^2 + \frac{1}{\gamma_R^2} |\mathbf{g}_{R, r_0}^{sc}(\hat{\mathbf{r}} | \hat{\mathbf{p}}_L)|^2 \right] ds(\hat{\mathbf{r}}) = \\ &= (\pi a^2) \left\{ \frac{(1 + \beta k)^2}{64} \left[\frac{16}{3} \tau^4 + (\gamma_L a)^2 \left(\frac{64}{3} \tau^2 + 16\tau^6 \right) + (\gamma_L a)^4 \left(\frac{64}{3} + \frac{16}{9} \tau^4 \right) \right] + \right. \\ &+ \frac{(1 - \beta k)^4}{(1 + \beta k)^2} \left[\frac{3}{4} \tau^4 + (\gamma_L a)^2 (3\tau^2 + \frac{5(1 - \beta k)^2}{16(1 + \beta k)^2} \tau^6) + \right. \\ &\left. \left. + (\gamma_L a)^4 \left(3 + \frac{5(1 - \beta k)}{9(1 + \beta k)^2} \tau^4 \right) \right] \right\} + O((\gamma_L a)^6), \quad \gamma_L a \rightarrow 0 \end{aligned} \quad (46)$$

or

$$\begin{aligned} \sigma_{R, r_0}^{sc} &= \int_{S^2} \left[\frac{1}{\gamma_L^2} |\mathbf{g}_{L, r_0}^{sc}(\hat{\mathbf{r}} | \hat{\mathbf{p}}_R)|^2 + \frac{1}{\gamma_R^2} |\mathbf{g}_{R, r_0}^{sc}(\hat{\mathbf{r}} | \hat{\mathbf{p}}_R)|^2 \right] ds(\hat{\mathbf{r}}) = \\ &= (\pi a^2) \left\{ \frac{(1 - \beta k)^2}{64} \left[\frac{16}{3} \tau^4 + (\gamma_R a)^2 \left(\frac{64}{3} \tau^2 + 16\tau^6 \right) + (\gamma_R a)^4 \left(\frac{64}{3} + \frac{16}{9} \tau^4 \right) \right] + \right. \\ &+ \frac{(1 + \beta k)^4}{(1 - \beta k)^2} \left[\frac{3}{4} \tau^4 + (\gamma_R a)^2 (3\tau^2 + \frac{5(1 + \beta k)^2}{16(1 - \beta k)^2} \tau^6) + \right. \\ &\left. \left. + (\gamma_R a)^4 \left(3 + \frac{5(1 + \beta k)}{9(1 - \beta k)^2} \tau^4 \right) \right] \right\} + O((\gamma_R a)^6), \quad \gamma_R a \rightarrow 0 \end{aligned} \quad (47)$$

In the special case $r_0 \rightarrow \infty$ ($\tau \rightarrow 0$), by the relations (46), (47) we obtain [2],

$$\sigma = (\pi a^2) \left\{ \frac{(1 + \beta k)^2}{3} + \frac{3(1 - \beta k)^4}{(1 + \beta k)^2} \right\} (\gamma_L a)^4 + O((\gamma_L a)^6), \quad \gamma_L a \rightarrow 0 \quad (48)$$

or

$$\sigma = (\pi a^2) \left\{ \frac{(1 - \beta k)^2}{3} + \frac{3(1 + \beta k)^4}{(1 - \beta k)^2} \right\} (y_R a)^4 + O((y_R a)^6), \quad y_R a \rightarrow 0 \quad (49)$$

likewise in the case $y_L a \rightarrow 0$ and $y_R a \rightarrow 0$, by the relations (46), (47) we obtain [2],

$$\sigma_{A, r_0}^{sc} = \frac{1}{4} f_A(\beta, k) (\pi a^2) (a/r_0)^4 \quad (50)$$

where $A = L, R$, with $f_A(\beta, k) = \frac{(1 - \varpi_A \beta k)^2}{3} + \frac{3(1 + \varpi_A \beta k)^4}{(1 - \varpi_A \beta k)^2}$ (51)

Choose a Cartesian coordinate system $Ox\psi z$, and five point-source locations, namely $(0, 0, 0)$, $(1, 0, 0)$, $(0, 1, 0)$, $(0, 0, 1)$ and $(0, 0, 2l)$, which are at (unknown) distances r_0, r_1, r_2, r_3 and r_4 , respectively from the sphere's center. The parameter l is a chosen fixed length. For each location, measure the leading order term in the low-frequency expansion of the scattering cross-section.

Thus, our five measurements are [2],

$$m_j = \frac{1}{4} f_A(\beta, k) \pi a^2 \left(\frac{a}{r_j}\right)^4 \quad (52)$$

$$j = 0, 1, 2, 3, 4$$

Dimensionless quantities related to m_j are

$$Y_j = \frac{l}{\sqrt{m_j}} = 2 \sqrt{\frac{1}{f_A(\beta, k) \pi}} \frac{l}{a} \left(\frac{r_j}{a}\right)^2 \quad (53)$$

$$j = 0, 1, 2, 3, 4$$

equivalently, we obtain [2],

$$r_j^2 = \frac{1}{2} \sqrt{f_A(\beta, k) \pi} \frac{a^3}{l} Y_j \quad (54)$$

$$j = 0, 1, 2, 3, 4$$

There are six unknowns namely r_0, r_1, r_2, r_3, r_4 and a . Furthermore, r_0, r_3 and r_4 are related using the cosine rule, $r_4^2 + r_0^2 = 2r_3^2 + 2l^2$. So, we can find the six unknowns. The center of the spherical scatterer is obtained from the intersection of the four spheres centers at $(0, 0, 0)$, $(1, 0, 0)$, $(0, 1, 0)$ and $(0, 0, 1)$, with corresponding radius r_0, r_1, r_2, r_3 respectively.

References

- [1] Athanasiadis C., Berketis N., "Scattering relations for point - source excitation in chiral media", *Mathematical Methods in the Applied Sciences*, Vol. 29, 2006, pp. 27-48
- [2] Berketis M. Nikolaos, "Scattering spherical Electro-magnetic waves in chiral media", PhD thesis, University of Athens - Department of Mathematics, December 2007
- [3] Arnaoudov Y, Dassios G, Hadjinicolaou M., "The resistive coated sphere in the presence of a point generated wave field", *Mathematical Methods in the Applied Sciences*, Vol. 22, 1999, pp. 73-90
- [4] Lakhtakia A., "Beltrami Fields in Chiral Media", *World Scientific*, Singapore, 1994, §2-1.3 (pp. 42-44), §2-2.3 (pp. 49-52), §4-1 (p. 130 Chapter 4), §5-1 (p. 164 Chapter 5), §6-1.1 (pp. 214-397), §8-2.1 (pp. 391-397), §9-2.3 (pp. 468- 473).
- [5] Lakhtakia A, Varadan V.K., Varadan V.V., "Time-Harmonic Electromagnetic Fields in Chiral Media", *Lecture Notes in Physics*, Vol. 335, Springer, Berlin, 1989, §3-§4-§7-§11-§12-§13
- [6] Athanasiadis C., "On the far field patterns for electromagnetic scattering by a chiral obstacle in a chiral environment", *Journal of Mathematical Analysis and Applications*, Vol. 309, 2005, pp. 517-533
- [7] Morse P.M, Feshbach H., "Methods of Theoretical Physics, Part II", *Mc Graw-Hill*, 1953, pp. 1864-1866, 1870, 1871, 1887

Preprint Versions

"Direct and inverse scattering problems for spherical
Electromagnetic waves in chiral media"
Christodoulos Athanasiadis and Nikolaos Berketis
"<http://arxiv.org/abs/0812.2169>"

* About the Author

Nikolaos Berketis, was born in Athens, Greece, 1952. Mathematics degree, Aristotle University of Thessaloniki, 1976. MSc in Applied Mathematics-Numerical Functional Analysis, Department of Mathematics, National and Kapodistrian University of Athens (UoA), 2003. Ph.D. in Applied Mathematics, Department of Mathematics, UoA, 2007. Professor of Secondary Education, 1980-2006. High school Principal, 2007-2012. Teacher at the UoA: Department of Informatics and Telecommunications, 2002-2003. Postgraduate program of the Department of Geology and Paleontology, 2003-2004. Research experience: Participation in the following research projects: 1) "The far-field operator in solving inverse scattering problem". Special Research Account 70/4/6412, UoA, 2002. 2) "Scattering of spherical electromagnetic waves by chiral materials". Special Research Account 70/4/6412, UoA, 2004. 3) "Mathematical analysis of wave propagation in chiral electromagnetic and elastic media." Pythagoras II: Reinforcing of University research groups (EPEAEK II), Department of Mathematics, UoA, 2005. Member of the Question Bank department of Evaluation and Training Research Center, Hellenic Mathematical Society (HMS), 2001-2004. Editorial Board experience: Member of the Scientific Committee of Euclid C' journal, Hellenic Mathematical Society (HMS). Member of the Scientific Committee of the project "Digital Training Textbooks for Pan-Hellenic examinations" -for Mathematics, Science and Technology Educational Path, 3rd grade, High School and Mathematics & Elementary Statistics, General Education, 3rd grade, High School- implemented by Computer Technology Institute University of Patra, for the Ministry of Education. Eighteen published peer-reviewed papers, more than 150 references, in peer-reviewed journals, utilizing both Hellenic and international bibliography. Participation in the project: "Change of speed of pulse wave after surgical narrowing of the descending thoracic aorta, "1st prize, Best Project award, 28th Annual Pan-Hellenic Medical Conference in the field of basic research, oral presentation, Athens, May 21-25, 2002. Personal work on the scattering of spherical electromagnetic waves in chiral media is posted at "The Smithsonian/NASA Astrophysics Data System" website. Authoring experience: Scientific research articles and books.
nberketis@gmail.com

This paper is licensed under a Creative Commons Attribution 4.0 International License – <https://creativecommons.org/licenses/by/4.0/>

Experimental Results on the Behavior of Water Droplets on Polymeric Surfaces Under the Influence of Electric Fields: the Case of an Inclined Test Arrangement for PVC, Rubber and Silicone Rubber

M.G. Danikas, P. Ramnalis, R. Sarathi *

Department of Electrical and Computer Engineering,
Democritus University of Thrace, Xanthi, Greece [1, 2]
Department of Electrical Engineering,
IIT Madras, Chennai- 600 036, India [3]

Abstract

This paper investigates the influence of various parameters on the behavior of water droplets on polymeric surfaces under electric fields. An inclined plane test was carried out to understand the droplet behavior in strong electric field. Parameters such as, water droplet conductivity, droplet volume, polymeric surface roughness and droplet positioning with respect to the electrodes were studied. The flashover voltage is affected by all aforementioned parameters. The droplet positioning is in some cases more vital than the droplet volume.

Introduction

Water droplets on a polymeric surface may cause corona under the influence of an electric field and can cause deterioration to insulation surface even in conditions of low pollution level. Water droplets on a polymeric surface increase locally the applied electric field. Local field intensifications lead to partial discharges (PD) and/or localized arcs, which may render possible the dry bands on the polymeric sur-

face. Local arcing will eventually bridge the dry bands and a complete flashover will finally ensue. This mechanism is valid to a greater or lesser extent for both outdoor and indoor insulation, although each of the aforementioned categories have their own particular characteristics, namely that indoor insulation is stressed more and is subjected to a different type of environmental influences than outdoor insulation [1], [2]. A combination

of water droplets and dust-like impurities on the surface of a polymeric surface may lead to a conducting contamination layer, which may cause a reduction of the flashover voltage. The design of high voltage insulators, they can be for indoor or outdoor use, one should take into account not only the pollution level, the insulator material and the appropriate voltage level, but also the influence of water droplets on the flashover voltage. Previous work, carried out in this laboratory, tackled the behavior of water droplets for a wide range of water conductivities ($1.7 \mu\text{S/cm} - 10000 \mu\text{S/cm}$) [3], [4]. In both publications, it was shown that, among the factors influencing the behavior of the water droplets, were the water conductivity, polymer surface roughness, droplet volume and droplet positioning with respect to the electrodes.

In the present work, a study of the aforementioned parameters on the water droplet behavior under the influence of a uniform electric field in the range of $1.7 \mu\text{S/cm} - 2000 \mu\text{S/cm}$ was carried out. All tests were performed with an inclined test arrangement, in order to simulate the behavior of water droplets on the surface

of a real insulator. The angle used with respect to the horizontal was 10° . Such an angle was chosen because of its immediate relevance to industrial insulators.

Force balance at the droplet/polymer surface interface

A modeling of a wet contaminated surface was given in other publications and only a brief outline is provided here [5]. Condensation of droplets on the surface of a high voltage insulator can come about from droplet germs. In Fig. 1, the forces exercised on the droplet are shown in case where no electrical field is applied. Such forces are the surface tension of the liquid (τ_L), the surface tension of the solid (τ_S) and the interfacial tension between liquid and solid (δ_{sl}). When an electric field is applied, the droplet deforms because of an additional force. The tangential electric field on the surface of the insulator creates a force on the surface of the droplet which causes its deformation. The deformation of the droplet affects the field distribution. Local field intensifications may result, which will cause micro-discharges between the droplets. This is the beginning of the chemical deterioration of the insulator surface.

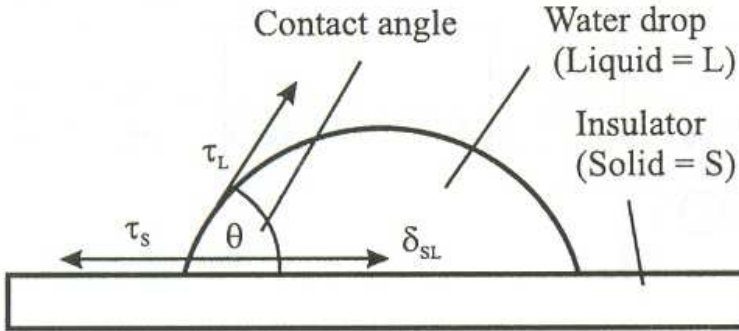


Fig. 1: Force balance at the interface solid/liquid at a water droplet on an insulating Surface (after [5])

Hydrophobicity may locally be lost. The voltage difference across the droplet will be diminished and micro-discharges will follow. Solvable nitrates, which are the result of the electrochemical deterioration, cause a higher conductivity of the water droplets. Dry zones may follow. It is important to bear in mind that not only the influence of the applied electric field on the shape of the droplet is of great significance, but also the influence of the disintegrated droplet on the electric field distribution [5], [6].

Hydrophobic polymeric surfaces are characterized by a low surface conductivity which in turn gives a low discharge activity and a higher flashover voltage. This holds also for polluted environments. Reduced hy-

drophobicity implies a higher risk for flashover of the insulator. Hydrophilic materials, on the other hand, are very sensitive to polluted environments, and are characterized by a significant activity of local discharges [7]. It is well known the classification of the Swedish Transmission Research Institute (STRI) regarding the hydrophobic and hydrophilic surfaces. STRI classifies the various surfaces according to their hydrophobicity from class 1 (most hydrophobic, with only discrete droplets on the surface with contact angle larger than 80°) to class 7 (most hydrophilic, with continuous water films forming on the surface). However, the truth is that no matter if the insulator has some sort of humidity and it is only slightly polluted or

it is heavily polluted, in both cases surface discharges play a most important role, and such discharges may start from water droplets.

Experimental arrangement and preparation of the samples

The aim of this paper is to study the behavior of water droplets under the influence of an electric field. The voltage supplied was from a 20 kV transformer (in practice the transformer may deliver voltages up to 1.2 times of its nominal voltage without loss of the accuracy of the measurement. Consequently, the applied voltages were accurate up to 24 kV). The electrodes used were of copper. A top view as well as

a cross section of an electrode is shown in Fig. 2. The electrodes were half cylindrical in shape. Attention was paid to the smoothness of the electrode surfaces, so that no unnecessary field enhancements could be noticed.

The water droplets were positioned on the polymeric material surface with the aid of a special arrangement consisting of a metallic frame and three laser rules, one of which had two laser indicators. The water droplets were put on the surface with a syringe. Detailed information on the way the droplets were positioned on the polymeric surface is given in [3]. The photograph of the inclined plane test is shown in Fig. 3.

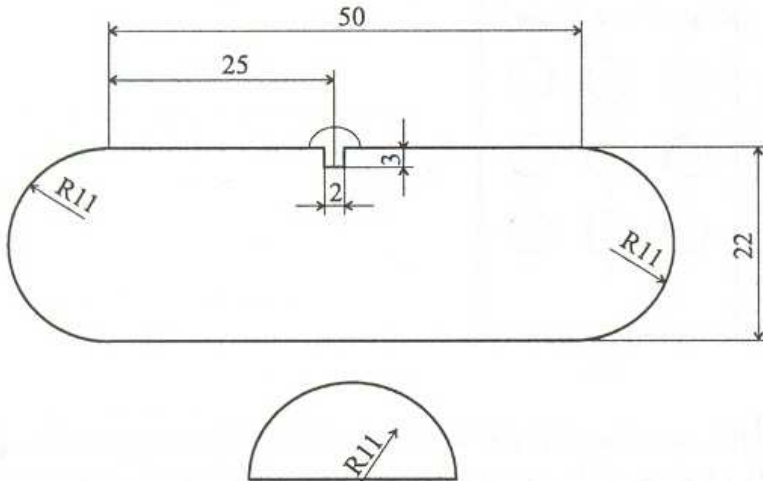


Fig. 2: Top view (above) and cross section (bottom) of the electrodes used (all dimensions in mm)

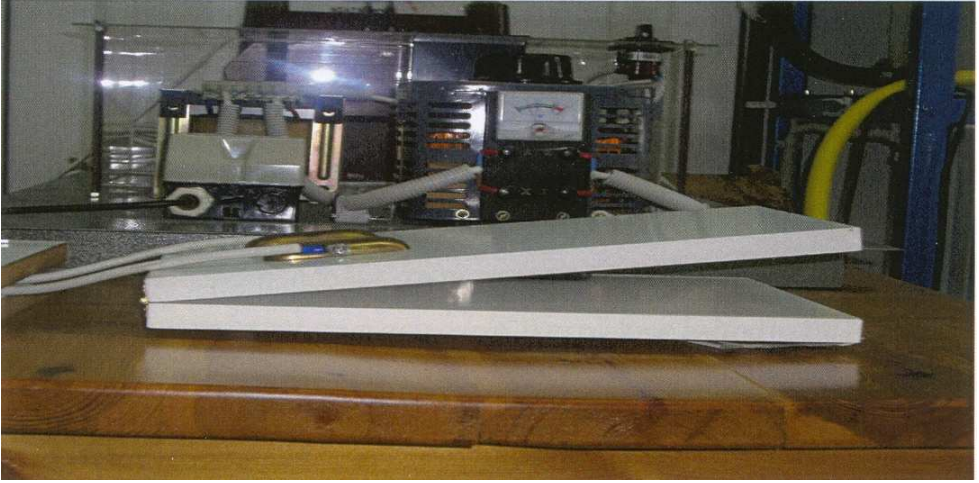


Fig. 3: The inclined Plane test setup (side view)

The polymeric materials used were PVC, rubber and silicone rubber. Surface roughness and resistivity of the material were measured. Surface roughness were measured using perthometer (Type Perthometer M4P). They gave a roughness of $0.25 \mu\text{m}$ for PVC, $0.79 \mu\text{m}$ for silicone rubber and $1.10 \mu\text{m}$ for rubber. Resistivity of the material were performed with a Megger (BM25 type) and they gave a resistivity of $206 \text{ G}\Omega$ for PVC, a resistivity of $3100 \text{ G}\Omega$ silicone rubber and a resistivity of $2660 \text{ G}\Omega$ for rubber. The above values of surface roughness and surface resistivity were not isolated values, but each of them was the mean of three measurements [8], [9].

In the present work, by

mixing known quantity of NaCl in distilled water forming solutions with conductivity in the range $1.7 \mu\text{S}/\text{cm}$ to $2000 \mu\text{S}/\text{cm}$, were used as droplet. The range of conductivity were chosen based on the conductivity of natural rain and its values lie in the range $50 - 150 \mu\text{S}/\text{cm}$, whereas the tests with porcelain and glass insulators are performed with conductivities of $2500 \mu\text{S}/\text{cm}$ [10].

Experimental procedure

The materials used were PVC, silicone rubber and rubber. Various droplet arrangements were studied. These arrangements are given in Fig. 4. Each droplet had a volume of 0.2 ml . The electrodes were positioned at a distance of 4 cm from each other.

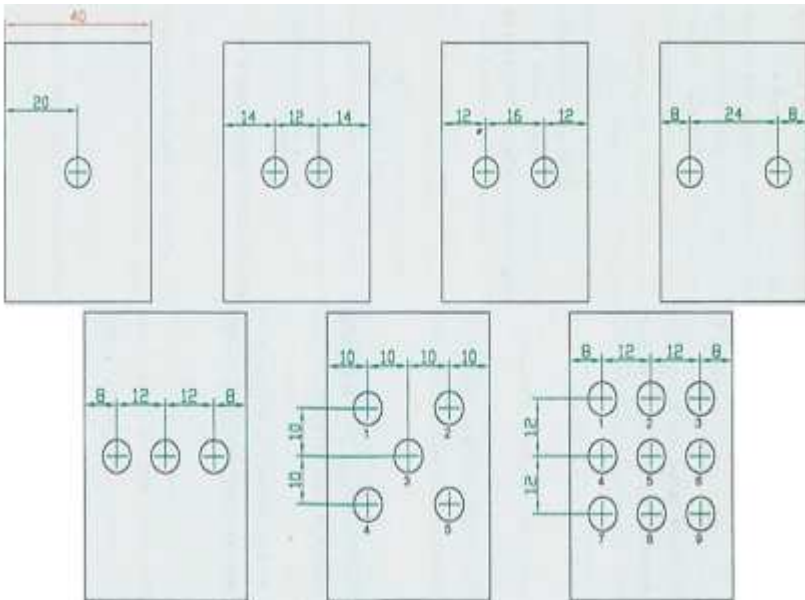


Fig. 4: Top view showing the droplet arrangements. Starting from top left, the arrangements were named as
 (1) arrangement with 1 droplet,
 (2a) arrangement with 2 droplets, 14-12-14,
 (2b) arrangement with 2 droplets, 12-16-12,
 (2c) arrangement with 2 droplets, 8-24-8,
 (3) arrangement with 3 droplets,
 (5) arrangement with 5 droplets and
 (9) arrangement with 9 droplets
 All dimensions given are in mm and they symbolize the distances of the droplets from the respective electrodes and the distances between them

The parameters investigated were the water conductivity, the roughness of the insulating surface, the positioning of the droplets and their volume. The insulating surfaces were used as they were received from the manufacturer without any further treatment. After putting the

droplets on the polymeric surface, the voltage was slowly raised until flashover occurred. After that and after cleaning the surface and putting new droplets on it, the voltage was raised again up to the previous flashover value minus 1.2 kV, so that no new flashover would occur.

At this voltage the arrangement would stay for 1 min. If no flashover occurred, the voltage was raised by 0.4 kV and the procedure was repeated until flashover occurred. The reason we left every time the voltage on for 1 min, was in order to give necessary time interval for the droplet(s) to deform and for the partial discharge to initiate.

It should be noted that it is observed a tendency for the droplets to slide, especially for PVC because of its smooth surface. The droplet slide was minimal in the case of rubber, which was the roughest of the three materials used. An elongation of the droplets was observed, as the applied voltage was larger. A more evident oscillation of the droplet was observed with silicone rubber. The reason for that was because the aforementioned material is more hydrophobic than the other two. Consequently, the droplet, for a defined droplet volume, has a smaller contact area with silicone rubber, and for this reason it oscillates more [8]. In some cases, such as with PVC with a droplet conductivity of 1.7 $\mu\text{S}/\text{cm}$ and with the arrangement (1) of Fig. 4, ejection of minute charged droplets was observed just before flashover [11].

Experimental results

At first, experiments were performed without any droplets between the electrodes. This was done in order to have reference values of the flashover voltage and also to understand influence of number of droplets between the electrodes that would result in a reduction of the flashover voltage. The flashover voltages without any droplets measured were 23 kV (± 0.5) for PVC, 25 kV (± 0.5) for silicone rubber and 24 kV (± 0.5) for rubber. The flash-over voltages of the three materials used were very similar.

In Figs. 5 - 11 the variation of flashover voltage with respect to the droplet conductivity for different droplet arrangements is shown.

It is evident that silicone rubber presents a higher flashover voltage than the other two materials. It should be noted, however, that in the case of droplet arrangements (5) and (9) where rubber seems to be as good as silicone rubber. A possible explanation might be that in such a case, the droplets cover a significant part of the polymeric surface and hence they play an even more important role than the polymer itself. This in combination with the fact that

the rubber has a rougher surface compared to the other two materials, has as a result the lesser oscillation in the case of rubber.

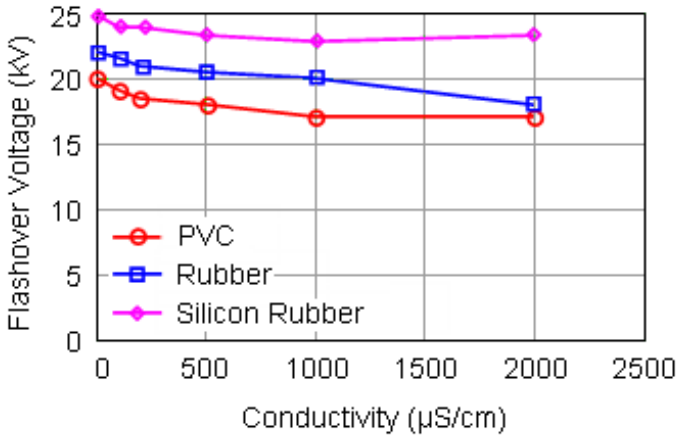


Fig. 5: Flashover voltage for droplet arrangement (1)

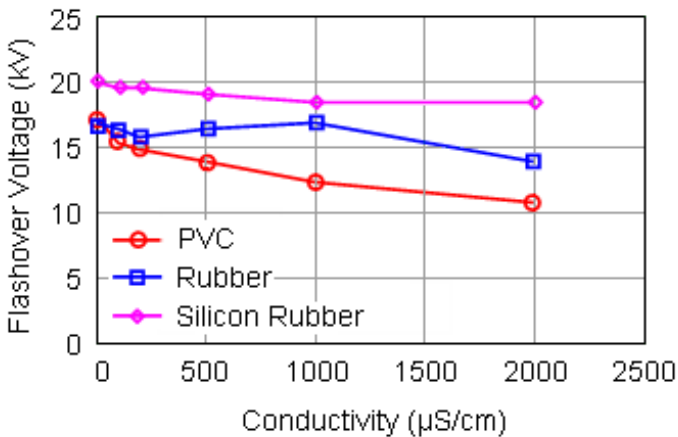


Fig. 6: Flashover voltage for droplet arrangement (2a)

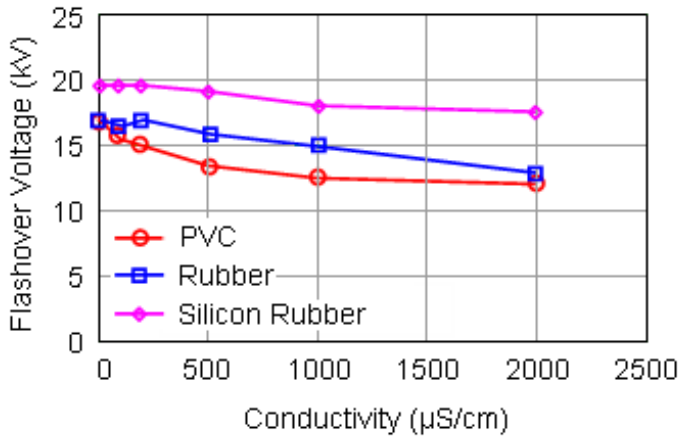


Fig. 7: Flashover voltage for droplet arrangement (2b)

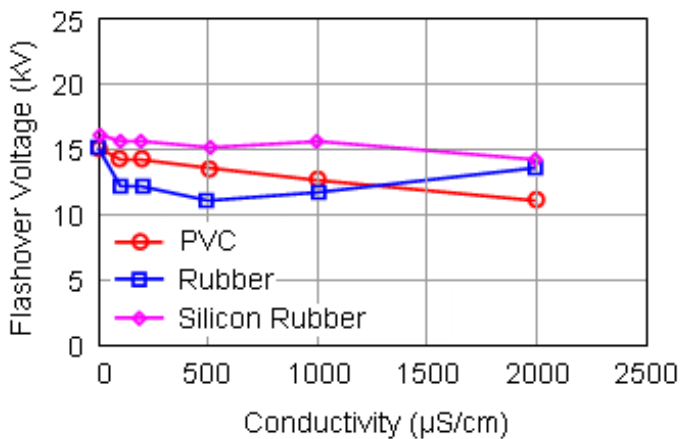


Fig. 8: Flashover voltage for droplet arrangement (2c)

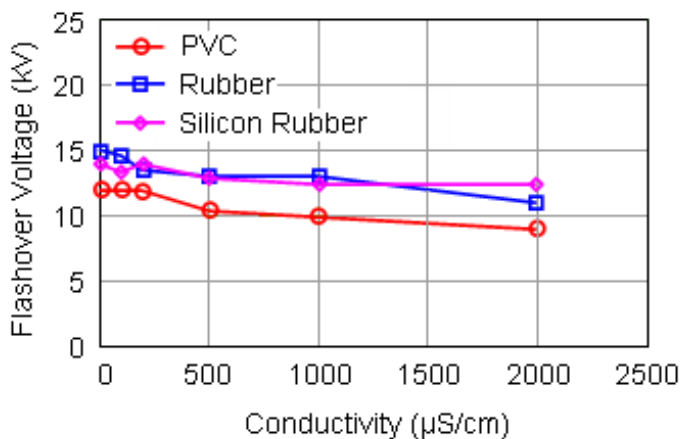


Fig. 9: Flashover voltage for droplet arrangement (3)

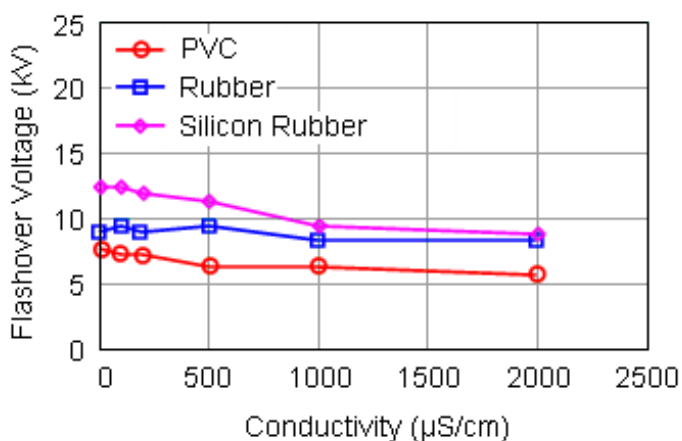


Fig. 10: Flashover voltage for droplet arrangement (5)

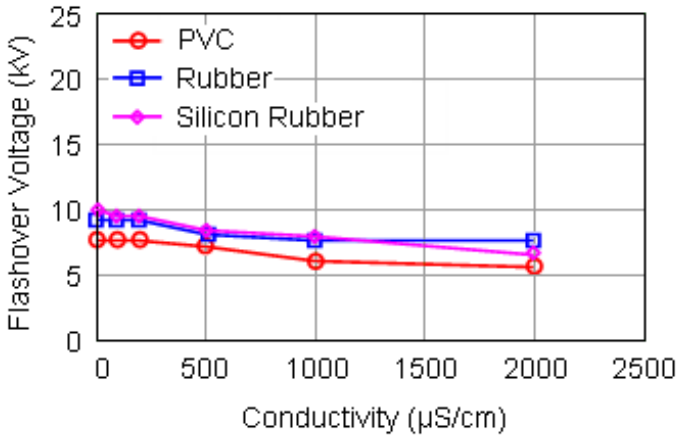


Fig. 11: Flashover voltage for droplet arrangement (9)

The better performance of silicone rubber is due to its hydrophobicity [5], [12]. The larger contact angle the droplets have minimum contact with the insulation material as in the case of silicone rubber. Figs. 12 - 14 show the influence of droplet volume on the flashover voltage. It is clear that the number of droplets affects the flashover voltage, i.e. the larger the number, the lesser the flashover voltage. An exception to that we have with the arrangement of 3 and 5 droplets. It is evident that larger flashover voltages were observed with 5 droplets than with 3 drop-

lets. A possible explanation of that is that in the case of 3 droplets, the distance between electrode and droplet is smaller than in the case of 5 droplets. Consequently, one might say that there are occasions where the positioning of the droplets with respect to the electrodes which plays a more vital role than the whole droplet volume. A further validation of the above consists of the comparison of the flashover voltages in the cases of 3 and 9 droplets. It is observed that the flashover voltages for both these arrangements are not that different although the droplet volume triples.

An interesting case consists also of the droplets arrangements 2a, 2b and 2c. Higher values for flashover voltage were observed for arrangement 2a, then for arrangement 2b and the lower flashover voltage was observed for droplet arrangement 2c. This fact reinforces the above observations, namely that the positioning of the droplets play a crucial role, i.e. the closer the droplets to the electrodes, the lower the flashover voltage. It is to be noted that similar observations were made also in [3], [4], where not an inclined arrangement was used but a horizontal one. What is presented in this paper is an approach of the behavior of water droplets on polymeric surfaces with an inclined electrode arrangement. The results were reproducible but not that many tests were carried out which would allow a statistical study of the collected data. The main interest of this paper concentrates on the study of the behavior of the droplets. In the present context, no emphasis was given to the quantification of the studied parameters.

A comment should be made on the results with the conductivity of $1.7 \mu\text{S}/\text{cm}$: in such a case, with such a low conductivity, the water path behaves like a load, i.e. like a resistance connecting the two electrodes. It is for this reason that we observed a lowering of the voltage at the output of the power source. The flow of current through water of low conductivity (i.e. of large resistance) means practically an increase of water temperature because of the power loss in the resistance of the water path. From the relation $P = I^2R$, we can conclude that as the resistance is larger, as in our case the water path of very low conductivity, the power loss at this resistance is larger. Consequently, the temperature developed in such a resistance is enough for the boiling of the water. A quantity of water evaporates and the water path becomes narrower. Dry zones are formed, micro-discharges ensue and finally the flashover follows. Such a phenomenon was observed in the inclined arrangement experiments, as they were observed before with non-inclined test arrangements [8].

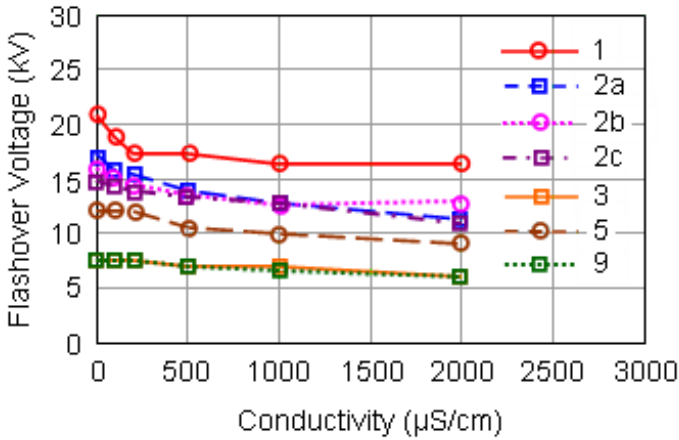


Fig. 12: Flashover voltage for various conductivities, positioning and volume of the droplets. PVC used

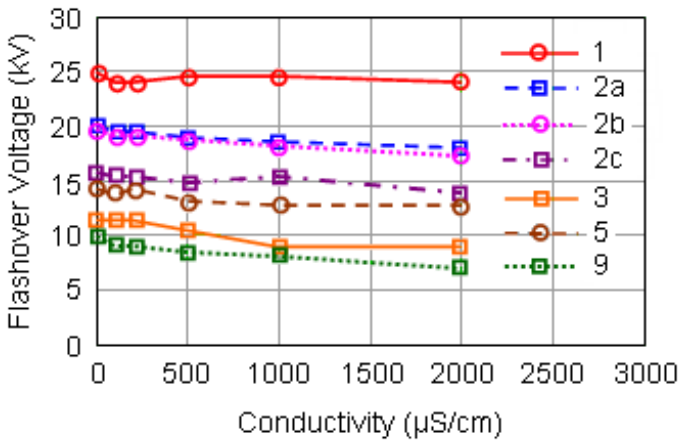


Fig. 13: Flashover voltage for various conductivities, positioning and volume of the droplets. Silicone rubber used

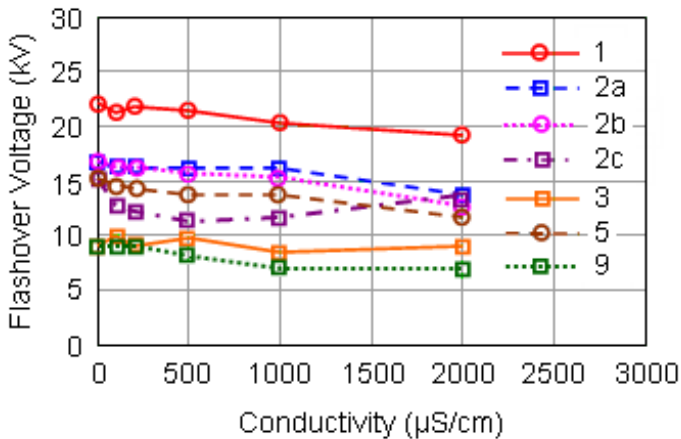


Fig. 14: Flashover voltage for various conductivities, positioning and volume of the droplets. Rubber used

Discussion and thoughts for further research

In the present paper, some parameters influencing the droplet behavior on polymeric surfaces were investigated, such as water conductivity, droplet volume, polymeric surface roughness and droplet positioning. An increase of conductivity causes a decrease of flashover voltage. This is a statement valid irrespective of the polymer used. The surface roughness affects in a positive way the flashover voltage, when the number of droplets is large. The surface roughness functions as a hindrance to the movement of the droplets, and consequently renders their oscillation more difficult.

An increase of droplet volume causes a decrease of flashover voltage. This is in agreement with experimental observations published before with either ac or dc electric fields [13]. The position of the droplets with respect to the electrodes is of vital importance. With the droplets nearer the electrodes, the flashover voltage decreases. This is a phenomenon observed, albeit in different circumstances and conditions, also with enclosed cavities in solid dielectrics, where discharges become much more intense when one of the enclosing walls is an electrode [14].

The above show clearly that the polymeric material

plays a predominant role in determining the flashover voltage and the behavior of water droplets. Hydrophobic materials, such as silicone rubber, perform better than PVC or rubber. With this in mind, one should also note that most polymeric materials for outdoor applications present some sort of hydrophobicity. However, the advantage of silicone rubber consists in the fact that it does not only have this property, it can also regenerate it [15].

The formation of water paths, between the droplets as well as between the droplets and the electrodes, generally follow the direction of the applied electric field. The general activity in the form of discharges and droplet movement with rougher surfaces, sets in at higher voltages. In the case of just one droplet, with the application of the field, a deformation starts turning later to instability. Such behavior was observed with the inclined arrangement as well as with previous horizontal arrangements [3], [4]. Also in the case of the inclined arrangement, the role of the 'triple points' (i.e. the points where air, polymeric surface and droplet meet each other) is vital. The forces exercised on the droplets,

because of the applied electric field, are quite strong, and therefore, the 'triple points' move towards the electrodes. Experimental data published recently, validate what is reported here [16]. Such movement of 'triple points' causes the spread of the droplets. The spread of droplets is perhaps the most characteristic phenomenon observed with the inclined electrode arrangement. It is not, however, the only one observed. Droplet oscillation, formation of water paths, collapsing of two droplets into a larger one, ejection of small charged droplets from a larger one, were also noted during the experiments. In this respect, the present work offers similar conclusions with those in [3], [4], [8], [9], [16], [17]. The importance of the triple points should be emphasized. In other works, it has been reported that partial discharge (PD) activity is sometimes marginal, not easily detectable by a conventional electrical PD system but by a photomultiplier. Smaller water droplets offer higher flashover voltages. This can also be explained by considering - in the case of smaller droplets - that the intermolecular forces are in equilibrium with the surface tension and, consequently, the electrical forces required to

disturb the equilibrium are higher. On the other hand, for larger droplets, the inner forces may be lower and, if the surface tension stays the same, the equilibrium can more easily be disturbed. In such a case, the PD activity will start earlier and at lower voltages, and therefore, the flashover voltage will be lower [18]. The fact that the contact angle increases with the decrease of water droplet volume, is something that cannot be underestimated [18]. Generally speaking, although the observations of [18] refer to silicone rubber samples only, the relevant conclusions are not different from the ones presented in this paper.

It is to be noted that the inclined electrode arrangement, used here, should not be compared by any means with the well known arrangement of the inclined plane test [19]. In the latter, a film of electrolyte is arranged to trickle down the back surface of a sheet and the samples are rated in terms of the voltage which causes a track to form in one hour [20]. In other words, the inclined plane test is a means of evaluating resistance to tracking and erosion of insulating materials for outdoor use, whereas the inclined electrode arrangement used in

this work is a setup to study some parameters affecting the droplet movement on polymeric materials. The inclined plane test is an accelerating test [19]. The angle which was used in our experiments, i.e. the angle of 10° , was taken from real insulators. The purpose was to see the droplet behavior under an electric field in, as much as possible, real conditions. The present work confirms some general tendencies noted in [3], [4].

It would be interesting to try experiments, in which the contact angle will be accurately measured for both smaller and larger water droplets w.r.t. time. The purpose would be to see whether the contact angle diminishes with the passing of time and which diminution is more dramatic, that of the contact angle of smaller droplets or that of the contact angle of the larger droplets. Recent research indicated that the contact angle of droplets decreases with time, without, however, precisising whether the rate of decrease is larger for smaller or for larger droplets [21]. Moreover, as noted before, an interesting point can be to study different modes of droplet deformation in terms of the four parameters investigated in this pa-

per [18], [22].

One last point should be raised: the research mentioned above was carried out with conventional polymers. It is remarkable that, most of the aforementioned points, i.e. the importance of the positioning of the droplets, the significance of the droplet volume and/or of the droplet number as well as the importance of the water conductivity, are points which are also important for non-conventional polymers, i.e. for nanocomposite polymers. Work done recently in this laboratory emphasizes that parameters such as those investigated here, are also significant for nanocomposite polymers. In fact, the nature of phenomena such as surface discharges or flashovers, must have a common underlying denominator for both conventional polymers and nanocomposite polymers. Future research must also be directed in order to find the common grounds for surface discharge phenomena in both conventional and nanocomposite polymers [23], [24].

Conclusion

Water droplet conductivity, polymer surface roughness, droplet volume and the positioning of droplets with respect to the electrodes constitute important param-

eters affecting the behavior of droplets under the influence of an electric field with an inclined plane electrode arrangement. Increased conductivity, smoother polymer surfaces and increased droplet volume cause a reduction of the flashover voltage. The droplet positioning with respect to the electrodes plays a vital role in reducing the flashover voltage and, on occasions, is more important than the droplet volume.

Appendix - Elementary modeling

As mentioned above, the behavior of a droplet was modeled in [25], where the electric field E_N developed at one edge of the droplet is given by

$$E_N = U h / [a(h - a)] \quad (1)$$

where, U is the applied voltage, a is the droplet radius and h is the distance of the center of the droplet from one of the electrodes. The electric field E_M on the opposite edge of the droplet is given by

$$E_M = U h(L - h) / [a(L - h - a)] \quad (2)$$

where, L is the distance between the electrodes and the other symbols as in Eq. (1). As a droplet is positioned in the middle of the electrodes, the ratio E_N/E_M is expected to

be unity, and this was what was exactly obtained with the above equations. Considering Eq. (1), as $h \rightarrow a$, E_n tends to infinity. This is what we observed in the context of this work, namely that the closer a droplet is in one of the electrodes, the larger the electric field is getting, and consequently the more deleterious the consequences are. The above simple modeling is due to [25]. It was elaborated in [26], albeit with a non-inclined test arrangement. It must be mentioned that phenomena of very similar nature were observed also with the inclined test arrangement.

Remark

Main aspects of this paper were published in M.G. Danikas, P. Ramnalis and R. Sarathi, "A study of the behavior of water droplets on polymeric surfaces under the influence of electric fields in an inclined test arrangement", Journal of Electrical Engineering, Vol. 60, No. 2, 2009, pp. 94-99. The present version, however, contains additional comments on some aspects of the investigated polymeric materials as well as on a possible relation of the observed phenomena in nanocomposite polymers.

References

- [1] Kind D., Kaerner H., "High Voltage Insulation Technology", Braunschweig: Eds. Vieweg, 1985
- [2] Danikas M.G., "Surface Phenomena on Resin-Type Insulators under Different Electrical and Non-electrical Stresses in the Early Stage of Ageing", Facta Universitatis, Vol. 13, 2000, pp. 335-352
- [3] Karakoulidis K., Danikas M.G., Rakitzis P., "Deterioration Phenomena on Insulating Surfaces due to Water Droplets", Journal of Electrical Engineering, Vol. 56, 2005, pp. 169-175
- [4] Danikas M.G., Rakitzis P., Karakoulidis K., "Study of Parameters Related to Deterioration Phenomena due to Water Droplets on Polymeric Surfaces", Journal of Electrical Engineering, Vol. 57, 2006, pp. 130-137
- [5] Kloes H.J., Koenig D., Danikas M.G., "Electrical Surface Discharges on Wet Polymer Surfaces", Proceedings of the 8th International Symposium of Gaseous Dielectrics, Virginia beach, Virginia, USA, June 1998, pp. 489-495

- [6] Koenig D., "Surface and Aging Phenomena on Organic Insulation under the Condition of Light Contamination and High Electric Stress", Proceedings of the Nordic Insulation Symposium, Vaasa, Finland, June 1994, pp. 17-35
- [7] Hartings R., "The AC-Behavior of a Hydrophilic and Hydrophobic Post Insulator During Rain", IEEE Winter Power Meeting, New York, USA, 1994
- [8] Karakoulidis K., "Breakdown Phenomena on Insulating Surfaces", M.Sc. Thesis, Democritus University of Thrace, Xanthi, Greece, 2002 (in Greek)
- [9] Rakitzis P., "Flashover Phenomena on Polymeric Surfaces under the Influence of a Uniform Electric Field", M.Sc. Thesis, Democritus University of Thrace, Xanthi, Greece, 2003 (in Greek).
- [10] Danikas M.G., "Ageing Properties of Silicone Rubber Materials Used in High Voltage Composite Insulators", Journal of Electrical and Electronics Engineering, Australia, Vol. 15, 1995, pp. 193-202
- [11] Dan Windmar, "Water Droplet Initiated Discharges in Air", PhD Thesis, Uppsala, University, Uppsala, Sweden, 1994
- [12] Gorur R.S., "High Voltage Outdoor Insulation Technology", Control and Dynamic Systems, Vol. 44, 1991, pp. 131-191
- [13] Schutte, T., "Water Drop Dynamics and Flashover Mechanisms on Hydrophobic Surfaces", Proceedings of the Nordic Insulation Symposium, Vasteras, Sweden, paper 8.1, June, 1992
- [14] Mason J.H., "Discharges", IEEE Transactions on Electrical Insulation, Vol. 13, 1978, pp. 211-238
- [15] Vlastos A., Gubanski S., "Surface Structural Changes of Naturally Aged Silicone Rubber and EPDM Composite Insulators", IEEE Transactions on Power Delivery, Vol. 6, 1991, pp. 888-900
- [16] Keim S., Koenig D., Hinrichsen V., "Experimental Investigations on Electrohydrodynamic Phenomena at Single Droplets on Insulating Surfaces", Annual Report of the Conference on Electrical Insulation and Dielectric Phenomena, Albuquerque, New Mexico, USA, October 2003, pp. 133-136
- [17] Keim S., "Optical Diagnostic of Single Droplets on Polymeric Insulating Surfaces in an Electric Field to Describe the Phenomena of the Beginning of Aging Mechanisms", PhD Thesis, Darmstadt University of Technology, Darmstadt, Germany, 2003 (in German).

- [18] Feier-Iova S., "The Behaviour of Water Droplets on Insulating Surfaces Stressed by Electric Field", PhD Thesis, Darmstadt University of Technology, Darmstadt, Germany, 2009
- [19] IEC 60 587 and BS 5604 Method of Test for Evaluating Resistance to Tracking and Erosion of Electrical Insulating Materials Used under Severe Ambient Conditions
- [20] Stannett A.W., "Breakdown Testing and Measurements on Installed Equipment, In: Electrical Insulation", A. Bradwell (Ed.), London: Peter Peregrinus Ltd., 1983, pp. 261-276
- [21] Fijii O., Honsali K., Mizuno Y., Naito K., "A Basic Study on the Effect of Voltage Stress on a Water Droplet on a Silicone Rubber Surface", IEEE Transactions on Dielectrics and Electrical Insulation, Vol. 16, 2009, pp. 116-122
- [22] Fijii O., Honsali K., Mizuno Y., Naito K., "Vibration of a water Droplet on a Polymeric Insulating Material Subjected to AC Voltage Stress", IEEE Transactions on Dielectrics and Electrical Insulation, Vol. 17, 2010, pp. 566-571
- [23] Kechagia S., Danikas M.G., Sarathi R., "Water Droplets and Breakdown Phenomena on Polymer Nanocomposite Surfaces under the Influence of Uniform Electric Fields", Malaysian Polymer Journal, Vol. 8, No. 2, 2013, pp. 41-47
- [24] Bairaktari A., Danikas M.G., Zhao X., Cheng Y., Zhang Y., "Behaviour of Water Droplets under the Influence of a Uniform Electric Field in Nanocomposite Samples of Epoxy Resin/TiO₂", Engineering, Technology & Applied Science Research, Vol. 3, No. 5, 2013, pp. 511-515
- [25] Imano A.M., Beroual A., "Deformation of Water Droplets on Solid Surface in Electric Field", Journal of Colloidal Interfacial Science, Vol. 298, 2006, pp. 869-879
- [26] Cheng Y., Zhao X., Danikas M.G., Christantoni D., Zairis P., "A Study of the Behaviour of Water Droplets under the Influence of Uniform Electric Field in Epoxy Resin Samples, Journal of Electrical Engineering, Vol. 63, No. 3, 2012, pp. 196-200

*** About The Authors**

Michael Danikas, received the B.Sc. and M. Sc. from the University of Newcastle-upon-Tyne, England, in 1980 and 1982 respectively. He received the Ph.D. from the University of London, Queen Mary College, London, England, in 1985. He was employed at Eindhoven University of Technology, The Netherlands, and at ABB, Switzerland during the years 1987-1993. At present he is Professor at the Dept. of Electrical and Computer Engineering, Democritus University of Thrace, Xanthi, Greece. His research interests were and still are electrical trees in polymeric materials, the role of humidity on flashover voltage, transformer oil ageing and solid/liquid insulation ageing.

mdanikas@ee.duth.gr

Pavlos Ramnalis, graduated from the Dept. of Electrical and Computer Engineering, Democritus University of Thrace, in 2010. Afterwards he was employed in private companies in Athens, Greece.

Ramanujam Sarathi, is Professor at the Dept. of Electrical Engineering, Indian Institute of Technology Madras, Chennai, India. During his career, he spent a lot of time having worked with researchers at Akita University, Japan, and at Waseda University, Japan, on subjects such as properties of insulating materials, nanopowder technology and characterization of electrical trees in insulating structures.

[This Page Intentionally Left Blank]

Measurement Uncertainty in Network Analyzers: Differential Error Analysis of Error Models Part 3: Short One-Port Calibration – Comparison

N.I. Yannopoulou, P.E. Zimourtopoulos *

Antennas Research Group, Austria – Hellas [1, 2]
EECE Dept, Democritus University of Thrace, Hellas [2]

Abstract

In order to demonstrate the usefulness of the only one existing method for systematic error estimation in VNA (Vector Network Analyzer) measurements by using complex DERS (Differential Error Regions), we compare one-port VNA measurements after the two well-known calibration techniques: the quick reflection response, that uses only a single S (Short circuit) standard, and the time-consuming full one-port, that uses a triple of SLO standards (Short circuit, matching Load, Open circuit). For both calibration techniques, the comparison concerns: (a) a 3D geometric representation of the difference between VNA readings and measurements, and (b) a number of presentation figures for the DERS and their polar DEIs (Differential Error Intervals) of the reflection coefficient, as well as, the DERS and their rectangular DEIs of the corresponding input impedance. In this paper, we present the application of this method to an AUT (Antenna Under Test) selected to highlight the existence of practical cases in which the time consuming calibration technique results a systematic error estimation stripe including almost all of that of quick calibration.

Introduction

The systematic error in a full one-port calibrated VNA measurement ρ of a given one-port DUT (Device Under Test) is already estimated by its DER [1]-[2]:

$$\rho = (m - D) / [M(m - D) + R] \quad (1)$$

$$d\rho = [-RdD - (m - D)^2dM - (m - D)dR + RdM] / [M(m - D) + R]^2 \quad (2)$$

where m is the VNA complex reading and D , M and R are the complex system errors of Fig. 1.

The relations holding between this complex reflection

coefficient ρ and its respective impedance Z , as well as, between their DERs are [1]-[2]:

$$Z = Z_0(1 + \rho)/(1 - \rho) \quad (3)$$

$$dZ = 2Z_0 d\rho / (1 - \rho)^2 \quad (4)$$

In this paper, we express the DERs for systematic error estimation in VNA measurements calibrated by the much simpler and quicker reflection response technique, in order to be in place to make some practical decisions from the different calibration techniques comparison.

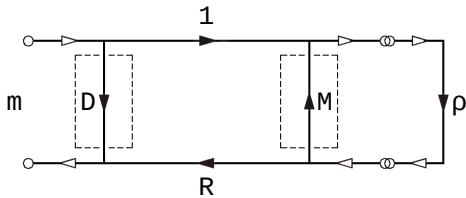


Fig. 1: Full one-port error model

Response Calibration

The reflection response calibration technique can be accomplished with the measurement of only one standard load, instead of three in full one-port, usually of a S short circuit [3]-[4]. This means that the flow graph of Fig. 1 is simplified a lot, since the two surrounded by dashed boxes system error branches of directivity D and source match M do not exist, equivalently $D = 0$ and $M = 0$ and (1) results to:

$$R = m/\rho_s = s/S \quad (5)$$

where s is the VNA complex reading of the S short circuit standard with a nominal value of $S = -1$, m is the complex reading of a given DUT and ρ_s is its complex reflection coefficient as it is measured after this response calibration:

$$\rho_s = (m/s)S \quad (6)$$

which, from (2), has the differential error:

$$d\rho_s = (S/s)dm - (Sm/s^2)ds + (m/s)dS \quad (7)$$

The corresponding total DER is then the sum of $L = 3$ parallelograms. Therefore, this DER contour is a polygonal line with $4L = 12$ line segments and vertices at most, in contrast with the DER of the measurement after a SLO full one-port calibration, which is a piecewise curve composed of $4(L - 1) = 24$ line segments, $4(L - 1) = 24$ circular arcs and $8(L - 1) = 48$ vertices, at most [1]-[2].

Application Results

By following the error estimation process, we already detailed in [1]-[2], we take as dS the considered manufacturers' standard S uncertainty data:

$$-0.01 \leq d|S| \leq 0, \quad -2^\circ \leq d\angle S \leq +2^\circ$$

and as d_m and d_s the VNA inaccuracy of ± 1 digit in LSD of their corresponding readings, for either the amplitude in decibels or the phase in degrees. Moreover, the one-port DUT that was considered is the same typical UHF ground-plane antenna (that is: AUT) mentioned in [1].

The difference between the 3 nominal values (-1, 0, 1) of the 3 full one-port calibration standards (S, L, O), respectively, and their 3 corresponding VNA readings (s , l , o), can be estimated by the extent of the surfaces shown in the triptych of Fig. 2, where the vertical axis segment represents the range of the distinct stepped frequencies. Each surface is formed by parallel to horizontal plane lines. Each such line expresses the complex difference between the standard nominal value and its corresponding VNA reading, in each stepped frequency.

In the triptych of Fig. 3, and from left to right we have the difference surfaces made by distance lines between:

(a) the measured reflection coefficient ρ after a full SLO one-port calibration (black solid points) and the corresponding VNA readings m for the AUT measurement (colored magenta points),

(b) the measured reflection coefficient ρ_s after S response calibration (black ring points) and the corresponding VNA readings m for the AUT measurement (colored magenta points), and

(c) the two measurements (ρ , ρ_s).

All the involved, previously shown, quantities are projected on the horizontal complex plane of Fig. 4. The magenta colored spiral represents m , while, the black curves the reflection coefficient: solid points, for ρ , and ring points for ρ_s . All of 1 VNA readings are close enough to complex origin (colored green points). It is rather difficult to distinguish the two curves for s and o VNA readings, which are close enough to the unit circle circumference (colored red solid points and colored blue ring point, respectively).

The ρ -DERs and ρ_s -DERs, for all 4 MHz stepped frequencies covering the range of [600, 1000] MHz, are overlapped on the complex plane of Fig. 5, forming a light and a dark gray stripes, respectively. From each stripe we selected 11 DERs out of 101, drawn with dark gray and white colors respectively, to illustrate their outline dependence on frequency.

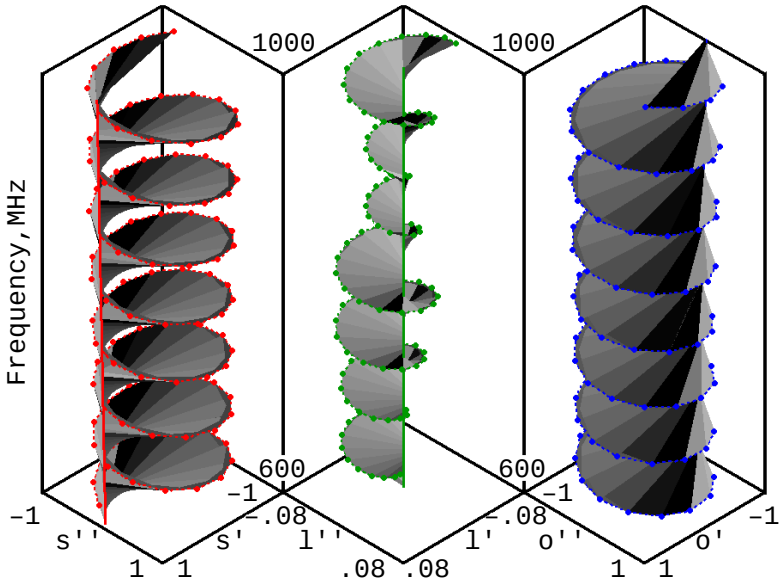


Fig. 2: Difference between s and S , l and L , o and O

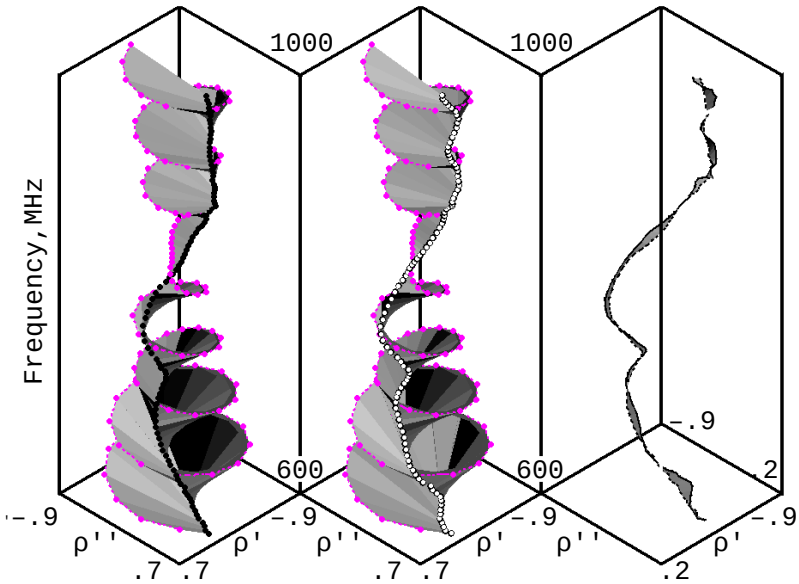


Fig. 3: Difference between m and ρ , m and ρ_s , ρ and ρ_s .

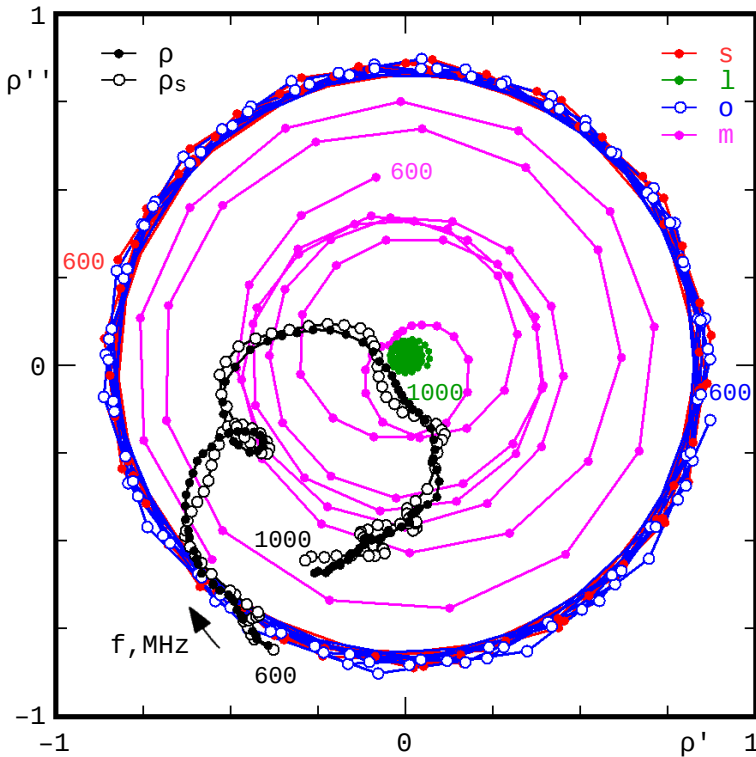


Fig. 4: VNA s , l , o , m readings and ρ , ρ_s measurements.

Moreover, we selected to magnify a part of this figure in the sub-range of [892, 1000] MHz, to further illustrate the DER outlines and their overlapping in Fig. 6, where the clearly shown ripple of the simple response calibration stripe over the relatively smooth full one-port calibration stripe reveals the superiority of the latter in the production of more accurate measurements.

The comparison between the AUT measurements based on

these two calibration techniques is extended to the comparison against the frequency:

- (a) of the computed polar DEIs of the reflection coefficient magnitude and argument stripes in Fig. 7,
- (b) of the rectangular DEIs for the corresponding R input resistance and X input reactance stripes, in Fig. 8 and
- (c) of the Z-DERs, and Z_s -DERs stripes in Fig. 9.

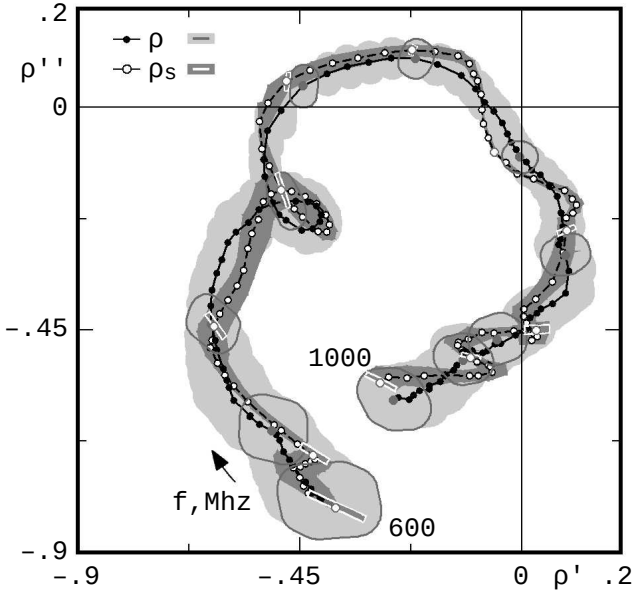


Fig. 5: Complex ρ -DERs and ρ_s -DERs in [600, 1000] MHz

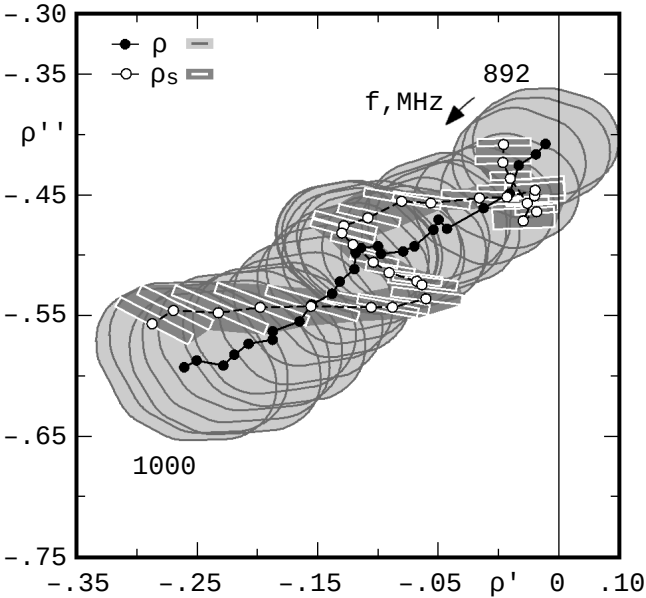


Fig. 6: Complex ρ -DERs and ρ_s -DERs in [892, 1000] MHz

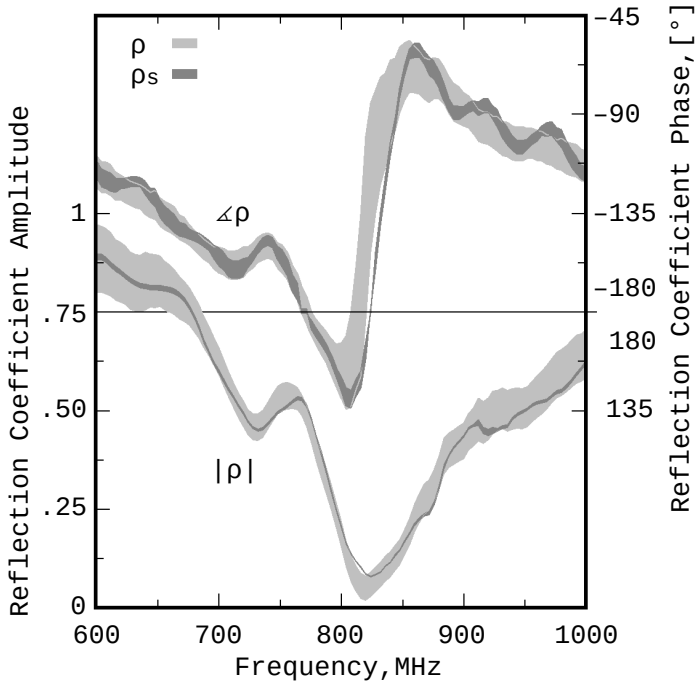


Fig. 7: Polar DEIs of reflection coefficient

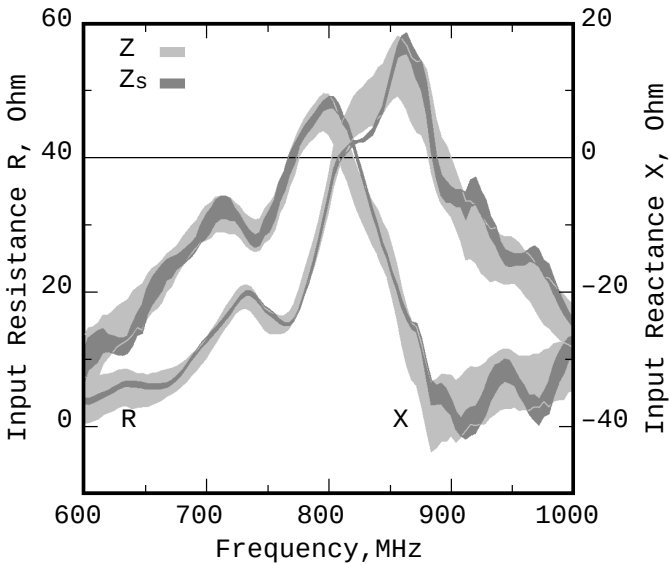


Fig. 8: Rectangular DEIs of input impedance

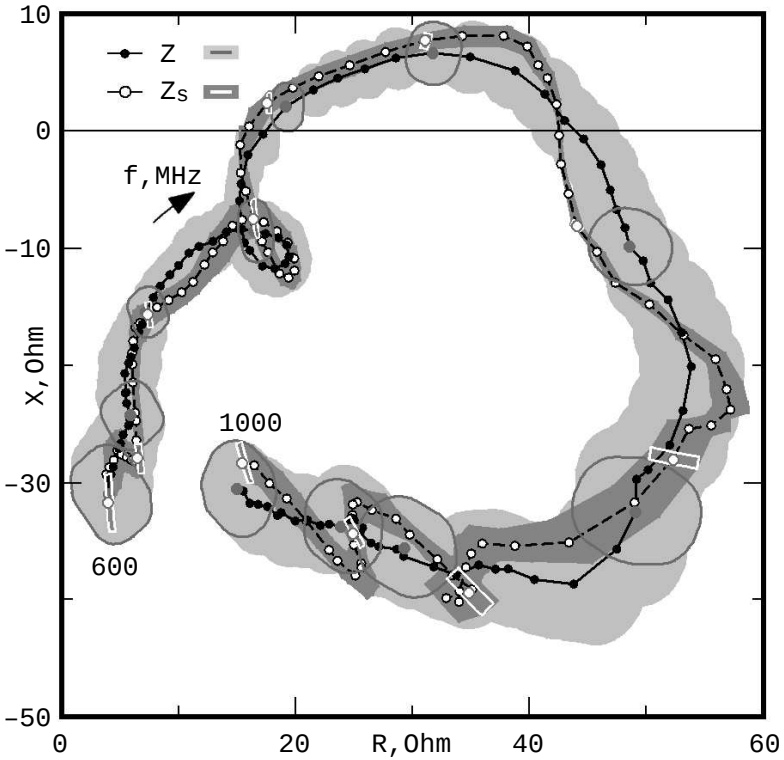


Fig. 9: Complex Z-DERS and Z_s-DERS in [600, 1000] MHz

Conclusion

From all that, it must be clear now that in this intentionally selected for presentation particular AUT case there was no advantage at all

in selection of full one-port calibration over the reflection response one, due to their remarkable in all aspects coincidence. Of course this is just another one conclusion a-posteriori.

References *

- [1] Yannopoulou N., Zimourtopoulos P., "Total Differential Errors in One Port Network Analyzer Measurements with Application to Antenna Impedance", Radioengineering, Vol. 16, No. 2, June 2007, pp. 1-8
"www.radioeng.cz/fulltexts/2007/07_02_01_08.pdf"
 - [2] Yannopoulou N.I., Zimourtopoulos P.E., "Measurement Uncertainty in Network Analyzers: Differential Error Analysis of Error Models Part 1: Full One-Port Calibration", FunkTechnikPlus # Journal, Issue 1, October 2013, pp. 17-22
"www.otoiser.org/index.php/ftpj/article/view/42"
 - [3] HP, "Vector Measurements of High Frequency Networks", Hewlett-Packard, 1989, pp. 2-13, 2-15, 3-11, 3-12
 - [4] AGILENT, "OPEN/SHORT Response Calibration (reflection test), Calibration Types and Characteristics"
"http://ena.support.keysight.com/e5071c/manuals/webhelp/eng/measurement/calibration/calibration.htm"
- *Active Links: 15.12.2013 - Inactive Links : FTP#J Link Updates: "http://updates.ftpj.otoiser.org/"

Preprint Versions

"Comparison of Error Estimation by DERs in One-Port S and SLO Calibrated VNA Measurements and Application"
Nikolitsa Yannopoulou, Petros Zimourtopoulos
"http://arxiv.org/abs/1102.4239"

Follow-Up Research Paper

Not until now

Previous Publication in FUNKTECHNIKPLUS # JOURNAL

"Measurement Uncertainty in Network Analyzers: Differential Error Analysis of Error Models Part 2: Full Two-Port Calibration", Issue 1, pp. 23-30

* About The Authors

Nikolitsa Yannopoulou, Issue 1, p. 15

Petros Zimourtopoulos, Issue 1, p. 15

This paper is licensed under a Creative Commons Attribution 4.0 International License – <https://creativecommons.org/licenses/by/4.0/>

[This Page Intentionally Left Blank]

[This Page Intentionally Left Blank]

In case of any doubt,
download the genuine papers from
genuine.ftpj.otoiser.org

FRONT COVER VIGNETTE

A faded synthesis of an anthemion rooted in a meandros

The thirteen-leaf is a symbol for a life tree leaf.
"Herakles and Kerberos", ca. 530–500 BC,
by Paseas, the Kerberos Painter,
Museum of Fine Arts, Boston.

www.mfa.org/collections/object/plate-153852

The simple meandros is a symbol for eternal immortality.
"Warrior with a phiale", ca. 480–460 BC,
by Berliner Maler,
Museo Archeologico Regionale "Antonio Salinas" di Palermo.

commons.wikimedia.org/wiki/File:Warrior_MAR_Palermo_NI2134.jpg

ISSN 2310-6697

toiser—open transactions on independent scientific-engineering research

FUNKTECHNIKPLUS # JOURNAL

Théorie—Expérimentation—Métrologie—Logiciel—Applications

ISSUE 3 – FRIDAY 31 JANUARY 2014 – YEAR 1

- 1 Contents
- 2 About
- 3 Editorial Board – Technical Support
- 4 Information for Peers – Guiding Principles
- # Telecommunications Engineering – Logiciel
- 7 The Very First Ever Made 3D/4D Virtual Laboratory for Antennas
N.I. Yannopoulou, P.E. Zimourtopoulos
- # Applied Electromagnetics – Théorie
- 19 Near-field Method in Solving Inverse Scattering Problem of Spherical Electromagnetic Waves in Chiral media
Nikolaos M. Berketis



About

This European Journal defends
honesty in science and ethics in engineering

Publisher – **otoiser** open transactions on independent scientific-engineering research – **ARG NP UoP** Antennas Research Group Non Profit Union of Persons – Hauptstraße 52, 2831 Scheiblingkirchen, Austria – **www.otoiser.org** – **www.antennas.gr**

Language – We declare the origins of the Journal by using English, German and French, as well as, a Hellenic vignette, in the cover page. However, since we recognize the dominance of USA English in technical literature, we adopted it as the Journal's language, although it is not our native language.

Focus – We consider Radio-FUNK, which still creates a vivid impression of the untouchable, and its Technology-TECHNIK, from an Advanced-PLUS point of view. That is, we dynamically focus at any scientific-engineering discipline producing FUNKTECHNIKPLUS Théorie, Expérimentation, Métrologie, Logiciel, ou Applications.

Scope – We emphasize this scope broadness by extending the title of the Journal with a Doppelkreuz-Zeichen #, which we use as a placeholder for the disciplines of Editorial Board:

Electrical – # Electronics – # Computer – # Telecommunications – Engineering # Computer Science # Applied Mathematics, etc.

Frequency – We regularly publish 3 issues per year on January, May, and September as well as an issue every 3 papers.

Editions – We follow the arXiv.org system, that is the 1st edition date of every issue is on the cover page and any update date is on the odd pages with its version on all pages.

Format – We use the uncommon for Journals A5 paper size and the much readable Liberation Mono fixed-space font, with hyphenation, justification, and unfixed word spacing, to display 2 pages side-by-side on widescreen monitors with WYSIWYG printout. We can consider only papers in ODF odt or MS doc format written in LibreOffice or MS Office with MathType. We use PDFCreator and PDF-Xchange to produce pdf and export to images for printing on demand and electronic publishing.

License – We use the free Open Journal System OJS from the PKP Public Knowledge Project for internet publication

Copyright – Creative Commons Attribution 3 Unported CC-BY 3

Please download the latest *About* edition from
about.ftpj.otoiser.org

Editorial Board

Electrical Engineering

High Voltage Engineering # Insulating Materials

Professor Michael Danikas

EECE, Democritus University of Thrace, mdanikas@ee.duth.gr

Electrical Machines and Drives # Renewable Energies

Electric Vehicles

Assistant Professor Athanasios Karlis

EECE, Democritus University of Thrace, akarlis@ee.duth.gr

Computer Engineering # Software Engineering

Cyber Security

Associate Professor Vasileios Katos

EECE, Democritus University of Thrace, vkatos@ee.duth.gr

Internet Engineering # Computer Science

Simulation # Applied Education # Learning Management Systems

Lecturer Sotirios Kontogiannis

BA, TE Institute of Western Macedonia, skontog@gmail.com

Applied Mathematics # Applied Functional & Numerical Analysis

Applied Electromagnetics # Control Theory

Dr. Nikolaos Berketis, Athens, Greece

BS-Math, MSc-Appl.Math, PhD-Appl.Math, nberketis@gmail.com

Telecommunications Engineering # Applied Electromagnetics

Antennas # RF & Microwave Metrology # Software Applications

Simulation # Virtual Reality # Amateur Radio # FLOSS

Applied Education # Applied Physics # Electronics Engineering

Dr. Nikolitsa Yannopoulou, Scheiblingkirchen, Austria

Diploma Eng-EE, MEng-EECE, PhD-EECE, yin@arg-at.eu

Assistant Professor Petros Zimourtopoulos

EECE, Democritus University of Thrace, pez@ee.duth.gr

Technical Support

Konstantinos Kondylis, Doha, Qatar

Diploma Eng-EECE, MEng-EECE, k8k@arg-at.eu

Christos Koutsos, Bratislava, Slovakia

Diploma Eng-EECE, MEng-EECE, cak@arg-at.eu

Information for Peers Guiding Principles

This is a small, but independent, low profile Journal, in which we are all – Authors – Reviewers – Readers – Editors – free at last to be Peers in Knowledge, without suffering from either:

- Journal roles or positions,
- Professional, amateur, or academic statuses, or
- Established impact factorizations,

but with the following Guiding Principles:

Authors – We do know what work means; and we do respect the research work of the scientist – engineer; and we do want to highlight this work; and we do decided to found this Journal; and we do publish this work openly; and furthermore, we do care for the work of the technical author, especially the beginner one, whom we do support strongly as follows:

- 1 We encourage the author to submit his own paper written just in Basic English plus Technical Terminology.
- 2 We encourage the author even to select a pen name, which may drop it at any time to reveal his identity.
- 3 We encourage the author to submit an accepted for publication paper, which he was forced to decline that publication because it would be based on a review with unacceptable evaluation or comments.
- 4 We encourage the author to resubmit a non accepted for publication paper that was rejected after a poor, inadequate, unreasonable, irresponsible, incompetent, or ticking only, review.
- 5 We encourage the author to submit a paper that he already self-archived on some open repository, such as arXiv.org.
- 6 We encourage the author to self-archive all of the preprint and postprint versions of his paper.
- 7 We provide the author with a decent, express review process of up to just 4 weeks, by at least 2 peers, never have been co-authors with him.
- 8 We provide the author with a selection of review process between: a traditional, anonymous, peer review decision, and an immediate online pre-publication of his paper followed by an open discussion with at least 2 reviewers.

About

- 9 We immediately accept for publication a research paper directly resulting from a Project Report, Diploma-, Master-, or PhD-thesis, which the author already has successfully defended before a committee of experts and he can mention 2 members of it, who reviewed and approved his work.
- 10 We immediately publish online a paper, as soon as, it is accepted for publication in the Journal.
- 11 We quickly print-on-demand an issue every 3 papers, in excess of the 3 issues we regularly publish 3 times a year.
- 12 We do not demand from the author to transfer his own copyright to us.
- 13 Nevertheless, we publish only an original research work paper and only if the author does assure us that he owns the copyright of his own paper and submit this paper or a revised version of it to the Journal for publication or even for republication under the Creative Commons–Attribution 3.0 Unported License, CC-BY 3.

Reviewers – Any peer may voluntarily become a reviewer of the Journal in his expertise for as long as he wishes. Each author of the Journal has to support the peer-to-peer review process by reviewing one paper, written by non co-author(s) of him, for every one of his papers published in the Journal.

Readers – Any reader is a potential reviewer. We welcome online comments and post-reviews by the readers.

Editors – Any editor holds a PhD degree, to objectively prove that he really has the working experience of passing through the established publishing system. An editor pre-reviews a paper in order to check its compliance to the Guiding Principles and to select the appropriate reviewers of the Journal. We can only accept for consideration papers in the expertise areas currently shown in the Editorial Board page. However, since we are willing to amplify and extend the Scope of the Journal, we welcome the volunteer expert, in any subject included into it, who wants to join the Board, if he unreservedly accepts our Guiding Principles.

Antennas Research Group – Non-Profit 12(3) * Union of Persons

* The Constitution of Greece, Article: 12(3) 2008:

www.hellenicparliament.gr/en/Vouli-ton-Ellinon/To-Politevma

* The Hellenic Supreme Court of Civil and Penal Law:

www.areiospagos.gr/en/ – Court Rulings:Civil|A1|511|2008

Submissions

sub@ftpj.otoiser.org

Electronic Publishing

www.ftpj.otoiser.org

Printing-on-Demand

pod@ftpj.otoiser.org

Directly:

Georgios Tontrias, msn.expresscopy.xan@hotmail.com

ExpressCopy, V.Sofias 8, 671 00, Xanthi, Greece

More – Detailed information will be available soon at:

www.ftpj.otoiser.org/gp

The Very First Ever Made 3D/4D Virtual Laboratory for Antennas

N.I. Yannopoulou, P.E. Zimourtopoulos *

Antennas Research Group, Austria – Hellas [1, 2]
EECE Dept, Democritus University of Thrace, Hellas [2]

Abstract

Based on the experience we have gained so far, as independent reviewers, we thought that may be proved useful to publicly share with the interested author, especially the young one, some practical implementations of our ideas for the interactive representation of data using 3D/4D movement and animation, in an attempt to motivate and support him in the development of similar dynamic presentations, when he is looking for a way to locate the stronger aspects of his research results in order to prepare a clear, most appropriate for publication, static presentation figure. For this purpose, we selected to demonstrate a number of presentations, from the simplest to the most complicated, concerning well-known antenna issues with rather hard to imagine details, as it happens perhaps in cases involving Spherical Coordinates and Polarization, which we created to enrich the very first ever made Virtual Laboratories of Antennas, that we distribute over the Open Internet through our website Virtual Antennas. These presentations were developed in a general way, without using antenna simulators, to handle output text and image data from third-party CAS Computer Algebra Systems, such as the Mathematica commercial software we use or the Maxima FLOSS we track its evolution.

Introduction

The very first ever made Virtual Laboratories of Antennas, which are available on the Internet through Virtual Antennas website [1], are exclusively based on our alternative form of Antenna Theory [2], and are founded, by applying the learning by

teaching method to Antennas education [3], in order to support the quick comprehension of 3D space matters unavoidably related to antennas. The initial material of Virtual Antennas was prepared during the years 1996-1997 and presented to Antenna students during the spring seme-

Presentation Development and Use

ster of 1998 [4]. On 1999, the existence of this visual material was announced to the first ever appeared on the web EMLIB Electromagnetics Library, maintained those years by Jet Propulsion Laboratory of NASA [5]. On the same year, all of the material was approved for inclusion to MathSource repository of Mathematica [6].

Since 2000 and until today, the Virtual Antennas material is constantly increased and improved. Moreover, a number of websites either use this material or suggest its use [7]. On 2009, a sample of its current development state was approved for publication by the Wolfram Demonstrations Project [8], an event that was announced in our Creative Commons Network web pages [9].

During the last years, our voluntary reviewing work revealed some needs of potential authors -especially the young ones- related to the presentation of their research results, which perhaps may be confronted by similar to our interactive presentation techniques, and thus we decided to present in this paper our continuing work for the Virtual Laboratories of Antennas.

The implementation of a presentation idea demands the expression of the theoretical idea formulation in the CAS language we select to produce output data in the appropriate file format for movement or/and animation (we would like to emphasize that in the case of Mathematica we use, while we abandoned the package written by Novak [10], we still run the one written by Donley [11]). These files are: (a) WRL (WoRLd: Open by Web3D Consortium), a plain text file with a known structure described in the VRML Virtual Reality Modeling Language [12] for a visual object, (b) a bunch of images in a selected non-destructive format; usually BMP, and (c) NBP text file (Note Book Player: Mathematica proprietary). After that, the development of the presentation requires: (a) either a text editor to correct bugs or to add special features into WRL output file, (b) a graphics editor to align images or correct blemishes, as well as, a video editor to handle these images as frames of the final movie file in a selected format, usually AVI (Audio Visual Interleave: Microsoft proprietary). It is worth to notice that accord-

ing to our experience, the non-computing time needed: (a) to design the idea implementation, has been reduced by the years, from a couple of weeks at the beginning to just a couple of days now, and (b) to develop the presentation, after a tedious, routine work of editing each frame, varies considerably according to the frame theme, e.g. from 1.5 minutes for that in Fig. 7, to 10 minutes of Fig. 10.

The software needed for presentations to work under MS Windows is: a web browser (MS-IE 3.02r+), a VRML viewer add-on to that browser (World-View 2.1), an AVI player (Mplayer2), and the Mathematica 7 Notebook Player.

3D/4D Presentation Samples

In order to abbreviate the figure descriptions in the following, we have to notice that: (a) for every animation presentation, a typical full-window screen capture of the recommended AVI player is shown after its pause button was pressed, (b) for every movement presentation, a typical full-window screen capture of the recommended online WRL viewer, with a cursor perhaps to indicate the existence of an additional feature, and (c) for both presentation types, the basic colors (R, G, B) are used in

that order to correspond either to the CCS Cartesian Coordinate System (x, y, z) axes, (xoy, yoz, zox) planes, and its unit vectors, or to the SCS Spherical Coordinate System (r -radius, θ -semi-circle, ϕ -circle) curves, (r -sphere, θ -semi-cone, ϕ -semi-plane) surfaces, and its unit vectors, while the same color correspondence holds for the radiation pattern cuts by the mentioned CCS planes or SCS surfaces.

After that, short descriptions of the samples, are following, while all of these presentations will be always available in authors' group repositories in Virtual Antennas [13] and Google Code Repository [14].

Fig. 1 shows 1 frame out of 12 of an AVI repeated-for-ever animation for the 3D plane-time presentation of the considered as time-harmonic sinusoidal current wave amplitude, on a 3 wavelengths portion of a long thin wire loop antenna terminated on some complex impedance. The propagated current wave p is decomposed in the dual couples: (incident wave i , reflected wave r) and (standing wave s , transmitted wave t), while the imposed letters and arrows on the figure indicate these current waves as well as the direction of their motion.

Fig. 2 shows a screen-shot of a WRL presentation with 5 additional predefined view points of 12 frames animation, as the cursor indicates, of a 4D space-time asynchronous movement, from a view-point in the 1st-octant. In essence, this presentation is an alternative geometric meaning of the considered as standing wave current on an adequate length of a thin wire dipole antenna.

Fig. 3 shows a screen-shot of a WRL presentation of 4D space-time asynchronous movement from a view point in the 1st-octant, of the 3D difference volume element formed by adjacent SCS coordinate surfaces and lying between the 1st and 2nd octant.

Fig. 4 shows a screen-shot of a WRL presentation of a 4D space-time asynchronous movement from a view-point in the 1st-octant, for the triples of SCS unit vectors in the shown directions, that is 13 triples on the CCS main-planes, as well as, 2 undefined triples on the irregular z-axis of the CCS-to-SCS transformation.

Fig. 5 shows a screen-shot of a WRL presentation of a 4D space-time asynchronous movement from a view-point in the 1st-octant, for all 3 SCS surfaces, curves, and unit vectors in a direction of the 1st- octant.

Fig. 6 shows 1 frame out of 37 of an AVI animation for the 4D plane-time presentation of a SCS phi-circle curve as the intersection between 2 SCS surfaces, that is of a r-sphere and a theta-semi-cone, while theta angle -which changes from 0° to 180° - has the value of 50° . Different colors illustrate the inner and outer surfaces of the r-sphere and a cut off spherical section between adjacent meridians permit us to see the interior of that sphere.

Fig. 7 shows a screen-shot of a WRL presentation of a 4D space-time asynchronous movement for three different polarizations at three different points: linear, circular and elliptical on each of the coordinate axes x, y and z respectively to emphasize that, in general, the polarization of an antenna is not constant.

Fig. 8 shows 1 frame out of 20 of an AVI animation for the 4D space-time presentation of the non-linearly CCW polarized time-harmonic real electric field E, from an antenna, as well as, its decomposition to two linearly polarized time-harmonic real electromagnetic fields, as they are uniquely defined by the constant of time linearly independent space vectors E_c and E_s .

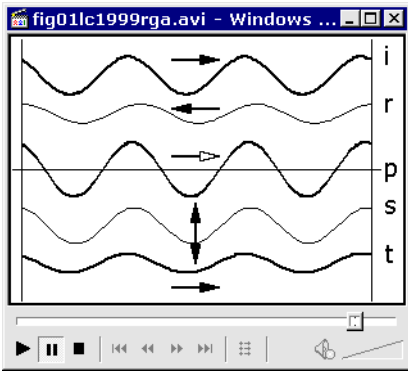


Fig. 1: Current waves

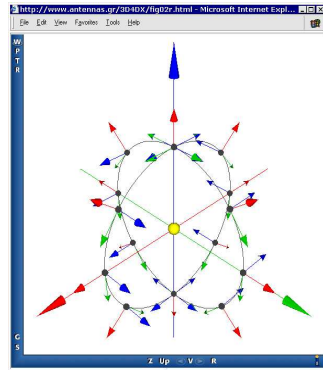


Fig. 4: SCS: Unit vectors

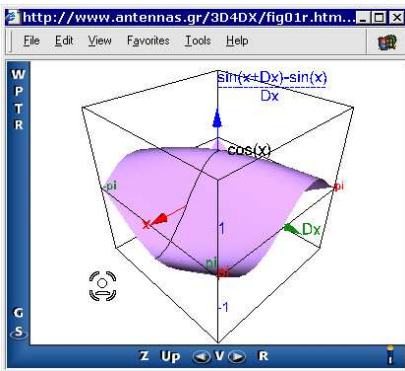


Fig. 2: Standing current-voltage waves relation

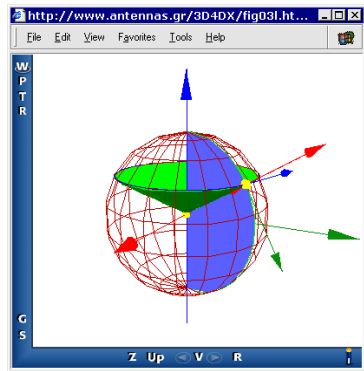


Fig. 5: Coordinate curves, surfaces and unit vectors

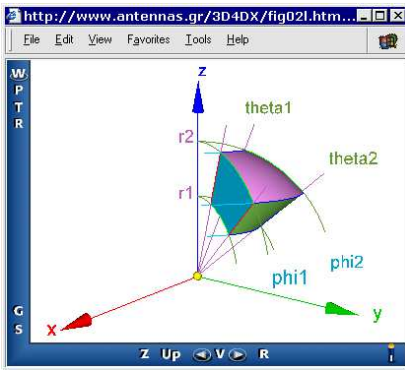


Fig. 3: SCS: Volume element

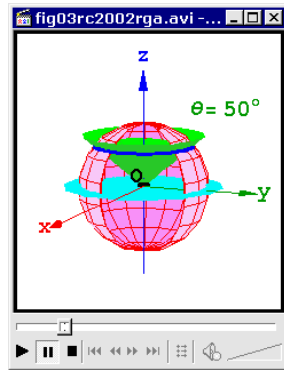


Fig. 6: Coordinate surfaces

Fig. 9 shows the last frame out of 23 of an AVI animation for the 4D space-time presentation of the path traced by the electric far-field arrow tip, which is CW elliptically polarized in the direction of y-axis.

Fig. 10 shows 1 frame out of 19 of an AVI for the 4D space-time presentation of a normalized CCW elliptically polarized electromagnetic far-field in the shown direction of propagation, from a point of view in the 1st octant of an observer mirrored to (r, theta) plane.

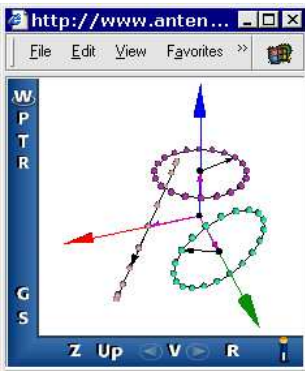


Fig. 7: Polarization: Directional dependence

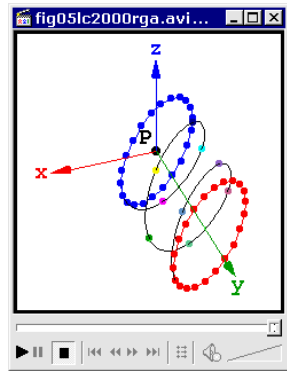


Fig. 9: Polarization: CW elliptical

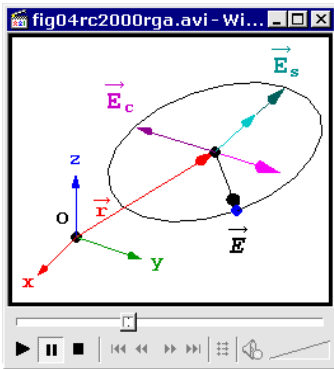


Fig. 8: Polarization: Non-linear CCW

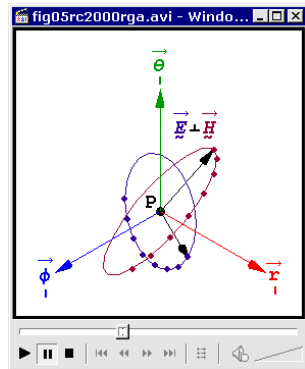


Fig. 10: Polarization: Far-Field CCW elliptical.

Fig. 11 shows 3 frames out of 73 of an AVI for the 4D space-time presentation of the direction dependency of antenna polarization from a center fed short crossed dipoles on y and z axes, which have a current phase difference of 90° . The three different polarizations are shown with their orientation for an observer on the xOy plane (theta = 90° and in three different phi angles of 0° , 240° and 270°).

Fig. 12 shows 4 frames out of 38 of an AVI animation for the 4D space-time presentation of the space radiation pattern and its three main-planes cuts, for the specific case of an antenna consisting of 2 dipoles, with the same direction of the unit vector (0.2, 0.4 0.894), each of 2.4λ length long, with their centers placed 0.25λ apart on an axis with a unit directional vector (0.3 0.5 0.812), fed with a 30° current phase difference.

Fig. 13 shows a screenshot of a WRL presentation with 1 additional predefined view point of 12 frames animation possibility, as the cursor indicates, of a 4D space-time asynchronous movement, from a view-point in the 1st-octant. This presentation concerns the interior of an anechoic chamber and imitates a discone antenna

rotation in order to visualize the way by which the measurement of a plane-cut of its radiation pattern is accomplished.

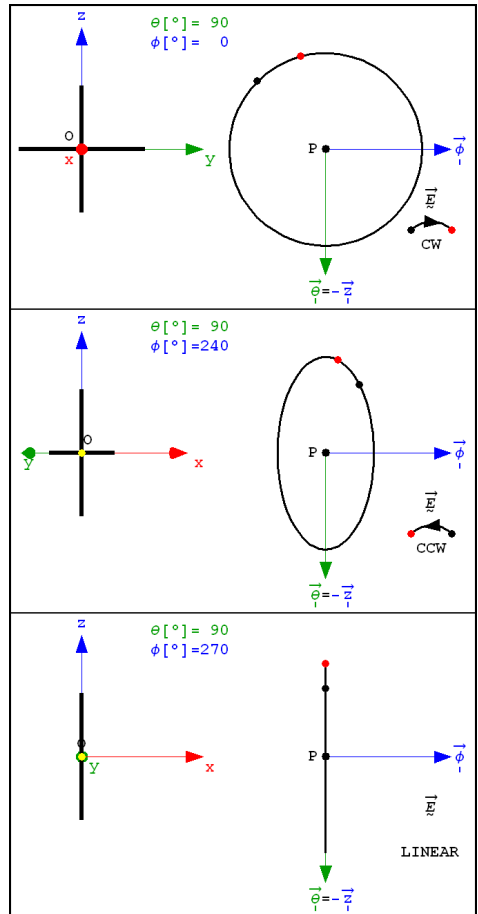


Fig. 11: Polarization: CW Circular - CCW Elliptical - Linear

Fig. 14 shows a sophisticated combination of a movement with an animation presentation, which in fact is an application that was developed using the version 7 of Mathematica, in a way that permits the definition of any (θ, ϕ) direction in space for a dipole of variable length. Notably, this application has all the available VRML movement features, with 6 predefined view points, while 3 different animations can be run simultaneously. In addition, the

mesh, opacity, rendering goal, and the evaluation step for the radiation pattern can be also defined.

Fig. 15 shows the last frame out of 100 of an AVI for the 4D space-time presentation of a detailed study for some of the linear dipole characteristics regarding the plane and space radiation patterns, the direction from the dipole axis of their first common maximum, the directivity, and the input radiation resistance; this really is a 4-tuple of frames.

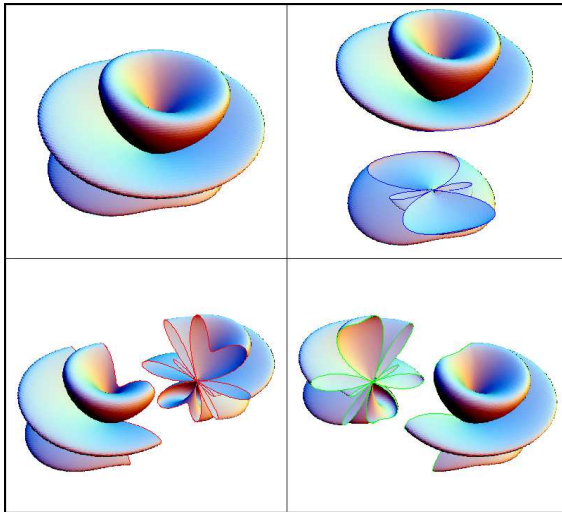


Fig. 12: Radiation Pattern: 3D and its 2D main-plane cuts

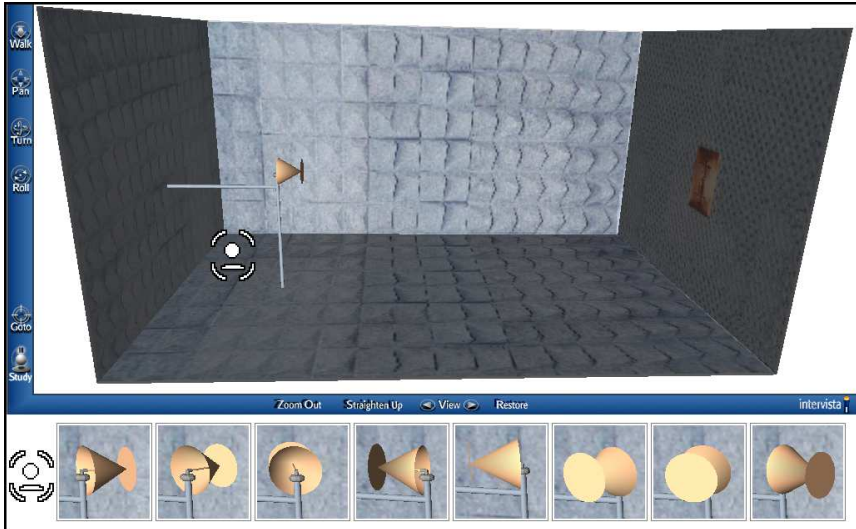


Fig. 13: Anechoic chamber – discone antenna

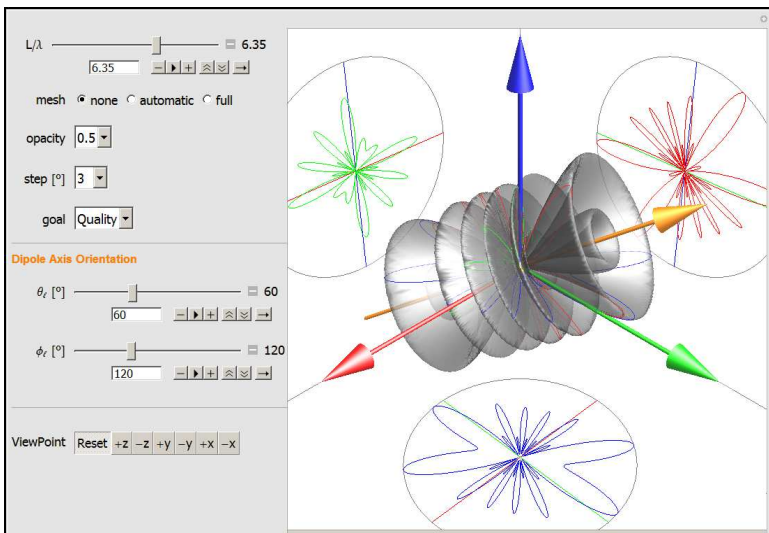


Fig. 14 Radiation Pattern: A composite 3D/4D presentation

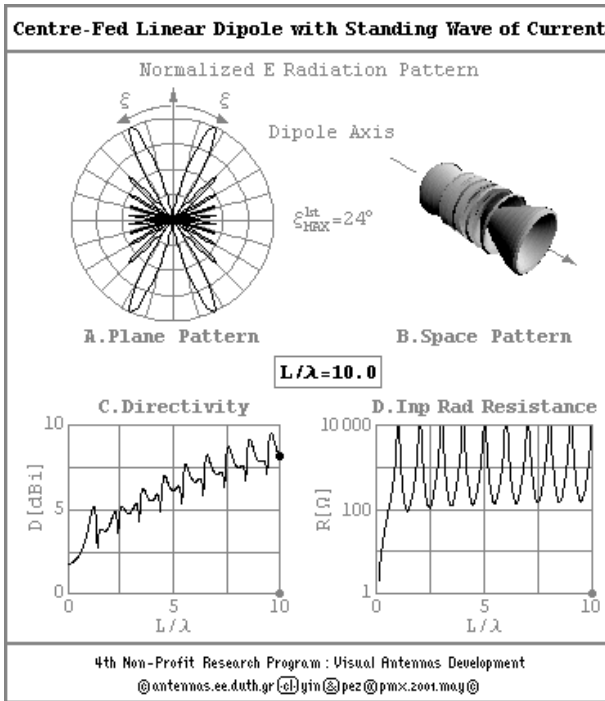


Fig. 15: Antenna characteristics

Conclusion

The Antennas Research Group (ARG) carries on for the enhancement of this low-cost Virtual Laboratory with new material placed to web site www.antennas.gr [13], as well as to Google Code Repository [14], and Fig. 13 and Fig. 14 are only two of many more possible examples.

The evolution on computer systems in recent years has increased the demand for new teaching, learning and re-

searching methodologies, which this paper supports by describing available material for a web-based Virtual Laboratory for Antennas that provides interactive computer aided visualization in various Antenna Theory topics.

The main goal is constantly attained since this continuously developed material cannot be produced by the means of the conventional literature.

References *

- [1] ANTENNAS RESEARCH GROUP, "Virtual Antennas 1996-2011"
"www.antennas.gr"
 - [2] Zimourtopoulos P., Yannopoulou N., "Antennal Calculus",
(forthcoming book) "www.antennas.gr/zyacbook/"
 - [3] WIKIPEDIA, "Learning by Teaching"
"http://en.wikipedia.org/wiki/Learning_by_teaching"
 - [4] VIRTUAL ANTENNAS, "An On-Line Course", DUTH Computer
Center, Spring 1998
"www.antennas.gr/TheLaboratory/VirtualAntennas/VirtualA
ntennas33A.htm"
 - [5] EMLIB, "EM Educational Resources: Virtual Antennas",
Last modified: 14 January 1999 - Wayback Machine:
"http://web.archive.org/web/19990221012605/emlib.jpl.na
sa.gov/EMLIB/education.html"
 - [6] Yannopoulou N., Zimourtopoulos P., "Virtual Antennas",
Antennas Research Group DUTH, 1999-2000
"http://library.wolfram.com/database/MathSource/868"
 - [7] VIRTUAL ANTENNAS, Backlinks
"www.antennas.gr/backlinks/"
 - [8] Yannopoulou N., Zimourtopoulos P., "Dipole Antenna Ra-
diation Pattern", Wolfram Demonstrations Project, 2009
"http://demonstrations.wolfram.com/DipoleAntennaRadiatio
nPattern"
 - [9] CREATIVE COMMONS NET, Licensed Works
"http://creativecommons.net/yin/"
"http://creativecommons.net/pez/"
 - [10] Noval J.M., "Arrow3D 1.0 Package for Mathematica", 1996
"http://forums.wolfram.com/mathgroup/archive/1998/Mar/m
sg00102.html"
 - [11] Donley E.H., "VRMLConvert 1.0 Package for Mathematica",
1996 ["www.ma.iup.edu/projects/VRMLConvert/"]
"http://ftp.carnet.hr./misc/VRML/utilities/converters/"
 - [12] ISO/IEC 14772-1:1997, 14772-2:2004, "Virtual Reality
Modeling Language (VRML97 Specifications)"
"www.web3d.org/x3d/specifications/vrml/ISO-IEC-14772-VR
ML97"
 - [13] ANTENNAS RESEARCH GROUP, File Repository
"www.antennas.gr/3D4DX"
 - [14] GOOGLE CODE, Antennas Research Group File Repository
"http://code.google.com/p/rga/"
- * Active Links: 30.01.2014 - Inactive Links : FTP#J Link
Updates: "http://updates.ftpj.otoiser.org/"

Preprint Versions

"Support of Interactive 3D/4D Presentations by the
Very First Ever Made Virtual Laboratories of Antennas"
Nikolitsa Yannopoulou, Petros Zimourtopoulos
"http://arxiv.org/abs/1102.4241"

Previous Publication in FUNKTECHNIKPLUS # JOURNAL

"Measurement Uncertainty in Network Analyzers:
Differential Error Analysis of Error Models Part 3:
Short One-Port Calibration – Comparison"
Issue 2, pp. 41-49

* About The Authors

Nikolitsa Yannopoulou, Issue 1, p. 15

Petros Zimourtopoulos, Issue 1, p. 15

Near-field Method in Solving Inverse Scattering Problem of Spherical Electromagnetic Waves in Chiral media

Nikolaos M. Berketis *

Independent Researcher, Athens, Greece

Abstract

We have developed two methods to study an inverse scattering problem of electromagnetic waves in chiral media, for a spherical scatterer perfect conductor. The first called Far-field inverse problem was described analytical in our previous work. The second called Near-field method is given in detail in the present paper. It is a geometrical method based on the scattered fields. Using Near-field experiments, in which the scattered field is measured at the source, we solve the corresponding inverse scattering problem that is to determine the coordinates of the center and the radius of the spherical scatterer.

Introduction

We study an inverse scattering problem of electromagnetic waves with time harmonic dependence applying the method of Near-field [1]-[3]. Spherical electromagnetic waves generated by a point source incident on a spherical scatterer perfect conductor in a chiral media.

Knowing the incident and scattered wave fields in the inverse problem we are looking for the coordinates of the sphere center and its radius.

The corresponding problem is solved by geometrical methods using either energy scattering cross-section, or

the scattered fields. In the first case we refer to the inverse Far-field problem [4] and in the second case to a Near-field inverse problem.

The chiral materials exhibit the phenomenon of optical activity i.e., the phenomenon that in which the plane of polarizations of linearly polarized light is rotated as the light passes through an optically active medium.

The chirality is a property which is often found in nature and reflects the asymmetry in the spatial inversion. An electromagnetic wave into a chiral media is analyzed in a counter-clockwise

(LCP) and a clockwise (RCP) Beltrami field. Using vector spherical harmonic functions and appropriate expansions of the Beltrami fields and by extension the development of spherical electromagnetic waves in spherical wave functions, we calculate the exact solution of the scattering problem for a spherical perfect conductor in chiral media, and the corresponding back scattering [3]-[4].

In the inverse problem we calculate the scattered Near-field, when the source is in position $\mathbf{r} = \mathbf{r}_0$. A similar problem for achiral materials has been studied in the works [1], [2].

Statement of the problem

Consider a point source at the position \mathbf{r}_0 that produces spherical electromagnetic waves in a chiral media near a scatterer Ω^- , perfect conductor, i.e. the surface of the boundary condition is satisfied

$$\hat{\mathbf{n}} \times (\mathbf{E}^{inc}(\mathbf{r}) + \mathbf{E}^{sc}(\mathbf{r})) = \mathbf{0} \quad (1)$$

$r = a$

We consider that the exterior $\Omega^+ = \mathbb{R}^3 / \Omega^-$ of the scatterer is homogeneous chiral media with fixed chirality β , dielectric constant ϵ and magnetic permeability μ .

A spherical incident electromagnetic wave $(\mathbf{E}_{\mathbf{r}_0}^{inc}(\mathbf{r}), \mathbf{H}_{\mathbf{r}_0}^{inc}(\mathbf{r}))$ with time harmonic dependence in accordance with the Bohren transformation, analyzed in spherical Beltrami fields $\mathbf{Q}_{L,\mathbf{r}_0}^{inc}(\mathbf{r})$ and $\mathbf{Q}_{R,\mathbf{r}_0}^{inc}(\mathbf{r})$ as follows:

$$\begin{cases} \mathbf{E}_{\mathbf{r}_0}^{inc}(\mathbf{r}) = \mathbf{Q}_{L,\mathbf{r}_0}^{inc}(\mathbf{r}) + \mathbf{Q}_{R,\mathbf{r}_0}^{inc}(\mathbf{r}) \\ \mathbf{H}_{\mathbf{r}_0}^{inc}(\mathbf{r}) = \frac{1}{i\eta} (\mathbf{Q}_{L,\mathbf{r}_0}^{inc}(\mathbf{r}) - \mathbf{Q}_{R,\mathbf{r}_0}^{inc}(\mathbf{r})) \end{cases} \quad (2)$$

where $\eta = (\mu/\epsilon)^{1/2}$ is the intrinsic impedance of the chiral medium. The Beltrami fields satisfy the equations, [5], [6],

$$\begin{cases} \nabla \times \mathbf{Q}_{L,\mathbf{r}_0}(\mathbf{r}) = \gamma_L \mathbf{Q}_{L,\mathbf{r}_0}(\mathbf{r}) \\ \nabla \times \mathbf{Q}_{R,\mathbf{r}_0}(\mathbf{r}) = -\gamma_R \mathbf{Q}_{L,\mathbf{r}_0}(\mathbf{r}) \end{cases} \quad (3)$$

where γ_L, γ_R are wave numbers for Beltrami fields and are given by,

$$\gamma_L = \frac{k}{1 - k\beta}, \gamma_R = \frac{k}{1 + k\beta} \quad (4)$$

With $k = \omega(\epsilon\mu)^{1/2}$, ω being the angular frequency. The indices L and R denote the LCP and RCP fields respectively. The spherical incident Beltrami fields with suitable normalization have the form, as defined in the following works: [4] (issue 2, p. 9, relations (4), (5)), and [3].

If $\mathbf{Q}_{L,r_0}^{inc}(\mathbf{r})$ and $\mathbf{Q}_{R,r_0}^{inc}(\mathbf{r})$ are Beltrami fields corresponding via transformation to Bohren in $\mathbf{E}_{r_0}^{inc}$ and $\mathbf{H}_{r_0}^{inc}$, then the scattering problem for the perfect conductor can be formulated in the following way: be found $\mathbf{Q}_{L,r_0}^{tot}(\mathbf{r})$, $\mathbf{Q}_{R,r_0}^{tot}(\mathbf{r})$, which belong to the space $C^1(\Omega^+) \cap C(\overline{\Omega^+})$, such that:

$$(i): \begin{cases} \nabla \times \mathbf{Q}_{L,r_0}^{tot}(\mathbf{r}) = \gamma_L \mathbf{Q}_{L,r_0}^{tot}(\mathbf{r}) \\ \nabla \times \mathbf{Q}_{R,r_0}^{tot}(\mathbf{r}) = -\gamma_R \mathbf{Q}_{R,r_0}^{tot}(\mathbf{r}) \\ \mathbf{r} \in \Omega^+ \end{cases}$$

$$(ii): \hat{\mathbf{n}} \times \mathbf{Q}_{L,r_0}^{tot}(\mathbf{r}) = -\hat{\mathbf{n}} \times \mathbf{Q}_{R,r_0}^{tot}(\mathbf{r}) \quad (5)$$

$$\mathbf{r} \in S = \partial\Omega^-$$

$$(iii): \begin{cases} \hat{\mathbf{r}} \times \mathbf{Q}_{L,r_0}^{sc}(\mathbf{r}) + i\mathbf{Q}_{L,r_0}^{sc}(\mathbf{r}) = o(\frac{1}{r}) \\ \hat{\mathbf{r}} \times \mathbf{Q}_{R,r_0}^{sc}(\mathbf{r}) - i\mathbf{Q}_{R,r_0}^{sc}(\mathbf{r}) = o(\frac{1}{r}) \\ r \rightarrow \infty \end{cases}$$

The limits on radiation conditions (5(iii)), are taken uniformly in all directions $\hat{\mathbf{r}} \in S^2$, where S^2 is the unit sphere in \mathbb{R}^3 and $\hat{\mathbf{n}}$ is the outward normal unit vector perpendicular to the surface on the scatterer.

The incident electromagnetic wave ($\mathbf{E}_{r_0}^{inc}(\mathbf{r})$, $\mathbf{H}_{r_0}^{inc}(\mathbf{r})$) on the scatterer Ω^- generates the corresponding scattered field

($\mathbf{E}_{r_0}^{sc}(\mathbf{r})$, $\mathbf{H}_{r_0}^{sc}(\mathbf{r})$). The scattered electric field will be depended on the polarizations $\hat{\mathbf{p}}_L$, $\hat{\mathbf{p}}_R$, (see [4] (issue 2, p. 9, relation (6))) and will have the decomposition

$$\mathbf{E}_{r_0}^{sc}(\mathbf{r} | \hat{\mathbf{p}}_L, \hat{\mathbf{p}}_R) = \mathbf{Q}_{L,r_0}^{sc}(\mathbf{r} | \hat{\mathbf{p}}_L, \hat{\mathbf{p}}_R) + \mathbf{Q}_{R,r_0}^{sc}(\mathbf{r} | \hat{\mathbf{p}}_L, \hat{\mathbf{p}}_R) \quad (6)$$

where $\mathbf{Q}_{L,r_0}^{sc}(\mathbf{r} | \hat{\mathbf{p}}_L, \hat{\mathbf{p}}_R)$ and $\mathbf{Q}_{R,r_0}^{sc}(\mathbf{r} | \hat{\mathbf{p}}_L, \hat{\mathbf{p}}_R)$ are the corresponding scattered Beltrami fields which have the following behavior, when $r \rightarrow \infty$, [5], [7],

$$\mathbf{Q}_{A,r_0}^{sc}(\mathbf{r} | \hat{\mathbf{p}}_L, \hat{\mathbf{p}}_R) = h_0(\gamma_A r) \cdot \mathbf{g}_{A,r_0}(\hat{\mathbf{r}} | \hat{\mathbf{p}}_L, \hat{\mathbf{p}}_R) + o(\frac{1}{r^2}) \quad (7)$$

with $A = L, R$. The functions \mathbf{g}_{L,r_0} and \mathbf{g}_{R,r_0} are the LCP and RCP far-field patterns respectively, which are defined by the following relationship [7],

$$\mathbf{g}_{A,r_0}(\hat{\mathbf{r}} | \hat{\mathbf{p}}_L, \hat{\mathbf{p}}_R) = \int_S \hat{\mathbf{n}} \times [Y_A \nabla \times \mathbf{E}_{r_0}^{sc}(\mathbf{r}' | \hat{\mathbf{p}}_L, \hat{\mathbf{p}}_R) - \varpi_A \gamma^2 \mathbf{E}_{r_0}^{sc}(\mathbf{r}' | \hat{\mathbf{p}}_L, \hat{\mathbf{p}}_R) e^{-i\gamma_A \mathbf{r} \cdot \mathbf{r}'} ds(\mathbf{r}') \quad (8)$$

$$\text{With } \varpi_A = \begin{cases} -1, A = L \\ 1, A = R \end{cases}, \quad \gamma^2 = \gamma_L \gamma_R.$$

Near-field Inverse problem

Using the exact solution found in the paper [4] (issue 2, pp. 10-12) and considering appropriate asymptotic forms of the Bessel and Hankel functions in low frequencies, i.e. $|y_A a| \ll 1$, calculate asymptotic expressions of the coefficients a_n^L , a_n^R , b_n^L and b_n^R . Specifically we have [3],

$$\begin{aligned}
 a_n^L &\sim \frac{1 + \beta k}{2i\zeta_n^2(2n + 1)} (y_L a)^{2n+1} \\
 y_L a &\rightarrow 0 \\
 a_n^R &\sim -\frac{i}{2n\zeta_n^2} \frac{(1 - \beta k)^{n+2}}{(1 + \beta k)^{n+1}} (y_L a)^{2n+1}
 \end{aligned} \tag{9}$$

$$\begin{aligned}
 \mathbf{E}_{r_0}^{sc}(\mathbf{r}_0 | \hat{\mathbf{p}}_L) &= \\
 &= \sum_{n=1}^{\infty} \frac{n(n+1)}{2} B_n^L a_n^L \{ (h_n(y_L r_0) \hat{\mathbf{x}} + \tilde{h}_n(y_L r_0) \hat{\Psi}) + i(\tilde{h}_n(y_L r_0) \hat{\mathbf{x}} - h_n(y_L r_0) \hat{\Psi}) \} + \\
 &+ \sum_{n=1}^{\infty} \frac{n(n+1)}{2} B_n^L a_n^R \{ (h_n(y_R r_0) \hat{\mathbf{x}} - \tilde{h}_n(y_R r_0) \hat{\Psi}) + i(-\tilde{h}_n(y_R r_0) \hat{\mathbf{x}} - h_n(y_R r_0) \hat{\Psi}) \}
 \end{aligned} \tag{11}$$

Using the asymptotic relations:

$$\begin{aligned}
 \frac{h_n(y_A r_0)}{h_0(y_A r_0)} &\sim \frac{\zeta_n}{(y_A r_0)^n} \\
 \frac{\tilde{h}_n(y_A r_0)}{h_0(y_A r_0)} &\sim \frac{-n\zeta_n}{(y_A r_0)^{n+1}} \\
 \tilde{h}_n(y_A a) &\sim -\frac{n\zeta_n}{i(y_A a)^{n+2}}
 \end{aligned} \tag{12}$$

or

$$\begin{aligned}
 b_n^L &\sim -\frac{i}{2n\zeta_n^2} \frac{(1 + \beta k)^{n+2}}{(1 - \beta k)^{n+1}} (y_R a)^{2n+1} \\
 y_R a &\rightarrow 0
 \end{aligned} \tag{10}$$

$$b_n^R \sim -\frac{i(1 - \beta k)}{2\zeta_n^2(2n + 1)} (y_R a)^{2n+1}$$

Where

$$\zeta_n = 1 \cdot 3 \cdot 5 \cdots (2n - 1) = (2n)! / (2^n n!)$$

In the inverse problem we calculate the scattered Near-field in the source $\mathbf{r} = \mathbf{r}_0$. By the relation (21), in work [4], with $\mathbf{r} = \mathbf{r}_0$ and for LCP incidence, we obtain [3],

with $y_A r_0 \rightarrow 0$, $A = L, R$ and the series,

$$\begin{cases} \sum_{n=1}^{\infty} \tau^{2n+1} = \frac{\tau^3}{1 - \tau^2} \\ \sum_{n=1}^{\infty} n^2 \tau^{2n+1} = \frac{\tau^3(1 + \tau^2)}{(1 - \tau^2)^3} \end{cases} \tag{13}$$

$$\sum_{n=1}^{\infty} (2n + 1) \tau^{2n+1} = \frac{\tau(3\tau^2 - \tau^4)}{(1 - \tau^2)^2} \tag{14}$$

$$\sum_{n=1}^{\infty} n(2n+1)\tau^{2n+1} = \frac{\tau(3\tau^2 + \tau^4)}{(1-\tau^2)^3} \quad (15)$$

$$\sum_{n=1}^{\infty} \frac{2n+1}{n} \tau^{2n+1} = \quad (16)$$

$$= \frac{\tau[\tau^2 \ln(1-\tau^2) + 2\tau^2 - \ln(1-\tau^2)]}{\tau^2 - 1}$$

and because of the relationships:

$$\frac{y_R}{y_L} = \frac{1 - \beta k}{1 + \beta k}, \quad 0 < \tau < 1,$$

where $\tau = a/r_0$, we obtain from (11) [3],

$$\mathbf{E}_{r_0}^{sc}(\mathbf{r}_0 | \hat{\mathbf{p}}_L) \sim \quad (17)$$

$$\sim \frac{(1 + \beta k)}{2(y_L a)^2} \frac{\tau^5}{(1 - \tau^2)^3} \cdot \hat{\mathbf{p}}_L$$

Therefore the measure of the scattered field $\mathbf{E}_{r_0}^{sc}(\mathbf{r}_0 | \hat{\mathbf{p}}_L)$ is

$$|\mathbf{E}_{r_0}^{sc}(\mathbf{r}_0 | \hat{\mathbf{p}}_L)| \sim \frac{(1 + \beta k)}{2(y_L a)^2} \frac{\tau^5}{(1 - \tau^2)^3} \quad (18)$$

$$y_L a \rightarrow 0$$

Similarly for the RCP incidence, we have that

$$|\mathbf{E}_{r_0}^{sc}(\mathbf{r}_0 | \hat{\mathbf{p}}_R)| \sim \frac{(1 - \beta k)}{2(y_R a)^2} \frac{\tau^5}{(1 - \tau^2)^3} \quad (19)$$

$$y_R a \rightarrow 0$$

Finally, based on the relationships (18) and (19), we conclude that

$$|\mathbf{E}_{A,r_0}^{sc}(\mathbf{r}_0 | \hat{\mathbf{p}}_A)| \sim \quad (20)$$

$$\sim \frac{(1 - \varpi_A \beta k)}{2(y_A a)^2} \frac{\tau^5}{(1 - \tau^2)^3}$$

$$y_A a \rightarrow 0, \quad A = L, R$$

Choose a Cartesian coordinate system $Ox\psi z$, and five point-source locations, namely $O(0, 0, 0)$, $A_1(l, 0, 0)$, $A_2(0, l, 0)$, and $A_4(0, 0, 2l)$, which are at (unknown) distances r_0 , r_1 , r_2 , r_3 and r_4 , respectively from the sphere's center K . The parameter l is a chosen fixed length. The sizes of the resulting five measurements $|\mathbf{E}_{A,r_j}^{sc}(\mathbf{r}_j | \hat{\mathbf{p}}_A)|$ are

$$M_j = \frac{2(y_L y_R)l}{(1 - \varpi_A \beta k)} |\mathbf{E}_{A,r_j}^{sc}(\mathbf{r}_j | \hat{\mathbf{p}}_A)| \quad (21)$$

and

$$\rho_j = \frac{r_j}{l}, \quad b = \sqrt{\frac{a}{l}} \quad (22)$$

where $j = 0, 1, 2, 3, 4$. Therefore we have the following five measurements

$$M_j = \frac{b^5 \rho_j}{(\rho_j^2 - b^4)^3} \quad (23)$$

with $\rho_j > b^2 > 0$. Applying the law of cosines in triangle KOA_4 and using that

$$r_j = \rho_j l \quad (24)$$

we obtain

$$\rho_4 = 2 + 2\rho_3 - \rho_0 \quad (25)$$

Because of (24), we take

$$\rho_j^6 - 3\rho_j^4 b^4 + 3\rho_j^2 b^8 - b^{12} - b^5 \frac{\rho_j}{M_j} = 0 \quad (26)$$

Thus in equation (26) identified the ρ , with $j=0, 1, 2, 3, 4$. If the radius a of the sphere is known, solve the system of six algebraic equations (25) and (26). Also if you consider that the radius

a is too small so that $a \ll 1$, then the relationship (23) shows [3],

$$M_j = \frac{b^5}{\rho_j^5} \quad (27)$$

so we have the following system of equations

$$\begin{cases} \rho_4 = 2 + 2\rho_3 - \rho_0 \\ \rho_j^5 M_j - b^5 = 0 \end{cases} \quad (28)$$

where $j = 0, 1, 2, 3, 4$.

References

- [1] Athanasiadis C., Martin P.A., Stratis I.G., "On spherical-wave scattering by a spherical scatterer and related near-field inverse problems", IMA Journal of Applied Mathematics, Vol. 66, 2001, pp. 539-549
- [2] Athanasiadis C., Martin P.A., Stratis I.G., "On the Scattering of Point-generated Electromagnetic Waves by a perfectly Conducting Sphere, and Related Near-field Inverse Problems", Zeitschrift für Angewandte Mathematik und Mechanik, Vol. 83, Issue 2, 2003, pp. 129-136
- [3] Berketis M. Nikolaos, "Scattering spherical Electromagnetic waves in chiral media", PhD thesis, University of Athens - Department of Mathematics, December 2007
- [4] Berketis N.M., "Direct and related far-field inverse scattering problems for spherical electromagnetic waves in chiral media", FunkTechnikPlus # Journal, Issue 2, November 2013, pp. 7-18
["www.otoiser.org/index.php/ftpj/article/view/26"](http://www.otoiser.org/index.php/ftpj/article/view/26)
- [5] Lakhtakia A., "Beltrami Fields in Chiral Media", World Scientific, Singapore, 1994, §2-1.3 (pp. 42-44), §2-2.3 (pp. 49-52), §4-1 (p. 130 Chapter 4), §5-1 (p. 164 Chapter 5), §6-1.1 (pp. 214-397), §8-2.1 (pp. 391-397), §9-2.3 (pp. 468- 473)

- [6] Lakhtakia A, Varadan V.K., Varadan V.V., "Time-Harmonic Electromagnetic Fields in Chiral Media", Lecture Notes in Physics, Vol. 335, Springer, Berlin, 1989, §3-§4-§7-§11-§12-§13
- [7] Athanasiadis C., "On the far field patterns for electromagnetic scattering by a chiral obstacle in a chiral environment", Journal of Mathematical Analysis and Applications, Vol. 309, 2005, pp. 517-533
- [8] Morse P.M, Feshbach H., "Methods of Theoretical Physics, Part II", Mc Graw-Hill, 1953, pp. 1864-1866, 1870, 1871, 1887

Previous Publication in FUNKTECHNIKPLUS # JOURNAL

"Direct and Related Far-Field Inverse Scattering Problems for Spherical Electromagnetic Waves in Chiral Media", Issue 2, pp. 7-18

Preprint Versions

"Direct and inverse scattering problems for spherical Electromagnetic waves in chiral media", Christodoulos Athanasiadis and Nikolaos Berketis, "<http://arxiv.org/abs/0812.2169>"

*** About the Author**

Nikolaos Berketis, Issue 2, p. 18

[This Page Intentionally Left Blank]

[This Page Intentionally Left Blank]

In case of any doubt,
download the genuine papers from
genuine.ftpj.otoiser.org

FRONT COVER VIGNETTE

A faded synthesis of an anthemion rooted in a meandros

The thirteen-leaf is a symbol for a life tree leaf.
"Herakles and Kerberos", ca. 530–500 BC,
by Paseas, the Kerberos Painter,
Museum of Fine Arts, Boston.

www.mfa.org/collections/object/plate-153852

The simple meandros is a symbol for eternal immortality.
"Warrior with a phiale", ca. 480–460 BC,
by Berliner Maler,
Museo Archeologico Regionale "Antonio Salinas" di Palermo.

commons.wikimedia.org/wiki/File:Warrior_MAR_Palermo_NI2134.jpg

ISSN 2310-6697

toiser—open transactions on independent scientific-engineering research

FUNKTECHNIKPLUS # JOURNAL

Théorie—Expérimentation—Métrologie—Logiciel—Applications

ISSUE 4 – SATURDAY 31 MAY 2014 – YEAR 1

- 1 Contents
- 2 About
- 3 Editorial Board – Technical Support
- 4 Information for Peers – Guiding Principles
- # Electrical Engineering – Expérimentation
- 7 Interfaces in High Voltage Engineering: A Most Important Question for Conventional Solid Insulating Materials as well as for Nanocomposite Polymers
M.G. Danikas, R. Sarathi
- # Applied Electromagnetics – Théorie
- 33 Spherical Beltrami Fields in Chiral Media: Reciprocity and General Theorems
Nikolaos M. Berketis
- # Telecommunications Engineering – Applications
- 43 Self-Standing End-Fed Geometrically Uniform Linear Arrays: Analysis, Design, Construction, Measurements and FLOSS
K.Th. Kondylis, N.I. Yannopoulou, P.E. Zimourtopoulos
- # Electrical Engineering – Expérimentation
- 53 Parameters Affecting the Lifetime of Transformer Oil in Distribution Transformers: Parameter Monitoring of 50 Transformers from the Athens Area
M.G. Danikas, E. Rapti, I. Liapis, A.B.B.Abd. Ghani



About

This European Journal defends
honesty in science and ethics in engineering

Publisher – **otoiser** open transactions on independent scientific-engineering research – **ARG NP UoP** Antennas Research Group Non Profit Union of Persons – Hauptstraße 52, 2831 Scheiblingkirchen, Austria – **www.otoiser.org** – **www.antennas.gr**

Language – We declare the origins of the Journal by using English, German and French, as well as, a Hellenic vignette, in the cover page. However, since we recognize the dominance of USA English in technical literature, we adopted it as the Journal's language, although it is not our native language.

Focus – We consider Radio-FUNK, which still creates a vivid impression of the untouchable, and its Technology-TECHNIK, from an Advanced-PLUS point of view. That is, we dynamically focus at any scientific-engineering discipline producing FUNKTECHNIKPLUS Théorie, Expérimentation, Métrologie, Logiciel, ou Applications.

Scope – We emphasize this scope broadness by extending the title of the Journal with a Doppelkreuz-Zeichen #, which we use as a placeholder for the disciplines of Editorial Board:

Electrical – # Electronics – # Computer – # Telecommunications – Engineering # Computer Science # Applied Mathematics, etc.

Frequency – We regularly publish 3 issues per year on January, May, and September as well as an issue every 3 papers.

Editions – We follow the arXiv.org system, that is the 1st edition date of every issue is on the cover page and any update date is on the odd pages with its version on all pages.

Format – We use the uncommon for Journals A5 paper size and the much readable Liberation Mono fixed-space font, with hyphenation, justification, and unfixed word spacing, to display 2 pages side-by-side on widescreen monitors with WYSIWYG printout. We can consider only papers in ODF odt or MS doc format written in LibreOffice or MS Office with MathType. We use PDFCreator and PDF-Xchange to produce pdf and export to images for printing on demand and electronic publishing.

License – We use the free Open Journal System OJS from the PKP Public Knowledge Project for internet publication.

Copyright – Creative Commons Attribution 3 Unported CC-BY 3

Please download the latest *About* edition from
about.ftpj.otoiser.org

Editorial Board

Electrical Engineering

High Voltage Engineering # Insulating Materials

Professor Michael Danikas

EECE, Democritus University of Thrace, mdanikas@ee.duth.gr

Electrical Machines and Drives # Renewable Energies

Electric Vehicles

Assistant Professor Athanasios Karlis

EECE, Democritus University of Thrace, akarlis@ee.duth.gr

Computer Engineering # Software Engineering

Cyber Security

Associate Professor Vasileios Katos

EECE, Democritus University of Thrace, vkatos@ee.duth.gr

Internet Engineering # Computer Science

Simulation # Applied Education # Learning Management Systems

Lecturer Sotirios Kontogiannis

BA, TE Institute of Western Macedonia, skontog@gmail.com

Hypercomputation # Fuzzy Computation # Digital Typography

Dr. Apostolos Syropoulos, Xanthi, Greece

BSc-Physics, MSc-, PhD-Comp. Science, asyropoulos@yahoo.com

Applied Mathematics # Functional and Numerical Analysis

Applied Electromagnetics # Control Theory

Dr. Nikolaos Berketis, Athens, Greece

BSc-Math, MSc-Appl.Math, PhD-Appl.Math, nberketis@gmail.com

Telecommunications Engineering

Applied Electromagnetics # Metrology # Applied Education

Simulation # Virtual Reality # Amateur Radio # FLOSS

Applied Physics # Electronics Engineering

Dr. Nikolitsa Yannopoulou, Scheiblingkirchen, Austria

Diploma Eng-EE, MEng-EECE, PhD-EECE, yin@arg.op4.eu

Dr. Petros Zimourtopoulos, Scheiblingkirchen, Austria

BSc-Physics, MSc-Electronics-Radio, PhD-EE, pez@arg.op4.eu

Technical Support

Konstantinos Kondylis, Doha, Qatar

Diploma Eng-EECE, MEng-EECE, kkondylis@gmail.com

Christos Koutsos, Bratislava, Slovakia

Diploma Eng-EECE, MEng-EECE, ckoutsos@gmail.com

Information for Peers Guiding Principles

This is a small, but independent, low profile Journal, in which we are all – Authors – Reviewers – Readers – Editors – free at last to be Peers in Knowledge, without suffering from either:

- Journal roles or positions,
- Professional, amateur, or academic statuses, or
- Established impact factorizations,

but with the following Guiding Principles:

Authors – We do know what work means; and we do respect the research work of the scientist – engineer; and we do want to highlight this work; and we do decided to found this Journal; and we do publish this work openly; and furthermore, we do care for the work of the technical author, especially the beginner one, whom we do support strongly as follows:

- 1 We encourage the author to submit his own paper written just in Basic English plus Technical Terminology.
- 2 We encourage the author even to select a pen name, which may drop it at any time to reveal his identity.
- 3 We encourage the author to submit an accepted for publication paper, which he was forced to decline that publication because it would be based on a review with unacceptable evaluation or comments.
- 4 We encourage the author to resubmit a non accepted for publication paper that was rejected after a poor, inadequate, unreasonable, irresponsible, incompetent, or ticking only, review.
- 5 We encourage the author to submit a paper that he already self-archived on some open repository, such as arXiv.org.
- 6 We encourage the author to self-archive all of the preprint and postprint versions of his paper.
- 7 We provide the author with a decent, express review process of up to just 4 weeks, by at least 2 peers, never have been co-authors with him.
- 8 We provide the author with a selection of review process between: a traditional, anonymous, peer review decision, and an immediate online pre-publication of his paper followed by an open discussion with at least 2 reviewers.

About

- 9 We immediately accept for publication a research paper directly resulting from a Project Report, Diploma-, Master-, or PhD-thesis, which the author already has successfully defended before a committee of experts and he can mention 2 members of it, who reviewed and approved his work.
- 10 We immediately publish online a paper, as soon as, it is accepted for publication in the Journal.
- 11 We quickly print-on-demand an issue every 3 papers, in excess of the 3 issues we regularly publish 3 times a year on January, May, and September.
- 12 We do not demand from the author to transfer his own copyright to us. Instead, we only consider papers resulting only from original research work, and only if the author does assure us that he owns the copyright of his paper and that he submits to the Journal either an original or a revised version of his paper, for either publication after review, or even an immediate re-publication if this paper has already been published after review, under the Creative Commons Attribution 3.0 Unported License CC-BY 3, in any case.

Reviewers – Any peer may voluntarily becomes a reviewer of the Journal in his expertise for as long as he wishes. Each author of the Journal has to support the peer-to-peer review process by reviewing one paper, written by non co-author(s) of him, for every one of his papers published in the Journal.

Readers – Any reader is a potential reviewer. We welcome online comments and post-reviews by the readers.

Editors – Any editor holds a PhD degree, to objectively prove that he really has the working experience of passing through the established publishing system. An editor pre-reviews a paper in order to check its compliance to the Guiding Principles and to select the appropriate reviewers of the Journal. We can only accept for consideration papers in the expertise areas currently shown in the Editorial Board page. However, since we are willing to amplify and extend the Scope of the Journal, we welcome the volunteer expert, in any subject included into it, who wants to join the Board, if he unreservedly accepts our Guiding Principles.

Electronic Publishing

www.ftpj.otoiser.org

Printing-on-Demand

pod@ftpj.otoiser.org

Directly:

Georgios Tontrias, msn.expresscopy.xan@hotmail.com
ExpressCopy, V.Sofias 8, 671 00, Xanthi, Greece

Submissions

sub@ftpj.otoiser.org

Online:

www.ftpj.otoiser.org

More – Detailed information will be available soon at:

www.ftpj.otoiser.org/gp

Antennas Research Group – Non Profit 12(3)* Union of Persons

* The Constitution of Greece, Article: 12(3) 2008:
www.hellenicparliament.gr/en/Vouli-ton-Ellinon/To-Politevma

* The Hellenic Supreme Court of Civil and Penal Law:
www.areiospagos.gr/en/ – Court Rulings:Civil|A1|511|2008

This document is licensed under a Creative Commons Attribution 4.0 International License – <https://creativecommons.org/licenses/by/4.0/>

Interfaces in High Voltage Engineering: A Most Important Question for Conventional Solid Insulating Materials as well as for Nanocomposite Polymers

M.G. Danikas, R. Sarathi *

Power Systems Laboratory, Department of Electrical and
Computer Engineering, Democritus University of Thrace,
Xanthi, Greece [1]

Department of Electrical Engineering,
Indian Institute of Technology Madras, Chennai, India [2]

Abstract

Interfaces consist a most important part of conventional insulating systems at high voltages. They are considered to be problem areas which have to be dealt with. Numerous publications have contributed in rendering the mechanisms of interfaces understandable. On the other hand, interfaces in nanocomposite polymers seem to function in an entirely different manner from that in conventional insulating systems. The present paper reviews past work on both the conventional insulations and in nanocomposites. Differences regarding the interfaces are mentioned and discussed. Whereas interfaces in conventional insulating systems are to be avoided, interfaces in nanocomposite polymers seem to be desirable - at least - up to a certain percentage of nanoparticles in the base polymer. Although things are better understood in conventional insulating materials, more work has to be performed in order to clarify several aspects, such as space charges and electrical trees emanating from enclosed cavities. Needless to say that much more work has to be done in nanocomposites w.r.t. their modeling and possible explanations of the surprising performance of interfaces, a performance that deviates strongly from the performance in classical insulating materials.

Keywords

Breakdown, breakdown strength, conventional insulating materials/systems, nanocomposite polymers, partial discharges, electrical treeing/trees

Introduction

With some sort of exaggeration, a well known professor said once that "the problems of high voltage insulations are problems of interfaces" [1]. Interfaces result when there are two different insulating materials next to each other or when an insulating material meets a conductor. An interface may become, e.g., the source of partial discharges or even the cause for a complete breakdown of an insulating system. When two insulating materials of different dielectric constants have a common interface, then the material with the lowest dielectric constant will undergo the more intense electric stressing [2]. Depending also on other parameters, such stressing may result in a gradual deterioration of the insulating system and consequently in a complete breakdown [3].

In this paper, the questions raised by the existence of interfaces in high-voltage insulating systems are discussed. Interfaces play an important role in determining the robustness of an insulating system, when conventional insulating materials are used. Interfaces play also a vital role in insulating systems with nanocomposite polymers. Their functioning, however, is of another nature.

This short review is by no means exhaustive since the topic of interfaces is a vast one. It is the aim of the authors to give the gist of the problems and questions the researchers may face and to offer some comments. In the context of this paper, the terms "insulating material" and "dielectric material" or simply "dielectric" are sometimes interchanged meaning the same thing.

Interfaces in Conventional Insulating Materials

Dielectric breakdown in insulating materials depends on electrode configuration, insulating material thickness, electrode materials, presence of microcavities, temperature, pressure, nature and morphology of material under test, type of applied voltage, damage path (surface or volume) [4]. Various dielectric breakdown theories have been put forward [5]-[13]. No matter whether the proposed theory was based on cumulative impact ionization by electrons - creating thus positive space charges which distort the field distribution and weaken the dielectric [5] -, on the notion of "intrinsic breakdown" - according to which a large number of electrons trapped in energy levels due to lattice imperfections can transfer

energy to the lattice vibrations [6]-[8], on the "40 generations avalanche theory" [9], on the importance of space charges which modify the local electric field value [10], on the right assumption that the breakdown is a property of the dielectric material plus its electrode system [11] or on the theory based on the ionizing electrons and the hole traps [12], [13], the fact remains that all the above mentioned phenomena result from electric field intensifications, i.e. from either electrode imperfections or mismatch of dielectric materials. This brings us to the point mentioned in the Introduction of the present paper: that interfaces may create the conditions which may cause electric field intensifications.

The subject of partial discharges (PD) which may ensue because of electric field intensifications and/or because of gas (or foreign particle) inclusions in a solid dielectric material, has been studied by Mason in his fundamental publications [14]-[18]. Having in mind all the above, it is fitting to say that interfaces - created either by a mismatch of dielectric materials or because of intrusion of foreign particles and/or air cavities in the insulating material under

question -, are the problem areas of an insulating system.

As was pointed out quite early [19], interfaces play a most significant role in the discharge and breakdown processes: even if an insulation does not contain any cavities, at a sufficient stress "some event" releases gas with the subsequent formation of a cavity. The cavity is occupied by a gas discharge which increases the rate of gas formation with the subsequent growth of both the cavity size and the discharge intensity. The importance of the differing nature of interfaces was also stressed in another publication, where it was pointed out that damage in internal cavities in polyethylene is little compared to the electrode adjacent cavities of the same dimensions and tested under the same experimental conditions [20]. It is evident that in [20], interfaces between polyethylene and gas were compared with interfaces between polyethylene and electrodes, and the latter were found to be more dangerous and deleterious to the insulating material. On the same lines, Kreuger showed that with PVC-insulated cables, the number of discharges increased with increasing electric stress in the dielectric [21]. In yet

another paper, it was indicated that the nature of internal discharges was greatly affected by the assembly of the electrode system and the adhesion of the insulating tapes [22]. Discharges always start in the electrically weaker insulating material, as was commented in previous works [23]-[25].

Needless to say that phenomena related to PD, such as electrical treeing, are also closely connected to the mismatch of the dielectric constants of insulating materials and/or to the existence of gas cavities in their volume. Earlier papers indicated that the treeing phenomenon in polyethylene cables started from both inner and outer surfaces and also from solid particles and fibres [26]. Pioneering work performed with 15 kV and 22 kV polyethylene insulated cables reported that trees originated from contaminants and cavities, the tendency for tree initiation from a contaminant being probably more affected by the contaminant material than by the size, location or shape of the contaminant [27]. The importance of enclosed cavities in the initiation of trees was also reported more recently [28]. According to Ieda [29], tree propagation can be induced by internal gas discharge in the

tree. It is to be borne in mind that in numerous publications dealing with experimental work, the electrode arrangement that was used was a needle-plane electrode arrangement, indicating again that an electrode arrangement was chosen, with pronounced interfaces, in order to study the treeing phenomenon [30]-[33].

Interfaces which may play a role in determining the breakdown strength of an insulating material need not be only interfaces between insulating material and metal or between insulating material and gas cavity or contaminant. Differing phases may play also a role, as was noted in [34], where the interfacial domain of crystalline and amorphous phases may determine the various properties of semi-crystalline polymers, such as biaxially orientated polypropylene (BOPP). Stressing the importance of interfaces and experimenting with cross-linked polyethylene (XLPE), McKean showed that a considerable improvement in cable breakdown can be achieved by impregnation with silicone oil or diethyleneglycol. Such liquids can impregnate gas microspaces in the main insulation and thus result in an increase of the breakdown strength [35]. Similar observations were also

reported with polypropylene and polyethylene impregnated with suitable dipolar liquids [36].

Interfacial breakdown was studied with various electrode geometries and insulating systems consisting of paper typical for transformers and transformer oil [37]. It was reported that interfacial breakdown will occur if the paper is not carefully dried or if many gaseous micro-porosities are left in or on the paper. In [37], however, it was also noticed that using a carefully prepared paper-oil interface structure, the breakdown does not necessarily take place at the interface. Similar observations were made more recently by using silicone rubber interfaces, where both perpendicular and parallel to the applied electric field were investigated [38].

Conventional paper-oil cable insulation was studied quite early and the problems of interfaces were noted [39]. Alternative insulating systems, based mainly on polymeric materials, were proposed with considerable commercial success [40] - [43]. Modern cables with solid polymeric insulation did not avoid the problems of interfaces, namely those of extrusions of semi-conducting sheaths with the main insula-

tion or the inclusion of microcavities and/or impurities [44], [45]. Extruded cable insulation exposed to wet conditions suffered from electrochemical treeing and impurities greatly deteriorated its electrical performance [46]. Moreover, operating electrical stresses may also cause premature insulation failure in 15 kV polyethylene cables, if combined with unfavorable interface profiles and moisture [47]. Interfaces between polyethylene and small contaminants or microcavities may cause bow-tie trees in polyethylene cables [48].

Interfaces either perpendicular to the applied electric field or parallel to it or at an angle with it were dealt with in [49], where it was noted that such a variety of interfaces may be encountered in applications, such as capacitors, cables and in transformer windings. Composite insulating systems must preserve low dielectric losses. Higher dielectric losses may imply high ionic concentration in a solid/liquid insulating system, i.e. high ionic concentration in the liquid component of such a system [50].

Before concluding this section, it is fitting to mention the composite insulating systems of electrical machi-

nes, which consist mainly of epoxy resin and mica sheets. Previous work done in this context indicated that electrical treeing propagates through the epoxy resin and generally stops at the mica sheets, as mica is harder and electrically stronger than epoxy resin. The importance of such interfaces was reported before using a needle-plane electrode arrangement [51], where experiments were carried out without and with a mica sheet inserted in epoxy resin (Figs. 1 and 2). Evidently electrical trees were propagating more easily in the case of absence of the mica sheet and with much more difficulty with mica sheet.

Simulation work done recently showed that mica sheets prevent electrical trees from reaching the opposite electrode [52]. The purpose of mentioning experimental results regarding the composite system of epoxy resin/mica sheets is to show that the electrical trees propagate through the electrically weaker insulating medium. The simulation results indicate that even the slightest variations of dielectric constant may cause the electrical tree growth. In other words, the simulation data indicate that

local fluctuations of dielectric constant imply local - even microscopically minute - formations of interfaces, which in turn may mean local field intensifications, encouraging thus the growth of electrical trees (Figs. 3 and 4). Such observations w.r.t. the local variations of dielectric constant have also been reported for polyethylene [53], [54].

It is evident from all the above that interfaces in classical insulating systems seem to cause problems (possible dielectric constant mismatch, PD, treeing phenomena and ultimately risk of ultimate insulation failure). Due attention should be paid in choosing the insulating materials for specific applications and to the construction of the composite insulating system. Too many things depend on the quality of the construction of the interfaces [55]-[58], too many things that cannot be ignored. Interfaces in traditional insulating systems are considered as the weak aspects of such systems. Keeping this in mind and without exaggerating, it is not far from the truth if we state that an insulating system is as good as its weakest interfaces.

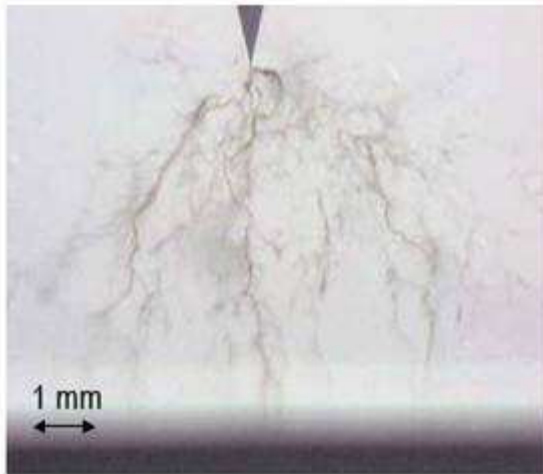


Fig. 1: Electrical tree propagation without the presence of mica sheet (applied voltage 28 kVrms, 50 Hz) (after [51])

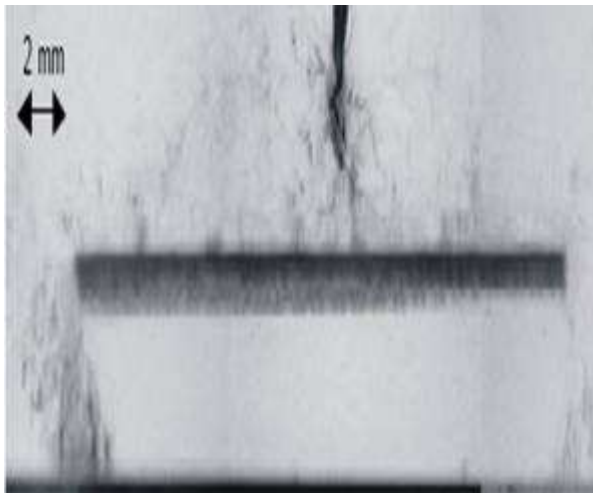


Fig. 2: Electrical tree propagation with the presence of mica sheet. The mica sheet increases the propagation time of the tree (applied voltage 28 kVrms, 50 Hz) (after [51])

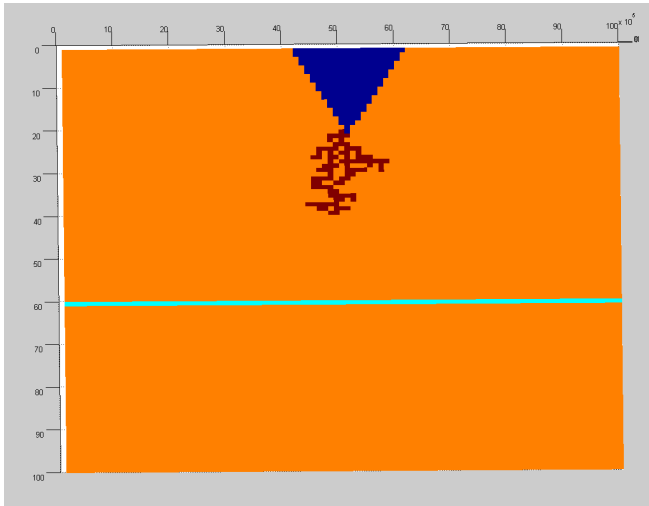


Fig. 3: Simulated electrical tree propagation with one mica sheet. Needle-plane electrode arrangement used

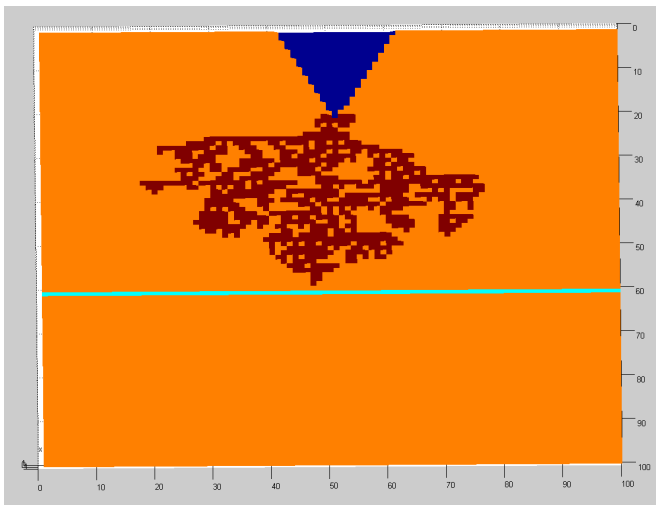


Fig. 4: Further expansion of electrical trees. Electrical trees stop at mica sheet. Needle-plane electrode arrangement used

It goes without say that this short review regarding classical interfaces does not by any means cover the whole subject and variety of solid insulating materials (for example, no mention in this paper was offered about the interfaces in outdoor polymeric insulators [59], [60] or in indoor polymeric insulators [61]). Both in the libraries and in the Internet, the interested reader may find practically tens of thousands of publications referring to the questions and problem areas of the solid insulating materials and insulating systems. What this short review tried to do is to show that interfaces, electric field intensifications, pre - breakdown phenomena (such as PD and electrical trees) and breakdown mechanisms are all interwoven and interrelated. Having said that, the next question related to interfaces, is whether they play the same detrimental role in the new generation of insulating materials, the nanocomposite polymers. This is to be examined in the following section.

Interfaces in Nanocomposite Polymers

More than twenty years ago, nanocomposite polymers came to our lives [62]. The first application of nanocom-

posites appeared in 1990, when Toyota Motor Corporation introduced nanocomposite nylon in their car industry [63]. Since that year, many car industries introduced the use of nanocomposite polymers. Use of nanocomposite polymers was noted in other industries, such as in the optics and the electronics industries as well as in the food industry. A seminal paper by Lewis gave the impetus for research also in the insulation branch [64].

For the electrical insulation, nanocomposite polymers are defined as conventional polymers in which particles smaller than 100 nm are added and dispersed in such a way that at the end one gets a homogeneous mixture [63]. The addition of such nanoparticles (the term "nanofillers" is also widely used) is being done in very small quantities, usually less than 10 wt%. Nanocomposite polymers consist of three components:

- a) the base polymer (or polymer matrix),
- b) the nanoparticles (or nanofillers) and
- c) the interaction zone (or interface zone) between the matrix and the nanoparticles [63].

Regarding the polymers used, these may be either thermoplastics, thermosettings or

elastomers. Nanoparticles may be classified w.r.t. their dimensions, and they can be distinguished as

- 1) mono-dimensional (i.e. extremely thin),
- 2) two-dimensional (nanotubes) and
- 3) three-dimensional (inorganic oxides).

The most usual nanoparticles for the purposes of electrical insulation are

- 1) silica nanoparticles SiO_2 ,
- 2) montmorillonite nanoparticles (layered silica),
- 3) metallic oxides such as Al_2O_3 , TiO_2 , MgO and ZnO and
- 4) carbon nanotubes.

Nanocomposite polymers can be obtained in two types of structures, namely,

- (i) intercalated nanocomposites (formed when there is limited inclusion of polymer chain between the clay layers with a corresponding small increase in the interlayer spacing of a few nanometers and
- (ii) exfoliated nanocomposites (formed when the clay layers are well separated from one another and individually dispersed in the continuous polymer matrix [65], [66].

As mentioned above, nanoparticles are added and dispersed in relatively small

quantities in the base polymer (usually no more than 10 wt%). Since nanoparticles are smaller than microparticles (smaller by three orders of magnitude), their interaction with the surrounding polymer matrix is much greater [62]. The so-called interaction zone is the main factor contributing in the improvement of the properties of the base polymer [67]. In the case of addition of nanoparticles into a polymer, the interfaces are far more numerous and far larger than in the case of microparticles. As the size of the added particles is reduced, the interface becomes larger and larger. The distance between the nanoparticles is also extremely small. It seems that interfaces determine to a great extent the properties of nanocomposite polymers.

The size of nanoparticles and the distance between them is of the order of magnitude on nanometers. Such particles may interact with the polymer matrix both physically and chemically in the nanometer scale. This has as consequence the appearance of properties that are somehow different from those we already know in a more macroscopic scale [68]. In contradistinction to the interfaces in classical insulating materials, and also to what we know

from classical high voltage textbooks, the improved insulating properties of the nanocomposite polymers are due to

- a) the large surface area of nanoparticles, which creates a large interaction zone,
- b) the changes in polymer morphology because of the large interaction zone,
- c) the changes in the space charge distribution and
- d) a dispersion mechanism [69].

Both the size of the nanoparticles and the chemical properties of their surface play an important role in determining the electrical, thermal and mechanical properties of nanocomposites. Needless to say that the chemical compatibility between the introduced nanoparticles and the polymer matrix is of paramount importance for the general properties of the nanocomposite [70].

One of the most significant characteristics of nanocomposite polymers is the increase of their breakdown strength as the size of the added nanoparticles tends to extremely small values. This increase is not in agreement with the conventional wisdom, which suggests that as the number of interfaces increases, the breakdown strength decreases dramatically

[2], [3]. Nanocomposite polymers seem not to agree with what we already know for classical insulating materials or systems [71]. Differences in breakdown strength between conventional epoxy resin and epoxy resin with nanoparticles was reported in [72]. Such observations were also noted later, when six different materials based on epoxy resin with various with and/or micro- and nanoparticles of alumina/silica were tested. It was shown that epoxy resin with nanosilica particles was the most suitable to obtain high values of breakdown strength [73].

Addition of the percentage of nanoparticles to epoxy resin up to a certain level favors the increase of breakdown strength both with a.c. and d.c. voltage, as was noticed in [74]. Why nanoparticles act in such a favorable way, despite the numerous interfaces they create? The increase of the breakdown strength may be due to

- (i) the increase of the surface area of the interfaces, which somehow alters the behavior of the polymer,
- (ii) the changes of space charge distribution inside the insulation structure,
- (iii) the dispersion mechanism, and
- (iv) the changing properties of the insulating material,

more specifically its volume resistivity, its $\tan\delta$ and its dielectric constant.

It is possible that the electrons moving in such a nanocomposite polymer, lose their kinetic energy because of the nanoparticles. Since the distances between the nanoparticles are extremely small, the electrons cannot acquire enough speed so that they can contribute to the breakdown process. Consequently, epoxy resin with nanoparticles presents a higher breakdown strength than conventional epoxy resin [74].

Normally the introduction of particles in polymeric materials has as result the introduction of defects and subsequently the worsening of its electrical properties. Nanocomposite polymers seem not to obey the above rule, as the mechanisms of conductivity during the breakdown process are influenced from the applied electric field, the dielectric constant of the nanoparticles and their number. The combined effect of these factors is difficult to fully understand at this stage and we need more work [71]. Similar results were obtained with epoxy resin with nanoparticles of TiO_2 as it presented a much higher breakdown strength than conventional epoxy resin [75].

On the other hand, electrical treeing propagation was found to be easier in conventional polymers than in nanocomposite polymers [76], [77]. Even a small wt% addition of nanoparticles affects in a positive way the electrical treeing resistance of the nanocomposite polymer. It seems that electrical tree propagation paths go through the base polymer and around the nanoparticles (experimental evidence for this was presented in SEM photographs published in [76]). Consequently, the more the nanoparticles in a polymer, the more difficult the formation of treeing paths. It seems that nanoparticles act as extremely small barriers, thus preventing the easy growth of electrical trees. Electrical trees propagate through the base polymer (in other words through the polymer matrix) and not through the nanoparticles. In some cases the electrical trees stop at the nanoparticles and they do not progress any further. Such observations were made in simulation studies recently [78]-[80].

Further research showed that a small percentage introduction of nanoparticles into a conventional polymer may increase its resistance to electrical treeing [81]. It is interesting to note

that nanoparticles may function as barriers preventing the tree growth even in minute quantities [82]. Earlier work indicated that as soon as the electrical tree touches the nanoparticle, the physico-chemical properties of it are such that very high energies are required in order to cause its deterioration [83]. Although the latter paper is an old one, it may give a clue as to why nanoparticles act as elementary barriers and why they prevent (or they delay) electrical treeing. More recently, a similar argument was given by some Japanese researchers [84].

Loading (i.e. the percentage of included nanoparticles expressed in wt%) plays also a vital role in determining the resistance to electrical treeing. More loading (i.e. more nanoparticles, that is more interfaces) implies a better resistance to treeing. This is probably because trees interact with many more nanoparticles and this delays their growth [85]. Another possible explanation was offered some years ago, where the authors proposed that in front of a tree a damage process zone is formed in a conventional polymer. Such a zone cannot progress easily when it meets nanoparticles [86]. Simulation data indi-

cated that loading affects the tree growth. The nanoparticle size plays also a role in delaying tree propagation, smaller nanoparticles offer a better tree resistance than the larger ones [79]. In Figs. 5-8 simulation results regarding the loading of nanoparticles as well as the size of nanoparticles are shown. It is evident that more loading makes tree growth more difficult. It goes also without say that smaller nanoparticles offer a better resistance to tree propagation.

There is no need to emphasize that there is also in the field of nanocomposite polymers a vast body of technical literature, too vast to be mentioned here in the context of this paper. From this short review it is obvious that interfaces in nanocomposites play an entirely different role from the one they play in classical insulating materials. Why is this so? This may be because the physics and/or chemistry somehow change in the nanoscopic world of such materials. Interfaces become highly desirable - at least up to a certain percentage of added nanoparticles. The surface area of the nanoparticles is huge if compared with that of microparticles for other high voltage applications.

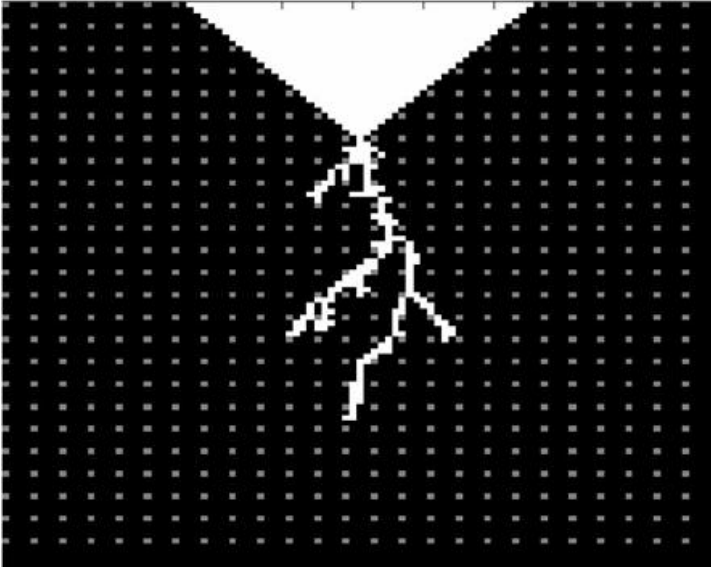


Fig. 5: Simulation with epoxy resin filled with TiO_2 nanoparticles (loading of 2 wt%, nanoparticle diameter 100 nm)

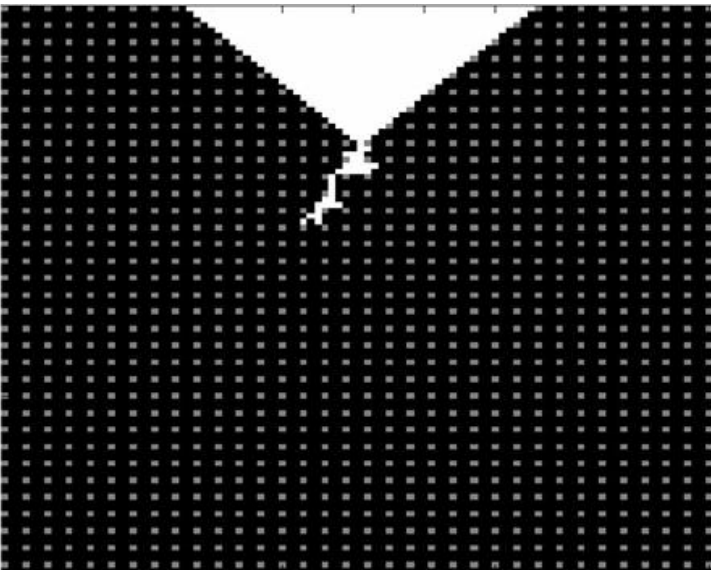


Fig. 6: Simulation with epoxy resin filled with TiO_2 nanoparticles (loading of 6 wt%, nanoparticle diameter 100 nm)

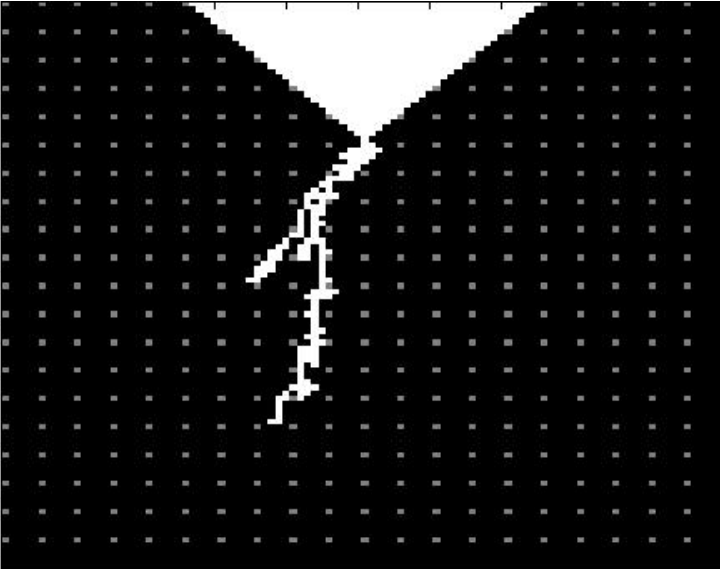


Fig. 7: Simulation with epoxy resin filled with TiO_2 nanoparticles (loading of 6 wt%, nanoparticle diameter 200 nm)

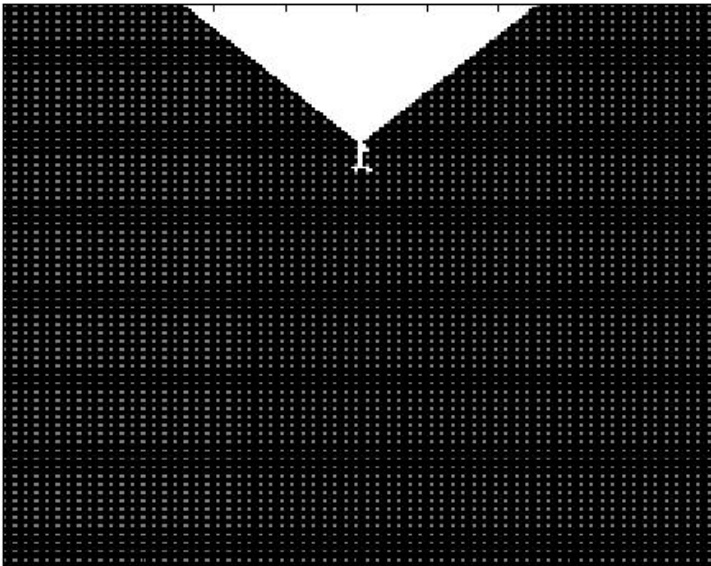


Fig. 8: Simulation with epoxy resin filled with TiO_2 nanoparticles (loading of 6 wt%, nanoparticle diameter 100 nm)

Models regarding the explanation of the functioning of nanocomposites were proposed as well as how the nanoparticles behave inside the base polymeric material [62], [87], [88]. Such models try to explain the higher breakdown strength values of nanocomposites and also their higher resistance to electrical treeing. The explanations seem to be plausible but more hard evidence is needed. Such evidence will be offered by many more photographs (SEM and TEM photos) showing in detail how the electrical trees circumvent the nanoparticles and how they propagate through the polymer matrix. Such photographs are very difficult to obtain.

Where all this leaves us? How can we understand in a unified way interfaces in both classical and nanocomposite insulating systems? Can the experimental results and simulations on electrical treeing with typical machine insulation ([52]) provide a hint also for a possible explanation in the nanoscopic world? A recent paper on interfaces posed some pertinent questions regarding classical and nanocomposite insulating materials [89]. From this paper it is obvious that although more questions are in need of an answer for the nanocomposites, the subject of

interfaces in classical insulating systems is by no means finished. For example, charging of larger interfaces, such as found in cable joints and terminations, needs to be further explored regarding the mechanisms of space charges. Another aspect in need of further discussion is whether electrical trees may emanate from enclosed cavities in conventional polymers. The latter question has been partly answered in [28], [90] - where some experimental evidence was offered as to the possibility of electrical trees stemming from enclosed cavities - but further experimental data is needed.

One thing that should not be forgotten - and it is common to conventional as well as nanocomposite polymers - is that an insulating system to a great extent is as good as its interfaces. This means that, no matter whether we deal with conventional insulating materials or nanocomposites, preparation and construction in both cases has to be not only careful but meticulous.

A last remark on the literature presented here: the interested reader may find that the authors dwell perhaps too much in the older scientific literature. This is not done because they tend to ignore the more recent re-

search: they simply would like to show that even in the old days, the problems were more or less the same. Moreover, they would also like to show that fundamental ideas - which are with us even today - on the various mechanisms in insulating materials came about quite early.

Conclusion

This review - by no means exhaustive - tackled the subject of the importance of interfaces both in conventional insulating materials and in nanocomposite polymers. Whereas interfaces are to be avoided in conventional materials, they seem to be a blessing in nanocomposites.

Whereas in conventional materials they cause problems of compatibility and sometimes high field intensifications with all the bad consequences such intensifications entail (i.e. PD, trees), in nanocomposites they seem - up to a certain loading - to be desirable and they prevent (or the delay) tree growth. Whereas in conventional insulating systems the introduction of more interfaces seems to cause sometimes insurmountable problems, the introduction of interfaces (because of the nanoparticles' introduction to the polymer matrix) seems to alleviate electrical trees and to distribute more evenly electric fields and space charges.

References

- [1] Misikian M., Personal Communication, August 1991
- [2] Kuffel E., Zaengl W.S., Kuffel J., "High Voltage Engineering: Fundamentals", Eds. Newnes, Oxford, UK, 2000
- [3] Kind D., Kaerner H., "High Voltage Insulation Technology", Eds. Vieweg, Braunschweig, Germany, 1985
- [4] Budenstein P., "On the mechanism of dielectric breakdown of solids", IEEE Transactions on Electrical Insulation, Vol. 15, No. 3, 1980, pp. 225-240
- [5] Von Hippel A., "Electric breakdown of solid and liquid insulators", Journal of Applied Physics, Vol. 8, 1937, pp. 815-832
- [6] Froehlich H., "Theory of electrical breakdown in ionic crystals", Proceedings of the Royal Society A, Vol. 160, 1937, pp. 230-241
- [7] Froehlich H., "On the dielectric strength of mixed crystals", Proceedings of the Royal Society A, Vol. 178, 1941, pp. 493-498

- [8] Froehlich H., "On the theory of dielectric breakdown in solids", Proceedings of the Royal Society A, Vol. 188, 1947, pp. 521-532
- [9] Seitz F., "On the theory of electron multiplication in crystals", Physical Review, Vol. 76, 1949, pp. 1376-1393
- [10] Croitotu Z., "Space charges in dielectrics", Progress in Dielectrics, Vol. 6, 1959, pp. 105-146
- [11] O'Dwyer J.J., "Breakdown in solid dielectrics", IEEE Transactions on Electrical Insulation, Vol. 17, No. 6, 1982, pp. 484-487
- [12] Klein N., "Electrical breakdown mechanisms in thin insulators", Thin Solid Films, Vol. 50, 1978, pp. 223-232
- [13] Klein N., "Electrical breakdown of insulators by one-carrier impact ionization", Journal of Applied Physics, Vol. 53, No. 8, 1982, pp. 5828-5839
- [14] Mason J.H., "The deterioration and breakdown of dielectrics resulting from internal discharges", Proceedings of IEE, Vol. 98, Pt. I, 1951, pp. 44-59
- [15] Mason J.H., "Breakdown of insulation by discharges", Proceedings of IEE, Vol. 100 (IIA), 1953, pp. 149-158
- [16] Mason J.H., "Breakdown of solid dielectrics in divergent fields", Proceedings of IEE, Vol. 102, Pt. C, 1955, pp. 254-263
- [17] Mason J.H., "Assessing the resistance of polymers to electrical treeing", Proceedings of IEE, Vol. 128, Pt. A, no. 3, 1981, pp. 193-201
- [18] Mason J.H., "Enhancing the significance of PD measurements", IEEE Transactions on Dielectrics and Electrical Insulation, Vol. 2, No. 5, 1995, pp. 876-888
- [19] Church H.F., Garton C.G., "Some mechanisms of insulation failure", Proceedings of IEE, Vol. 100 (IIA), 1953, pp. 111-120
- [20] Rogers E.C., "The self-extinction of gaseous discharges in cavities in dielectrics", Proceedings of IEE, Vol. 105A, 1958, pp. 621-630
- [21] Kreuger F.H., "Discharge Detection in High Voltage Engineering", Eds. Heywood, London, UK, 1964
- [22] Okamoto H., et al., "Deterioration of insulating materials by internal discharge", IEEE Transactions on Power Apparatus and Systems, Vol. PAS-96, No. 1, 1977, pp. 166-177

- [23] Nikolopoulos P.N., Diamantopoulos D.N., "Behaviour of press-board - oil insulation under alternating voltages of industrial frequency in a non-uniform electric field", Proceedings of IEE, Vol. 130, Pt. A, No. 3, 1983, pp, 145-151
- [24] Danikas M.G., "A study of the behaviour of a uniaxially orientated polyethylene tape/oil insulating system subjected to electrical and thermal stresses", Ph.D. Thesis, University of London, Queen Mary College, UK, 1985
- [25] Kelen A., Danikas M.G., "Evidence and presumption in PD diagnostics", IEEE Transactions on Dielectrics and Electrical Insulation, Vol. 2, No. 5, 1995, pp. 780-795
- [26] Kitchin D.W., Pratt O.S., "Treeing in polyethylene as a prelude to breakdown", AIEE Transactions on Power Apparatus and Systems, Vol. PAS-77, Pt. III, 1958, pp. 180-186
- [27] Vahstrom W.Jr., "Investigation of insulation deterioration in 15 kV and 22 kV polyethylene cables removed from service", IEEE Transactions on Power Apparatus and Systems, Vol. PAS-91, No. 1-3, 1972, pp. 1023-1035
- [28] Danikas M.G., Adamidis G.A, "Partial discharges in epoxy resin voids and the interpretational possibilities and limitations of Pedersen's model", Archiv fuer Elektrotechnik, Vol. 80, No. 2, 1997, pp. 105-110
- [29] Ieda M., "Dielectric breakdown process of polymers", IEEE Transactions on Electrical Insulation, Vol. 15, No. 3, 1980, pp. 206-224
- [30] Laurent C., et al., "Electrical breakdown due to discharges in different types of insulation", IEEE Transactions on Electrical Insulation, Vol. 16, No. 1, 1981, pp. 52-58
- [31] Kao K.C., De Min Tu, "Formation of electrical treeing in polyethylene", Annual Report of Conference on Electrical Insulation and Dielectric Phenomena (CEIDP), Amherst, MA, USA, October 17-21, 1982, pp. 598-603
- [32] El Moslemany M.A., et al., "Some observations on tree patterns in PMMA under alternating voltages", IEEE Transactions on Electrical Insulation, Vol. 17, No. 1, 1982, pp. 76-80
- [33] Tanaka T., Greenwood, "Advanced Power Cable Technology", Eds. CRC Press, Inc., Boca Raton, Florida, 1983
- [34] Umemura T., Couderc D., "Dielectric behaviour of solid/liquid insulation system", IEEE Transactions on Elec-

- trical Insulation, Vol. 17, No. 3, 1982, pp. 276-280
- [35] McKean A.L., "Breakdown mechanism studies in cross-linked polyethylene cable", IEEE Transactions on Power Apparatus and Systems, Vol. PAS-95, No. 1, 1976, pp. 253-260
- [36] Fendley J.J., Parkman N., "Effect of impregnation, compression and temperature on electric strength of polythene and polypropylene", Proceedings of IEE, Vol. 129, Pt. A, No. 2, 1982, pp. 113-118
- [37] Kelley E.F., Hebner R.E., "Electrical breakdown in composite insulating systems: Liquid-solid interface parallel to the field", IEEE Transactions on Electrical Insulation, Vol. 16, No. 4, 1981, pp. 297-303
- [38] Danikas M.G., "On the breakdown strength of silicone rubber", IEEE Transactions on Dielectrics and Electrical Insulation, Vol. 1, No. 6, 1994, pp. 1196-1200
- [39] Gazzana-Priaroggia P., et al, "The influence of ageing on the characteristics of oil-filled cable dielectrics", Proceedings of IEE, Vol. 108A, 1961, pp. 467-479
- [40] Buntin R., et al, "A study of the electrical insulation characteristics of oil impregnated polypropylene paper", IEEE Transactions on Electrical Insulation, Vol. 7, No. 4, 1972, pp. 162-169
- [41] Gibbons J.A.M., Stannett A.W., "Plastics in transmission cables", 2nd International Electrical Insulation Conference, BEAMA, Brighton, UK, May 1974
- [42] Forsyth E., et al., "The development of synthetic insulating tape for EHV cables", IEE 2nd International Conference on Progress in Cables and Overhead Lines For 220 kV and Above, London, UK, September 1979
- [43] Ernst A., Muller A., "The state of development of 100% synthetic tape at Brookhaven National Laboratory", Inf. Rep., BNL-28981, Brookhaven National Laboratory, January 1981
- [44] Yoda B., Muraki K., "Development of EHV cross-linked polyethylene insulated power cables", IEEE Transactions on Power Apparatus and Systems, Vol. PAS-91, 1972, pp. 506-513
- [45] Bahder G., et al., "Electrical and electrochemical treeing effect in polyethylene and crosslinked polyethylene cables", IEEE Transactions on Power Apparatus and Syst., Vol. PAS-93, No. 1-3, 1974, pp. 977-990
- [46] Charoy M.A., Jocteur R. F., "Very high tension cables

- with extruded polyethylene insulation", IEEE Transactions on Power Apparatus and Systems, Vol. PAS-90, No. 2, 1971, pp. 777-782
- [47] Wilkens W.D., "A study of treeing in medium voltage power cables", IEEE Transactions on Power Apparatus and Systems, Vol. PAS-93, No. 4-6, 1974, pp. 1201-1207
- [48] Lyle R., Kirkland J.W., "An accelerated life test for evaluating power cable insulation", IEEE Transactions on Power Apparatus and Systems, Vol. PAS-100, No. 8, 1981, pp. 3764-3770
- [49] Kreuger F.H., "Industrial High Voltage: Electric Fields, Dielectrics, constructions", Eds. Delft University Press, Delft, The Netherlands, 1991
- [50] Parkman N., "Breakdown in composites", pp. 52-69, in the book: "Electrical Insulation", edited by A. Bradwell, Eds. Peter Peregrinus Ltd., London, UK, 1983
- [51] Vogelsang R., Fruth B., Farr T., Froehlich K., "Detection of electrical tree propagation by partial discharge measurements", Proceedings of 15th International Conference on Electrical Machines, Brugge, Belgium, 2002
- [52] Christantoni D.D., Danikas M.G., Vardakis G.E., Lekou A.T., "Simulation of electrical tree growth in a composite insulating system consisted from epoxy resin and mica sheets", International Review on Modeling and Simulation (IREMOS), Vol. 3, No. 2, 2010, pp. 241-249
- [53] Vardakis G.E., Danikas M.G., "Simulation of electrical tree propagation in a solid insulating material containing spherical insulating particle of a different permittivity with the aid of Cellular Automata", Facta Universitatis, Series Electronics and Energetics, Vol. 17, 2004, pp. 377-389
- [54] Vardakis G.E., Danikas M.G., "Simulation of electrical tree propagation using Cellular Automata: The case of conducting particle included in a dielectric in point-plane electrode arrangement", Journal of Electrostatics, Vol. 63, 2005, pp. 129-142
- [55] Benken H.-G., "Ueber die elektrische Festigkeit von Fugen zwischen festen' Isolierstoffen", Elektrotechnische Zeitschrift (ETZ-A), Vol. 89, 1968, pp. 356-361
- [56] Benken H.-G., "Ueber die elektrische Festigkeit von Fugen zwischen festen' Isolierstoffen", Ph.D. Thesis, Technische Universitaet Braunschweig, 1967
- [57] Kahle M., "Elektrische Isoliertechnik", Eds. VEB Verlag

- Technik, Berlin, Germany, 1988
- [58] Naidu M.S., Kamaraju V., "High Voltage Engineering", Eds. Tata McGraw-Hill Publ. Co. Ltd., New Delhi, India, 2000
- [59] Danikas M.G., "Ageing properties of silicone rubber materials used in high voltage composite insulators", Journal of Electrical and Electronics Engineering, Australia, Vol.15, No. 2, 1995, pp. 193-202
- [60] Danikas M.G., "Polymer outdoor insulators", Acta Electrotechnica Napocensis, Vol. 40, No. 1, 1999, pp. 3-10
- [61] Danikas M.G., "Surface phenomena on resin-type insulators under different electrical and non-electrical stresses in the early stage of ageing", Facta Universitatis, Series Electronics and Energetics, Vol. 13, No. 3, 2000, pp. 335-352
- [62] Nelson J.K., "Dielectric Polymer Nanocomposites", Eds. Springer, Heidelberg, Germany, 2010
- [63] Lau K.Y., Piah M.A.M., "Polymer nanocomposites in high voltage electrical insulation perspective: A review", Malaysian Polymer Journal, Vol. 6, No. 1, 2011, pp. 58-69
- [64] Lewis T.J., "Nanometric dielectrics", IEEE Transactions on Dielectrics and Electrical Insulation, Vol. 1, No. 5, 1994, pp. 812-825
- [65] Alexandre M., Dubois F., "Polymer-layered silicate nanocomposites: Preparation, properties and uses of a new class of materials", Materials Science and Engineering, Vol. 28, 2000, pp. 1-63
- [66] Sahu R.K., "Understanding the electrical, thermal and mechanical properties of epoxy nanocomposites", Ph.D. Thesis, Indian Institute of Technology Madras, Department of Electrical Engineering, Chennai, India, 2007
- [67] Nelson J.K., "The promise of dielectric nanocomposites", Conference Record of 2006 IEEE International Symposium on Electrical Insulation, pp. 452-457
- [68] Tanaka T., Montanari G.C., Mulhaupt R., "Polymer nanocomposites as dielectrics and electrical insulation - Perspectives for processing technologies, material characterization and future applications", IEEE Transactions on Dielectrics and Electrical Insulation, Vol. 11, No. 5, 2004, pp. 763-784
- [69] Roy M., Nelson J.K., McCrone R.K., Schaldler L.S., Reed C.W., Keefe R., Zenger W., "Polymer nanocomposite dielectrics - The role of the interface", IEEE Transa-

- ctions on Dielectrics and Electrical Insulation, Vol. 12, No. 4, 2005, pp. 629-643
- [70] Roy M., Nelson J.K., McCrone R.K., Schaldler L.S., "Candidate mechanisms controlling the electrical characteristics of silica/XLPE nanodielectrics", Journal of Materials Science, Vol. 42, No. 11, 2007, "http://homepages.rpi.edu/~nelsoj/JMS_Paper_07.pdf"
- [71] Singha S., Joy Thomas M., "Dielectric properties of epoxy nanocomposites", IEEE Transactions on Dielectrics and Electrical Insulation, Vol. 15, No. 1, 2008, pp. 12-23
- [72] Tanaka T., "Dielectric nanocomposites with insulating properties", IEEE Transactions on Dielectrics and Electrical Insulation, Vol. 12, No. 5, 2005, pp. 914-928
- [73] Okazaki Y., Kozako M., Hikita M., Tanaka T., "Effects of addition of nano-scale alumina and silica fillers on thermal conductivity and dielectric strength of epoxy/alumina microcomposites", Proceedings of 2010 IEEE International Conference on Solid Dielectrics, Potsdam, Germany, July 4-9, 2010, pp. 279-282
- [74] Sarathi R., Sahu R.K., Rajeshkumar P., "Understanding the thermal, mechanical and electrical properties of epoxy nanocomposites", Journal of Materials Science and Engineering: A, Vol. 445-446, 2007, pp. 567-578
- [75] Imai T., Sawa F., Ozaki T., Inoue Y., Shimizu T., Tanaka T., "Comparison of insulation breakdown properties of epoxy nanocomposites under homogeneous and divergent electric fields", 2006 Annual Report of Conference on Electrical Insulation and Dielectric Phenomena, Kansas City, USA, October 25-18, 2006, pp. 306-309.
- [76] Danikas M.G., Tanaka T., "Nanocomposites - A review of electrical treeing and breakdown", IEEE Electrical Insulation Magazine, Vol. 25, No. 4, 2009, pp. 19-25
- [77] Alapati S., Joy Thomas M., "Electrical treeing in polymer nanocomposites", Proceedings of 15th National Power Systems Conference (NPSC), IIT Bombay, India, December 2008, pp. 351-355
- [78] Pitsa D., Vardakis G., Danikas M.G., Kozako M., "Electrical treeing propagation in nanocomposites and the role of nanofillers: Simulation with the aid of Cellular Automata", Journal of Electrical Engineering, Vol. 61, No. 2, 2010, pp. 125-128

- [79] Pitsa D., Danikas M.G., "A 2D Cellular Automata model for tree propagation in nanocomposites: Influence of nanoparticles size, loading and the presence of microvoids", *NANO: Brief Reports and Reviews*, Vol. 8, No. 1, 2013 (DOI: 10.1142/S1793292013500021)
- [80] Pitsa D., Danikas M.G., "Modeling relative permittivity and electrical treeing in polymer nanocomposites", *Proceedings of 2013 IEEE International Conference on Solid Dielectrics*, Bologna, Italy, June 30 - July 4, 2013, pp. 832-835
- [81] Ding H.-Z., Varlow B.R., "Effect of nano-fillers on electrical treeing in epoxy resin subjected to AC voltage", *2004 Annual Report of Conference on Electrical Insulation and Dielectric Phenomena*, Colorado, USA, 17-20 October, 2004, pp. 332-335
- [82] Tanaka T., Yokoyama K., Ohki Y., Murata Y., Sekiguchi Y., Goshowaki M., "High field light emission in LDPE/MgO nanocomposites", *Proceedings of 2008 International Symposium on Electrical Insulating Materials*, Mie, Japan, September 7-11, 2008, pp. 506-509
- [83] MacKenzie B.T., Prober M., Lever R.C., "Filler effects and treeing phenomena in laboratory models and cable sections", *Annual Report of Conference on Electrical Insulation and Dielectric Phenomena*, 1972, pp. 233-238
- [84] Tanaka T., Matsunawa A., Ohki Y., Kozako M., Kohtoh M., Okabe S., "Treeing phenomena in epoxy/alumina nanocomposite and interpretation by a multi-core model", *IEEE Transactions on Fundamentals and Materials*, Vol. 126, No. 11, 2006, pp. 1128-1135
- [85] Imai T., Sawa F., Ozaki T., Inoue Y., Shimizu T., Tanaka T., "Roles of fillers on properties of nano-TiO₂ and micro-SiO₂ filler mixed composites", *Proceedings of International Conference on Solid Dielectrics*, Winchester, UK, July 8-13, 2007, pp. 407-410
- [86] Ding H.-Z., Varlow B.R., "Thermodynamic model for electrical tree propagation in combined electrical and mechanical stresses", *IEEE Transactions on Dielectrics and Electrical Insulation*, Vol. 12, No. 1, 2005 pp. 81-89
- [87] Danikas M.G., "On two nanocomposite models: Differences, similarities and interpretational possibilities regarding Tsagaropoulos' model and Tanaka's model", *Journal of Electrical Engineering*, Vol. 61, No. 4, 2010, pp. 241-246

- [88] Pitsa D., Danikas M.G., "Interfaces features in polymer nanocomposites: A review of proposed models", NANO: Brief Reports and Reviews, Vol. 6, No. 6, 2011, pp. 497-508
- [89] Morshuis P., "Interfaces: to be avoided or to be treasured?", Proceedings of 2013 IEEE International Conference on Solid Dielectrics, Bologna, Italy, June 30 - July 4, 2013, pp. 1-9
- [90] Danikas M.G., Karlis A.D., "Some observations on the dielectric breakdown and the importance of cavities in insulating materials used for cables and electrical machines", Advances in Electrical and Computer Engineering, Vol. 11, No. 2, 2011, pp. 123-126

Previous Publication in FUNKTECHNIKPLUS # JOURNAL

"Experimental Results on the Behavior of Water Droplets on Polymeric Surfaces Under the Influence of Electric Fields: the Case of an Inclined Test Arrangement for PVC, Rubber and Silicone Rubber"
Issue 2, pp. 19-39

*** About The Authors**

Michael Danikas, Issue 2, p. 39

Ramanujam Sarathi, Issue 2, p. 39

[This Page Intentionally Left Blank]

Spherical Beltrami Fields in Chiral Media: Reciprocity and General Theorems

Nikolaos M. Berketis *

Independent Researcher, Athens, Greece

Abstract

The Beltrami fields are extremely important for the description of time-harmonic electromagnetic fields in chiral media. This paper introduces the spherical Beltrami fields in chiral media, extending the corresponding known results for plane electromagnetic waves. Two key theorems are given for the scattering of spherical electromagnetic waves in chiral environment from a perfect conductor: the Reciprocity and the General Scattering theorems.

Keywords

Chiral media, spherical Beltrami fields, reciprocity relation, general scattering theorem

Introduction

The name "Beltrami field" comes from the fact that these fields \mathbf{A} satisfy the equation type $\nabla \times \mathbf{A} = \alpha \mathbf{A}$, where $\alpha \neq 0$ is a reciprocal length [1]. The word chiral regards the concept of "chirality", derived from the Greek word hand. In geometry, a figure is chiral if it cannot be mapped to its mirror image by rotations and translations alone. Typical examples are human hands, snail shells, spirals and spirals in general.

The discoveries of natural optical activity in special

materials have been known since the beginning of last century. Though optical activity has been considered in optics and in quantum mechanics for many years, its analysis within the framework of classical electromagnetic field theory arose much later. Recently, there has been a considerable interest in the study of scattering and diffraction by chiral medium. Chiral media are isotropic birefringent substances that respond to either electric or magnetic excitation with both electric and magnetic polarizations. Such media have been known since the end of the

nineteenth century (e.g. the study of chirality by Pasteur) and find a wide range of applications from many sciences [1].

In general, the electromagnetic fields inside the chiral medium are governed by Maxwell equations together with Drude-Born-Fedorov equations in which the electric and magnetic fields are coupled [1]. The chiral medium is characterized by the electric permittivity ϵ , magnetic permeability μ and chirality measure β .

Scattering problems with incident waves have been studied: for spherical acoustic waves in the works [2]-[4], as well in the works [2], [5] for spherical electromagnetic waves in non-chiral electromagnetic waves and finally for spherical electromagnetic waves in chiral media in the works [6], [7].

In this work, we derive reciprocity relation and general scattering theorem, from spherical electromagnetic waves emanating from point sources in chiral media and scattered by a perfect conductor. Similar theorems are proved, analogously, for a chiral dielectric [6], [7].

As it is well known [1], in a homogeneous isotropic chiral medium the electromagnetic field is composed of left-circularly polarized (LCP)

and right-circularly polarized (RCP) components which are propagated independently and with different phase speeds. When either a LCP or a RCP or a linear combination of LCP and RCP electromagnetic waves is incident upon a chiral scatterer then the scattered field is composed of both LCP and RCP components. So, using Bohren decomposition [1], [6], [7], the electromagnetic waves are expressed in terms of LCP and RCP Beltrami fields. The use of the Beltrami fields for problems of scattering in chiral material leads to a more simplified relationship.

This is due to the fact that the differential equations which satisfy Beltrami fields is of first order while the electric and magnetic field satisfy the Helmholtz modified equation which is of second-order. Moreover, the Beltrami equations and the conditions of radiation for the Beltrami fields are in effect separately for each one of them but on the scatterer surface, when applying the boundary conditions, both Beltrami fields are present. This fact makes easier to use these equations mainly in scattering problems where the behavior of the scattered field away from the scatterer is studied.

In the second section, we formulate the problem for

spherical electromagnetic wave in a chiral medium. In the third section we formulate the problem of electromagnetic wave scattering from a perfect conductor as a function of the Beltrami fields using the Bohren transformation. The spherical Beltrami fields are defined in the fourth section. Finally, Reciprocity relation and the General Scattering theorem are given in fifth section.

Problem Formulation

Let Ω^- be a bounded and closed subset of \mathbb{R}^3 having a C^2 -boundary S , i.e. $\partial\Omega^- = S$. The set Ω^- will be referred to as the scatterer. The exterior $\Omega^+ = \mathbb{R}^3/\Omega^-$ of the scatterer is an infinite isotropic homogeneous chiral medium with electric permittivity ε , magnetic permeability μ and chirality measure β .

The scatterer is filled with a isotropic chiral medium with corresponding physical parameters ε^-, μ^- and β^- . All the physical parameters are assumed to be real positive constants.

Let $(\mathbf{E}_0^{inc}, \mathbf{H}_0^{inc})$ be a time-Harmonic spherical electromagnetic wave, due a point source located at a point with position vector \mathbf{r}_0 with

respect to an origin O in the vicinity of Ω^- .

This wave is incident upon the scatterer Ω^- and let $(\mathbf{E}_0^{sc}, \mathbf{H}_0^{sc})$ be the corresponding scattered field. Then the total electromagnetic field $(\mathbf{E}_0^t, \mathbf{H}_0^t)$ in Ω^+ is given by

$$\begin{cases} \mathbf{E}_0^t(\mathbf{r}) = \mathbf{E}_0^{inc}(\mathbf{r}) + \mathbf{E}_0^{sc}(\mathbf{r}) \\ \mathbf{H}_0^t(\mathbf{r}) = \mathbf{H}_0^{inc}(\mathbf{r}) + \mathbf{H}_0^{sc}(\mathbf{r}) \end{cases} \quad (1)$$

We assume that the scattered field satisfies the Silver-Müller radiation condition

$$\frac{1}{\eta} \mathbf{E}_0^{sc}(\mathbf{r}) + \hat{\mathbf{r}} \times \mathbf{H}_0^{sc}(\mathbf{r}) = o(r^{-1}), \quad (2)$$

$$r \rightarrow \infty$$

uniformly in all directions, $\hat{\mathbf{r}} \in S^2$, where S^2 is the unit sphere in \mathbb{R}^3 , $r = |\mathbf{r}|$, $\hat{\mathbf{r}} = \mathbf{r}/r$ and $\eta = (\mu/\varepsilon)^{1/2}$ is the intrinsic impedance of the chiral medium in Ω^+ . It is known [8], that (2) can be replaced by

$$\hat{\mathbf{r}} \times \mathbf{E}_0^{sc}(\mathbf{r}) - \eta \mathbf{H}_0^{sc}(\mathbf{r}) = o(r^{-1}), \quad (3)$$

$$r \rightarrow \infty$$

uniformly in all directions, $\hat{\mathbf{r}} \in S^2$. The total electric field \mathbf{E}^{tot} satisfies the boundary condition:

$$\hat{\mathbf{n}} \times \mathbf{E}^t(\mathbf{r}) = \mathbf{0}, \quad \mathbf{r} \in S \quad (4)$$

where \hat{n} is the unit vector perpendicular to the outer surface S . In view of the Drude-Born-Fedorov constitutive relations [1], the total exterior electromagnetic field satisfies in the source-free region Ω^+ the modified Maxwell equations

$$\nabla \times \mathbf{E}_{r_0}^t(\mathbf{r}) = \beta \gamma^2 \mathbf{E}_{r_0}^t(\mathbf{r}) + i\omega\mu \left(\frac{\gamma}{k}\right)^2 \mathbf{H}_{r_0}^t(\mathbf{r}) \quad (5)$$

$$\nabla \times \mathbf{H}_{r_0}^t(\mathbf{r}) = \beta \gamma^2 \mathbf{H}_{r_0}^t(\mathbf{r}) - i\omega\varepsilon \left(\frac{\gamma}{k}\right)^2 \mathbf{E}_{r_0}^t(\mathbf{r}) \quad (6)$$

where

$$k^2 = \omega^2 \varepsilon \mu, \quad \gamma^2 = \frac{k^2}{1 - k^2 \beta^2} \quad (7)$$

with $|\beta k| < 1$, [1].

We note that (in contrast to the non-chiral case) k is not a wave number, but just a parameter without physical significance which has dimensions of inverse length and $\omega > 0$ is the angular frequency. The system of relations (5), (6) can be written as

$$\begin{bmatrix} \nabla \times \mathbf{E}_{r_0}^t \\ \nabla \times \mathbf{H}_{r_0}^t \end{bmatrix} = \left(\frac{\gamma}{k}\right)^2 \begin{bmatrix} k^2 \beta & i\omega\mu \\ -i\omega\varepsilon & k^2 \beta \end{bmatrix} \begin{bmatrix} \mathbf{E}_{r_0}^t \\ \mathbf{H}_{r_0}^t \end{bmatrix} \quad (8)$$

Beltrami Fields

As it is well known [1], [10], in chiral media LCP and RCP waves can both propagate

independently and with different phase speeds. So, we consider the Bohren [9], decomposition of \mathbf{E}_{r_0} and \mathbf{H}_{r_0} into suitable Beltrami fields \mathbf{Q}_{L,r_0} and \mathbf{Q}_{R,r_0} , as follows

$$\mathbf{E}_{r_0}^t = \mathbf{Q}_{L,r_0} + \mathbf{Q}_{R,r_0} \quad (9)$$

$$\mathbf{H}_{r_0}^t = \frac{1}{i\eta} (\mathbf{Q}_{L,r_0} - \mathbf{Q}_{R,r_0}) \quad (10)$$

where $\eta = (\mu/\varepsilon)^{1/2}$ is the impedance of the material.

Because the transformation Bohren the relation (8) is written:

$$\begin{bmatrix} \nabla \times \mathbf{Q}_{L,r_0} \\ \nabla \times \mathbf{Q}_{R,r_0} \end{bmatrix} = \begin{bmatrix} \gamma_L & 0 \\ 0 & -\gamma_R \end{bmatrix} \begin{bmatrix} \mathbf{Q}_{L,r_0} \\ \mathbf{Q}_{R,r_0} \end{bmatrix} \quad (11)$$

or equivalent

$$\begin{cases} \nabla \times \mathbf{Q}_{L,r_0} = \gamma_L \mathbf{Q}_{L,r_0} \\ \nabla \times \mathbf{Q}_{R,r_0} = -\gamma_R \mathbf{Q}_{R,r_0} \end{cases} \quad (12)$$

where γ_L, γ_R are wave numbers for Beltrami fields $\mathbf{Q}_{L,r_0}, \mathbf{Q}_{R,r_0}$ and are given by,

$$\gamma_L = \frac{k}{1 - k\beta}, \quad \gamma_R = \frac{k}{1 + k\beta} \quad (13)$$

respectively. Applying the transformation Bohren we split the field $\mathbf{E}_{r_0}^t, \mathbf{H}_{r_0}^t$ into the Beltrami fields $\mathbf{Q}_L, \mathbf{Q}_R$, so that the problem (2)-(6) becomes equivalent to the following problem: We are

looking for \mathbf{Q}_L , \mathbf{Q}_R in Ω^+ such that

$$\nabla \times \mathbf{Q}_L(\mathbf{r}) = \gamma_L \mathbf{Q}_L(\mathbf{r}), \quad \mathbf{r} \in \Omega^+ \quad (14)$$

$$\nabla \times \mathbf{Q}_R(\mathbf{r}) = -\gamma_R \mathbf{Q}_R(\mathbf{r}), \quad \mathbf{r} \in \Omega^+ \quad (15)$$

$$\hat{\mathbf{n}} \times \mathbf{Q}_L(\mathbf{r}) = i\sqrt{\frac{\mu}{\varepsilon}} \hat{\mathbf{n}} \times \mathbf{Q}_R(\mathbf{r}), \quad \mathbf{r} \in S \quad (16)$$

$$\hat{\mathbf{r}} \times \mathbf{Q}_L(\mathbf{r}) + i\mathbf{Q}_L(\mathbf{r}) = o\left(\frac{1}{r}\right), \quad r \rightarrow \infty \quad (17)$$

$$\hat{\mathbf{r}} \times \mathbf{Q}_R(\mathbf{r}) - i\mathbf{Q}_R(\mathbf{r}) = o\left(\frac{1}{r}\right), \quad r \rightarrow \infty \quad (18)$$

Spherical Beltrami Fields

So, we consider the Bohren decomposition of $\mathbf{E}_{\mathbf{r}_0}^{inc}$ and $\mathbf{H}_{\mathbf{r}_0}^{inc}$ into suitable incident spherical Beltrami fields $\mathbf{Q}_{L,\mathbf{r}_0}^{inc}$ and $\mathbf{Q}_{R,\mathbf{r}_0}^{inc}$ which have the form [6], [7],

$$\mathbf{Q}_{L,\mathbf{r}_0}^{inc}(\mathbf{r} | \hat{\mathbf{p}}_L) = A_L \tilde{\mathbf{B}}_L(\mathbf{r}, \mathbf{r}_0) \cdot \hat{\mathbf{p}}_L \quad (19)$$

$$\mathbf{Q}_{R,\mathbf{r}_0}^{inc}(\mathbf{r} | \hat{\mathbf{p}}_R) = A_R \tilde{\mathbf{B}}_R(\mathbf{r}, \mathbf{r}_0) \cdot \hat{\mathbf{p}}_R \quad (20)$$

where

$$\tilde{\mathbf{B}}_L(\mathbf{r}, \mathbf{r}_0) = \frac{iky_L}{8\pi y^2} (\gamma_L \tilde{\mathbf{I}} + \frac{1}{\gamma_L} \nabla \nabla + \nabla \times \tilde{\mathbf{I}}) h(\gamma_L |\mathbf{r} - \mathbf{r}_0|) \quad (21)$$

$$\tilde{\mathbf{B}}_R(\mathbf{r}, \mathbf{r}_0) = \frac{iky_R}{8\pi y^2} (\gamma_R \tilde{\mathbf{I}} + \frac{1}{\gamma_R} \nabla \nabla - \nabla \times \tilde{\mathbf{I}}) h(\gamma_R |\mathbf{r} - \mathbf{r}_0|) \quad (22)$$

and $h(x) = e^{ix}/(ix)$ is the zeroth order spherical Hankel function of the first kind and $\tilde{\mathbf{I}} = \hat{\mathbf{x}}\hat{\mathbf{x}} + \hat{\mathbf{y}}\hat{\mathbf{y}} + \hat{\mathbf{z}}\hat{\mathbf{z}}$ is the identity dyadic. We recall that $\tilde{\mathbf{B}}_L$ and $\tilde{\mathbf{B}}_R$ are the fundamental Green dyadics, for the Beltrami fields [1], [11]. The constant unit vectors $\hat{\mathbf{p}}_L$ and $\hat{\mathbf{p}}_R$ are assumed to satisfy the relations:

$$\begin{aligned} \hat{\mathbf{r}}_0 \cdot \hat{\mathbf{p}}_L &= \hat{\mathbf{r}}_0 \cdot \hat{\mathbf{p}}_R = 0 \\ \hat{\mathbf{r}}_0 \times \hat{\mathbf{p}}_L &= i\hat{\mathbf{p}}_L \\ \hat{\mathbf{r}}_0 \times \hat{\mathbf{p}}_R &= -i\hat{\mathbf{p}}_R \end{aligned} \quad (23)$$

The constants A_L and A_R are evaluated so that as the location of the point source goes to infinity along the ray in the direction $\hat{\mathbf{r}}_0$, the spherical fields degenerate into plane LCP and RCP Beltrami fields propagated in a direction from \mathbf{r}_0 towards $\mathbf{0}$, with polarizations $\hat{\mathbf{p}}_L$ and $\hat{\mathbf{p}}_R$, respectively. Using the asymptotic forms:

$$\begin{aligned} |\mathbf{r} - \mathbf{r}_0| &= r_0 - \hat{\mathbf{r}}_0 \cdot \mathbf{r} + o\left(\frac{1}{r_0}\right), \\ \frac{\mathbf{r} - \mathbf{r}_0}{|\mathbf{r} - \mathbf{r}_0|} &= -\hat{\mathbf{r}}_0 + o\left(\frac{1}{r_0}\right), \end{aligned} \quad (24)$$

$$r_0 \rightarrow \infty$$

in the relations (19) and (20) we obtain [6], [7],

$$\mathbf{Q}_{j,r_0}^{inc}(\mathbf{r} | \hat{\mathbf{p}}_j) = A_j \frac{2e^{-iy_j r_0}}{r_0} \tilde{\mathbf{K}}_j(-\hat{\mathbf{r}}_0) \cdot \hat{\mathbf{p}}_j e^{-iy_j \hat{\mathbf{r}}_0 \cdot \mathbf{r}} + O\left(\frac{1}{r_0^2}\right), \quad (25)$$

$$r_0 \rightarrow \infty$$

for $j = L, R$, where

$$\tilde{\mathbf{K}}_L(-\hat{\mathbf{r}}_0) = \frac{1}{2}(\tilde{\mathbf{I}} - \hat{\mathbf{r}}_0 \hat{\mathbf{r}}_0 - i\hat{\mathbf{r}}_0 \times \tilde{\mathbf{I}}) \quad (26)$$

$$\tilde{\mathbf{K}}_R(-\hat{\mathbf{r}}_0) = \frac{1}{2}(\tilde{\mathbf{I}} - \hat{\mathbf{r}}_0 \hat{\mathbf{r}}_0 + i\hat{\mathbf{r}}_0 \times \tilde{\mathbf{I}}) \quad (27)$$

In view of (23) the dyadics $\tilde{\mathbf{K}}_L$ and $\tilde{\mathbf{K}}_R$ satisfy the relations

$$\begin{cases} \hat{\mathbf{p}}_L = \tilde{\mathbf{K}}_L(-\hat{\mathbf{r}}_0) \cdot \hat{\mathbf{p}}_L \\ \hat{\mathbf{p}}_R = \tilde{\mathbf{K}}_R(-\hat{\mathbf{r}}_0) \cdot \hat{\mathbf{p}}_R \end{cases} \quad (28)$$

Hence, if we take

$$\begin{cases} A_L = r_0 e^{-iy_L r_0} \frac{4\pi y^2}{k y_L} \\ A_R = r_0 e^{-iy_R r_0} \frac{4\pi y^2}{k y_R} \end{cases} \quad (29)$$

then

$$\begin{aligned} \lim_{r_0 \rightarrow \infty} \mathbf{Q}_{L,r_0}^{inc}(\mathbf{r} | \hat{\mathbf{p}}_j) &= e^{-iy_L \hat{\mathbf{r}}_0 \cdot \mathbf{r}} \hat{\mathbf{p}}_j = \\ &= \mathbf{Q}_j^{inc}(\mathbf{r}; -\hat{\mathbf{r}}_0, \hat{\mathbf{p}}_j) \end{aligned} \quad (30)$$

It is convenient to write the incident spherical Beltrami fields as [6], [7],

$$\mathbf{Q}_{L,r_0}^{inc}(\mathbf{r} | \hat{\mathbf{p}}_L) = \tilde{\mathbf{r}}_L \left(\frac{h(y_L u)}{h(y_L r_0)} \right) \cdot \hat{\mathbf{p}}_L \quad (31)$$

$$\mathbf{Q}_{R,r_0}^{inc}(\mathbf{r} | \hat{\mathbf{p}}_R) = \tilde{\mathbf{r}}_R \left(\frac{h(y_R u)}{h(y_R r_0)} \right) \cdot \hat{\mathbf{p}}_R \quad (32)$$

where

$$\tilde{\mathbf{r}}_L = \frac{1}{2y_L}(y_L \tilde{\mathbf{I}} + \frac{1}{y_L} \nabla \nabla + \nabla \times \tilde{\mathbf{I}}) \quad (33)$$

$$\tilde{\mathbf{r}}_R = \frac{1}{2y_R}(y_R \tilde{\mathbf{I}} + \frac{1}{y_R} \nabla \nabla - \nabla \times \tilde{\mathbf{I}}) \quad (34)$$

and $u = |\mathbf{r} - \mathbf{r}_0|$. Using asymptotic forms (24) for $r \rightarrow \infty$ we obtain [6], [7],

$$\mathbf{Q}_{j,r_0}^{inc}(\mathbf{r} | \hat{\mathbf{p}}_j) = \mathbf{F}_{j,r_0}^{inc}(\hat{\mathbf{r}} | \hat{\mathbf{p}}_j) h(y_j r) + O\left(\frac{1}{r^2}\right) \quad (35)$$

where

$$\mathbf{F}_{j,r_0}^{inc}(\hat{\mathbf{r}} | \hat{\mathbf{p}}_j) = \frac{e^{-iy_j \hat{\mathbf{r}} \cdot \mathbf{r}_0}}{h(y_j r_0)} \tilde{\mathbf{K}}_j(\hat{\mathbf{r}}) \cdot \hat{\mathbf{p}}_j \quad (36)$$

are the far-field patterns of the point source incident Beltrami fields, which satisfy the relations

$$\hat{\mathbf{r}} \cdot \mathbf{F}_{j,r_0}^{inc}(\hat{\mathbf{r}} | \hat{\mathbf{p}}_j) = 0 \quad (37)$$

The scattered electric field $\mathbf{E}_{r_0}^{sc}$ will be dependent on the polarization $\hat{\mathbf{p}}_L, \hat{\mathbf{p}}_R$ and will be have the decomposition

$$\begin{aligned} \mathbf{E}_{r_0}^{sc}(\mathbf{r} | \hat{\mathbf{p}}_L, \hat{\mathbf{p}}_R) &= \mathbf{Q}_{L,r_0}^{sc}(\mathbf{r} | \hat{\mathbf{p}}_L, \hat{\mathbf{p}}_R) \\ &+ \mathbf{Q}_{R,r_0}^{sc}(\mathbf{r} | \hat{\mathbf{p}}_L, \hat{\mathbf{p}}_R) \end{aligned} \quad (38)$$

where

$\mathbf{Q}_{L,r_0}^{sc}(\mathbf{r} | \hat{\mathbf{p}}_L, \hat{\mathbf{p}}_R)$ and $\mathbf{Q}_{R,r_0}^{sc}(\mathbf{r} | \hat{\mathbf{p}}_L, \hat{\mathbf{p}}_R)$ are the corresponding scattered Beltrami fields, which have the following behavior, when $r \rightarrow \infty$ [1], [10], [12]

$$\mathbf{g}_{L,r_0}(\hat{\mathbf{r}}) = \frac{iky_L}{8\pi y^2} \tilde{\mathbf{K}}_L(\hat{\mathbf{r}}) \cdot \int_S \hat{\mathbf{n}} \times (y_L \nabla \times \mathbf{E}_{r_0}^{sc}(\mathbf{r}') + y^2 \mathbf{E}_{r_0}^{sc}(\mathbf{r}')) e^{-iy_L \hat{\mathbf{r}} \cdot \mathbf{r}'} ds(\mathbf{r}') \quad (40)$$

$$\mathbf{g}_{R,r_0}(\hat{\mathbf{r}}) = \frac{iky_R}{8\pi y^2} \tilde{\mathbf{K}}_R(\hat{\mathbf{r}}) \cdot \int_S \hat{\mathbf{n}} \times (y_R \nabla \times \mathbf{E}_{r_0}^{sc}(\mathbf{r}') - y^2 \mathbf{E}_{r_0}^{sc}(\mathbf{r}')) e^{-iy_R \hat{\mathbf{r}} \cdot \mathbf{r}'} ds(\mathbf{r}') \quad (41)$$

are the LCP and RCP far-field patterns, respectively [10], and they are dependent also on the polarization $\hat{\mathbf{p}}_L$ and $\hat{\mathbf{p}}_R$. We note that the far-field patterns $\mathbf{g}_{j,r_0}(\hat{\mathbf{r}})$ satisfy the relations

$$\begin{cases} \hat{\mathbf{r}} \cdot \mathbf{g}_{j,r_0}(\hat{\mathbf{r}}) = 0 \\ \hat{\mathbf{r}} \times \mathbf{g}_{L,r_0}(\hat{\mathbf{r}}) = -i\mathbf{g}_{L,r_0}(\hat{\mathbf{r}}) \\ \hat{\mathbf{r}} \times \mathbf{g}_{R,r_0}(\hat{\mathbf{r}}) = i\mathbf{g}_{R,r_0}(\hat{\mathbf{r}}) \end{cases} \quad (42)$$

Reciprocity and General Scattering Theorems

For two vector functions \mathbf{u} and \mathbf{v} we introduce the bilinear form [10],

$$\begin{aligned} \{\mathbf{u}, \mathbf{v}\}_S &= \\ &= \int_S \hat{\mathbf{n}} \cdot (\mathbf{u} \times \nabla \times \mathbf{v} - \mathbf{v} \times \nabla \times \mathbf{u}) dS - \\ &- 2\beta y^2 \int_S \hat{\mathbf{n}} \cdot (\mathbf{u} \times \mathbf{v}) dS \end{aligned} \quad (43)$$

$$\mathbf{Q}_{j,r_0}^{sc}(\mathbf{r} | \hat{\mathbf{p}}_L, \hat{\mathbf{p}}_R) = h(y_j r) \mathbf{g}_{j,r_0}(\hat{\mathbf{r}}) + o\left(\frac{1}{r^2}\right) \quad (39)$$

The functions $\mathbf{g}_{j,r_0}(\hat{\mathbf{r}})$ given by

where S is the surface of the scatterer Ω^- and $\hat{\mathbf{n}}$ is the outward unit vector on S . We, also, consider two locations for the point source, \mathbf{a} and \mathbf{b} from which the time-harmonic incident spherical electric waves

$$\begin{aligned} \mathbf{E}_\sigma^{inc}(\mathbf{r} | \hat{\mathbf{p}}_L, \hat{\mathbf{p}}_R) &= \\ &= \mathbf{Q}_{L,\sigma}^{inc}(\mathbf{r} | \hat{\mathbf{p}}_L) + \mathbf{Q}_{R,\sigma}^{inc}(\mathbf{r} | \hat{\mathbf{p}}_R) \end{aligned} \quad (44)$$

for $\sigma = \mathbf{a}, \mathbf{b}$, emanate. \mathbf{E}_σ^{sc} and the corresponding scattered electric waves \mathbf{E}_σ^{sc} of form (38), have the Bohren decomposition of (9) in terms of LCP and RCP Beltrami fields. In particular, we have

$$\begin{cases} \mathbf{E}_\sigma^{inc} = \mathbf{Q}_{L,\sigma}^{inc} + \mathbf{Q}_{R,\sigma}^{inc} \\ \mathbf{E}_\sigma^{sc} = \mathbf{Q}_{L,\sigma}^{sc} + \mathbf{Q}_{R,\sigma}^{sc} \end{cases} \quad (45)$$

and the following properties for the fields $\mathbf{Q}_{j,\sigma}^{inc}$ and $\mathbf{Q}_{j,\sigma}^{sc}$ [6], [7]:

$$\{\bar{\mathbf{Q}}_{L,a}^{inc}(\mathbf{r}; \hat{\mathbf{p}}_L), \mathbf{Q}_{L,b}^{sc}(\mathbf{r} | \hat{\mathbf{q}}_L, \hat{\mathbf{q}}_R)\}_S = \frac{2Y^2}{K} \int_S \hat{\mathbf{n}} \cdot (\bar{\mathbf{Q}}_{L,a}^{inc}(\mathbf{r}; \hat{\mathbf{p}}_L) \times \mathbf{Q}_{L,b}^{sc}(\mathbf{r} | \hat{\mathbf{q}}_L, \hat{\mathbf{q}}_R)) ds(\mathbf{r}) \quad (46)$$

$$\{\bar{\mathbf{Q}}_{L,a}^{inc}(\mathbf{r}; \hat{\mathbf{p}}_L), \mathbf{Q}_{R,b}^{sc}(\mathbf{r} | \hat{\mathbf{q}}_L, \hat{\mathbf{q}}_R)\}_S = 0 \quad (47)$$

$$\{\bar{\mathbf{Q}}_{R,a}^{inc}(\mathbf{r}; \hat{\mathbf{p}}_R), \mathbf{Q}_{R,b}^{sc}(\mathbf{r} | \hat{\mathbf{q}}_L, \hat{\mathbf{q}}_R)\}_S = -\frac{2Y^2}{K} \int_S \hat{\mathbf{n}} \cdot (\bar{\mathbf{Q}}_{R,a}^{inc}(\mathbf{r}; \hat{\mathbf{p}}_R) \times \mathbf{Q}_{R,b}^{sc}(\mathbf{r} | \hat{\mathbf{q}}_L, \hat{\mathbf{q}}_R)) ds(\mathbf{r}) \quad (48)$$

$$\{\bar{\mathbf{Q}}_{R,a}^{inc}(\mathbf{r}; \hat{\mathbf{p}}_R), \mathbf{Q}_{L,b}^{sc}(\mathbf{r} | \hat{\mathbf{q}}_L, \hat{\mathbf{q}}_R)\}_S = 0 \quad (49)$$

Now a "reciprocity theorem" for spherical electromagnetic waves in chiral media is formulated as follows [6], [7]:

For any two incident spherical electric waves $\mathbf{E}_a^{inc}(\mathbf{r} | \hat{\mathbf{p}}_L, \hat{\mathbf{p}}_R)$ and $\mathbf{E}_b^{inc}(\mathbf{r} | \hat{\mathbf{p}}_L, \hat{\mathbf{p}}_R)$ of (44) and for any scatterer in a homogeneous isotropic chiral medium, we have:

$$\begin{aligned} & \frac{ae^{-iy_L a}}{Y_L} \mathbf{Q}_{L,b}^{sc}(\mathbf{a} | \hat{\mathbf{q}}_L, \hat{\mathbf{q}}_R) \cdot \hat{\mathbf{p}}_L + \\ & + \frac{ae^{-iy_R a}}{Y_R} \mathbf{Q}_{R,b}^{sc}(\mathbf{a} | \hat{\mathbf{q}}_L, \hat{\mathbf{q}}_R) \cdot \hat{\mathbf{p}}_R = \\ & = \frac{be^{-iy_L b}}{Y_L} \mathbf{Q}_{L,a}^{sc}(\mathbf{b} | \hat{\mathbf{q}}_L, \hat{\mathbf{q}}_R) \cdot \hat{\mathbf{q}}_L + \\ & + \frac{be^{-iy_R b}}{Y_R} \mathbf{Q}_{R,a}^{sc}(\mathbf{b} | \hat{\mathbf{q}}_L, \hat{\mathbf{q}}_R) \cdot \hat{\mathbf{q}}_R \end{aligned} \quad (50)$$

Let

$\mathbf{E}_a^{inc}(\mathbf{r} | \hat{\mathbf{p}}_L, \hat{\mathbf{p}}_R)$ and $\mathbf{E}_b^{inc}(\mathbf{r} | \hat{\mathbf{p}}_L, \hat{\mathbf{p}}_R)$ be two incident spherical waves of the form (44). We define spherical far-field pattern generators for LCP and RCP spherical Beltrami fields by

$$\begin{aligned} \mathbf{G}_{j,b}(\mathbf{a} | \hat{\mathbf{q}}_L, \hat{\mathbf{q}}_R) &= \frac{ae^{iy_L a}}{iy_j} \cdot \\ & \cdot \left\{ \frac{1}{4\pi} \int_{S^2} \mathbf{g}_{j,b}(\mathbf{a} | \hat{\mathbf{q}}_L, \hat{\mathbf{q}}_R) \cdot \overline{\tilde{\mathbf{K}}_j(\hat{\mathbf{r}})} e^{iy_A \hat{\mathbf{r}} \cdot \mathbf{a}} ds(\hat{\mathbf{r}}) - \right. \\ & \left. - \mathbf{Q}_{j,b}^{sc}(\mathbf{a} | \hat{\mathbf{q}}_L, \hat{\mathbf{q}}_R) \right\} \end{aligned} \quad (51)$$

for $j = L, R$.

This terminology and definition is appropriate because when both the observation point and the source goes to infinity, $\mathbf{G}_{j,b}(\mathbf{a} | \hat{\mathbf{q}}_L, \hat{\mathbf{q}}_R)$, reduce to the far-field patterns for an incident plane electric wave propagating in the direction $-\hat{\mathbf{b}}$ and of polarizations $\hat{\mathbf{q}}_L$ for LCP and $\hat{\mathbf{q}}_R$ for RCP fields. Far-field pattern generators in acoustic and achiral electromagnetic scattering have been defined in [13]. When the point sources are transferred at infinity, the generators $\mathbf{G}_{j,b}(\mathbf{a} | \hat{\mathbf{q}}_L, \hat{\mathbf{q}}_R)$ are transformed into far-field patterns scattering spherical electrical wave, namely [6], [7],

$$\lim_{a \rightarrow \infty} \mathbf{G}_{j,b}(\mathbf{a} | \hat{\mathbf{q}}_L, \hat{\mathbf{q}}_R) = \mathbf{g}_{j,b}(-\hat{\mathbf{a}} | \hat{\mathbf{q}}_L, \hat{\mathbf{q}}_R) \quad (52)$$

Using this notation, the "general scattering theorem" for spherical electric waves in chiral media is formulated as follows [6], [7]:

Let

$\mathbf{E}_a^{inc}(\mathbf{r} | \hat{\mathbf{p}}_L, \hat{\mathbf{p}}_R)$ and $\mathbf{E}_b^{inc}(\mathbf{r} | \hat{\mathbf{p}}_L, \hat{\mathbf{p}}_R)$ be two spherical electric waves of (44) incident upon a

scatterer in a chiral medium. Then it is valid

$$\begin{aligned} & \mathbf{G}_{L,b}(\mathbf{a} | \hat{\mathbf{q}}_L, \hat{\mathbf{q}}_R) \cdot \hat{\mathbf{p}}_L + \mathbf{G}_{R,b}(\mathbf{a} | \hat{\mathbf{q}}_L, \hat{\mathbf{q}}_R) \cdot \hat{\mathbf{p}}_R + \\ & + \overline{\mathbf{G}_{L,a}(\mathbf{b} | \hat{\mathbf{p}}_L, \hat{\mathbf{p}}_R)} \cdot \hat{\mathbf{q}}_L + \overline{\mathbf{G}_{R,a}(\mathbf{b} | \hat{\mathbf{p}}_L, \hat{\mathbf{p}}_R)} \cdot \hat{\mathbf{q}}_R = \\ & = -\frac{1}{2\pi} \left\{ \int_{S^2} \frac{1}{V_L^2} \overline{\mathbf{F}_{L,a}^{sc}(\hat{\mathbf{r}})} \cdot \mathbf{F}_{L,b}^{sc}(\hat{\mathbf{r}}) dS(\hat{\mathbf{r}}) + \right. \\ & \left. + \int_{S^2} \frac{1}{V_R^2} \overline{\mathbf{F}_{R,a}^{sc}(\hat{\mathbf{r}})} \cdot \mathbf{F}_{R,b}^{sc}(\hat{\mathbf{r}}) dS(\hat{\mathbf{r}}) \right\} \quad (53) \end{aligned}$$

References

- [1] Lakhtakia A., "Beltrami Fields in Chiral Media", World Scientific, Singapore, 1993, §1-1 (p. 3), §3-1 (p. 83), §3-2.2 (p. 110), §4-1 (p. 130), §4-3, (p. 150), §5-1, (p. 164)
- [2] Athanasiadis C., Martin P.A., Stratis I.G., "On the scattering of spherical electromagnetic waves by a penetrable chiral obstacle", 6th International Workshop on Mathematical Methods in Scattering Theory and Biomedical Engineering, Tsepelovo, Greece, 2003
- [3] Charalambopoulos A., Dassios G., Kamvyssas G., "Reciprocity theorems for point source scalar scattering", In: Dassios G., Fotiadis D., Kiriaki C., Massalas C. (eds) *Mathematical Methods in Scattering Theory and Biomedical Technology*, Longman, London 1998, pp. 12-19
- [4] Dassios G, Kamvyssas G. "The impedance scattering problem for a point source field. The small resistive sphere", *Quarterly Journal of Mechanics and Applied Mathematics*, Vol. 50, 1999, pp. 321-332
- [5] Athanasiadis C., Martin P.A., Stratis I.G., "On the Scattering of Point-generated Electromagnetic Waves by a Perfectly Conducting Sphere, and Related Near-field Inverse Problems", *Zeitschrift für Angewandte Mathematik und Mechanik*, Vol. 83, Issue 2, 2003, pp. 129-136
- [6] Athanasiadis C, Berketis N., "Scattering relations for point - source excitation in chiral media", *Mathematical Methods in the Applied sciences*, Vol. 29, 2006, pp. 27-48

- [7] Berketis M. Nikolaos, "Scattering spherical Electromagnetic waves in chiral media", PhD thesis, University of Athens – Department of Mathematics, December 2007
- [8] Colton D., Kress R., "Inverse Acoustic and Electromagnetic Scattering Theory" Springer, Berlin, 1992, §6.2, (p. 153)
- [9] Bohren C. F., "Light scattering by an optically active Sphere", Chemical Physics Letters, Vol. 29, Issue 3, 1974, pp. 458-462
- [10] Athanasiadis C., "On the far field patterns for electromagnetic scattering by a chiral obstacle in a chiral environment", Journal of Mathematical Analysis and Applications, Vol. 309, 2005, pp. 517-533
- [11] Athanasiadis C., Giotopoulos S., "Scattering theorem for dyadic chiral fields", Reports on Mathematical Physics, Vol. 53, 2004, pp. 339-350
- [12] Berketis M. Nikolaos, "Direct and Related Far-Field Inverse Scattering Problems for Spherical Electromagnetic Waves in Chiral Media", FunkTechnikPlus # Journal, Issue 2, November 2013, pp. 7-18
- [13] Athanasiadis C., Martin P.A., Spyropoylos A., Stratis I.G., "Scattering relations for point source acoustic and electromagnetic waves", Journal of Mathematical Physics Vol. 43, Issue 11, 2002, pp. 5683-5697

Previous Publication in FUNKTECHNIKPLUS # JOURNAL

"Near-field Method in Solving Inverse Scattering Problem of Spherical Electromagnetic Waves in Chiral media",
Issue 3, pp. 19-25

*** About the Author**

Nikolaos Berketis, Issue 2, p. 18

Self-Standing End-Fed Geometrically Uniform Linear Arrays: Analysis, Design, Construction, Measurements and FLOSS

K.Th. Kondylis, N.I. Yannopoulou, P.E. Zimourtopoulos *

Antennas Research Group, Athens, Greece [1]
Antennas Research Group, Austria – Hellas [2, 3]

Abstract

The array factor of a both geometrically and electrically uniform array is the simple formula for the complex geometric progression sum. This fact, although results in the simplest of all possible analytical designs, obviously does not in the least simplify the complicated practical problem of feeding the array elements using multiple driving points. In order to begin the examination of uniform linear arrays with a single driving point, this paper presents a compact study of the end-fed space arrays with application to geometrically uniform, self-standing linear arrays of parallel dipoles. A number of test array models were simulated, constructed and their radiation pattern was then measured. The experimental and computational results were found to be in good agreement. The developed software applications are available through the Internet as FLOSS Free Libre Open Source Software.

Keywords

End-fed, single driving-point, self-standing arrays

Introduction

A space array of $1 \leq k \leq N$ parallel, arbitrarily shaped, dipoles with identical current density distributions, has a complex vector radiation pattern $E = AG$ (by applying the "Principle of Radiation Patterns Multiplication", i.e. by the linear property of the volume integral), where G is the radiation pattern of the first dipole (which

"generates the array"; the "Generator Pattern"), and A is the Array Factor,

$$A = \sum_{k=1}^N \left(\frac{I_k}{I_1} \right) e^{i\beta(R_{k_r} - R_{1_r})} \quad (1)$$

i.e. the complex numerical radiation pattern of N invented "isotropic point sources", each of current I_k and pointed by the dipole center vector R_k , with projection R_{k_r} to

the unit direction vector r . Linear Arrays have dipole centers on a straight line. Fully Uniform Linear Arrays are both geometrically uniform, i.e. the dipoles are equidistant, and electrically uniform, i.e. the consecutive dipole currents are of equal amplitude and constant phase difference [1].

End-Fed Arrays

Perhaps, the simplest practical array is the one constructed from a linear two-wire transmission line that supports the arms of parallel, linear, symmetrical dipoles, vertical to its plane. In order to operate the line as a balanced one, it is end-fed through a coaxial line balun from a coaxial connector, which at the same time supports the weight of the whole, self-standing, array. A possible analysis of such an array is shown in Fig. 1.

In this one port linear network, the number of circuit voltage and current variables is equal to the sum of 2 variables for the input port plus 2N variables for the dipole ports plus 4(N-1) variables for the line seg-

ment ports, that is a total number of 6N-2 variables. The number of the linear relations between these variables is equal to the sum of 3 relations, for the generator dipole

$$1 \leq N : \begin{aligned} V &= V_1 = {}_i V_1, \\ I &= I_1 + {}_i I_1 \end{aligned} \quad (2)$$

plus 2 relations, for the last dipole

$$2 \leq N : \begin{aligned} {}_o V_{N-1} &= V_N, \\ {}_o I_{N-1} + I_N &= 0 \end{aligned} \quad (3)$$

plus 3(N-2) relations, for the intermediate dipoles

$$3 \leq N, 1 \leq k \leq N-2 : \begin{aligned} {}_o V_k &= V_{k+1} = {}_i V_{k+1}, \\ {}_o I_k + I_{k+1} + {}_i I_{k+1} &= 0 \end{aligned} \quad (4)$$

plus N relations, for the coupling between these dipoles

$$1 \leq k \leq N : V_k = \sum_{\mu=1}^N Z_{k\mu} I_{\mu} \quad (5)$$

plus 2(N-1) relations, for each one of the lossless transmission line segments of electrical length βl_k and characteristic impedance Z_{0k}

$$\theta < \beta l_k \neq v\pi, v = 1, 2, 3, \dots : \begin{bmatrix} {}_{ii} Z_k & {}_{io} Z_k \\ {}_{oi} Z_k & {}_{oo} Z_k \end{bmatrix} = -i \frac{Z_{0k}}{\sin \beta l_k} \begin{bmatrix} \cos \beta l_k & 1 \\ 1 & \cos \beta l_k \end{bmatrix} \quad (6)$$

$$\beta l_k = v\pi, v = 2\mu + 1, \mu = 0, 1, 2, \dots : \begin{aligned} {}_o V_k &= -{}_i V_k, \\ {}_o I_k - {}_i I_k &= 0 \end{aligned} \quad (7)$$

$$\beta l_k = v\pi, v = 2\mu + 2, \mu = 0, 1, 2, \dots : {}_oV_k = {}_iV_k, {}_oI_k + {}_iI_k = 0 \quad (8)$$

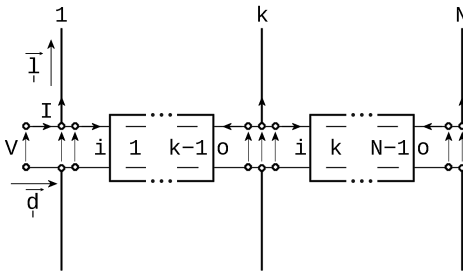


Fig. 1: End-fed linear array of linear dipoles

that is a total of $6N-3$ linear relations to solve for $6N-2$ variables, in terms of the source voltage V , which is considered as a parameter. Anyhow, the resulting current ratios are clearly independent of V .

Single Driving-Point Self-Standing Linear Array

The authors' group has limited available technical resources for antenna construction. This fact restricts the experimentation to thin-wire self-standing array models of a low total weight that is of a small total transmission line length and of a small number of dipoles. Thus, the practical application of the analysis was carried-out for $N = 2, 3$ and 4 dipoles only. In order to demonstrate the procedure in use, the smallest case of $N = 2$ dipoles is

presented in some detail. In Fig. 2, the resulting $6N-3 = 9$ linear relations between $6N-2 = 9$ variables + 1 parameter, are shown in a compact form, for the case of $\beta l_1 \neq v\pi, v = 1, 2, \dots$ in (6), with each cell value to be the coefficient of the variable in the first row of its column in an implied summation, while, if $\beta l_1 = v\pi, v = 1, 2, \dots$ then the two last rows with the gray background have to substituted by the rows of Fig. 3 or 4, according to the odd or even value of v given in (7)-(8).

V_1	V_2	I_1	I_2	${}_iV_1$	${}_oV_1$	${}_iI_1$	${}_oI_1$	I	$=$	V
1									$=$	1
1				-1					$=$	0
		1				1		-1	$=$	0
	1				-1				$=$	0
			1				1		$=$	0
-1		Z_{11}	Z_{12}						$=$	0
	-1	Z_{21}	Z_{22}						$=$	0
				-1		${}_iZ_{11}$	${}_iZ_{12}$		$=$	0
					-1	${}_oZ_{11}$	${}_oZ_{12}$		$=$	0

Fig. 2: The linear system of 9 relations for arrays with $N = 2$ and $\beta l_1 \neq v\pi, v = 1, 2, \dots$

Obviously, the complexity of the expressions increase with the number of dipoles, from the simple, of 2 dipoles

$$I_{21} = \frac{I_2}{I_1} = \frac{Z_{12}Z_{00}Z_1 - i_0Z_1Z_{22}}{i_0Z_1^2 + i_0Z_1Z_{12} - o_0Z_1(Z_{22} + o_0Z_1)} \quad (9)$$

in which the equality of self and mutual impedances have been taken into account, resulting from the system of Fig. 2, or of the simplest $I_2/I_1 = +1$ or $I_2/I_1 = -1$ of Fig. 3 or Fig. 4 respectively, to the most complex one for 4 dipoles, shown in Fig. 5, which covered about one and a half A4 page.

				1	1			=	0
						-1	1	=	0

Fig. 3: Last rows replacement for $v = 2\mu + 1, \mu = 0, 1, 2, \dots$

				-1	1			=	0
						1	1	=	0

Fig. 4: Last rows replacement for $v = 2\mu + 2, \mu = 0, 1, 2, \dots$

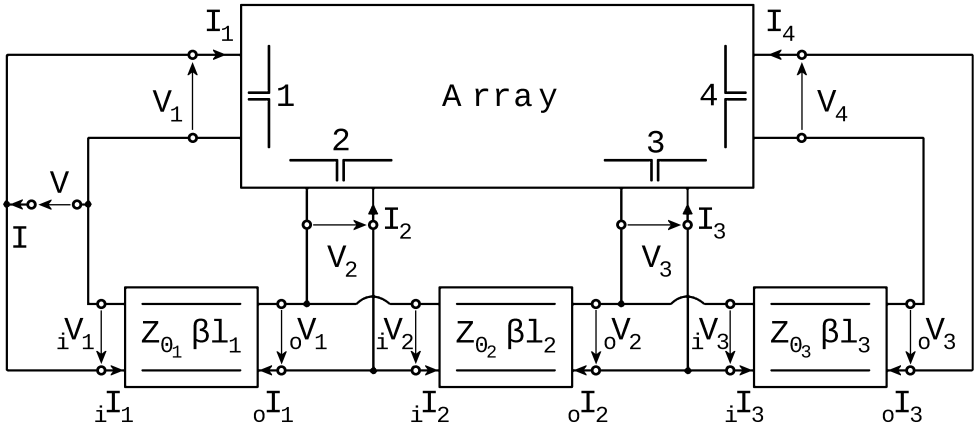


Fig. 5: Equivalent circuit of the 4 dipoles linear array

Three Visual Fortran applications were developed for the computation of current ratios. The GUI application form for $N = 4$ dipoles, is shown in Fig. 6 [2], [3]. In this form, the input data are the $N-1$ distances between dipoles, the dipole radius and length, the length, the characteristic impedance and the

velocity factor of each transmission line segment. In addition to current ratios, each application produces the text files needed by the [RadPat4W] application of a FLOSS mini-Suite of tools, which plots in Virtual Reality the Generator, Array Factor, and Array 3D radiation pattern, as well as, their 2D

main-plane cuts [4]. The deduced formulas for the determination of the $1 + 2 + 3 = 6$ current ratios (I_k/I_1), were mechanically verified using Mathematica.

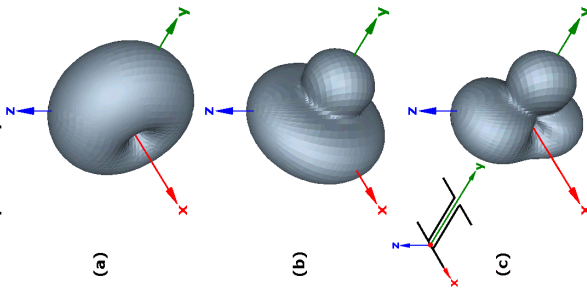
Array Design, Construction and Measurements

A number of dipole array designs were carried out using the developed applications and the [RichWire] simulation program, which is a fully analyzed, corrected and redeveloped edition of the original Moment Method thin-wire computer program [4], [5]. Eleven arrays were finally constructed and tested. The results for the current ratios of four selected arrays are shown in Tab. 1. The arrays were designed for operation at the frequency of 1.111 GHz. A two-wire transmission line, of $Z_0 = 200 \Omega$ and velocity factor $vf = 1$ was constructed to feed the dipoles [6]. This balanced line was then connected to an unbalanced 50Ω type-N/F base connector through a 4:1 balun made from a segment of RG-174U coaxial cable ($Z_0 = 50 \Omega$, $vf = 0.66$) with total length $\lambda/2$.

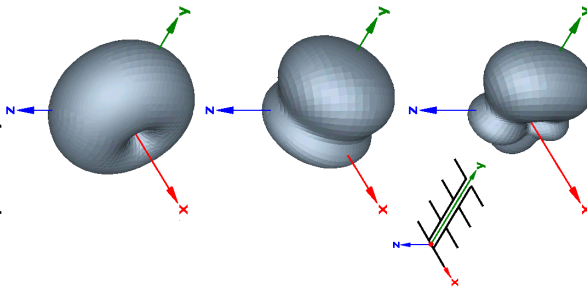
The arrays were constructed by bare copper wire of 1 mm (0.0037λ) radius and they are self-standing using an orthogonal piece of a two-

sided printed board (3 cm x 4.48 cm), on which the two-conductor line was soldered. A few Teflon spacers of low relative dielectric constant (≈ 2) were fabricated to fix the distance between the two line wires at 5.5 mm. The measurement system consists of a 50Ω Vector Network Analyzer external to an anechoic chamber [7]. Each array under test was azimuthally rotated around its three main axes, by a 360° built positioner, under the developed software control of a built hardware controller. The stationary antenna was a UHF standard gain antenna [8]. Fig. 7 and Fig. 8 show the results for the 4 test arrays, in 3 groups of rows, as follows: 1st group: The screen captures of the produced Virtual Reality radiation patterns in dB for (a) Generator, (b) Array Factor, and (c) Dipole Array - 2nd group: The constructed model, and 3rd group: The 2D radiation pattern cuts by (d) xOy , (e) yOz , and (f) zOx main-planes. In Fig. 7, the measurements for the array of $N = 2$, dipoles with equidistance $d = 0.325\lambda$, were carried out with and without balun. In Fig. 8, the array of $N = 2$ dipoles with equidistance $d = 0.633\lambda$, has been designed to exhibit the maximum radiation pattern direction off the 3 main-axes.

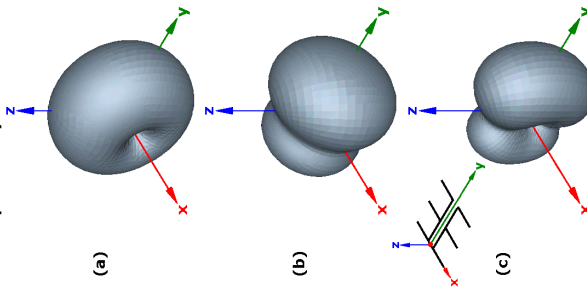
2 Dipoles Array, Distance 0.633 λ



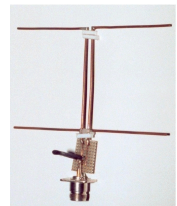
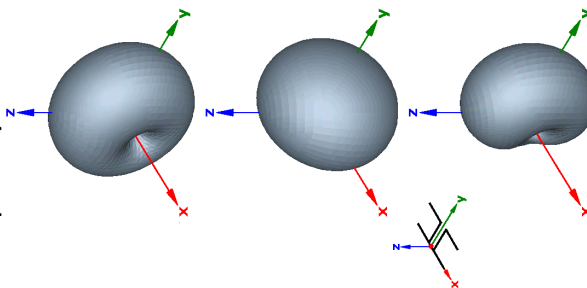
4 Dipoles Array, Distance 0.325 λ



3 Dipoles Array, Distance 0.325 λ



2 Dipoles Array, Distance 0.325 λ



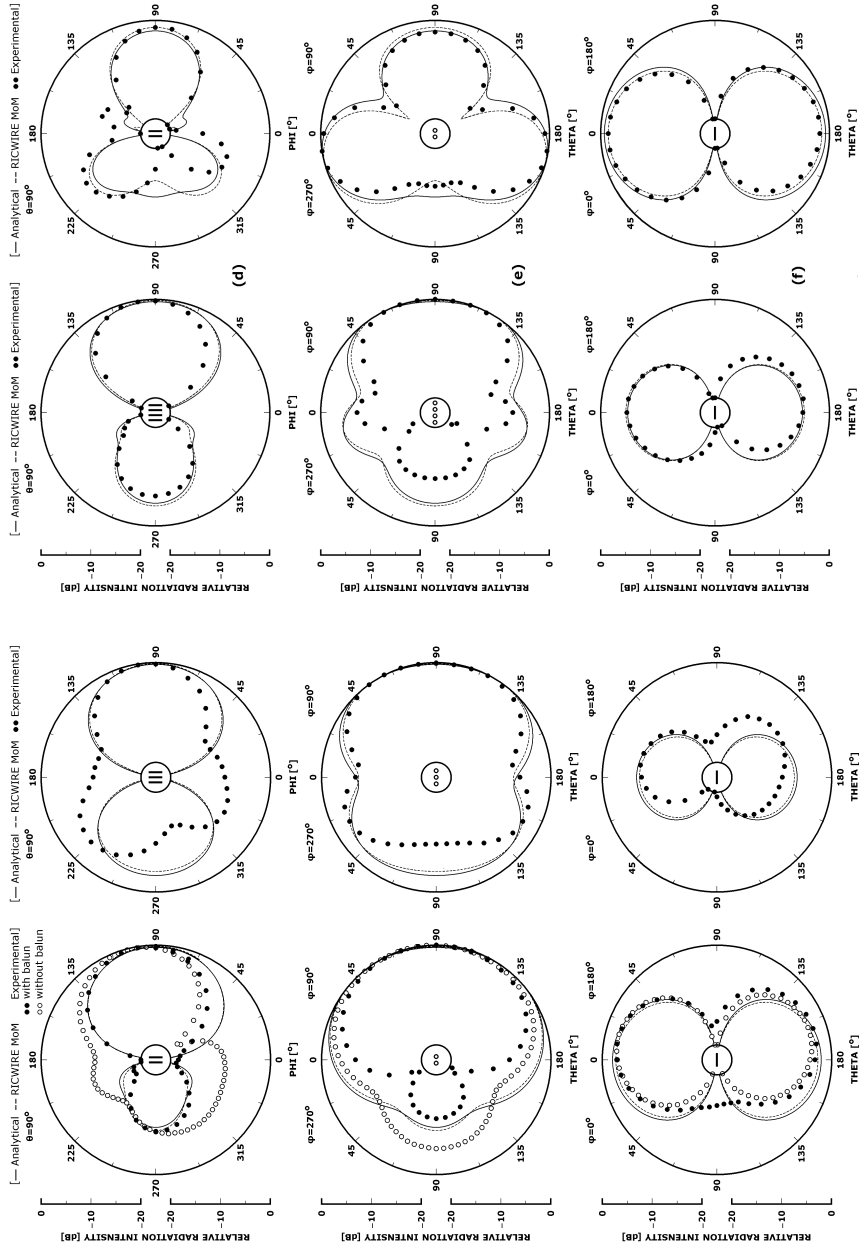


Fig. 7: Analysis, simulation and measurements for experimental arrays: $N = 2$, $N = 3$ and $d = 0.325\lambda$

Fig. 8: Analysis, simulation and measurements for experimental arrays: $N = 4$ $d = 0.325\lambda$, $N = 2$ and $d = 0.633\lambda$

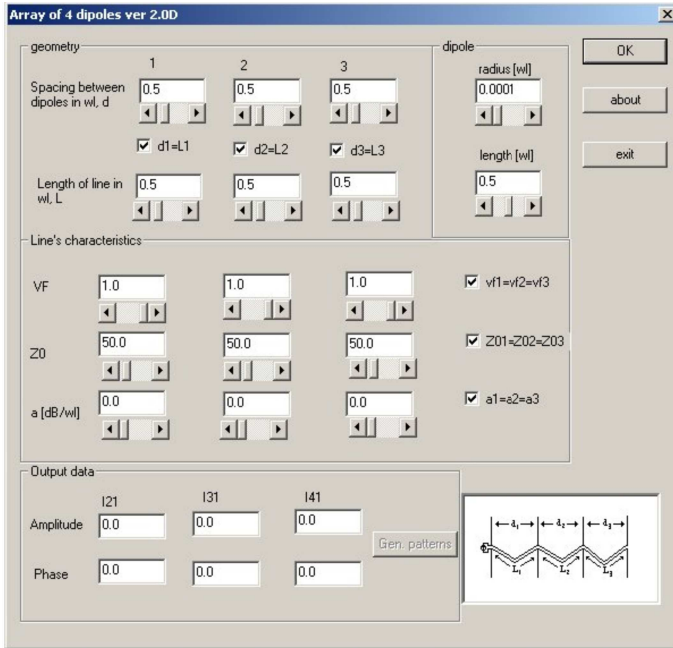


Fig. 6: GUI for the analysis of a linear array of $N = 4$ dipoles

Tab. 1: The experimental array characteristics and current ratios

Dipoles	2		3		4			2
L/λ	0.5185		0.5		0.5			0.44
d/λ	0.325		0.325		0.325			0.633
Ratios	I_2/I_1	I_2/I_1	I_2/I_1	I_3/I_1	I_2/I_1	I_3/I_1	I_4/I_1	I_2/I_1
$ I_k/I_1 $	0.534	0.205	0.286	0.280	0.115	0.226	0.527	
$\angle I_k/I_1 [^\circ]$	-80.5	-114.9	173	-115.9	150.4	68.1	49.5	

Conclusion

Although, the unavoidable mechanical supporting elements which exist in the anechoic chamber in the neighborhood of the antenna under test may affect the radiation pattern measurements, the observed differences in the 4 of the 12 patterns between the analysis and simulation results, on the one hand, and the measurements, on the other, have to be charged respectively: (1) On a cone-cut of the array radiation pattern, instead of the expected yOz main-plane cut, in Fig. 7(e), $N = 2$ and Fig. 8(e), $N = 4$, (2) On an inclination of the rotation axis relative to the expected linear polarization measurement plane, in Fig. 8(d), $N = 2$, and (3) On a

loosed connection during the array rotation, in Fig. 7(d), $N = 3$. These conclusions are amplified by the careful study of the corresponding Virtual Reality space radiation patterns. Therefore, under the given measurement circumstances, the experimental and computational results were found to be in good agreement and no attempt was made to modify any design or repeat any measurement.

The results for the single driving-point self-standing fully Uniform Linear Arrays, i.e. those including the electrical uniformity, along with their application to the constrained pattern design will be presented in a future paper (Part 2).

References *

- [1] Zimourtopoulos P., "Antenna Notes 1999-, Antenna Design Notes 2000-", "www.antennas.gr/antennanotes/" (in Greek)
- [2] Kondylis K., "Standard Antenna Arrays", Master Thesis #1, ARG-Antenas Research Group, DUTH, 2002 (in Greek)
- [3] Kondylis K., "FLOSS for Self-Standing Linear Arrays of Dipoles", "www.antennas.gr/floss" or "<http://code.google.com/p/rga/>"
- [4] Yannopoulou N., Zimourtopoulos P., "A FLOSS Tool for Antenna Radiation Patterns", Proceedings of 15th Conference on Microwave Techniques, COMITE 2010, Brno, Czech Republic, pp. 59-62
- [5] Richmond J.H., "Computer program for thin-wire structures in a homogeneous conducting medium", Publication Year: 1974, NTRS-Report/Patent Number: NASA-CR-2399, ESL-2902-12, DocumentID: 19740020595, "<http://ntrs.nasa.gov/>"

- [6] Chipman R.A., "Transmission Lines", McGraw-Hill, 1968, pp. 140-141, 104-105
- [7] Yannopoulou N., Zimourtopoulos P., "Total Differential Errors in One Port Network Analyzer Measurements with Application to Antenna Impedance", Radioengineering, Vol. 16, No. 2, June 2007, pp. 1-8
"www.radioeng.cz/fulltexts/2007/07_02_01_08.pdf"
- [8] Yang R.F.H., "A proposed gain standard for VHF antennas", IEEE Transactions on Antennas and Propagation, 1966, Vol. 14, No. 6, p. 792
- *Active Links: 27.04.2014 - Inactive Links : FTP#J Link Updates: "http://updates.ftpj.otoiser.org/"

Preprint Versions

"A Study of End-Fed Arrays with Application to Single Driving-Point Self-Standing Linear Arrays"

Konstantinos Kondylis, Nikolitsa Yannopoulou,
Petros Zimourtopoulos

"http://arxiv.org/abs/1002.3871"

Proceedings of 15th Conference on Microwave Techniques,
COMITE 2010, Brno, Czech Republic, pp. 43-46

Follow-Up Research Paper

Not until now

Previous Publication in FUNKTECHNIKPLUS # JOURNAL

"The Very First Ever Made 3D/4D Virtual Laboratory for Antennas", Issue 3, pp. 7-18

*** About The Authors**

Konstantinos Kondylis, was born in Athens, Greece in 1976. He graduated from Electrical Engineering and Computer Engineering in 2000 and received a MSc in Antennas in 2002, both from Democritus University of Thrace, Xanthi, Greece. Member of Antennas Research Group since 2000, he worked as R&D Engineer for Siemens and Nokia Solutions and Networks. He is currently working as Sr. Project Engineer in Doha, Qatar.

Nikolitsa Yannopoulou, Issue 1, p. 15

Petros Zimourtopoulos, Issue 1, p. 15

This paper is licensed under a Creative Commons Attribution 4.0 International License – <https://creativecommons.org/licenses/by/4.0/>

Parameters Affecting the Lifetime of Transformer Oil in Distribution Transformers: Parameter Monitoring of 50 Transformers from the Athens Area

M.G. Danikas, E. Rapti, I. Liapis, A.B.B.Abd. Ghani *

Department of Electrical and Computer Engineering,
Democritus University of Thrace, Xanthi, Greece [1, 2]
Public Electricity Corporation, Athens, Greece [3]
High Voltage Cable Diagnostics, Distribution Unit TNB
Research Sdn. Bhd. Selangor, Malaysia [4]

Abstract

The aim of this paper is the study of various parameters affecting the ageing of transformer oil in distribution transformers of 20/0.4 kV. Fifty (50) samples of oil were taken from such transformers. The transformers function in the major Athens area, Greece. Parameters, such as breakdown strength, oil color, humidity, interfacial tension and $\tan\delta$ were taken into account. Transformer ageing and lifetime are strictly related to the rate of ageing of the whole insulating system, and mainly of the oil.

Absence of transpiring system with silica gel has as a result the increase of oil humidity. The lengthy use of transformers under heavy load, and consequently under high temperatures, is a main factor for oil ageing and oxidation. Especially in the last few years, the increased loads required by the transformers which have to do also with the climatic changes, have as a result the additional stressing of the oil. Various arcs, resulting from short circuits in the network, have as a consequence the production of gases and sludge. Such gases and sludge influence in a negative way the insulating properties of the oil as well as its rate of ageing. The role of silica gel is stressed.

Keywords

Transformer oil, distribution transformer, diagnostic methods, breakdown voltage, dielectric strength

Introduction

Transformer oil is a most important component in transformers [1]. Transformer oil ageing has been studied as well as the parameters and factors influencing its behavior under a variety of stresses (electrical, thermal, etc.) [2]-[5]. Faults in power and distribution transformers are rare (of the order of 1% - 2% per year), but when they occur, they have very serious technical and economic consequences. They may even lead to dangerous situations for human life and the environment. Main factors affecting the acceleration of ageing of the insulation of a transformer are humidity, high temperature, oxidation and the acidity of its oil. The role of chemical byproducts of the transformer insulation is also very important for its ageing. There is no single measurement able to give a whole picture of the state of a transformer. It must be noted that the variety of the diagnostic methods used, does not have as an aim the prediction of the useful remaining lifetime of the insulation, but it tries to reveal the increasing probability of faults and the corresponding decrease of the insulation reliability. Needless to say, that reduced reliability implies also reduced remaining

insulation lifetime.

With this in mind, in the context of the present paper, diagnostic methods were used in order to study the state of distribution transformers of the major Athens area. The transformers investigated were 20/0.4 kV. The whole work was carried with the aid of Public Power Company (PPC) of Greece, and more specifically with the aid of PPC Transformer Division. Oil was taken from 50 distribution transformers.

Diagnostic Methods

Warning signs about the state of a transformer are, among others, a big increase of partial discharges ($>> 2500$ pC), a visible deterioration because of foreign metallic and carbon particles, the presence of humidity in the solid insulation about 3-4 % and the presence of sludge.

Several diagnostic methods were used in order to see the quality of the transformers in question. The characterization of the oil color (DIN 51517 - ASTM D155) was performed through a device (chromometer) including standard glass disks and two glass jars with lid. The control of dielectric strength was measured by a typical Foster test cell, according to IEC 156/95 (Fig. 1).

The control of humidity in the oil was measured by a Metrohm - 684 KF Coulometer, which consisted of a glass container with a stirrer titration in which the reagent from container storage is added. The device is fully automated and once the experimenter gives the settings, it

measures the moisture content of the oil. The measurements were performed according to IEC 814. The control of interfacial tension (ASTM D971 - 91) was performed via a tensimeter, which gives the value in dynes per centimeter in a direct reading (Fig. 2).



Fig. 1: Device for the measurement of dielectric strength

The device that performed measurements of $\tan\delta$ and of resistivity, is the BAUR-DTL fully automated device for measuring dielectric losses of oils. Such a system has a fully automated process for measuring dielectric loss, relative dielectric constant and resistivity. The measurements were performed with a

system counting $\tan\delta$ values with maximum accuracy from 0.00001 to 4.0, measured according to IEC 247.

It is true that no single diagnostic method can give full information as to the state of a transformer. The aforementioned methods may give a better picture of its state.



Fig. 2: Tensimeter Cenco du Nouy

Experimental Results

The sampling was performed with due care, and according to general standard practice, i.e. during sampling there must not be any dust and humidity in the nearby space, the sampling cells must be clean and dry and they must be washed with oil from the transformer which is to be checked, the samples must be protected from light and they must be taken while the oil is hot but due time should pass before the various particles settle down. Sampling was done from the bottom of the transformers. The glass cells used for oil sampling were big enough so that they contained enough oil volume for additional measurements, if needed. No measurement was performed based on only one value or sample. All results must be verified with additional samples and measurements. Color measurements of the oil samples were based on specification DIN 51517 - ASTM D155 (Fig. 3). Dielectric strength measurements were based on specification IEC 156/95. Humidity measurements were based on specification IEC 814. Interfacial tension measurements were based on specification ASTM D971-91. Loss factor measurements were based on specification IEC 247.

Transformer oil is charac-

terized as good, if its color is not dark, its breakdown voltage more than 40 kV, its humidity less than 10 ppm, its resistivity more than 3 GΩ·m, its loss factor 0.1, its interfacial tension more than 28 mN/m. It is acceptable if its breakdown voltage is between 30 to 40 kV, its humidity between 10 and 25 ppm, its resistivity between 0.2 and 3 GΩ·m, its loss factor between 0.1 and 0.5, its interfacial tension between 22 and 28 mN/m. In the case of an acceptable oil, samplings should be carried out more frequently, and the content in foreign particles and contained water should be controlled. If the breakdown voltage and humidity are near the limit values, then the oil should be filtered and cleaned. An oil is poor when its color is dark (the dark color is an indication of pollution or ageing), its breakdown voltage less than 30 kV (in this case the oil should be replaced or thoroughly cleaned), its humidity more than 25 ppm (in such a case the oil should be replaced or thoroughly cleaned), its resistivity less than 0.2 GΩ·m, its loss factor more than 0.5, its interfacial tension less than 22 mN/m (in this case a check should be carried out for the presence of sludge).

Generally it is suggested that in case one of the parameters mentioned (color, dielectric strength, humidity, interfacial tension, loss factor, resistivity) is acceptable, a more frequent sampling should be done in order to better monitor the oil quality. In the case any of the mentioned parameters is poor, cleaning or replacement of the oil is suggested. In any case, it is good to control all parameters concerned in order to have a clear picture of the state of the oil.

From the 50 oil samples investigated (taken from 50 distribution transformers), 3 of them showed breakdown voltage lower than 30 kV (i.e. percentage of 6%), 45 samples indicated humidity higher

than 25 ppm (i.e. percentage 90%), 28 samples presented interfacial tension lower than 15 dynes/cm (percentage 56%), whereas 44 samples showed a color higher than 1 1/2 (percentage 88%) (Fig. 4). It was evident from the data - mentioned in detail in [6] - that the more the number of years in service, the more the number of samples with lower dielectric strength. This is due to the fact that with the years there is also an increase of humidity in oil as well as an increase of the oxidation byproducts. Transformers which are in cities or in urban localities do not usually suffer lightning strokes, consequently the only stresses come from switching overvoltages and/or some high currents.



Fig. 3: Chromometer Hellige Comparator



Fig. 4: Typical glass colored disc

As the years pass by, humidity increases because fluctuations in temperature cause an increase of humidity entering the main oil volume. In distribution transformers having silica gel, the latter loses its absorbing property with an increasing number of years in service. Consequently silica gel should be replaced at regular intervals. The increasing number of years in service influences also the oil oxidation. Oxidation by-products in turn affect $\tan\delta$. The loss factor, however, is not influenced from the existence of humidity in the samples and for this reason is not a criterion for its exis-

tence. Interfacial tension is reduced with the years in service. This is due to the increasing quantity of humidity as well as to the byproducts of oxidation. There is, however, a number of samples with rather reduced interfacial tension although the number of years in service was not that big. This may be due to the quality of the oil used or to the fact that it contained only a small quantity of anti-oxidants. Finally, the oil color changes with the years in service. A change of color may also be due to the overcharging of a transformer.

Discussion

In this work, sampling from 50 transformers of 20/0.4 kV was carried out. Sampling and measurements were performed as suggested by the various international specifications [7]. All transformers were in the major Athens area. It should be noted that the transformers were not all from the same manufacturer. There were transformers from various manufacturers, both from Greece and abroad. This is one of the complications of the Greek Electricity System and certainly, this fact hinders any thought for a statistical approach. In case of poor oil color, this may be a symptom of humidity. Poor oil dielectric strength may imply that the oil should be cleaned or replaced. If the humidity level is high, the oil has to be again either cleaned or replaced. If the interfacial tension of oil is acceptable, this means that a control for the possible presence of by-products may be performed. Acceptable values of oil resistivity may be tolerated. In most cases, $\tan\delta$ was good. The parameters which changed most were the color, the oil dielectric strength, the levels of humidity and the oil interfacial tension. From the above, it is evident that one cannot pronounce any verdict

on the quality of a transformer oil based on only one parameter.

It is evident from the results that there was absence of a transpiring system with silica gel in most investigated transformers. This absence has as a result that the humidity of the atmosphere is in contact with the oil. The functioning of a transformer under heavy load, and consequently its functioning at high temperatures, results in an acceleration of its ageing. High temperatures cause oxidation of the oil. In addition to that, in the last years, increased loads – as a consequence of climatic changes (such as increased temperature and humidity) – are required and they result in the stressing of the oil. Arcs, because of short circuits, create gaseous byproducts and sludge. The latter influence in a negative way the dielectric strength of the oil. Another point which should be considered is that, with the continuing effort from the side of the manufacturers for the reduction in the size of the transformers, the oil tends to be more easily thermally stressed. This results in an accelerated rate of rise in temperature and an accelerated rate in its ageing.

Generally speaking, the frequent oil sampling helps in pointing out potential trouble spots in the network. It goes without saying that, as in this paper, a variety of measurements may give a better picture of the actual state of the transformers rather than isolated measurements or measurements confined only on a single quantity (e.g. dielectric strength). Ageing is a complex process and, as is well known, a variety of factors play a role. Ageing factors contribute not only to the ageing of the oil, but they may also interact among themselves, rendering thus the prediction of lifetime even more difficult [8], [9]. Breakdown of transformer oil is also a complex phenomenon determined mostly by the operating conditions [10].

As a way out of the various problems with transformer ageing, the construction of additional substations is proposed. This will reduce the load of each transformer. Needless to say that, the continuous checking of the whole distribution network and the requirement from the manufacturers to observe all the international norms and specifications, are necessary conditions for the good functioning of the whole system.

Special attention should be paid to the way one gets the oil samples. Sampling should be done with due care and care should be taken in order not for the sample to contain water. The samples should be taken from the transformers when the oil is still warm. Foreign particles should be allowed to settle at the bottom, so that no undue influence can be recorded in the various measurements.

In the case the results are contradictory, one has to repeat the sampling and the corresponding measurements. It is true that the manufacturers, try to reduce the production cost of the transformers and their respective materials by reducing the size of the transformers. This on one hand has as a result the possibly higher break-down strength of the oil, on the other hand, however, has as a result the faster increase of the oil temperature, and consequently the faster ageing and stressing of the mechanical parts of the transformer. Anyhow, a better maintenance of the distribution transformers should be followed as well as the placing of more transformers of larger power in localities with an increasing load demand.

The discussion as well as the conclusions of the pre-

sent paper are in line with previously published work [11], [12]. Such work was carried out on transformers of 20/0.4 kV as well as of 150/20 kV. A statistical approach cannot be offered for the time being, as it was done before [13], for the reasons given above.

It is to be hoped that the next steps in our work will be a classification of the distribution transformers according to manufacturer, according to their power (kVA) and according to the previous history (which includes years in service, all faults, short-circuits, lightning strokes, switching operations etc.). Thereafter, an effort will be made in order to statistically analyze the data.

Concluding, it is fitting to note that the present paper does not claim any originality regarding any new diagnostic techniques. This paper is an application of already existing and well known specifications. It is a continuation of an effort started few years ago, as mentioned in [7], [11], [12]. In this respect, the present paper presents new results, although the methods used are the same as in [6], [7], [11], [12]. In other words, this paper presents the state of transformer oil in some dis-

tribution transformers of a given area at a given moment in time. Needless to say that continuous monitoring is necessary in order to check and confirm the transformer oil quality. Continuous monitoring, however, is often not enough. If possible, it should go together with fault detection, namely partial discharge (PD) detection. PD detection can help preventing a defect from developing into a fault, e.g. a short circuit [14], [15], [16]. Nevertheless, condition monitoring as presented here, should be done on a regular basis.

Conclusion

Transformers of 20/0.4 kV from the major Athens area were investigated. Various parameters (oil color, dielectric strength, humidity, interfacial tension, $\tan\delta$ and resistivity) of the oil were studied with standard methods based on international specifications. No verdict on transformer oil quality can be based on only one parameter. A multitude of parameters is needed in order to pronounce a correct verdict on oil quality. The continuous control and monitoring of the distribution transformers is necessary in order to avoid problematic situations. The role of silica gel is emphasized.

Silica gel should be used in all transformers, so that humidity can be absorbed. The quantity of humidity increases with the number of years in service, consequently, distribution transformers should be checked at regular intervals.

References

- [1] Kind D., Kaerner H., "High-Voltage Insulation Technology", Eds. Friedr. Vieweg & Son, Braunschweig/Wiesbaden, Germany, 1985
- [2] Bell W.R., "Influence of specimen size on the dielectric strength of transformer oil", IEEE Transactions on Electrical Insulation, Vol. 12, 1977, pp. 281-292
- [3] Felici N.J., "Bubbles, partial discharges and liquid breakdown", Electrostatics 79, Institute of Physics Conference Ser. No. 48, 1979, pp. 181-190
- [4] Danikas M.G., "Breakdown of transformer oil", IEEE Electrical Insulation Magazine, Vol. 6, No. 5, 1990, pp. 27-34
- [5] Beroual A., Zahn M., Badent R., Kist K., Schwab A.J., Yamashita H., Yamazawa K., Danikas M., Chadband W.G., Torshin Y., "Propagation and structure of streamers in liquid dielectrics", IEEE Electrical Insulation Magazine, Vol. 14, 1998, pp. 6-17
- [6] Rapti E., "Parameters affecting the lifetime of transformer oil in distribution transformers", Diploma Thesis, Democritus University of Thrace, Department of Electrical and Computer Engineering, Power Systems Laboratory, Xanthi, Greece, 2009 (in Greek)
- [7] Liapis I., "Study of parameters influencing the ageing of the oil in distribution transformers", M.Sc. Thesis, Democritus University of Thrace, Department of Electrical and Computer Engineering, Power Systems Laboratory, Xanthi, Greece, 2010 (in Greek)
- [8] Kelen A., "Trends in PD diagnostics", IEEE Transactions on Dielectrics and Electrical Insulation, Vol. 2, 1995, pp. 529-534
- [9] Bernstein B.S., Brancato E., "Aging of equipment in the electric utilities", IEEE Transactions on Electrical Insulation, Vol. 28, 1993, pp. 866-875

- [10] Naidu M.S., Kamaraju V., "High Voltage Engineering", Eds. Tata McGraw-Hill Publishing Co. Ltd., New Delhi, India, 1995
- [11] Danikas M.G., Liapis I., "A study of parameters affecting the ageing of transformer oil in distribution transformers", Proceedings of 17th International Conference on Dielectric Liquids (ICDL 2011), Trondheim, Norway, 26-30 June 2011, Session 02, Paper 1
- [12] Danikas M.G., Missas S., Liapis I., "Factors affecting the ageing of transformer oil in 150/20 kV Transformers", Proceedings of 17th International Conference on Dielectric Liquids (ICDL 2011), Trondheim, Norway, 26-30 June 2011, Session 06, Paper 1
- [13] Spartalis S.I., Danikas M.G., Andreou G.P., Vekris G., "Statistical study of the oil dielectric strength in power distribution transformers", Journal of Electrical Engineering, Vol. 59, 2008, pp. 68-74
- [14] Borsi H., "Probleme der Teilentladungs-(TE-)Ueberwachung am Beispiel von TE-Messungen an Leistungstransformatoren im Betrieb", book (editors: Koenig D., Narayana Rao Y., "Teilentladungen in Betriebsmitteln der Energietechnik", vde verlag gmbh, Berlin und Offenbach, Germany, 1993), pp. 275-292
- [15] Gulski E., Smit J.J., Brooks R., Turner M., "Experiences with digital analysis of discharges in high voltage components", IEEE Electrical Insulation Magazine, Vol. 15, No. 3, 1999, pp. 15-24
- [16] Marques A.P., De Jesus Ribeiro C., Bezerra Azevedo C. H., Dos Santos J.A.L., De carvalho Sousa F.R., da Cunha Brito L., "Power transformer disruptions - A case study", IEEE Electrical Insulation Magazine, Vol. 30, No. 2, 2014, pp. 17-21

Previous Publication in FUNKTECHNIKPLUS # JOURNAL

"Interfaces in High Voltage Engineering: A Most Important Question for Conventional Solid Insulating Materials as well as for Nanocomposite Polymers", Issue 4, pp. 7-31

*** About The Authors**

Michael Danikas, Issue 2, p. 39

Elli Rapti, is a graduate of Democritus University of Thrace, Department of Electrical and Computer Engineering, Xanthi, Greece. She is currently employed in a private-owned company. Her research interests are in transformer oil diagnostics.

Ioannis Liapis, is a graduate of Democritus University of Thrace, Department of Electrical and Computer Engineering, Xanthi, Greece, and is currently working with Public Power Corporation in Athens. His research interests are in transformer oil diagnostic techniques.

j-liapis@hotmail.com

Ahmad Basri Bin Abdul Ghani, Dr., is a researcher at TNB Research Institute in Selangor, Malaysia. His research interests include among other topics, power cable diagnostics, transformer oil diagnostics and partial discharge measurements.

abasri.aghani@tnbr.com.my

[This Page Intentionally Left Blank]

[This Page Intentionally Left Blank]

In case of any doubt,
download the genuine papers from
genuine.ftpj.otoiser.org

FRONT COVER VIGNETTE

A faded synthesis of an anthemion rooted in a meandros

The thirteen-leaf is a symbol for a life tree leaf.
"Herakles and Kerberos", ca. 530–500 BC,
by Paseas, the Kerberos Painter,
Museum of Fine Arts, Boston.

www.mfa.org/collections/object/plate-153852

The simple meandros is a symbol for eternal immortality.
"Warrior with a phiale", ca. 480–460 BC,
by Berliner Maler,
Museo Archeologico Regionale "Antonio Salinas" di Palermo.

commons.wikimedia.org/wiki/File:Warrior_MAR_Palermo_NI2134.jpg

About

ISSN 2310-6697

toiser—open transactions on independent scientific-engineering research

FUNKTECHNIKPLUS # JOURNAL

Théorie—Expérimentation—Métrologie—Logiciel—Applications

ISSUE 5 – TUESDAY 30 SEPTEMBER 2014 – YEAR 2

1 Contents

2 About

3 Editorial Board – Technical Support

4 Information for Peers – Guiding Principles

Electrical Engineering – Expérimentation

7 Electrical Machine Insulation: Traditional Insulating Materials, Nanocomposite Polymers and the Question of Electrical Trees

M.G. Danikas, R. Sarathi

Telecommunications Engineering – Logiciel

33 Antenna Radiation Patterns: RadPat4W – FLOSS for MS Windows or Wine Linux

N.I. Yannopoulou, P.E. Zimourtopoulos



About

This European Journal defends
honesty in science and ethics in engineering

Publisher – **otoiser** open transactions on independent scientific-engineering research – **ARG NP UoP** Antennas Research Group Non Profit Union of Persons – Hauptstraße 52, 2831 Scheiblingkirchen, Austria – **www.otoiser.org** – **www.antennas.gr**

Language – We declare the origins of the Journal by using English, German and French, as well as, a Hellenic vignette, in the cover page. However, since we recognize the dominance of USA English in technical literature, we adopted it as the Journal's language, although it is not our native language.

Focus – We consider Radio-FUNK, which still creates a vivid impression of the untouchable, and its Technology-TECHNIK, from an Advanced-PLUS point of view. That is, we dynamically focus at any scientific-engineering discipline producing FUNKTECHNIKPLUS Théorie, Expérimentation, Métrologie, Logiciel, ou Applications.

Scope – We emphasize this scope broadness by extending the title of the Journal with a Doppelkreuz-Zeichen #, which we use as a placeholder for the disciplines of Editorial Board:

Electrical – # Electronics – # Computer – # Telecommunications – Engineering # Computer Science # Applied Mathematics, etc.

Frequency – We regularly publish 3 issues per year on January, May, and September as well as an issue every 3 papers.

Editions – We follow the arXiv.org system, that is the 1st edition date of every issue is on the cover page and any update date is on the odd pages with its version on all pages.

Format – We use the uncommon for Journals A5 paper size and the much readable Liberation Mono fixed-space font, with hyphenation, justification, and unfixed word spacing, to display 2 pages side-by-side on widescreen monitors with WYSIWYG printout. We can consider only papers in ODF odt or MS doc format written in LibreOffice or MS Office with MathType. We use PDFCreator and PDF-Xchange to produce pdf and export to images for printing on demand and electronic publishing.

License – We use the free Open Journal System OJS from the PKP Public Knowledge Project for internet publication.

Copyright – Creative Commons Attribution 3 Unported CC-BY 3

Please download the latest *About* edition from
about.ftpj.otoiser.org

Editorial Board

Electrical Engineering

High Voltage Engineering # Insulating Materials

Professor Michael Danikas

EECE, Democritus University of Thrace, mdanikas@ee.duth.gr

Electrical Machines and Drives # Renewable Energies

Electric Vehicles

Assistant Professor Athanasios Karlis

EECE, Democritus University of Thrace, akarlis@ee.duth.gr

Computer Engineering # Software Engineering

Cyber Security

Associate Professor Vasileios Katos

EECE, Democritus University of Thrace, vkatos@ee.duth.gr

Internet Engineering # Computer Science

Simulation # Applied Education # Learning Management Systems

Lecturer Sotirios Kontogiannis

BA, TE Institute of Western Macedonia, skontog@gmail.com

Hypercomputation # Fuzzy Computation # Digital Typography

Dr. Apostolos Syropoulos, Xanthi, Greece

BSc-Physics, MSc-, PhD-Comp. Science, asyropoulos@yahoo.com

Applied Mathematics # Functional and Numerical Analysis

Applied Electromagnetics # Control Theory

Dr. Nikolaos Berketis, Athens, Greece

BSc-Math, MSc-Appl.Math, PhD-Appl.Math, nberketis@gmail.com

Telecommunications Engineering

Applied Electromagnetics # Metrology # Applied Education

Simulation # Virtual Reality # Amateur Radio # FLOSS

Applied Physics # Electronics Engineering

Dr. Nikolitsa Yannopoulou, Scheiblingkirchen, Austria

Diploma Eng-EE, MEng-EECE, PhD-EECE, yin@arg.op4.eu

Dr. Petros Zimourtopoulos, Scheiblingkirchen, Austria

BSc-Physics, MSc-Electronics-Radio, PhD-EE, pez@arg.op4.eu

Technical Support

Konstantinos Kondylis, Doha, Qatar

Diploma Eng-EECE, MEng-EECE, kkondylis@gmail.com

Christos Koutsos, Bratislava, Slovakia

Diploma Eng-EECE, MEng-EECE, ckoutsos@gmail.com

Information for Peers Guiding Principles

This is a small, but independent, low profile Journal, in which we are all – Authors – Reviewers – Readers – Editors – free at last to be Peers in Knowledge, without suffering from either:

- Journal roles or positions,
- Professional, amateur, or academic statuses, or
- Established impact factorizations,

but with the following Guiding Principles:

Authors – We do know what work means; and we do respect the research work of the scientist – engineer; and we do want to highlight this work; and we do decided to found this Journal; and we do publish this work openly; and furthermore, we do care for the work of the technical author, especially the beginner one, whom we do support strongly as follows:

- 1 We encourage the author to submit his own paper written just in Basic English plus Technical Terminology.
- 2 We encourage the author even to select a pen name, which may drop it at any time to reveal his identity.
- 3 We encourage the author to submit an accepted for publication paper, which he was forced to decline that publication because it would be based on a review with unacceptable evaluation or comments.
- 4 We encourage the author to resubmit a non accepted for publication paper that was rejected after a poor, inadequate, unreasonable, irresponsible, incompetent, or ticking only, review.
- 5 We encourage the author to submit a paper that he already self-archived on some open repository, such as arXiv.org.
- 6 We encourage the author to self-archive all of the preprint and postprint versions of his paper.
- 7 We provide the author with a decent, express review process of up to just 4 weeks, by at least 2 peers, never have been co-authors with him.
- 8 We provide the author with a selection of review process between: a traditional, anonymous, peer review decision, and an immediate online pre-publication of his paper followed by an open discussion with at least 2 reviewers.

About

- 9 We immediately accept for publication a research paper directly resulting from a Project Report, Diploma-, Master-, or PhD-thesis, which the author already has successfully defended before a committee of experts and he can mention 2 members of it, who reviewed and approved his work.
- 10 We immediately publish online a paper, as soon as, it is accepted for publication in the Journal.
- 11 We quickly print-on-demand an issue every 3 papers, in excess of the 3 issues we regularly publish 3 times a year on January, May, and September.
- 12 We do not demand from the author to transfer his own copyright to us. Instead, we only consider papers resulting only from original research work, and only if the author does assure us that he owns the copyright of his paper and that he submits to the Journal either an original or a revised version of his paper, for either publication after review, or even an immediate re-publication if this paper has already been published after review, under the Creative Commons Attribution 3.0 Unported License CC-BY 3, in any case.

Reviewers – Any peer may voluntarily becomes a reviewer of the Journal in his expertize for as long as he wishes. Each author of the Journal has to support the peer-to-peer review process by reviewing one paper, written by non co-author(s) of him, for every one of his papers published in the Journal.

Readers – Any reader is a potential reviewer. We welcome online comments and post-reviews by the readers.

Editors – Any editor holds a PhD degree, to objectively prove that he really has the working experience of passing through the established publishing system. An editor pre-reviews a paper in order to check its compliance to the Guiding Principles and to select the appropriate reviewers of the Journal. We can only accept for consideration papers in the expertise areas currently shown in the Editorial Board page. However, since we are willing to amplify and extend the Scope of the Journal, we welcome the volunteer expert, in any subject included into it, who wants to join the Board, if he unreservedly accepts our Guiding Principles.

Electronic Publishing

www.ftpj.otoiser.org

Printing-on-Demand

pod@ftpj.otoiser.org

Directly:

Georgios Tontrias, msn.expresscopy.xan@hotmail.com
ExpressCopy, V.Sofias 8, 671 00, Xanthi, Greece

Submissions

sub@ftpj.otoiser.org

Online:

www.ftpj.otoiser.org

More – Detailed information will be available soon at:

www.ftpj.otoiser.org/gp

Antennas Research Group – Non Profit 12(3)* Union of Persons

* The Constitution of Greece, Article: 12(3) 2008:
www.hellenicparliament.gr/en/Vouli-ton-Ellinon/To-Politevma

* The Hellenic Supreme Court of Civil and Penal Law:
www.areiospagos.gr/en/ – Court Rulings:Civil|A1|511|2008

This document is licensed under a Creative Commons Attribution 4.0 International License – <https://creativecommons.org/licenses/by/4.0/>

Electrical Machine Insulation: Traditional Insulating Materials, Nanocomposite Polymers and the Question of Electrical Trees

M.G. Danikas, R. Sarathi *

Power Systems Laboratory, Department of Electrical and
Computer Engineering, Democritus University of Thrace,
Xanthi, Greece [1]

Department of Electrical Engineering,
Indian Institute of Technology Madras, Chennai, India [2]

Abstract

Electrical machine insulation consists basically of epoxy resin and mica foils. Both are good insulating materials and they proved to withstand large partial discharges and/or the combined attack from electrical, thermal and mechanical stresses. Nowadays alternatives to the traditional insulating materials exist, namely those of nanocomposite polymers, which present somehow improved performance regarding the aforementioned stresses. It is the aim of the present paper to investigate mechanisms of electrical treeing and/or breakdown in machine insulation as well as to study possible improvements with the aid of nanocomposite polymers.

Keywords

Machine insulation, nanocomposite polymers, breakdown, partial discharges, breakdown strength, pre-breakdown phenomena

Introduction

Machine insulation is generally characterized by hard materials, capable to withstand partial discharges of quite large magnitudes. An electrical insulation in high voltage machines must have a high breakdown strength, a good long term functioning without possible problems em-

anating from degradation effects (partial discharges (PD), treeing phenomena etc.) and certainly rather small - if any - leakage currents. Such insulation must also have a satisfactory thermal performance and must withstand relatively high temperatures. The electrical and thermal properties of such insulation

must not be deteriorated because of some extreme conditions, i.e. the highest possible temperature to be tolerated should not provoke any alterations to the insulation itself. The electrical machine insulation should have good long term functioning and it should present only small changes (to be tolerated) after many thermal cycles. Moreover, electrical machine insulation should have a satisfactory mechanical behavior, i.e. high mechanical strength which should stay high even at higher temperatures.

Thermal stressing may cause some sort of breakdown on the surface of mica sheets, whereas mechanical stressing may cause also fissures in epoxy resin and in mica. Electrical stressing may cause partial discharging in possible existing imperfections of the insulation and thus lead to electrical failure [1]. Needless to say that all properties - electrical, mechanical and thermal - are vital for the reliable operation of rotating machines. The insulation should have satisfactory electrical properties, it should withstand the expansion and contraction during temperature cycles and it should respond in a good way to mechanical stresses.

Rotating machines can be divided into two categories:

those with voltage ratings less than 6.6 kV and those with voltage ratings higher than 6.6 kV. Mica has been used for years in the electrical machine industry. Mica sheets with a backing of glass cloth and of binding material, like epoxy resin, have been the classical insulation systems for rotating machines. Generally speaking, such insulating systems have proved to be reliable [2]-[4].

Research on possible breakdown mechanisms in such systems revealed that PD and electrical treeing may lead to breakdown [5]. As is pointed out in published work, electrical trees propagate through the weaker material and they tend to reach the opposite electrode, resulting thus in total failure [2]-[5].

It is the aim of the present paper to explore mechanisms of failure both in conventional insulating materials used for rotating machines as well as to investigate alternative insulating systems based on a new series of insulating materials, namely, the nanocomposite polymers. Simulation data will be presented for conventional insulating materials and possible improvements will be suggested. It has to be noted that this review is by no means an

exhaustive one. Rotating machine insulation is a complex insulating system and, in the context of the present paper, only some aspects of it will be treated. It should also be added that the present review does not deal with the subject of enameled wiring, which will possibly consist the topic of another review paper.

At this stage, it would be fitting to state that review papers are useful even today. Why? Because they give some insight to the newcomer as well as to the experienced scientist regarding a particular subject. Although we are flooded with much information from the Internet with practically thousands and thousands of references (books, papers, journals etc.), a review paper can always be a starting point for the interested person. The purpose of a review paper is not simply to collect information on a particular subject, it is rather to offer - besides a wealth of information and the relevant references - comments and interrelations between experimental data, criticism and approaches for possible new theoretical models, it is probably the right place to also propose some new insights from the reviewer, it is the place to offer some thoughts for possibly new de-

velopments. This is why we believe in the validity of such efforts, this is why we think that reviews will always be useful, despite the flood of new scientific and technical information, almost on an every second-basis.

Conventional Insulating Materials for Rotating Machines

Mica sheets are used in rotating machine insulation as traditional insulating material. Mica is a natural mineral. Its crystalline nature gives very strong bonds in one plane and very weak Van-der-Waals's forces in the plane normal to this. The consequence of that is that mica can be split easily into flakes [2]. Mica has excellent tracking strength, high breakdown field strength, very good resistance to PD, high volume resistance as well as good thermal stability up to 6000 C [2]. For high voltage applications, mica sheets use as bonding material epoxy resin, a thermosetting material with very good electrical properties and good resistance to PD. Moreover, for a resin to be suitable for long-term operation, it requires high thermal stability with low electrical loss at service temperature and at power frequency, excellent adhesion to mica, high resistance to

moisture, chemicals and other contaminants, high mechanical strength over a range of service temperatures, dimensional stability, ability to operate at higher temperatures and a short cure time at 1500 C to 1600 C [6]. In typical rotating machine insulations, mica sheets form a sort of sandwich with epoxy resin, thus rendering the electrical breakdown of such a combined system rather difficult [7].

One of the problems facing the mica/epoxy resin insulation is the one of electrical trees, which may grow and eventually bridge the gap between the electrodes causing thus ultimate failure. Elongation of electrical trees has been experimentally observed in [8], [9]. In such a case, the mica sheets consist the harder material and the electrical trees propagate via the epoxy resin, which is the weaker material. Electrical trees propagate, generally speaking, more easily in epoxy resin, a fact also confirmed in another paper [10].

Normally prior to electrical treeing, PD take place in defects in the machine insulation. Such defects may come about from construction or from the stressing of the insulation. As said, the stressing in machine insulation can be multi-factor stressing, i.e. the insulation may

be stressed because of high voltage, thermal cycles as well as from mechanical loading [11]. Defects can come about as enclosed cavities, delaminations, problematic interfaces, possible enclosed foreign particles etc. The consequence of all these is local electric field enhancement, PD activity which subsequently may result to insulation damage. Such PD can be quite intense in the order of 1-10 nC [12], [13]. These phenomena can have a cumulative effect and cause aging and shortening of the lifetime of machine insulation [14], [15].

Rotating machine insulation systems suffer from what most of composite insulating systems suffer, i.e. the presence of interfaces. Mica sheets and epoxy resin consist of a system with multiple interfaces. Interfaces may encourage electric field intensifications in the weaker material and, thus, the cause of deteriorating phenomena. On the other hand, thinner (and consequently more) mica sheets may delay the discharge process in that discharges lose energy at the interfaces, i.e. a discharge having penetrated one layer could not enter the next layer of material until the spot on the interface, centred on the channel, had been charged to a potential which

could produce a field comparable with that of the channel at the level in question [16].

Breakdown mechanisms inside the insulation may start from defects due to excessive electrical field. Previous work done on epoxy resin samples showed that it is possible that trees emanate from enclosed cavities, causing thus conditions for further propagation and eventual failure [17]. Although such emanating trees are still put into question from some researchers [18], experimental evidence can hardly be refuted. PD cause pits on the inner surface of such cavities possible and then electrical trees may ensue. One aspect that should be stressed is that of the applied voltage: for meaningful comparisons of data (perhaps with several years interval) and/or comparison of data in the same laboratory or factory, it is essential to use identical wave shapes of voltages [19]. It is something that people tend to forget but something that comes out when PD measurements - comparisons of such measurements at different times - have to be performed.

Mica barriers delay tree propagation. Depending on the dielectric constants of mica sheets and of epoxy resin as

well as on the threshold voltages, electrical trees may take different forms but, in general, they seem not to penetrate the mica barriers [20]. Mica barriers may result in a major increase in breakdown time, this increase being depended on both the tree growth time and the set-in of the failure time [21].

The interplay and interdependence between PD and electrical treeing has been shown before, where in narrow holes of short length small PD in a rather high number may be produced whereas in holes of larger diameter and longer length, fewer PD but with larger magnitudes will ensue [22]. In any case, trees tend to grow around the mica barriers [23].

A crucial factor determining tree propagation along a mica barrier is the type of chemical bonding between mica and epoxy resin. The stronger the bonding, the higher the resistance to the tree propagation [24]. Imperfections may result from imperfect mica sheet overlapping, from the creation of cavities in parts which are at the edges of windings, from not so smooth mica sheets or from abrupt interruptions of mica sheets (because of constructional faults) [25]. Furthermore, the layered mica can delaminate under thermo-mechanical stresses and thus cause

cavities, which in turn will lead to PD [25]. Examples of imperfections are given below. In Fig. 1, a winding insulation is shown and the different radii of mica sheets are noted. In Fig. 2, imperfections in winding insulation are noted.

Experimental evidence that a mica barrier may withstand electrical treeing much better than epoxy resin was given in [10], where it was also noted that the breakdown strength of such a combination depends on the thickness of mica sheets, on the thickness of epoxy resin, the temperature, the type of epoxy resin as well as the cleanliness of both materials.

Generally speaking, the time to breakdown is the sum of the time from the initial PD activity and the creation of initial tree channels and the growth time of trees to the final breakdown. For some authors, there is an incubation period during which PD activity is barely detectable and trees grow only slightly, then a period of tree expansion follows and finally a widening of the smaller tree channels which eventually leads to bridging of the electrodes and the breakdown [9]. For others, two stages of treeing are observed: first, the inception period which may be for very many cycles, follo-

wed by a relatively short period of tree growth. PD detection reveals that a transition is accompanied by big increase in the PD magnitude, which persists until breakdown [26]. A good account of PD measurements and the effect of PD in rotating machines were given in [27], where examples of "good" (i.e. relatively free of PD) and "bad" (with delaminations) windings were presented. In [27], it was emphasized that for any comparison between PD measurements, the experimental conditions play a predominant role, a statement that echoes reference [19]. Certainly, a condition assessment of windings can be done by continuously monitoring the PD activity, taking into account that an increase in discharge activity occurs when the insulation is eroded and also that a PD activity can manifest itself both as internal PD activity and as surface discharges [28]. A good account of the relation between PD and tree structures was given in [29], where it was emphasized that electron avalanches, field fluctuations arising from the discharges themselves, local variations in permittivity and resistance of the insulation can play a decisive role for the electrical tree propagation. Minor variations of trapped space charges may

lead to preferred directions of propagation and, thus, may also affect the tree channel formation for new tree channel formation.

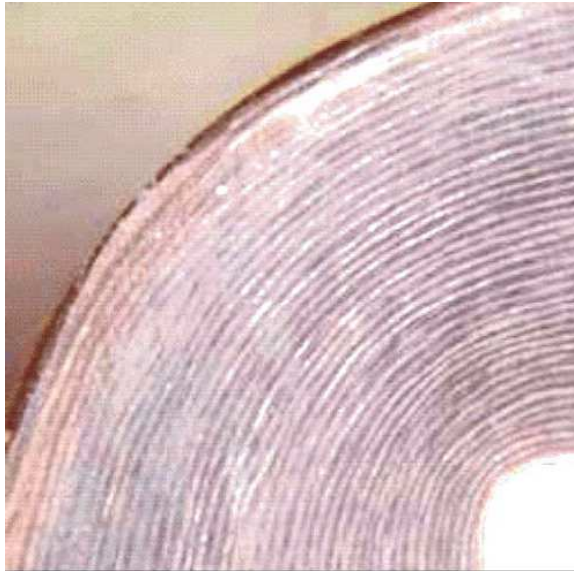


Fig. 1: Winding insulation. Note the different radii which cause the different bending of mica sheets (after [10])



Fig. 2: Imperfections of winding insulation at the edges (after [10])

It is not to underestimate that several years ago, problems with very small PD - not to say with phenomena below the inception voltage - were noticed in turbine generator armature winding insulations, namely that although such windings withstood standard testing, they failed short after the beginning of their service. Why was that? Possibly because extremely small PD, not easily detected by conventional methods, are at work and little by little could deteriorate the insulation of such windings [30].

Mica sheets offer a good protection to breakdown paths and/or to electrical treeing. This certainly depends on the applied voltage. Simulations in epoxy resin/mica sheets show that there is a voltage limit beyond which breakdown even of mica sheets is possible. From a certain voltage value upwards, mica sheets are also prone to treeing, as the following figures show. In Fig. 3, the applied voltage is 28 kV, which creates a rather distinguished form of treeing in the epoxy resin but which cannot penetrate the mica sheet. On the contrary, in Fig. 4, with another higher applied voltage, the mica sheet is penetrated by the electrical trees and in Fig. 5, there is a complete failure of the system epoxy

resin/mica sheet. It is to be noted that in Fig. 4 as well as in Fig. 5, the trees in the epoxy resin are of bush-type and in the mica sheet of branch-type. This is because trees in the weaker material are far more numerous and thus they are interconnected much more densely than in the stronger material. The simulations shown in Figs. 3, 4 and 5 were performed with the method of Cellular Automat [31]-[33]. The different types of electrical trees in epoxy resin (bush-type) and in mica sheet (branch-type) depend on the applied voltage as well as on the type of the insulating material [34]. In Figs. 4 and 5, the progression of treeing towards the opposite electrode can well be seen. It is indeed a question of time before the treeing structure reaches the opposite electrode.

All in all we observe that conventional insulating materials functioned more or less satisfactorily. Both experiments and simulations indicated that breakdown paths follow the easiest way to the other electrode, i.e. through the epoxy resin, which is the weaker of the two materials. Breakdown of the mica sheets may be possible but this depends on their thickness as well as on the voltage applied.

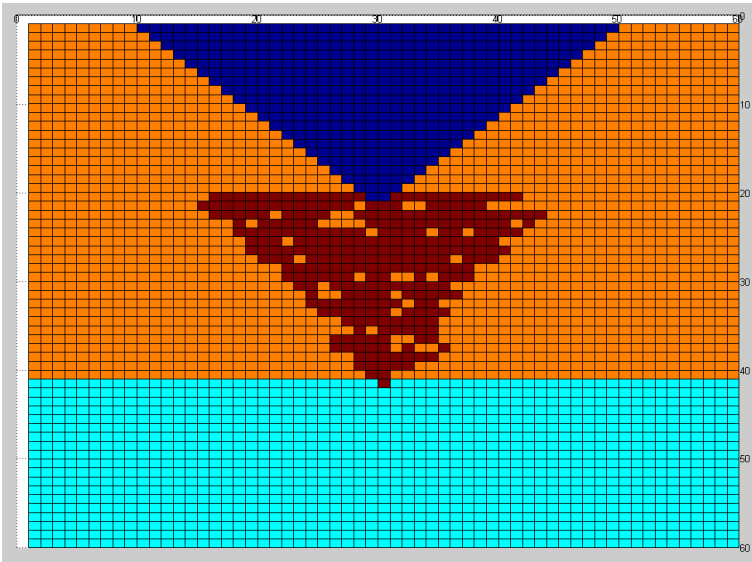


Fig. 3: Propagation of electrical tree in epoxy resin and mica sheet. Applied voltage 28 kV, breakdown strength of epoxy resin is 26 kV/mm, breakdown strength of mica sheet is 35 kV/mm

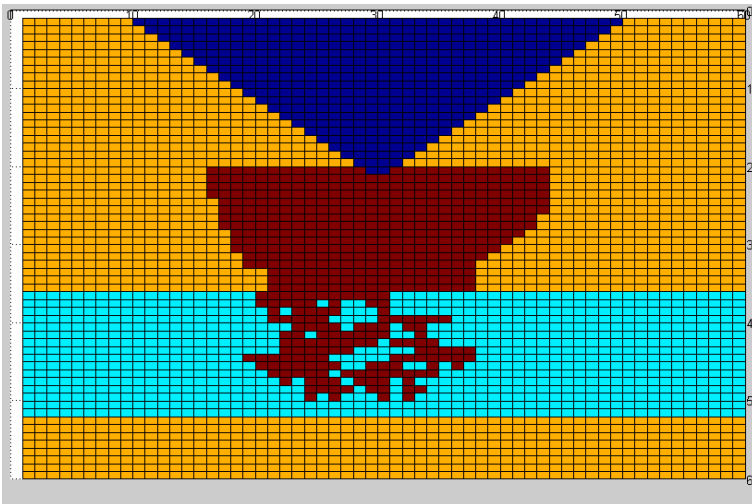


Fig. 4: Propagation of electrical tree in epoxy resin and mica sheet. Applied voltage 34 kV, breakdown strength of epoxy resin is 26 kV/mm, breakdown strength of mica sheet is 35 kV/mm

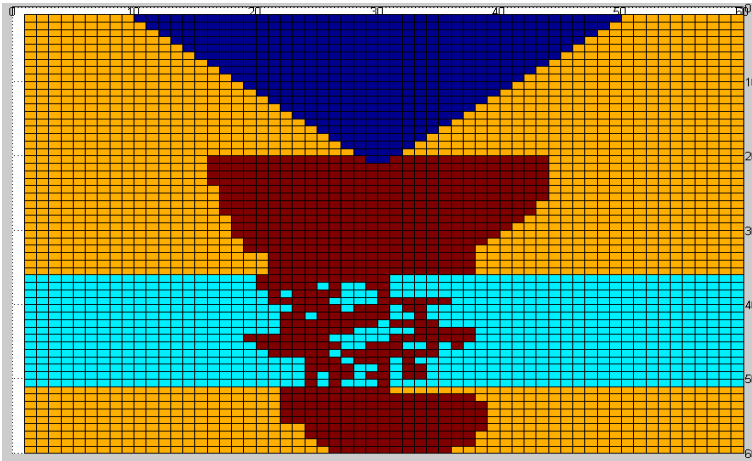


Fig. 5: Propagation of electrical tree in epoxy resin and mica sheet. Applied voltage 34 kV, breakdown strength of epoxy resin is 26 kV/mm, breakdown strength of mica sheet is 35 kV/mm

Is there a way to improve even more the electrical performance of such a composite system? The following section will concentrate on some of the modern materials proposed for machine insulation.

(As an explanatory note to this paper: It is evident from the present review that here we are not interested in an estimation of lifetime expectancies of the insulation in connection with the quality of the insulation itself. Models of lifetime expectancies have been developed and commented upon elsewhere [35]. It should also be emphasized that, the present paper is not concerned with the technicalities of the measurements of PD in rotating machine insu-

lation either [36]).

Nanocomposite Polymers for Rotating Machine Insulation

A recent paper on nanodielectrics applications has pointed out that "three types of insulations have been developed with great improvements in the resistance to partial discharges: first in random-wound wire enamel; second in form-wound strand enamel; and third in form-wound stator bar insulation or ground wall insulation" [37]. Of these aforementioned applications, the one that interests us most for the time being is the third one, i.e. that of stator bar insulation. The other two types of insulation may constitute

the subject of yet another review paper. In the context of the present paper, we will concentrate on some of the novel insulating materials concerning the stator bar insulation.

Results reported on 13.8 kV form-wound hydro generator bars made of epoxy resin with a high percentage of nanoparticles of silica, indicated a very optimum performance regarding their thermal and mechanical properties. The electrical performance of such an insulation w.r.t. the PD and electrical treeing resistance was also noted [37], [38]. Better resistance to PD and electrical treeing implies less insulation thickness.

Before starting an evaluation of nanocomposite materials for machine applications, let us be clear on a certain point: the novel materials may offer some new insights regarding the endurance of the insulation of electrical machines, but the condition-based maintenance treatment is not expected to change that dramatically. In other words, we are still far from new aging models and/or accelerated laboratory testing [40]. In yet other words, synergy effects may occur also with the new materials and, when two or more aging mechanisms are at work simultaneously, the total degradation

may not be a single algebraic sum of the separate degradation outcomes [39], [40].

It is rather clear that from the two basic components that constitute the rotating machine insulation, the one that is expected to be prone for the addition of nanoparticles, is the epoxy resin. Inorganic nitrides and oxides (such as, AlN, BN, SiO₂, ZnO, Al₂O₃ and TiO₂ among others) may be added in small amounts, and if homogeneously dispersed, they may show potentially better electrical and thermal properties than the conventional epoxy resin [41]. The need for good dispersion of the nanoparticles as well as the important role of interfaces in the nanocomposite polymers has been discussed elsewhere and there is no need for any repetition here [42]. Boron Nitride (BN) has been used to enhance the dielectric properties of the groundwall insulation system for generators because it has a reasonably high resistivity (10¹⁵ ohm.cm) and breakdown strength (53 kV/mm) as well as a rather small relative permittivity (around 4). Such inherent properties render BN a good nanoparticle material to be added to epoxy resin [41]. Moreover, the addition of BN nanoparticles improved the thermal conductivity of epoxy resin. In another pub-

lication, epoxy resin was mixed with Al₂O₃ nanoparticles [43]. The breakdown strength of such a nanocomposite was comparable to the breakdown strength of conventional epoxy resin but with a lower scatter in values. In [43], particular attention was paid to the fact that nanoparticle agglomerations were dependent on the method of preparation of the nanocomposite. As is well known, nanoparticle agglomerations affect the PD, the electrical tree propagation and the breakdown strength of nanocomposites [44]. Zirconia nanoparticles added to epoxy resin offer an improvement of the breakdown strength as well as of the thermal and dielectric properties. Addition of zirconia nanoparticles to about 5 wt% gives a higher breakdown strength compared to conventional epoxy resin [45]. It must, however, be noted that in [45], there are in certain parts of the paper discrepancies between the text and the experimental data.

Fillers in insulation systems for rotating machines are investigated in [46], a most thorough review publication. Without going into many details about the application of nanocomposites for machine insulation and the role of nanoparticles, that paper points out several vital as-

pects of insulation engineering, namely, the effect of electrical, mechanical and thermal stresses, which leads to delaminations and/or void formation. Nanoparticles are deemed to restrain the charge transport processes. As a consequence, nanocomposites exhibit less space charge formation than conventional polymers or their microparticle counterparts. The novel approach of [46] is that it insists on a concept for void formation that is based on a micro-mechanical approach, i. e. void formation can be considered as a process by which the insulating material accommodates mechanical energy, no matter whether this energy is purely mechanical, electro-mechanical or thermo-mechanical in nature. In the case of nanocomposites, crack initiation may be considered as having a critical nucleation size. Crack initiation sites may well come from nanoparticles aggregates, as was noted in [47]. In [47], the breakdown strength of epoxy resin/clay nanocomposites was investigated, the clays being Cloisite 20A (C20A) and Cloisite 30B (C30B) with different levels of loading. It was reported that the breakdown strength depends on the level of loading (around 5wt% being the optimum) and also on the type of nanocomposite structure (intercalated nano-

composite or exfoliated nano-composite), with the exfoliated type giving the higher breakdown strength. Clay C30B gave the better results since it is more hydrophilic than clay C20B and, consequently, it has a greater affinity for epoxy resin. Epoxy pre-polymers can more easily intercalate into C30B clay galleries, increasing thus the interlayer spacing (more details on intercalated and exfoliated structures in [48], [49]). In yet another paper, it was reported that appropriate nanoparticles, if suitably added, may enhance the breakdown time of conventional epoxy resin by a factor of ten [50].

Nanosized particles were also discussed in [51], where excellent voltage endurance results seemed to be very promising. Large percentages of silica nanoparticles (up to 25 wt%) were reported for making practical coils in VPI (vacuum pressure impregnation) epoxy resin successfully [52]. The reported percentage seems to be excessive in view of previous publications. Nevertheless, for nanocomposite materials in high voltage machinery, the problems remain much the same as with the more traditional insulations, namely that the heat transfer must be satisfactory also for the new

materials, the mechanical strength must be high enough and the risk from PD must be minimized [51]. Recent work on mechanical properties showed that, with epoxy resin and montmorillonite (MMT) clay mineral, natural frequency of vibration and damping factor of the said material increase by adding up to 5 wt% of nano clay [53]. Recent work also indicated that epoxy resin with 10 wt% TiO₂ nanoparticles improved greatly the ac breakdown strength and the time to breakdown [54].

The percentage of nanoparticles to be included in a base polymer matrix depends on the type of nanoparticles as well as on the base polymer. It has been reported, for example, that with epoxy resin and layered silicate, just small amounts of nanoparticles are enough for the improvement of partial discharge resistance, whereas in other publications, it was confirmed that only 2 wt% of nanoparticles is sufficient to improve the partial discharge resistance of polyamide/layered silicate nanocomposites [55]-[57]. Small amounts of nanoparticles (3 wt% of SiO₂ nanoparticles) were also reported to improve the glass transition temperature of epoxy resin in comparison with the neat epoxy resin. This is due to the re-

duction of polymer chains mobility. On the other hand, in the same paper, the resistivity of epoxy resin with 3 wt % of TiO₂ nanoparticles was lower by one order of magnitude with respect to pure epoxy resin [58]. Paper [58] is a good example of the dependence of the nanocomposite properties on the nature of the added nanoparticles to epoxy resin. Further evidence as to the effect of the percentage wt% of nanoparticles in epoxy resin is offered in [59], where POSS (polyhedral oligomeric silsesquioxane) nanoparticles were added to the base material. $\tan\delta$ measurements as well as thermogravimetric analysis showed that moderate percentages in wt% (between 1% and 4%) offered the best results. The importance of nanoparticle percentage and functionalization was also emphasized in [60], where poly (butylene terephthalate) based polymers containing alumina nanoparticles were investigated, as alternative to epoxy resin. It was reported that an optimum nanoparticle percentage exists for giving a lowering of the permittivity of the resulting nanocomposite as well as a lowering of $\tan\delta$. The lowering of the aforementioned parameters can probably be ascribed to the restriction of polymer chain movement by nanoparticles due

to the modified molecular structure and chain dynamics, which cause a strong surface interaction between the nanoparticle and the polymer matrix [61].

Treeing effects in nanocomposite epoxy resin propagate through the base material and do not go through the nanoparticles [44], [62]. Erosion depth was found to be minimal for a combination of micro- and nano- particles [62]. The desirable result of having good thermal conductivity and low dielectric constant is more difficult to obtain. In [60], it was shown that epoxy resin with h- or c- boron nitride nanoparticles presents higher thermal conductivity at the expense of a higher dielectric constant, whereas epoxy resin with silica nanoparticles has a much lower dielectric constant but with a far lower thermal conductivity. The reported lower thermal conductivity of epoxy resin with silica nanoparticles, however, was contradicted in [52], [63]. In [52], it was mentioned that nanosized SiO₂ particles act as barriers to the treeing phenomena and hinder propagation. Moreover, the mechanical and thermal properties are improved significantly, thus giving a promising new insulation system with less thickness and bet-

ter heat transfer. The disagreement between [62] and [52] may be due to the different processing methods as well as to the different size and/or shape of the nanoparticles.

Differentiation between short-time breakdown and long-term failure in nanocomposites was reported in [64]. As the authors pointed out, short-term breakdown properties depend on the applied voltage waveforms as well as the bonded region of the nanoparticles, whereas for long-term aging and failure, the transitional region and the cohesive energy density (CED) of the polymer matrix play the dominant role. They remarked that the percentage weight of nanoparticles to be included in a polymer matrix depends on the matrix itself, the chemical nature of the nanoparticles, their functionalization, their size and their bonding to the polymer matrix. For example, Ag nanoparticles of about 20 nm in size mixed with epoxy resin at about only 0.05 wt% may improve the short-term breakdown strength by about 30% w.r.t. the pure epoxy resin. Regarding nanoparticle content and the polymer matrix, it was shown that with 1 wt%, epoxy resin nanocomposite has a better long-term electrical aging resistance than its

polyethylene counterpart. The authors of [64] also remarked that PD resistance improves as the size of nanoparticles decreases because the probability of electron collision with nanoparticles increases leading the electron transport to become harder. The latter statement agrees with simulation results presented in [42].

Rotating machine insulation will be better served with nanomaterials, if such materials include nanometric layered silica nanoparticles, since the latter offer better PD resistance and improved mechanical properties. As the design field nowadays for conventional machine insulation is limited to only about 3 kV/mm [65], silica nanoparticles may help to increase the design field [66]. Such layered silica nanoparticles present a barrier behavior, rendering them interesting for applications.

Possible Charging Phenomena Below Inception Voltage

The present paper did not deal with either the technicalities of PD measurements in rotating machine insulation or the modeling of lifetime of such insulation under a variety of simultaneous stresses (electrical, thermal and mechanical) [67]-[69]. The literature on such topics

is very rich to be dealt with in the present work. This paper did not deal either with the possibility of charging phenomena below the so-called inception voltage. Relevant work done in the past revealed that it is possible to have sudden failures in insulation systems (including those of rotating machines), even though the equipment passed the relevant specification tests [30], [70]-[76]. More recent research on the topic of charging phenomena below inception voltage indicated that in both base epoxy resin [77], and in epoxy resin with TiO₂ nanoparticles and microparticles, charging phenomena were observed [78]. It has, however, to be noted that in the case of epoxy resin with nanoparticles and microparticles, charging phenomena below inception were rather sporadic. This may be due to the bonding strength between fillers and matrices, the interfiller space or matrix volume surrounded by neighboring fillers and to the morphology in the interfiller space [79]. The whole subject of possible charging effects below the so-called inception voltage cannot be dealt with in the present paper. It is, however, a subject which unjustly does not attract much attention from the insulation community. The authors intend to come back

to this subject, possibly with another review paper concentrated on this subject only. Certainly, for the treatment of this question, important publications such as [80]-[83], must be taken into account.

Further Developments

It is understandable that there may be alternatives to the epoxy resin as insulating material for rotating machines. Such alternatives may be silicone based, resin rich insulation materials due to their thermal stability, flexibility, anti-vibration and very good electrical properties. It would be interesting to see admixtures of such materials with nanoparticles, as a further exploration for possible applications [84]. Furthermore, more fundamental research has to be performed regarding the combined stresses on nanocomposite polymers. Since the various stresses (electrical, thermal, mechanical etc.) are applied not sequentially but combined [85]-[88], experimental work has to be done in this respect. In [63], detailed steps for future work have been proposed, such as thermal aging and classification tests at different temperatures, electrical aging - voltage endurance tests at various levels resulting in lifetime

curves, multifactor aging as well as thermo-mechanical bending endurance in parallel with electrical stress tests. On a more general basis, optimization of nanocomposite material fabrication methods, a better understanding of interfaces and possible combinations of micro- and nanocomposites may be research fields in the future. The need for nanocomposites having high breakdown strength, low thermal expansion coefficient, high thermal conductivity, satisfactory long-term aging and good withstanding capability to multi-stressing, will be even more pronounced in the coming years [89]. The variety of nanoparticle sizes and types, the variety of polymer matrices as well as the variety of processing methods, leaves us with the hope that optimal combinations w.r.t. the electrical, mechanical and thermal properties, may be found for the benefit of the electrical machines industry.

Conclusion

In this paper a review was performed for both traditional and modern insulating materials for rotating machine insulation. Traditional insulation mainly consists of mica sheets and epoxy resin,

with the former being the stronger of the two materials. Electrical trees tend to propagate through the epoxy resin and have greater difficulty in breaking through the mica sheets. Nanocomposites on the other hand offer generally better insulating properties. The nanoparticles that are dispersed in the polymer matrix tend to act as extremely small barriers, preventing thus the propagation and growth of electrical trees. The performance of the nanocomposite polymers depends on a variety of parameters, such as, for example, the type of polymer matrix, the type of nanoparticles, their functionalization and their size.

Acknowledgments

One of the authors (MGD) has to thank Miss D. Christantoni for the electrical tree simulations appearing in this paper. The same author has also to thank his colleagues at Xi'an Jiaotong University, State Key Laboratory of Electrical Insulation and Power Equipment, Xi'an, People's Republic of China, for letting him to carry out experiments on pure epoxy resin and nanocomposite samples and to study charging effects at and below inception voltage.

References

- [1] Pemen A.J.M., "Detection of partial discharges in stator windings of turbine generators", Ph.D. Thesis, Eindhoven University of Technology, ISBN 90-386-1720-8, 2000
- [2] Kind D., Kaerner H., "High-Voltage Insulation Technology", Eds. Friedr. Vieweg & Son, Braunschweig/Wiesbaden, Germany, 1985
- [3] Wadhwa C.L., "High voltage engineering", Eds. New Age International (P) Ltd. Publishers, New Delhi, 1994
- [4] Naidu M.S., Kamaraju V., "High voltage engineering", Eds. Tata McCraw-Hill Publishing Co. Ltd., New Delhi, 1995
- [5] Kuffel E., Zaengl W.S., Kuffel J., "High voltage engineering: Fundamentals", Eds. Newness, Oxford, 2000
- [6] Clemson C.S., "Evaluation of micaceous composites", in "Electrical Insulation", Edited by A. Bradwell, Eds. Peter Peregrinus Ltd. London, UK, 1983, pp. 219-233
- [7] Kim T.J., Nelson J.K., "Assessment of deterioration in epoxy/mica machine insulation", IEEE Transactions on Electrical Insulation, Vol. 27, No. 5, October 1992, pp. 1026-1039
- [8] Vogelsang R., Farr T., Froehlich K., "The effect of barriers on electrical tree propagation in composite insulation materials", IEEE Transactions on Dielectrics and Electrical Insulation, Vol. 13, No. 2, 2006, pp. 373-382
- [9] Vogelsang R., Fruth B., Farr T., Froehlich K., "Detection of electrical tree propagation by partial discharge measurements", Proceedings of 15th International Conference on Electrical Machines, Brugge, Belgium, 2002
- [10] Vogelsang R., Fruth B., Froehlich K., "Detection of electrical tree propagation in generator bar insulations by partial discharge measurements", Proceedings of 7th International Conference on Properties and Applications of Dielectric Materials, Nagoya, Japan, 2003, pp. 281-285
- [11] Lehmann K., "Teilentladungs-Monitoring an Grossgeneratoren", Ph.D. Thesis, ETH Zuerich, FG Hochspannungstechnik, 1994
- [12] Binder E., "Techniques of partial discharge measurements", CIGRE-Symposium, Vienna, Austria, May 1987

- [13] Lehmann K., Zaengl W.S., "Thoughts on partial discharge monitoring of rotating machines", Proceedings of 6th International Symposium on High Voltage Engineering, New Orleans, USA, August 1989, paper 43.07
- [14] Botts J.C., "Corona in high voltage rotating machine windings", IEEE Electrical Insulation Magazine, Vol. 4, No. 4, 1988, pp. 29-34
- [15] Gjaerde A.-C., "Multi-factor ageing of epoxy - The combined effect of temperature and partial discharges", Ph.D. Thesis, The Norwegian Institute of Technology, Faculty of Electrical Engineering and Computer Science, Department of Power Engineering, 1994
- [16] Morshuis P., "Interfaces: to be avoided or to be treasured?", Proceedings of IEEE International Conference on Solid Dielectrics, Bologna, Italy, June 30 - July 4, 2013, pp. 1-9
- [17] Danikas M.G., Karlis A.D., "Some observations on the dielectric breakdown and the importance of cavities in insulating materials used for cables and electrical machines", Advances in Electrical and Computer Engineering, Vol. 11, No. 2, 2011, pp. 123-126
- [18] Danikas M.G., Adamidis G., "Partial discharges in epoxy resin voids and the interpretational possibilities and limitations of Pedersen's model, to be avoided or to be treasured?", Archiv für Elektrotechnik, Vol. 80, No. 2, 1997, pp. 105-110
- [19] Boenig W., "Luftgehalt und Luftspaltverteilung Geschichteter Dielektrika", Archiv für Elektrotechnik, Vol. 48, No. 1, 1963, pp. 85-96
- [20] Sweeney P.J.J., Dissado L.A., Cooper J.M., "Simulation of the effect of barriers upon electrical tree propagation", Journal of Physics D: Applied Physics, Vol. 25, No. 1, 1992 pp. 113-119
- [21] Gefle O.S., Lebedev S.M., Uschakov Ya.V., "The mechanism of the barrier effect in solid dielectrics", Journal of Physics D: Applied Physics, Vol. 30, No. 23, 1997, pp. 3267-3273
- [22] Dissado L.A., Fothergill G.C., "Electrical degradation and breakdown in polymers", Eds. Peter Peregrinus Ltd., London, UK, 1992
- [23] Mitsui H., Yoshida K., Inoue Y., Kenjo S., "Thermal cyclic degradation of coil insulation for rotating machines", IEEE Transactions on Power Apparatus and Systems, Vol. PAS-102, No. 1, 1983, pp. 67-73

- [24] Vogelsang R., Farr T., Fröhlich K., "Electrical tree propagation along barrier-interfaces in epoxy resin", Annual Report on Conference of Electrical Insulation and Dielectric Phenomena (CEIDP), 2002, Cancun, Mexico, pp.946-950
- [25] Vogelsang R., Brutsch R., Froehlich K., "How imperfections in mica tape barriers influence tree growth and breakdown time", Annual Report on Conference of Electrical Insulation and Dielectric Phenomena (CEIDP), 2003, Albuquerque, USA, pp. 657-660
- [26] Cooper R., "Breakdown in solids", in "Electrical Insulation", edited by A. Bradwell, Eds. Peter Peregrinus Ltd. London, UK, 1983, pp. 33-51
- [27] Wichmann A., "Teilentladungen in Isolierungen rotierender Maschinen", edited by D. Koenig and Y. Narayana Rao, Eds. vde verlag, Berlin, Germany, 1993, pp. 139-161
- [28] Edwards D.G., "Slot discharge mechanisms in high voltage rotating machines", Proceedings of International Conference on Partial Discharge, University of Kent in Canterbury, UK, September 28030, 1993, pp. 113-114
- [29] Dissado L.A., "Discharges and the formation of tree-shaped breakdown structures", Proceedings of International Conference on Partial Discharge, University of Kent in Canterbury, UK, September 28030, 1993, pp. 60-63
- [30] Bruning A.M., "Design of electrical insulation systems", Ph.D. Thesis, University of Missouri-Columbia, USA, 1984
- [31] Danikas M.G., Karafyllidis I., Thanailakis A., Bruning, A.M., "Simulation of electrical tree growth in solid dielectrics containing voids of arbitrary shape", Modelling and Simulation in Materials Science and Engineering, Vol. 4, 1996, pp. 535-552
- [32] Vardakis G.E., Danikas M.G., "Simulation of electrical tree propagation in a solid insulating material containing spherical insulating particle of a different permittivity with the aid of cellular automata", Facta Universitatis, Series of Electronics and Energetics, Vol. 17, No. 3, 2004, pp. 377-389
- [33] Christantoni D.D., Danikas M.G., Vardakis G.E., Lekou A.T., "Simulation of electrical tree growth in a composite insulating system consisted from epoxy resin and mica sheets", International Review on Modelling and Simulation (IREMOS), Vol. 3, No. 2, 2010, pp. 241-249

- [34] Varlow B.R., Malkin G.J., "Electrical treeing in mechanically stressed insulation", IEEE Transactions on Dielectrics and Electrical Insulation, Vol. 7, No. 6, 2000, pp. 721-724
- [35] Brancato E., "Estimation of lifetime expectancies of motors", IEEE Electrical Insulation Magazine, Vol. 8, No. 3, 1992, pp. 5-13
- [36] Hutter W., "Partial discharges - Part XII: Partial discharge detection in rotating electrical machines", IEEE Electrical Insulation Magazine, Vol. 8, No. 3, 1992, pp. 21-32
- [37] Cherney E.A., "Nanodielectrics applications - Today and tomorrow", IEEE Electrical Insulation Magazine, Vol. 29, No. 6, 2013, pp. 59-65
- [38] Widner J.R., Pohlmann F., Groepel P., Hildinger T., "Nanotechnology in high voltage insulation systems for large rotating electrical machinery - First results", CIGRE WG D1.40 Functional Nanomaterials, CIGRE Session 44, Paris, France, August 27, 2012
- [39] Trnka P., Sirucek M., Svoboda M., Soucek J., "Condition-based maintenance of high-voltage machines - A practical application to electrical insulation", IEEE Electrical Insulation Magazine, Vol. 30, No. 1, 2014, pp. 32-38
- [40] Gjaerde A.-C., "Multifactor ageing of epoxy - The combined effect of temperature and partial discharges", Ph.D. Thesis, The Norwegian Institute of Technology, faculty of Electrical Engineering and Computer Science, Department of Power Engineering, 1994
- [41] Han Z., Garrett R., "Overview of polymer nanocomposites as dielectrics and electrical insulation materials for large high voltage rotating machines", NSTI-Nanotechnology Conference and Trade Show, Technical Proceedings, ISBN 978-1-4200-8504-4, Vol. 2, 2008, pp. 727-732
- [42] Danikas M.G., Sarathi R., "Interfaces in high voltage engineering: A most important question for conventional solid insulation materials as well as for nanocomposite polymers", FunkTechnikPlus # Journal, Issue 4, Year 1, May 2014, pp. 7-31
- [43] Zhao S., Hillborg H., Martensson E., Paulsson G., "Evaluation of epoxy nanocomposites for electrical insulation systems", Proceedings of the 2011 Electrical Insulation Conference, Annapolis, Maryland, USA, 5-8 June 2011, pp. 489-492

- [44] Tanaka T., "Interface properties and surface erosion resistance", in the book "Dielectric polymer nanocomposites", Edited by J. K. Nelson, Eds. Springer, Heidelberg, Germany, 2010, pp. 229-258
- [45] Pazhanimuthu C., "Investigation of dielectric and thermal properties of nano-dielectric materials in electrical applications", International Journal of Engineering and Innovative Technology (IJEIT), Vol. 2, No. 2, 2012, pp. 62-67
- [46] Wilder A.T., Neves R.S., "Fillers in insulation for rotating electrical machines", IEEE Transactions on Dielectrics and Electrical Insulation, Vol. 17, No. 5, 2010, pp. 1357-1363
- [47] Thelakkadan A.S., Coletti G., Guastavino F., Fina A., "Effect of clay on the electrical strength of epoxy/clay nanocomposites", Society of Plastics Engineers - Plastics Research on Line, "www.4spepro.org/pdf/003866/003866.pdf"
- [48] Alexandre M., Dubois P., "Polymer-layered silicate nanocomposites: Preparation, properties and uses of a new class of materials", Materials Science and Engineering, Vol. 28, No. 1-2, 2000, pp. 1-63
- [49] Sahu R.K., "Understanding the electrical, thermal and mechanical properties of epoxy nanocomposites", Ph.D. Thesis, Indian Institute of Technology Madras, Department of Electrical Engineering, Chennai, India, 2007
- [50] Imai T., Cho H., Nakamura Y., Yamazaki K., Komiya G., Murayama K., Sawa F., Sekiya H., Ozaki T., Shimizu T., "Application-oriented Researches on nanocomposite insulating materials", Proceedings of 2011 International Symposium on Electrical Insulating Materials (ISEIM 2011), September 6-10, 2011, Doshisha University, Kyoto, Japan, p. 162 (extended summary)
- [51] Stone G.C., Miller G.H., "Progress in rotating-machine insulation systems and processing", IEEE Electrical Insulation Magazine, Vol. 29, No. 4, 2013, pp. 45-51
- [52] Gropper P., Hildinger T., Pohlmann F., Weidner J.R., "Nanotechnology in high voltage insulation systems for large electrical machinery - First results", CIGRE, paper A1-103, August 2012
- [53] Sarathi R., Sahu R., Danikas M.G., "Understanding the mechanical properties of epoxy nanocomposite insulating materials", Journal of Electrical Engineering, Vol. 60, No. 6, 2009, pp. 358-361

- [54] Takala M., "Electrical insulation materials towards nanodielectrics", Ph.D. Thesis, Tampere University of Technology, Faculty of Computing and Electrical Engineering, Department of Electrical Energy Engineering, Finland, 2010
- [55] Tanaka T., Montanari G.C., Muelhaupt R., "Polymer nanocomposites as dielectrics and electrical insulation - Perspectives for processing technologies and future applications", IEEE Transactions on Dielectrics and Electrical Insulation, Vol. 11, No. 5, 2004, pp. 763-784
- [56] Kozako M., Fuse N., Ohki Y., Okamoto T., Tanaka T., "Surface degradation of polyamide nanocomposites caused by partial discharges using IEC (b) electrodes", IEEE Transactions on Dielectrics and Electrical Insulation, Vol. 11, No. 5, 2004, pp. 833-839
- [57] Lau K.Y., Piah M.A.M., "Polymer nanocomposites in high voltage electrical insulation perspective: A review", Malaysian Polymer Journal, Vol. 6, No. 1, 2011, pp. 58-69
- [58] Amendola E., Scamardella A.M., Petrarca C., Acierno D., "Epoxy nanocomposites containing ceramic fillers for electrical applications", Proceedings of 18th International Conference on Composites in Nano-Engineering, Anchorage, USA, 2010
- [59] Bocek J., Matejka L., Mentlik V., "Novel nanocomposite materials for power engineering", Proceedings of NANO-CON 2010, 12-14 October, 2010, Olomouc, Czech Republic
- [60] Russo P., Cimino F., Acierno D., Lupo G., Petrarca C., "Poly (butylenes terephthalate) based composites containing alumina whiskers: Influence of filler functionalization on dielectric properties", International Journal of Polymer Science, 2014, "<http://dx.doi.org/10.1155/2014/150589>"
- [61] Kochetov R., Andritsch T., Morshuis P.H.F., Smit J.J., "Anomalous behaviour of the dielectric spectroscopy response of nanocomposites", IEEE Transactions on Dielectrics and Electrical Insulation, Vol. 19, No. 1, 2012, pp. 107-117
- [62] Stevens G., "Nanodielectrics developments for future power sector needs", "<http://gnosysglobal.com/assets/files/Downloads/HiperNano%202013%20Recent%20Developments.pdf>"
- [63] Weidner J.R., "Nanotechnology in high voltage insulation systems for large electrical machinery - First results", CIGRE, Group Ref.: SC A1, Pref. Subject: 1,

Question No.: 1.2, Registration number: 2817

- [64] Li S., Yin G., Chen G., Li J., Bai S., Zhong L., Zhang Y., Lei Q., "Short-term breakdown and long-term failure in nanodielectrics: A review", IEEE Transactions on Dielectrics and Electrical Insulation, Vol. 17, No. 5, 2010, pp. 1523-1535
- [65] Mayoux C., "Degradation of insulating materials under electrical stress", IEEE Transactions on Dielectrics and Electrical Insulation, Vol. 7, No. 5, 2000, pp. 590-601
- [66] Cao Y., Irwin P.C., Younsi K., "The future of nanodielectrics in the electrical power industry", IEEE Transactions on Dielectrics and Electrical Insulation, Vol. 11, No. 5, 2004, pp. 797-807
- [67] Zhou Y., Qin Y., Leach C., "Cost-effective online partial discharge measurements for electrical machines: Preventing insulation failure", IEEE Electrical Insulation Magazine, Vol. 26, No. 5, 2010, pp. 23-29
- [68] Stone G.C., "A perspective on online partial discharge monitoring for assessment of the condition of rotating machine stator winding insulation", IEEE Electrical Insulation Magazine, Vol. 28, No. 5, 2012, pp. 8-13
- [69] Koenig D., "Erfassung von Teilentladungen in Hohlräumen von Epoxydharz-platten zur Beurteilung des Alterungsverhaltens bei Wechselspannung", Ph.D. Thesis, Technische Universität Braunschweig, Germany, 1968
- [70] Reynders J.P., "Electrical detection of degradation caused by partial discharges in polythene", Proceedings of International Conference on Dielectric Materials, Measurements and Applications, Cambridge, England, July 21-25, 1975, pp. 19-22
- [71] Bruning A.M., Kasture D.G., Campbell F.J., Turner N.H., "Effect of cavity sub-corona current on polymer insulation life", IEEE Transactions on Electrical Insulation, Vol. 26, No. 4, 1991, pp. 826-836
- [72] Turner N.H., Campbell F.J., Bruning A.M., Kasture D.G., "Surface chemical changes of polymer cavities with currents above and below corona inception voltage", Annual Report of Conference on Electrical Insulation and Dielectric Phenomena (DEIDP), Victoria, B.C., Canada, October 1992, pp. 687-693
- [73] Brancato E., "Electrical aging - A new insight", IEEE Electrical Insulation Magazine, Vol. 6, 1990, pp. 50-51

- [74] Danikas M.G., Prionistis F.K., "Detection and recording of partial discharges below the so-called inception voltage", *Facta Universitatis*, Vol. 17, 2004, pp. 99-110
- [75] Danikas M.G., Vrakotsolis N., "Experimental results with small air gaps: Further thought and comments on the discharge (or charging phenomena) below the so-called inception voltage", *Journal of Electrical Engineering*, Vol. 56, No. 9, 2005, pp. 246-251
- [76] Danikas M.G., Pitsa D., "Detection and registration of discharge events below the so-called inception voltage: The case of small air gaps", *Journal of Electrical Engineering*, Vol. 59, No. 3, 2008, pp. 160-164
- [77] Danikas M.G., Zhao X., Cheng Y., "Experimental data on epoxy resin samples: Small partial discharges at inception voltage and some thoughts on the possibility of the existence of charging phenomena below inception voltage", *Journal of Electrical Engineering*, Vol. 62, No. 5, 2011, pp. 292-296
- [78] Zhang Y., Danikas M.G., Zhao X., Cheng Y., "Charging phenomena below the inception voltage: Effects of nano-fillers on epoxy", *Malaysian Polymer Journal*, Vol. 7, No. 2, 2012, pp. 68-73
- [79] Kozako M., Kido R., Fuse N., Ohki Y., Okamoto T., Tanaka T., "Difference in surface degradation due to partial discharges between polyamide nanocomposite and microcomposite", *Annual report of Conference on Electrical Insulation and Dielectric Phenomena*, 2004, pp. 398-401
- [80] Maecker H., "Ueber die Charakteristiken zylindrischer Boegen", *Zeitschrift fuer Physik*, Vol. 157, 1959, pp. 1-29
- [81] Bauder U.H., Maecker H.H., "The determination of transport properties from arc experiments: Methods and results", *Proceedings of the Institute of Electrical and Electronics Engineers (IEEE)*, Vol. 59, No. 4, 1971, pp. 588-592
- [82] Maecker H.H., "Effects of chemical reactions in arcs", *Pure and Applied Chemistry*, Vol. 62, No. 9, 1980, pp. 1675-1680
- [83] Maecker H.H., Stablein H.G., "What keeps an arc standing in a cross flow?", *IEEE Transactions on Plasma Science*, Vol. PS-14, No. 4, 1986, pp. 291-299
- [84] Zhang H., Cloud A., "Silicone based electrical insulation material for high speed/voltage rotating machi-

- nes", Proceedings of Coil Winding/Insulation & Electrical manufacturing Exhibition (CWIEME), May 24-26, 2011, Messe Berlin, Germany, www.arlon-std.com/, www.coilwindingexpo.com
- [85] Fort E.M., Pietsch H.E., "Aging of insulation by thermal and electrical stresses", Proceedings of Electrical /Electronics Insulation Conference, November 1975, p. 143, Publication number 75 CH1014-0-EF54
- [86] Brancato E.L., "Insulation aging: A historical and critical review" IEEE Transactions on Electrical Insulation, Vol.EI-13, No. 4, 1978, pp. 308-317
- [87] Dakin T.W., "High voltage insulation applications", IEEE Transactions on Electrical Insulation, Vol. EI-13, No. 4, 1978, pp. 318-326
- [88] Greenwood A., "A perspective on insulation systems in the electric power industry", IEEE Transactions on Electrical Insulation, Vol. 15, No. 3, 1980, pp. 134-138
- [89] Tanaka T., Imai T., "Advances in nanodielectric materials over the past 50 years", IEEE Electrical Insulation magazine, Vol. 29, No. 1, 2013, pp. 10-23

Previous Publication in FUNKTECHNIKPLUS # JOURNAL

"Parameters Affecting the Lifetime of Transformer Oil in Distribution Transformers: Parameter Monitoring of 50 Transformers from the Athens Area", Issue 4, Year 1, pp. 53-65

*** About The Authors**

Michael Danikas, Issue 2, Year 1, p. 39

Ramanujam Sarathi, Issue 2, Year 1, p. 39

Antenna Radiation Patterns: RadPat4W – FLOSS for MS Windows or Wine Linux

N.I. Yannopoulou, P.E. Zimourtopoulos *

Antennas Research Group, Austria – Hellas [1, 2]

Abstract

This paper briefly highlights the features of the software tool [RadPat4W], named after Radiation Patterns for Windows, that is based on an alternative exposition of fundamental Antenna Theory. This stand-alone application is compatible with the [Wine] environment of Linux and is part of a freeware suite, which is under active development for many years. Nevertheless, the [RadPat4W] source code has been now released as FLOSS Free Libre Open Source Software and thus it may be freely used, copied, modified or redistributed, individually or cooperatively, by the interested user to suit her/his personal needs for reliable antenna applications, from the simplest to the more complex.

Keywords

FLOSS, antenna, radiation pattern, Virtual Reality

Introduction

Useful software has to work exactly as someone wants, so the authors' group decided to develop its own mini-Suite of software tools for antenna applications [1]. This project started in the middle of 90s, when the PC with www access became power enough to cover the increased requirements of antenna analysis and design, as well as of their results presentation and distribution. Since then, the development of the mini-Suite has been orientated towards

the personal needs of the individual user or of the independent member of a small, open, loosely connected group, like the authors' one, who is interested in antenna education, research and engineering, i.e., a student, an educator, a researcher, a professional engineer or a radio amateur. Such a user has enough bibliographical resources provided by the Open Access movement, but only limited technical resources for construction and measurement. The mini-Suite is intended

then for the informed user who at least can construct an experimental thin-wire antenna model and at most has access to a VNA Vector Network Analyzer to test this model - by the way, nowadays, the cost of a certified refurbished VNA is just a small percentage of its new price. For that reason, the mini-Suite specifically includes the stand-alone application [RadPat4W].

[RadPat4W]

The active development of this tool attempts to bridge the increasing gap of today approximate simulation techniques, which dominate antenna applications, to classic exact analysis methods, which concern the demanding user who wants to know what s/he is really doing with these marvellous antenna simulators. To achieve this goal and facilitate the study of antenna application results, either approximated or exact, [RadPat4W] computes and/or plots the antenna geometry, its characteristics, as well as 2D main-plane cuts of its radiation pattern and 3D Virtual Reality objects for its geometry and pattern. Currently, the tool uses by default: (1) working formulas produced by the analysis method of the authors' alternative exposition of funda-

mental Antenna Theory [2] that is quickly but rigorously results in the most general complex vector expression for the radiation pattern of any thin-wire antenna, and (2) numerical results from approximation techniques based on the Moment Method implemented by the two antenna simulators [DA] and [RichWire], which are included in the mini-Suite [1]. Finally, to support the serious user to judge the results, the current beta version of [RadPat4W] incorporates the superposition on the plotted results of scientific VNA measurements with systematic errors first estimated by the authors in 2008 [3], a process that is now accomplished semi-manually using a combination of other separate mini-Suite tools.

Besides [RadPat4W], which was always distributed through the internet as free-ware, other non-commercial software, less related to [RadPat4W] and from developers with a diverse knowledge of Antenna Theory, is distributed under various terms of use. These were kinds of the free have been exhaustively examined by the members of the USENET group [alt.comp.freeware] with the purpose to warn the candidate user about the actual content of the corresponding licenses. How-

ever, to the best of authors' knowledge, it seems that there is still no completely FLOSS for reliable antenna applications. Therefore, with the aim to further encourage the independent user to tweak [RadPat4W] according to her/his personal needs or even to be involved in this modern, most promising, cooperative activity of the FLOSS movement, the authors decided lately to release the entire source code of [RadPat4W] under the approved, by the OSI Open Source Initiative, MIT License.

The source code, now in version 4.4 with help in version 1.0, is developed from scratch, without using any other code, in MS Visual Basic 6 SP6 for 32-bit MS Windows and the executable, which is also compatible with the [Wine] environment of Linux, needs about 8.5 MB of free hard disk space for its installation. The application usability has been multiple checked during antenna courses and theses elaboration, thus its source code is in a mature state for a long time now although, from time to time, new features are added to it. The code is available for download from authors' group website "<http://www.annas.gr/floss>" or GoogleCode repository at "<http://code.google.com/p/rga/>".

The features of [RadPat4W] can be divided according to their functionality in two groups: (1) pattern computation and plotting using working formulas from Antenna Theory, and (2) pattern plotting using numerical results from antenna simulators. To exemplify these features by examples, a number of antenna education, research and engineering applications, from the simplest to the more complex, are presented in the following.

Working Formulas

Fig. 1 shows the software application form of [RadPat4W] for the three main-plane cuts of the E-normalized radiation pattern of a linear, center-fed, standing-wave dipole, which is parallel to z-axis and has a length of 2.35λ , where the length is the only one input parameter with values in the range $[0.001, 10]\lambda$. To overcome the practical constraints of the limited number of screen pixels that obscures the detailed view of zero-E directions, which determine the radiation pattern lobes, a useful feature has been introduced in all application forms that is the magnification of the pattern up to six times. Each magnified diagram shows the zero-E directions by magenta colored radial li-

nes on the screen. The [Max-Zero-D] button opens the window of Fig. 2 in which the computed directions of maxima and zeros, as well as, the

directivity and the maximum value of pre-normalized E radiation pattern, are shown [2].

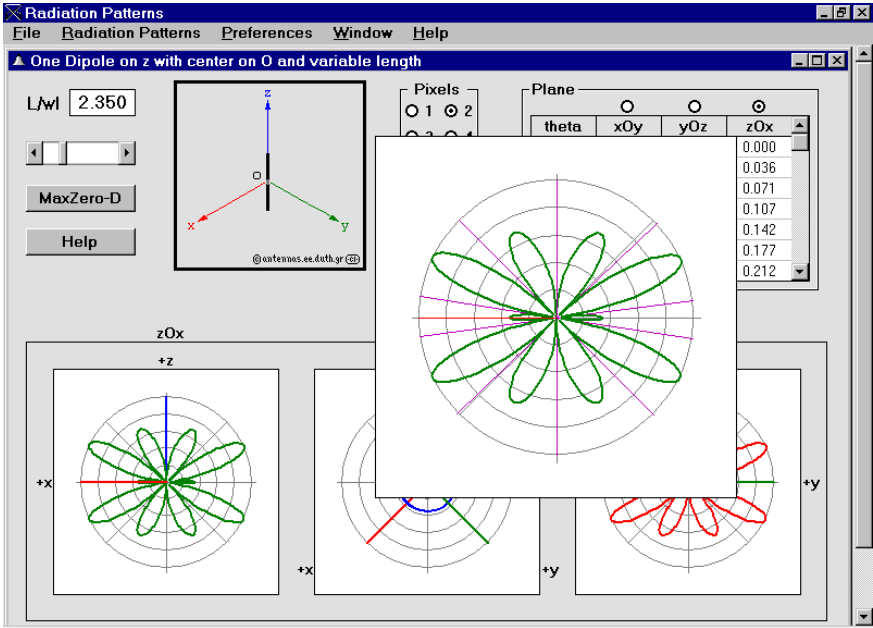


Fig. 1: [One Dipole on z]: A magnified main-plane cut

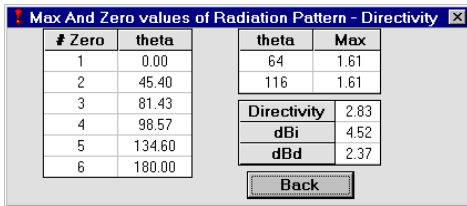


Fig. 2: [One Dipole on z]: Maximum, zeros and Directivity

Fig. 3 shows the three main-plane cuts of radiation pattern for the same dipole but in the space direction described by the input data of its unit directional vector: $(0.000, 0.707, -0.707)$. The [Zero] button opens the window of Fig. 4, where the computed directions of zeros on the three main-plane cuts, as well as on a plane that contains the dipole axis, are shown.

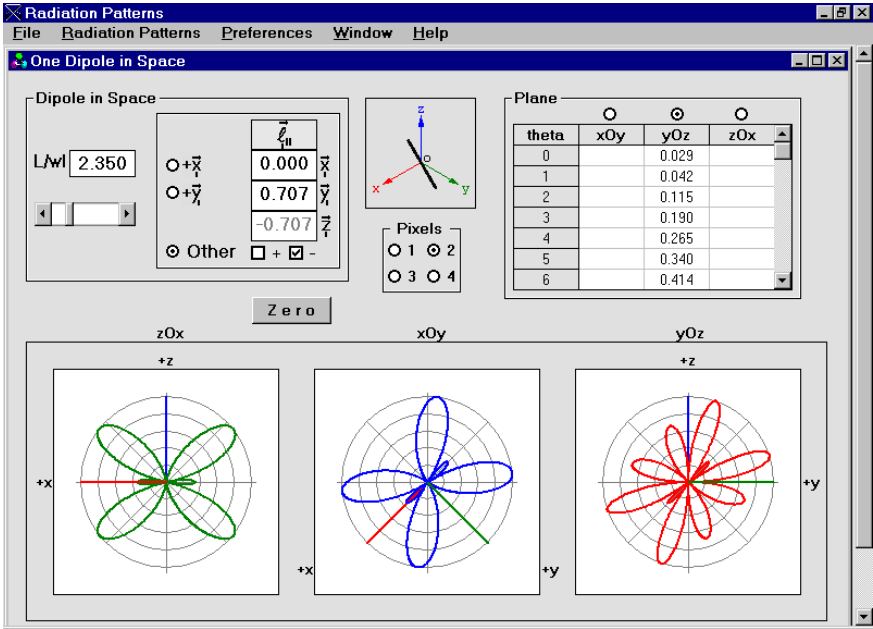


Fig. 3: [One Dipole in Space]: Three different main-plane cuts

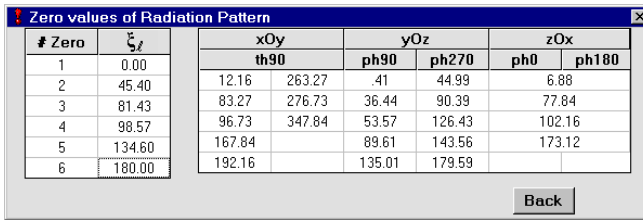


Fig. 4: [One Dipole in Space]: Zero pattern directions

Fig. 5 shows the input data for a uniform linear array of exactly parallel linear standing-wave dipoles, in two frames for the generator dipole with complex vector pattern G and the array of isotropic sources with complex number pattern A, respectively. The first frame

defines the length and the direction of the generator or reference dipole. The second frame defines the geometrical and electrical input data for the array: the number of isotropic point sources, their constant phase difference in degrees, their constant equidistance per wavelength, and

the unit directional vector of array axis. The shown values are for an array of 3 dipoles, 2λ each, in the direction of +y axis, with phase difference of -144° , 0.4λ apart, on the array axis direction of +x. The [Show Graphics] button opens the window of Fig. 6, in which the dipole array complex vector pattern $E = AG$, i.e., the Principle of Radiation Patterns Multiplication, is shown in absolute 3D form: the normalized norm pattern $||E||$ results as product of the normalized absolute pattern $|A|$ by the normalized norm pattern $||G||$ and by a non-shown constant spherical pattern $|A|_{\max} ||G||_{\max} / ||E||_{\max} \geq 1$ [2]. In the [Directivity] frame of the window, the directivities of the array D_A ,

of the generator D_G , and of the dipole array D are shown. The [Max-Zero of Array Factor] button opens the window of Fig. 7, in which the directions of zero-A and $|A|_{\max}$ and the values of $|A|_{\max}$, $||G||_{\max}$ and $||E||_{\max}$ are shown.

The buttons [A-3D], [G-3D] and [E-3D] produce the respective 3D Virtual Reality radiation patterns, which are shown in Fig. 8 as three screen captures of the free Platinum WorldView VRML viewer plug-in for MS Internet Explorer. By the way, the contemporary free VRML Cortona viewer is available for a number of other web browsers too, under MS Windows, while under Linux the most appropriate add-on for iceweasel (Mozilla Firefox) is the FreeWRL VRML viewer.

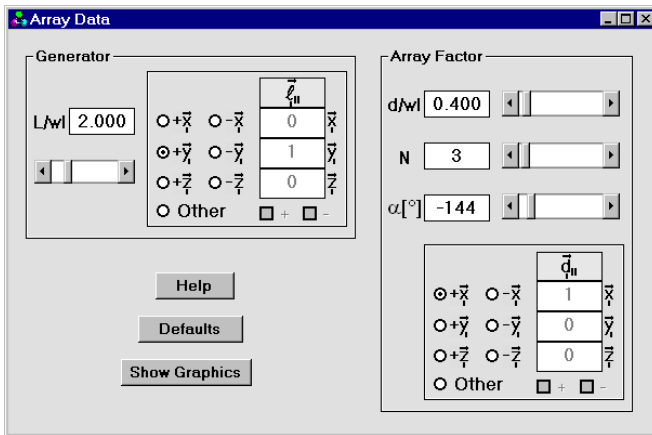


Fig. 5: [Array Data]: Uniform Linear Array input

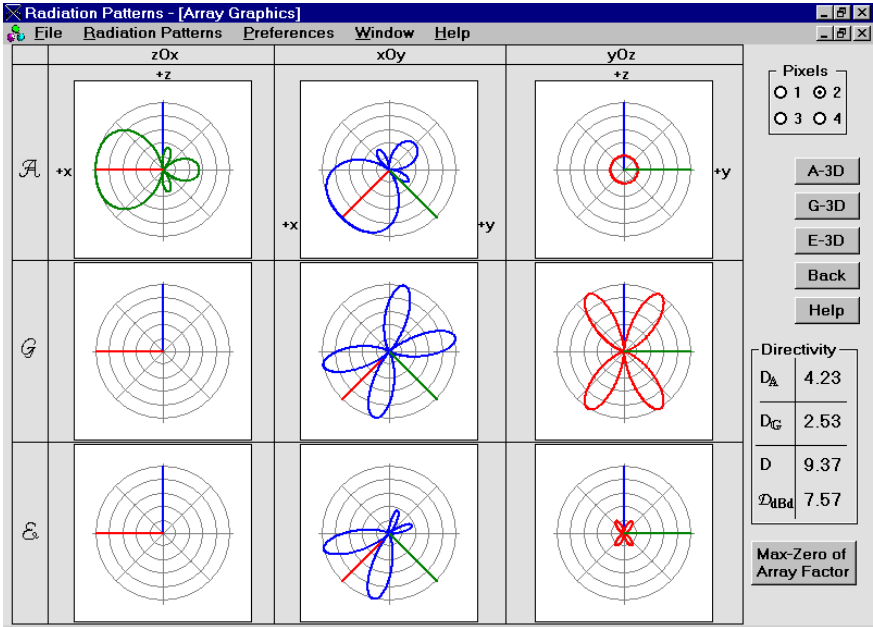


Fig. 6: [Array Graphics]: 9 main-plane pattern cuts, 2 zeros

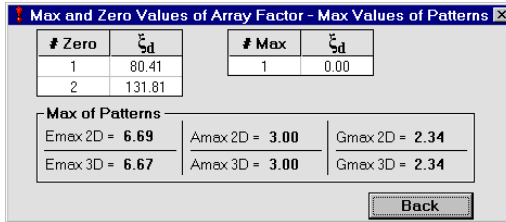


Fig. 7: [Max-Zero of Array Factor]: Computed results

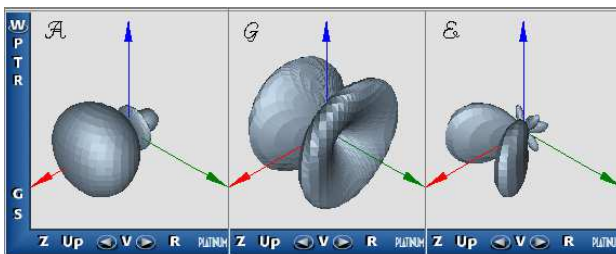


Fig. 8: Virtual 3D Principle of Radiation Pattern Multiplication

Antenna Simulators

The second group of [RadPat4W] features concerns its ability to plot antenna geometry and patterns from the clear text data files such those of the two antenna simulators of the mini-Suite: [DA] and [RichWire]. The source code of [DA], now in version 1.0.8, has been written in Compaq Visual Fortran 6.1 as Quick-Win 32-bit application for MS Windows, and the executable, which is also compatible with the [Wine] environment of Linux, can be easily installed on a PC with free hard disk space of only about ~500 KB.

In essence, this application is a restricted variation of [RichWire], which is a fully analyzed, corrected and redeveloped edition of the original Moment Method thin-wire computer program by J.H.Richmond, available in the public domain by NASA since 2005 [4]. [DA] is used for antenna simulation by half-wave dipoles, with just one active. The program requires an input data file to derive three output data files. All these data files are used by [RadPat4W]. In Fig. 9, the simplest data for only one dipole in space are shown. [RichWire] data files are similar. The usability of

both antenna simulators has been also multiple checked. The simulators are available as freeware from the mentioned repositories.

In Fig. 10, the [RadPat4W] engineering application for a commercial VHF Yagi-Uda antenna is shown. The [Antenna] button reads the antenna geometry [RichWire] data input file. The [geo.wrl] button produces the 3D Virtual Reality antenna geometry and simultaneously opens the [GL Viewer for Mathematica] for an immediate view [5]. In Fig. 11, the drawn results produced by [RadPat4W] are shown for an educational application of a flat airplane modeled with non-overlapping $\lambda/2$ dipoles in [DA] [6]. Fig. 12 illustrates the drawn results produced by the currently beta version of [RadPat4W] for a research application of a constructed Hentenna model, simulation designed with [RichWire] and measured with a VNA system [7].

[RadPat4W] Development Plans

Scheduled expansions of [RadPat4W] include the following facilities, which are already available in other mini-Suite tools: (1) choice of other plane- or conical-cuts, (2) key-in of any exact analysis working formula $E(\theta,$

φ), (3) selection of the ξ -, θ -, and φ - plotting step, (4) automation of fine Cartesian pattern plotting, (5) superposition of VNA measurements on 3D Virtual Reality patterns, such as that in the left part of Fig. 13 [8], and (6) superposition of VNA measurements with their differential error cloud [3] on 2D

plots, such that in the right part of Fig. 13 [9].

Any other expansion of the freely available code is of course welcomed. In authors' group, there are no plans in the near future to upgrade the mini-Suite to an integrated environment for its tools.

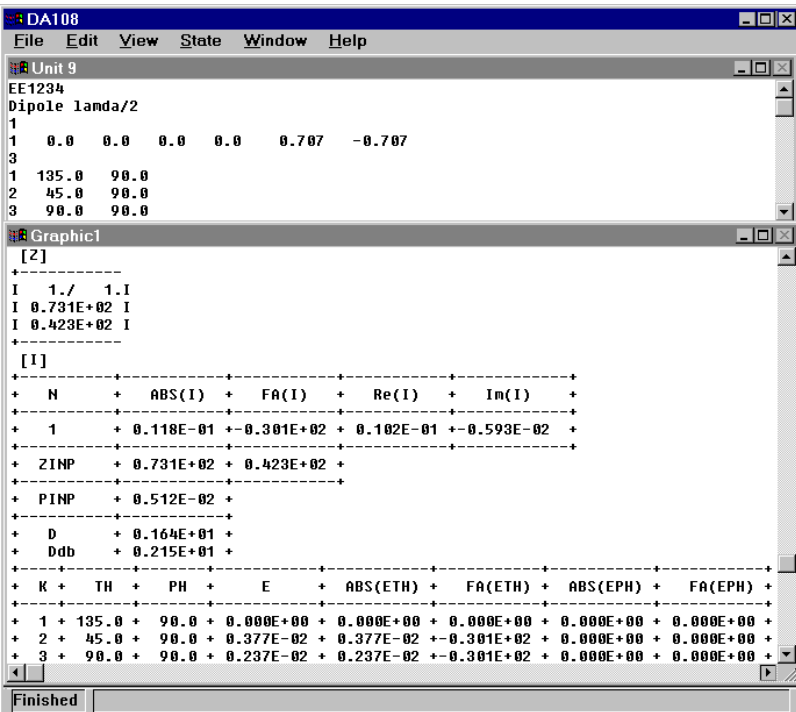


Fig. 9: [Da]: Input and output data for the simplest case

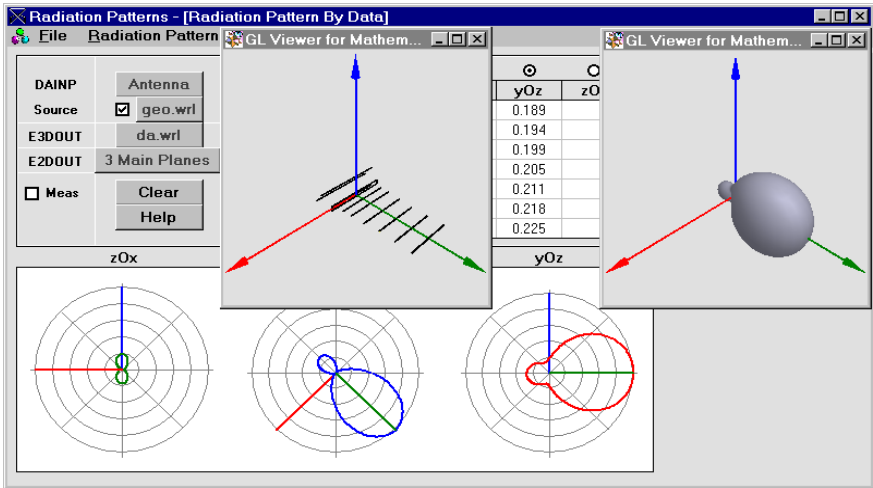


Fig. 10: [RichWire]: A commercial VHF Yagi-Uda antenna

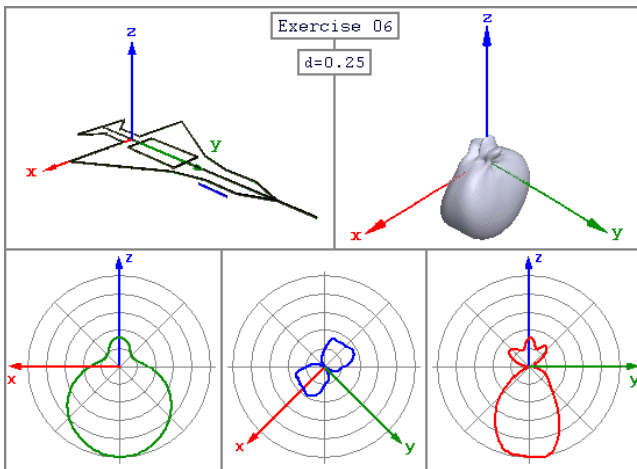


Fig. 11: [RadPat4W]: Results for a flat airplane model

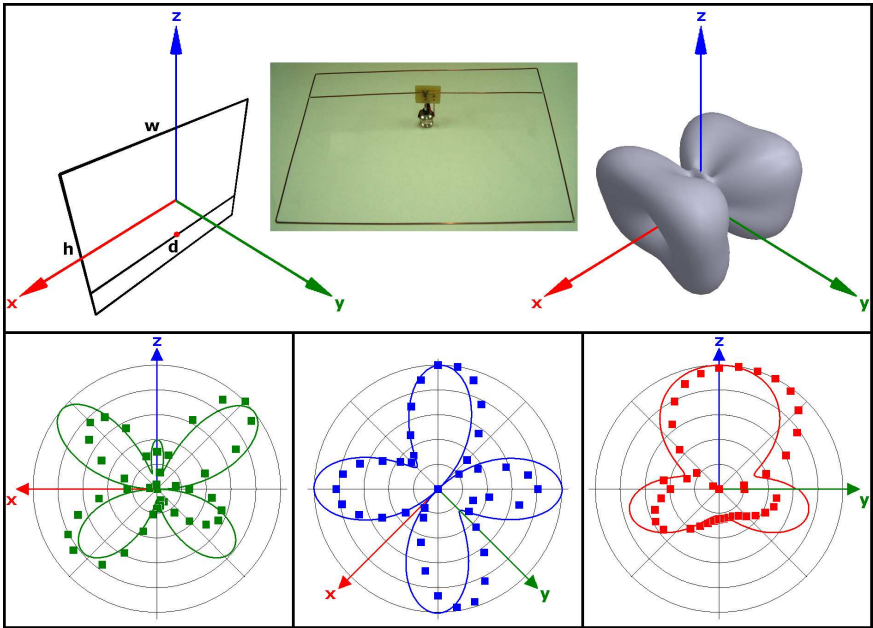


Fig. 12: [RadPat4W]: Design, Construction and Measurement

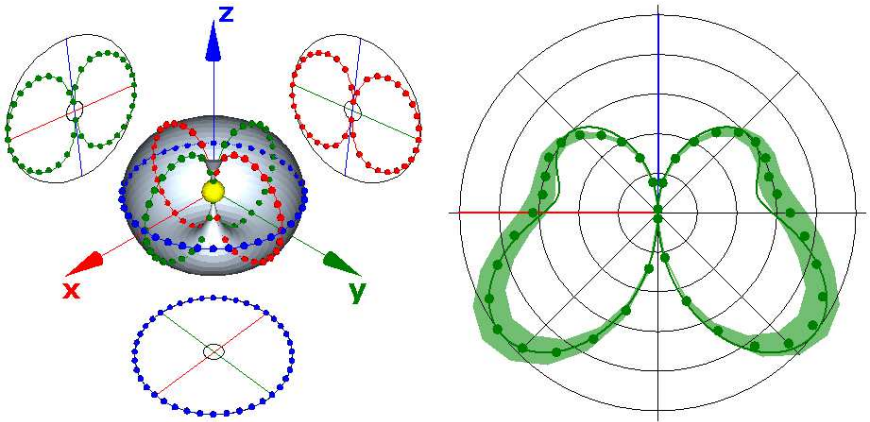


Fig. 13: 3D VNA measurements and their 2D error cloud

References *

- [1] Yannopoulou N., Zimourtopoulos P., "Mini Suite of Antenna Tools, Educational Laboratories, Antennas Research Group, 2006,
"www.antennas.gr/antsoft/minisuiteoftools/"
 - [2] Zimourtopoulos P., "Antenna Notes 1999-, Antenna Design Notes 2000-, "www.antennas.gr/antennanotes/" (in Greek)
 - [3] Yannopoulou N., Zimourtopoulos P., "S-Parameter Uncertainties in Network Analyzer Measurements with Application to Antenna Patterns", Radioengineering, Vol. 17, No. 1, April 2008, pp. 1-8
"www.radioeng.cz/fulltexts/2008/08_01_01_08.pdf"
 - [4] Richmond J.H., "Computer program for thin-wire structures in a homogeneous conducting medium", Publication Year: 1974, NTRS-Report/Patent Number: NASA-CR-2399, ESL-2902-12, DocumentID: 19740020595, "http://ntrs.nasa.gov/"
 - [5] Kuska J.-P., "MathGL3d: An Interactive OpenGL Based Viewer for Mathematica's 3D Graphics, Version 2.2,
"http://library.wolfram.com/infocenter/MathSource/2986/"
 - [6] Johnson R.C., "Antenna Engineering Handbook", 3rd Edition, McGraw-Hill, 1993, ch. 37, p. 11
 - [7] Babli E., "Hentenna", Diploma Thesis #31, ARG–Antennas Research Group, DUTH, 2004, ch. 6 (in Greek)
 - [8] Yannopoulou N., "Development of a broadband antenna for 3rd generation mobile telephony systems", MEng Thesis, ARG–Antennas Research Group, DUTH, 2003, ch. 6, p. 24 (in Greek)
 - [9] Yannopoulou N., "Study of monopole antennas over a multi-frequency decoupling cylinder", PhD Thesis, ARG–Antennas Research Group, DUTH, 2008, ch. 5 (in Greek)
- *Active Links: 04.08.2014 - Inactive Links : FTP#J Link Updates: "http://updates.ftpj.otoiser.org/"

Preprint Versions

"A FLOSS Tool for Antenna Radiation Patterns"

Nikolitsa Yannopoulou, Petros Zimourtopoulos
"http://arxiv.org/abs/1002.3072"

Proceedings of 15th Conference on Microwave Techniques,
COMITE 2010, Brno, Czech Republic, pp. 59-62

Follow-Up Research Paper

Not until now

Previous Publication in FUNKTECHNIKPLUS # JOURNAL

"Self-Standing End-Fed Geometrically Uniform Linear Arrays:
Analysis, Design, Construction, Measurements and FLOSS",
Issue 4, Year 1, pp.43-52

*** About The Authors**

Nikolitsa Yannopoulou, Issue 1, Year 1, p. 15

Petros Zimourtopoulos, Issue 1, Year 1, p. 15

[This Page Intentionally Left Blank]

[This Page Intentionally Left Blank]

In case of any doubt,
download the genuine papers from
genuine.ftpj.otoiser.org

FRONT COVER VIGNETTE

A faded synthesis of an anthemion rooted in a meandros

The thirteen-leaf is a symbol for a life tree leaf.
"Herakles and Kerberos", ca. 530–500 BC,
by Paseas, the Kerberos Painter,
Museum of Fine Arts, Boston.

www.mfa.org/collections/object/plate-153852

The simple meandros is a symbol for eternal immortality.
"Warrior with a phiale", ca. 480–460 BC,
by Berliner Maler,
Museo Archeologico Regionale "Antonio Salinas" di Palermo.

commons.wikimedia.org/wiki/File:Warrior_MAR_Palermo_NI2134.jpg

ISSN 2310-6697

toiser—open transactions on independent scientific-engineering research

FUNKTECHNIKPLUS # JOURNAL

Théorie—Expérimentation—Métrologie—Logiciel—Applications

ISSUE 6 – SATURDAY 31 JANUARY 2015 – YEAR 2

- 1 Contents
- 2 About
- 3 Editorial Board – Technical Support
- 4 Information for Peers – Guiding Principles
- # Telecommunications Engineering – Logiciel
- 7 Visual EM Simulator for 3D Antennas: VEMSA3D – FLOSS for MS Windows
C.A. Koutsos, N.I. Yannopoulou, P.E. Zimourtopoulos
- # Electrical Engineering – Expérimentation
- 27 Diagnostic Techniques in Transformer Oils: Factors Affecting the Lifetime of Transformer Oil in Transformers of 150/20 kV and the Problem of Relating Diagnostics Data with their Pre-history
M.G. Danikas, S. Georghiou, I. Liapis, A.B.B.Abd. Ghani



About

This European Journal defends
honesty in science and ethics in engineering

Publisher – **otoiser** open transactions on independent scientific-engineering research – **ARG NP UoP** Antennas Research Group Non Profit Union of Persons – Hauptstraße 52, 2831 Scheiblingkirchen, Austria – **www.otoiser.org** – **www.antennas.gr**

Language – We declare the origins of the Journal by using English, German and French, as well as, a Hellenic vignette, in the cover page. However, since we recognize the dominance of USA English in technical literature, we adopted it as the Journal's language, although it is not our native language.

Focus – We consider Radio-FUNK, which still creates a vivid impression of the untouchable, and its Technology-TECHNIK, from an Advanced-PLUS point of view. That is, we dynamically focus at any scientific-engineering discipline producing FUNKTECHNIKPLUS Théorie, Expérimentation, Métrologie, Logiciel, ou Applications.

Scope – We emphasize this scope broadness by extending the title of the Journal with a Doppelkreuz-Zeichen #, which we use as a placeholder for the disciplines of Editorial Board:

Electrical – # Electronics – # Computer – # Telecommunications – Engineering # Computer Science # Applied Mathematics, etc.

Frequency – We regularly publish 3 issues per year on January, May, and September as well as an issue every 3 papers.

Editions – We follow the arXiv.org system, that is the 1st edition date of every issue is on the cover page and any update date is on the odd pages with its version on all pages.

Format – We use the uncommon for Journals A5 paper size and the much readable Liberation Mono fixed-space font, with hyphenation, justification, and unfixed word spacing, to display 2 pages side-by-side on widescreen monitors with WYSIWYG printout. We can consider only papers in ODF odt or MS doc format written in LibreOffice or MS Office with MathType. We use PDFCreator and PDF-Xchange to produce pdf and export to images for printing on demand and electronic publishing.

License – We use the free Open Journal System OJS from the PKP Public Knowledge Project for internet publication.

Copyright – Creative Commons Attribution 3 Unported CC-BY 3

Please download the latest *About* edition from
about.ftpj.otoiser.org

Editorial Board

Electrical Engineering

High Voltage Engineering # Insulating Materials

Professor Michael Danikas

EECE, Democritus University of Thrace, mdanikas@ee.duth.gr

Electrical Machines and Drives # Renewable Energies

Electric Vehicles

Assistant Professor Athanasios Karlis

EECE, Democritus University of Thrace, akarlis@ee.duth.gr

Computer Engineering # Software Engineering

Cyber Security

Associate Professor Vasileios Katos

EECE, Democritus University of Thrace, vkatos@ee.duth.gr

Internet Engineering # Computer Science

Simulation # Applied Education # Learning Management Systems

Lecturer Sotirios Kontogiannis

BA, TE Institute of Western Macedonia, skontog@gmail.com

Hypercomputation # Fuzzy Computation # Digital Typography

Dr. Apostolos Syropoulos, Xanthi, Greece

BSc-Physics, MSc-, PhD-Comp. Science, asyropoulos@yahoo.com

Applied Mathematics # Functional and Numerical Analysis

Applied Electromagnetics # Control Theory

Dr. Nikolaos Berketis, Athens, Greece

BSc-Math, MSc-Appl.Math, PhD-Appl.Math, nberketis@gmail.com

Telecommunications Engineering

Applied Electromagnetics # Metrology # Applied Education

Simulation # Virtual Reality # Amateur Radio # FLOSS

Applied Physics # Electronics Engineering

Dr. Nikolitsa Yannopoulou, Scheiblingkirchen, Austria

Diploma Eng-EE, MEng-EECE, PhD-EECE, yin@arg.op4.eu

Dr. Petros Zimourtopoulos, Scheiblingkirchen, Austria

BSc-Physics, MSc-Electronics-Radio, PhD-EE, pez@arg.op4.eu

Technical Support

Konstantinos Kondylis, Doha, Qatar

Diploma Eng-EECE, MEng-EECE, kkondylis@gmail.com

Christos Koutsos, Bratislava, Slovakia

Diploma Eng-EECE, MEng-EECE, ckoutsos@gmail.com

Information for Peers Guiding Principles

This is a small, but independent, low profile Journal, in which we are all – Authors – Reviewers – Readers – Editors – free at last to be Peers in Knowledge, without suffering from either:

- Journal roles or positions,
- Professional, amateur, or academic statuses, or
- Established impact factorizations,

but with the following Guiding Principles:

Authors – We do know what work means; and we do respect the research work of the scientist – engineer; and we do want to highlight this work; and we do decided to found this Journal; and we do publish this work openly; and furthermore, we do care for the work of the technical author, especially the beginner one, whom we do support strongly as follows:

- 1 We encourage the author to submit his own paper written just in Basic English plus Technical Terminology.
- 2 We encourage the author even to select a pen name, which may drop it at any time to reveal his identity.
- 3 We encourage the author to submit an accepted for publication paper, which he was forced to decline that publication because it would be based on a review with unacceptable evaluation or comments.
- 4 We encourage the author to resubmit a non accepted for publication paper that was rejected after a poor, inadequate, unreasonable, irresponsible, incompetent, or ticking only, review.
- 5 We encourage the author to submit a paper that he already self-archived on some open repository, such as arXiv.org.
- 6 We encourage the author to self-archive all of the preprint and postprint versions of his paper.
- 7 We provide the author with a decent, express review process of up to just 4 weeks, by at least 2 peers, never have been co-authors with him.
- 8 We provide the author with a selection of review process between: a traditional, anonymous, peer review decision, and an immediate online pre-publication of his paper followed by an open discussion with at least 2 reviewers.

About

- 9 We immediately accept for publication a research paper directly resulting from a Project Report, Diploma-, Master-, or PhD-thesis, which the author already has successfully defended before a committee of experts and he can mention 2 members of it, who reviewed and approved his work.
- 10 We immediately publish online a paper, as soon as, it is accepted for publication in the Journal.
- 11 We quickly print-on-demand an issue every 3 papers, in excess of the 3 issues we regularly publish 3 times a year on January, May, and September.
- 12 We do not demand from the author to transfer his own copyright to us. Instead, we only consider papers resulting only from original research work, and only if the author does assure us that he owns the copyright of his paper and that he submits to the Journal either an original or a revised version of his paper, for either publication after review, or even an immediate re-publication if this paper has already been published after review, under the Creative Commons Attribution 3.0 Unported License CC-BY 3, in any case.

Reviewers – Any peer may voluntarily becomes a reviewer of the Journal in his expertise for as long as he wishes. Each author of the Journal has to support the peer-to-peer review process by reviewing one paper, written by non co-author(s) of him, for every one of his papers published in the Journal.

Readers – Any reader is a potential reviewer. We welcome online comments and post-reviews by the readers.

Editors – Any editor holds a PhD degree, to objectively prove that he really has the working experience of passing through the established publishing system. An editor pre-reviews a paper in order to check its compliance to the Guiding Principles and to select the appropriate reviewers of the Journal. We can only accept for consideration papers in the expertise areas currently shown in the Editorial Board page. However, since we are willing to amplify and extend the Scope of the Journal, we welcome the volunteer expert, in any subject included into it, who wants to join the Board, if he unreservedly accepts our Guiding Principles.

Electronic Publishing

www.ftpj.otoiser.org

Printing-on-Demand

pod@ftpj.otoiser.org

Directly:

Georgios Tontrias, msn.expresscopy.xan@hotmail.com
ExpressCopy, V.Sofias 8, 671 00, Xanthi, Greece

Submissions

sub@ftpj.otoiser.org

Online:

www.ftpj.otoiser.org

More – Detailed information will be available soon at:

www.ftpj.otoiser.org/gp

Antennas Research Group – Non Profit 12(3)* Union of Persons

* The Constitution of Greece, Article: 12(3) 2008:
www.hellenicparliament.gr/en/Vouli-ton-Ellinon/To-Politevma

* The Hellenic Supreme Court of Civil and Penal Law:
www.areiospagos.gr/en/ – Court Rulings:Civil|A1|511|2008

This document is licensed under a Creative Commons Attribution 4.0 International License – <https://creativecommons.org/licenses/by/4.0/>

Visual EM Simulator for 3D Antennas: VEMSA3D – FLOSS for MS Windows

C.A. Koutsos, N.I. Yannopoulou, P.E. Zimourtopoulos *

Antennas Research Group, Slovak Republic [1]
Antennas Research Group, Austria – Hellas [2, 3]

Abstract

This paper introduces the FLOSS Free Libre Open Source Software [VEMSA3D], a contraction of "Visual Electromagnetic Simulator for 3D Antennas", which are geometrically modeled, either exactly or approximately, as thin wire polygonal structures; presents its GUI Graphical User Interface capabilities, in interactive mode and/or in handling suitable formed antenna data files; demonstrates the effectiveness of its use in a number of practical antenna applications, with direct comparison to experimental measurements and other freeware results; and provides the inexperienced user with a specific list of instructions to successfully build the given source code by using only freely available IDE Integrated Development Environment tools—including a cross-platform one. The unrestricted access to source code, beyond the ability for immediate software improvement, offers to independent users and volunteer groups an expandable, in any way, visual antenna simulator, for a genuine research and development work in the field of antennas, adaptable to their needs.

Keywords

FLOSS, antennas, modeling, simulation

Introduction

A lot of amazing visual EM software simulators, both commercial and freeware, exist for many years now. However, to the best of authors' knowledge, none of these simulators has been ever released under an Open Source license—paid, free gratis or free libre. This situation, as it was discussed recently, pre-

cludes the independent users and volunteer groups with limited resources, like the authors' nonprofit group, from the genuine, state-of-the-art, scientific research, since, neither the code improvement, nor its adaptation to specific needs, is possible [1], [2].

For that reason, the authors decided to develop and

release under the GNU public license their own Visual Electromagnetic Simulator for 3D Antennas [VEMSA3D], although it certainly is a less well-equipped software application for the moment—but still a fully expandable one. That release is now perfectly permissible, because in 2005 NASA released in the public domain the FORTRAN source code of the well-known MoM Method of Moments Thin-Wire Computer Program, by J. H. Richmond [3], [4]. This is exactly the code on which the authors' group based its free-ware simulators: [RichWire], a CLI Command Line Interface, and [DA], a MS Quick-Win FORTRAN derivative of it. These two simulators are under uninterrupted revision, improvement, expansion, and redevelopment, since a long time ago [1], [2]. Therefore, the [Rich-Wire] FORTRAN code was translated—entirely, line-by-line, without using any paid or free translator—to C++, to form the core of scientific EM computations in [VEMSA3D].

On the other hand, the authors' group requirements for scientific accuracy in visual representation of the produced EM simulation antenna results from its simulators, were already enforced the software development of the Virtual Antennas, that is the Virtual Antennas laboratories,

in VRML [5], [6], the FLOSS application [RadPat4W] for antenna radiation pattern presentation, in MS VB6 [2], [7], as well as, the recently developed visual antenna application for the Wolfram Demonstrations Project in Mathematica [8]. The visualization ideas implemented in the aforementioned graphics applications were also expressed—from the scratch—in C++, to use the Open Source cross-platform [wxWidgets] library with OpenGL and form the core of scientific EM graphics in [VEMSA3D] [9].

The authors, having taken into account that no familiarization with software use is possible without getting hands-on experience, restrict themselves to a brief discussion of the current [VEMSA3D] characteristics. The code, the antenna applications data, as well as, any other information, referenced open bugs or future code releases, will be always available in authors' group repositories, at "www.antennas.gr/floss" and in GoogleCode website, at "<http://code.google.com/p/rgra/>".

GUI Interactive Mode of Operation

It is assumed that the user has already some experience in the sketching of a polygonal wire outline model,

for an antenna under consideration, consisting of numbered wire segments and nodes, with their 3D space coordinates, including the positions of any antenna circuit elements, that is voltage generators and lumped loads, and s/he wants then to key-in these model and circuit data into [VEMSA3D] using its GUI Graphical User Interface in interactive mode.

The GUI main window is shown in Fig. 1, while Fig. 2 shows the menu items along with their available submenu options numbered from 1 to 7.

The GUI itself is divided in three panels named [Antenna in space (3D)], [Antenna Elements], and [Data-sets].

The function of each panel is briefly described in the following.

The [Antenna in space (3D)] viewing panel is used to project all the generated 3D and 2D graphics. By default, the application starts with a simple linear dipole antenna in space, as it is shown in Fig. 1 from a viewpoint on the diagonal of trihedral angle OXYZ, where the usual letters associated with the Cartesian axes do not exist. Instead, a one-to-one correspondence implicitly exists between (X, Y, Z) axes and (R, G, B) colors [5]. The 3D image of any antenna can be manipulated through the [Study] options, as shown in Fig. 2.3.

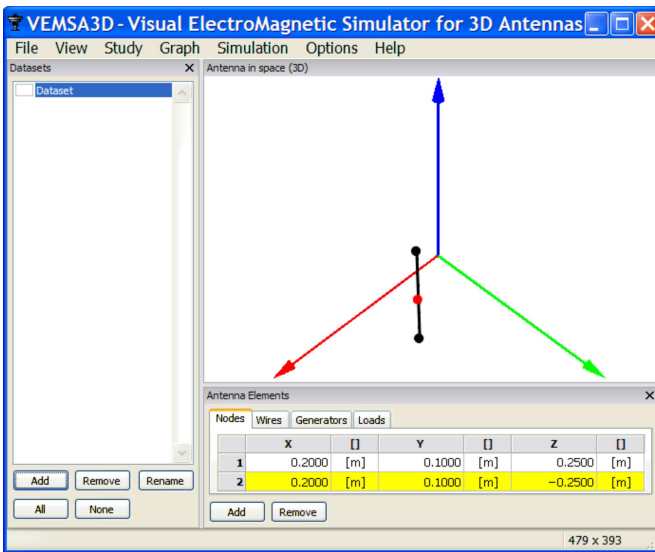


Fig. 1: GUI: The main window

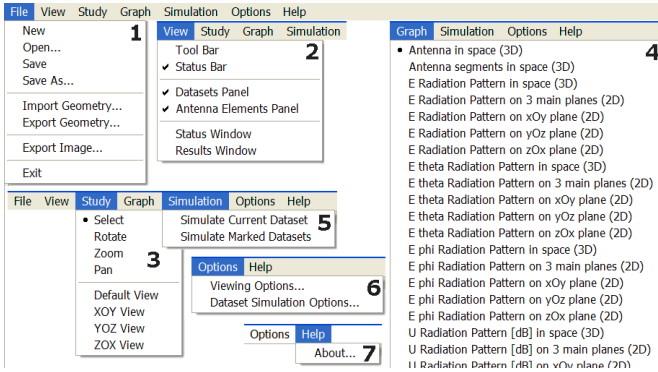


Fig. 2: Main window: The unfolded menu items

The [Antenna Elements] panel contains four tabs, corresponding to model and circuit data, in four self-explained building blocks. Instead of attempting to describe the block data in general the presentation continues with the default data:

[Nodes]: 2, with coordinates 1: (0.2, 0.1, 0.25), 2: (0.2, 0.1, -0.25), in meters [m] or in terms of wavelength λ [wl].

[Wires]: 1, starting at node: 1, ending at node: 2, that is a directed segment.

[Segments] is either: (a) a positive integer, (b) a zero or (c) a number between 0.00 and 0.25, to respectively define the division of this wire in segments: (a) in the indicated number of segments, (b) in a calculated number of segments of length no longer than 0.05λ (that is 10 segments, in this case),

(c) in segments with length no more to that number. Notably, no segment can be longer than 0.25λ [3].

[Generators]: 1, connected in the wire:1, at a distance of 0.5 times this wire length, from its starting node, with rms value of $1\angle 0^\circ$ [V]. There can be only one generator on each wire.

[Loads]: Has the same structure as [Generators]. Resistors, inductors and capacitors are inputted in [Ω], [H] and [F], respectively. It is empty in this case, since no lamped loads exist.

Notably, the GUI has been developed in such a way that efficiently supports the interactive handling of the antenna modeling by the user on the screen. Thus, the selection of an element in any of these four tabs simultaneously highlights this element on the viewing [Antenna in

space (3D)] panel—if the [Select] option under [Study] (Fig. 2.3) has been already chosen by the user, and this is the default selection in any case—and conversely: the selection of any element on this viewing [Antenna in space (3D)] panel highlights the element in its table. Consequently, a full control on the antenna modeling structure is achieved.

The [Datasets] panel may contain independent sets of model and circuit data for various antennas. Such a Dataset has its own [Dataset Simulation Options], which are chosen through submenu of Fig. 2.6, as the default selection of them is shown on the left part of Fig. 3.

A [Wire conductivity] of -1

corresponds to perfect wire conductivity, while the [Space conductivity] of 0 and the [Space dielectric constant] of 1 defines the Free Space EM environment. The [Integration steps] accepts a positive number for the steps of approximated integration used in the MoM impedance computations—a zero means closed-form integration.

Notably, the [Maximum segment length] affects the division of wires: the smaller this number is, the more segments will be considered. It is currently known that there is an implied, still programmatically unimproved, priority of the number of segments defined in [Wires] tab, over this selection—that is a bug, which may crash the application.

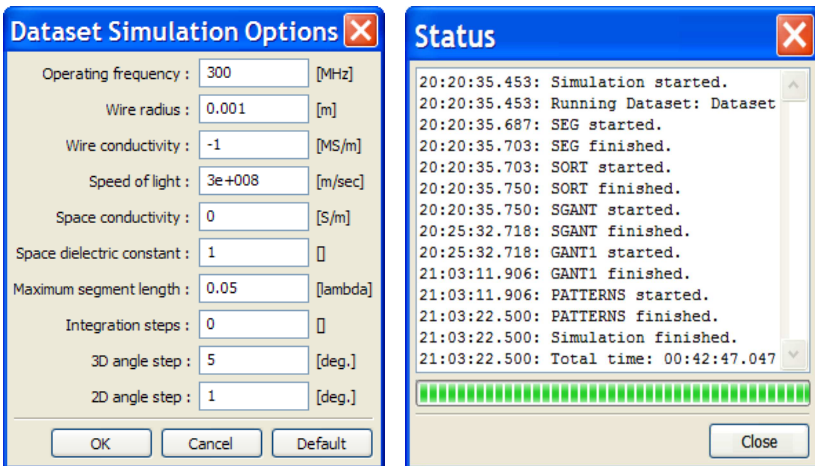


Fig. 3: Windows: [Dataset Simulation Options] - [Status]

The EM simulation of an antenna starts by selecting [Simulate Current Dataset], under [Simulation] (Fig. 2.5), while its progress is shown in the [Status] window, such as the one at the right of Fig. 3, which concerns the default dipole. Notably, multiple Datasets can be simulated, one after the other, through the [Simulate Marked Datasets] shown in Fig. 2.5.

The course of the simulation may be roughly described in five steps:

(1) Wires are automatically segmented, using the provided parameters, to produce the final model structure of points and segments

(2) Model structure is analyzed and adjacent segments are combined to form dipole current modes with sinusoidal

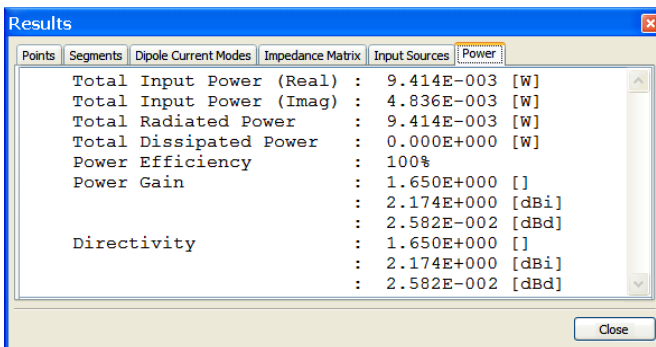
distribution

(3) Impedances are calculated and the MoM algebraic system of equations is formed

(4) The system of equations is solved and the segment currents are calculated

(5) 3D and 2D radiation patterns are calculated, as well as other useful results like those shown in Fig. 4.

In Fig. 5, the [Viewing Options] under the [Options] (Fig. 2.6) is given with all of the available options for the graphics. Through [Graph] menu item (Fig. 2.4), a variety of 3D and 2D plots, which include either the normalized electric far field E radiation pattern or the relative radiation intensity U in dB, as well as their θ and ϕ parts, can be illustrated.



The screenshot shows a window titled 'Results' with several tabs: 'Points', 'Segments', 'Dipole Current Modes', 'Impedance Matrix', 'Input Sources', and 'Power'. The 'Power' tab is active, displaying a table of power-related metrics. The table lists various power values and directivity in scientific notation and units.

Parameter	Value	Unit
Total Input Power (Real)	9.414E-003	[W]
Total Input Power (Imag)	4.836E-003	[W]
Total Radiated Power	9.414E-003	[W]
Total Dissipated Power	0.000E+000	[W]
Power Efficiency	100%	
Power Gain	1.650E+000	[]
	2.174E+000	[dBi]
	2.582E-002	[dBd]
Directivity	1.650E+000	[]
	2.174E+000	[dBi]
	2.582E-002	[dBd]

Fig. 4: Window: [Results] - Table: [Power]

The [Antenna segments in space (3D)] illustrates the final antenna structure with points, segments and segment currents in amplitude and phase, as shown in Fig. 6, where the resulting current distribution on default dipole it seems to be sinusoidal, that is as it was expected to be. The well-known

2D intersections of the 3D radiation patterns by the three main planes yOz , xOy , zOx , as well as these 3D patterns themselves are also shown for the default dipole.

Notably, modeled antennas can be imported and exported in [RichWire] data file format (Fig 2.1).



Fig. 5: [Viewing Options]

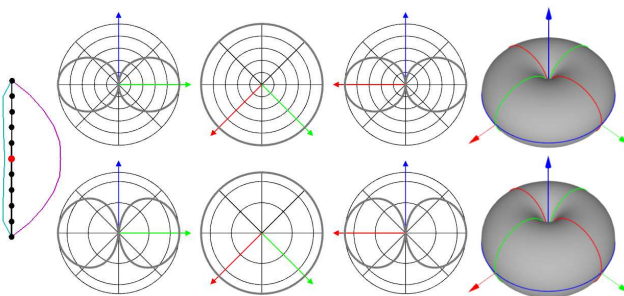


Fig. 6: GUI: Default dipole results

Build under MS Windows XP

To build [VESMA3D] MS Windows executables, the use of

IDE CodeBlocks with GCC/Mingw is suggested [10]:

```

Set below as X:\ the system disk, e.g. X:\ -> C:\

1 Download (~20MB), Install (~110MB):
  http://sourceforge.net/projects/codeblocks/files/Binaries/
[View all files][Binaries][8.02]
  codeblocks-8.02mingw-setup.exe
  Select: [Full], [Run], Compiler: [GCC/Mingw]

2 Download wxWidgets (~20MB), Extract (~120MB):
  http://sourceforge.net/projects/wxwindows/files/2.8.11/
[View all files] wxWidgets-2.8.11.zip
  wxWidgets-2.8.11.zip-> X:\ [Yes to All]

3 IDE CodeBlocks, Open:
  X:\wxWidgets-2.8.11\include\wx\msw\setup0.h
  Replace, at line 1006:
#define wxUSE_GLCANVAS 0 -> 1
  Repeat it, to file: setup.h

4 At system variable [path]:
[My Computer][Properties][Advanced]
[Environment Variables][System Variables]
Path[Edit][Variable value], Add:
";X:\Program Files\CodeBlocks\MingGW\bin;"

5 Command Prompt: >cd\
>cd X:\wxWidgets-2.8.11\build\msw
>mingw32-make -f makefile.gcc MONOLITHIC=0
  SHARED=0 UNICODE=0 USE_OPENGL=1
  BUILD=release

  Re-Command, with option:
  BUILD=release -> BUILD=debug

6 Download (~100KB), Extract (~700KB):
  http://code.google.com/p/rga/downloads/
  VEMSA3D_source_1.zip -> X:\

7 IDE CodeBlocks, [File][Open]:
  X:\VEMSA3D\build\win-cb\VEMSA3D.workspace

  * If system disk is not C:\ then:
(#)[Project][Build options...][VEMSA3D]
  * [Search directories] Correct in each of:
  * [Compiler],[Linker],[Resource compiler]
  * C:\ -> X:\ [Yes]
  * Repeat from (#), for [Release]
  * Repeat from (#), for [Debug]

[Build][Select target][Release][Build]
[Build][Select target][Debug][Build]

```

This process results in [VEMSA3D] executables of ~35 MB Debug and of ~5MB Release versions, which run under NT4, W2K and WXP, at least.

Alternatively, the use of the freeware IDE MS Visual Studio Express with C++ 2008 Compiler is also suggested. For that, first download MS Visual Studio 2008 Express iso-image from Microsoft website, burn it into a CD-R, and install it. Then, download from our repositories the file [VEMSA3Dfiles-4win-cb.zip], extract it, and follow the included setup instructions. This process results in [VEMSA3D] executables of ~5MB Debug and of ~2MB Release versions, which run under W2K and WXP, at least, but definitely do not run under NT4.

Practical Antenna Applications and Results

This section presents the implementation of [VEMSA3D] to produce eight antenna models, from simple to more complicated structures. The input data were imported through [Import Geometry] of the [File] menu (Fig. 2.1).

Fig. 7 shows an array of 2 dipoles for operation at the frequency of 1111 MHz, distanced by 0.85λ , constructed by bare copper wire of 1 mm (0.0037λ) radius, and measured. In the same figure,

the 3D radiation intensity pattern and its 2D main plane cuts are shown [11]. The continuous line represents [VEMSA3D] results, the dashed line, analytically produced patterns, and the dots, measurements made using the authors' group VNA system [12], [13].

Fig. 8 illustrates the results for a constructed and measured improved Hentenna model, at 1110 MHz, with height of $\lambda/2$, width of $\lambda/6$, and with the active element at a distance $7\lambda/12$ from its bottom [14].

The third antenna consists of a $\lambda/4$ monopole (5.83 cm) at 1286 MHz over a circular counterpoise of 14 cm radius. The monopole was constructed by 2 mm diameter copper wire and the counterpoise has been printed on a circuit board of 29 cm x 29 cm, as a circle with four radials of 2 mm width [15]. In Fig. 9, the left 3D and 2D patterns are for vertical polarization, while the right ones for horizontal. For a better representation, the patterns have been normalized.

A somehow more complicated antenna is shown in Fig. 10. The left 3D and 2D patterns correspond to the vertical polarization of a monopole over circular counterpoise with 16 radials, while the right column patterns are the corresponding 3D and 2D patterns

for the same antenna, but with an additional grounded disc below it, and without electrical connection to the counterpoise antenna, at a distance of 0.9 cm. The grounded

disc was constructed from thin copper sheet and was modeled in [VEMSA3D] with 5 concentric circles and 64 radials [15].

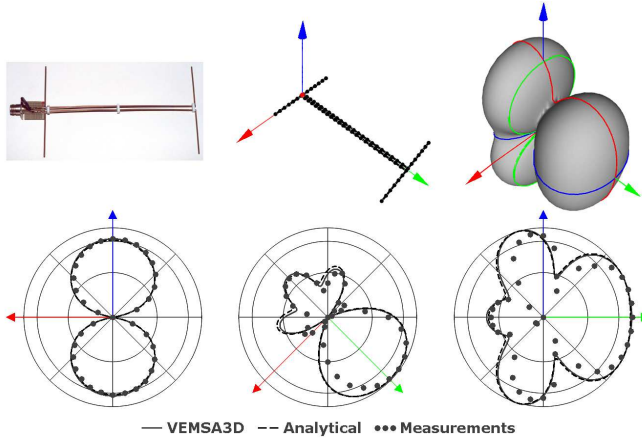


Fig. 7: Array of 2 dipoles: 73 dipole current modes

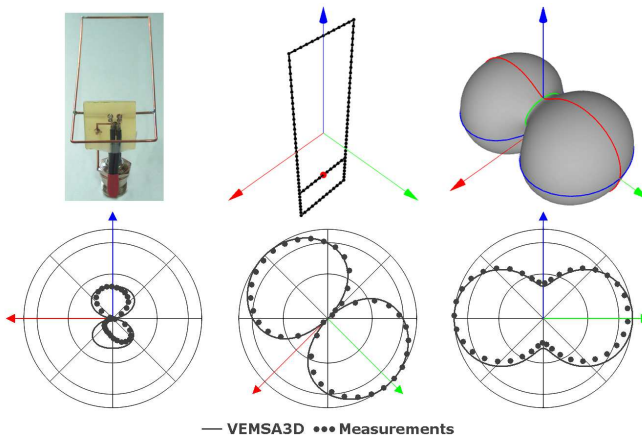


Fig. 8: Hentenna: 109 dipole current modes

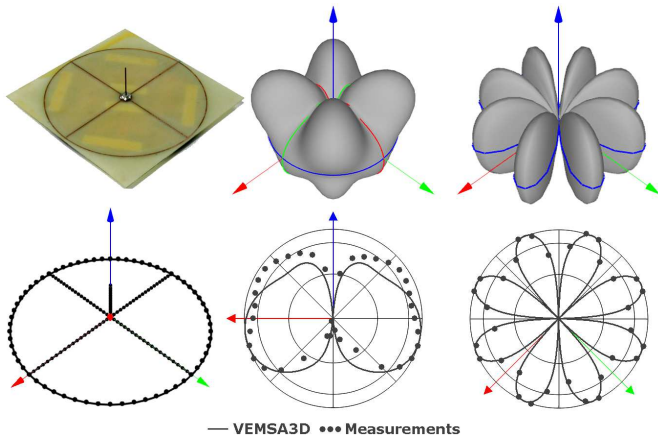


Fig. 9: Monopole over a counterpoise with 4 radials:
167 dipole current modes

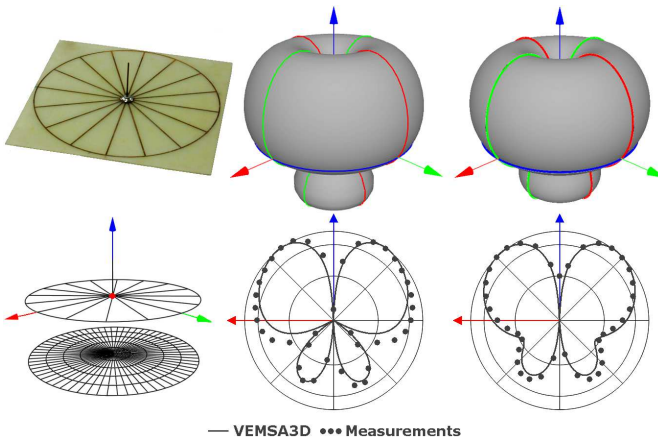


Fig. 10: Monopole over a counterpoise with 16 radials:
419 dipole current modes.
Monopole over a counterpoise with 16 radials over
a grounded disc: 2594 dipole current modes

In Fig. 11, the results of [VEMSA3D] for a commercial UHF antenna are shown [16]. The antenna model is presented in detail and separately, for the active element system, as well for the wire-frame reflector. The patterns correspond to the center frequency of its operation at 650 MHz.

Fig. 12 illustrates the model of a small jet airplane from the well-known freeware [4NEC2X] antenna simulator [17]. Simulation was carried out at the frequency of 10 MHz with the same number of points and segments in both simulators. There is a good agreement between them for

the radiation intensity patterns although some deviation in input impedance and directivity is observed.

Fig. 13 shows the results for a horn antenna with dimensions proposed by K. Pitra and Z. Raida [18]. A small bow-tie feeder with a triangular perimeter of 0.47λ and flare angle 37.50° , is considered. The antenna was initially simulated at the frequency of 40 GHz in both [4NEC2X] and [VEMSA3D] simulators, with 1205 segments to be consistent with the restricted maximum number of 1500 segments of [4NEC2X]. There is a good agreement between the produced results.

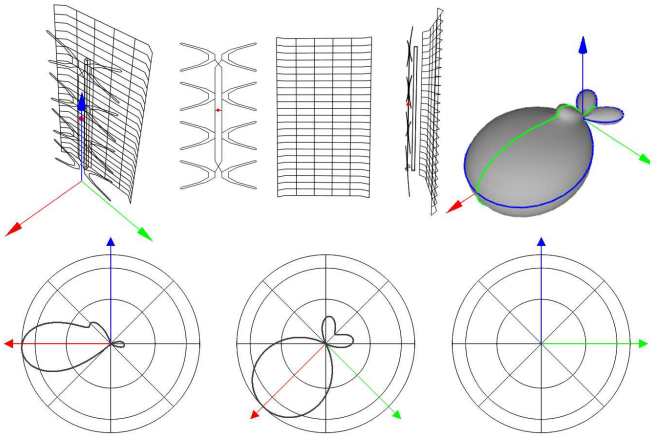


Fig. 11: Typical commercial TV UHF antenna:
723 dipole current modes.

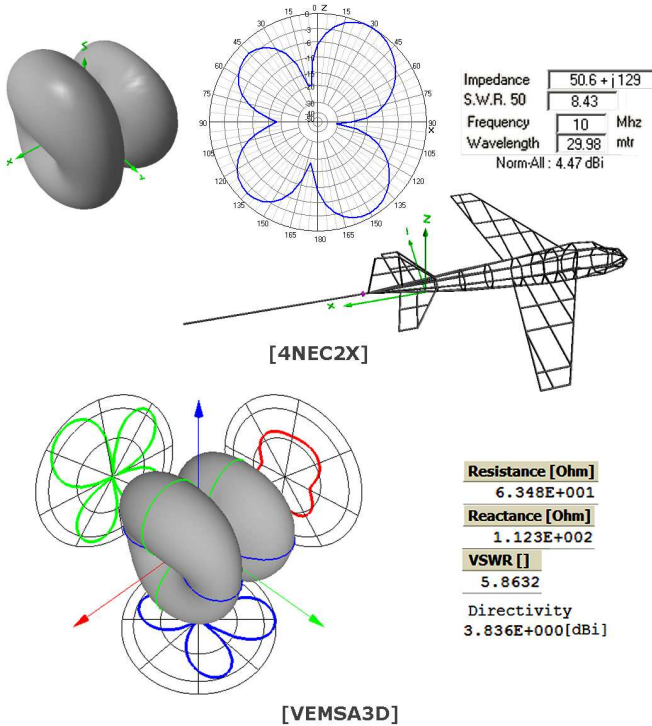


Fig. 12: Jet airplane modeled in [4NEC2X] and [VEMSA3D]: 391 dipole current modes

Finally, the most complicated antenna model, which is presented, corresponds to the same horn antenna at the same frequency of 40 GHz, with a dense wire-frame consisting of 3266 points and 4362 segments. The model is shown in Fig. 14. The total number of dipole current modes is 5458,

as shown in Fig. 15. The process time ranges from ~40 min in an AMD Phenom X2 550 3.11 GHz CPU to ~220 min, in an Intel Pentium 4 1.7 GHz CPU. Fig. 16 illustrates the resulting radiation patterns and Fig 17 the current amplitude and phase.

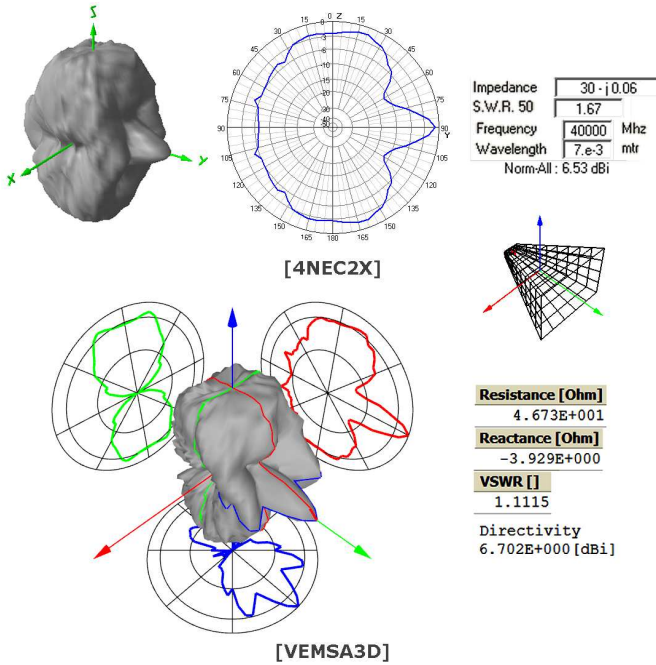


Fig. 13: Horn antenna with bow-tie feeder modeled in [4NEC2X] and [VEMSA3D]: 1370 dipole current modes

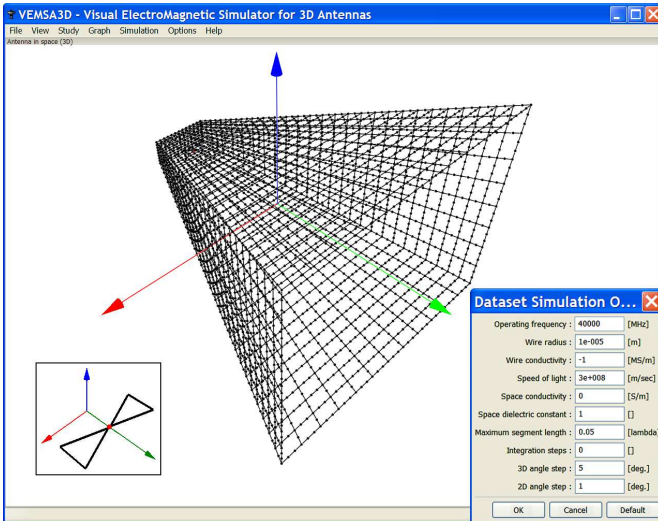


Fig. 14: Horn antenna with bow-tie feeder: 4362 segments

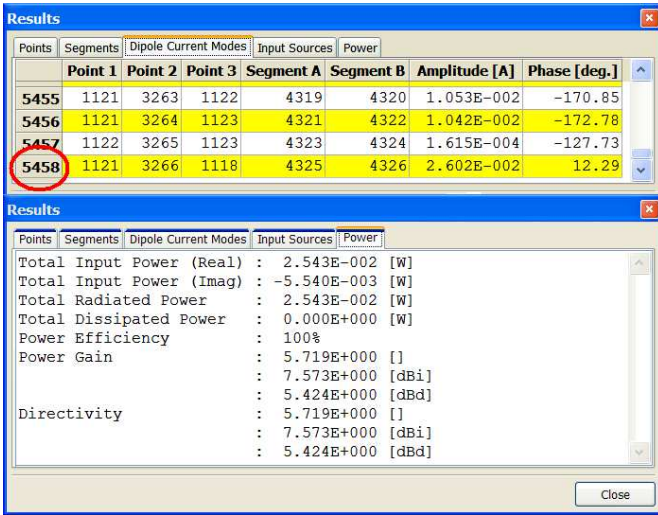


Fig. 15: Horn antenna with bow-tie feeder: 5458 dipole current modes

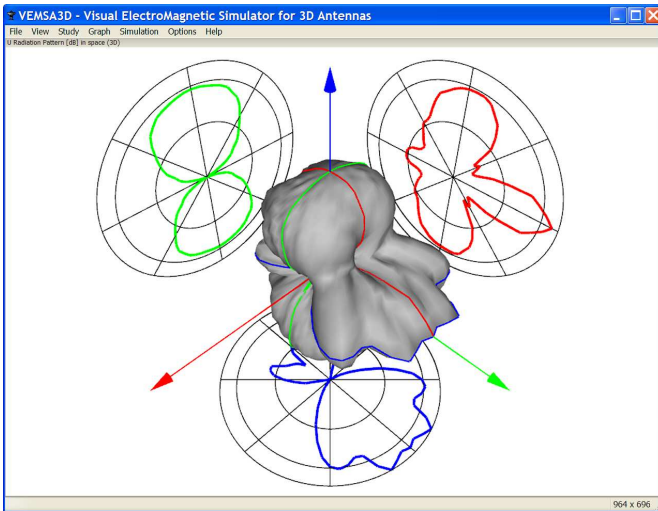


Fig. 16: Horn antenna with bow-tie feeder: Radiation intensity

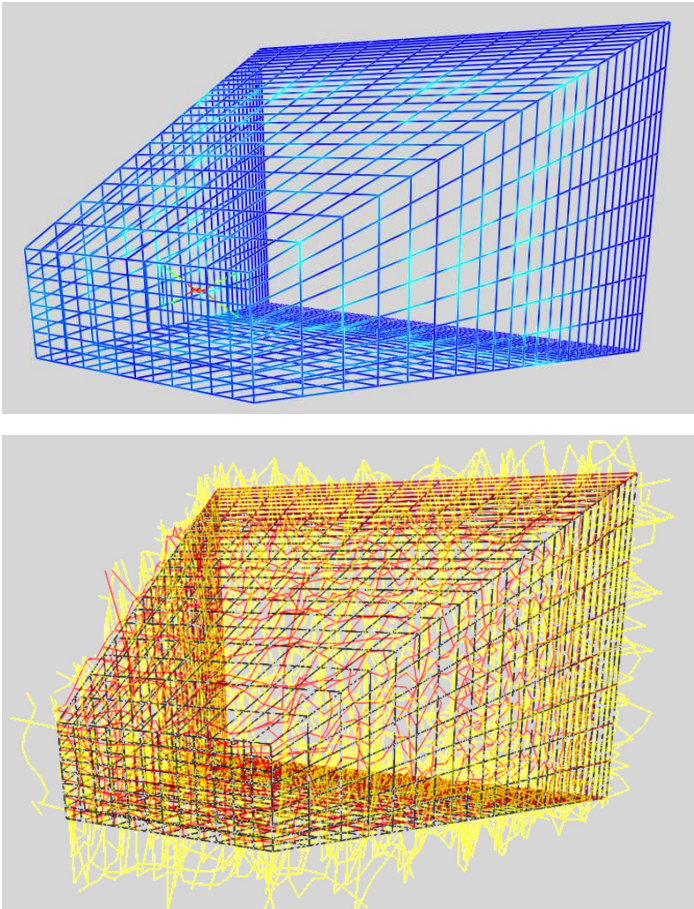


Fig. 17: Horn antenna with bow-tie feeder:
Current Amplitude and Phase

Conclusion

The first stable version of a visual EM simulator has been developed and released as FLOSS. The computational results of its use were found to be in good agreement with experimental measurements as well with the comparable free-

ware simulator [4NEC2X]. Since the number of possible modifications and additions to the attributes of [VEMSA3D] seems to be endless, no attempt will be made to suggest a particular direction for its future development: any contribution from the antenna community is very welcomed.

References *

- [1] Yannopoulou N. and Zimourtopoulos P., "A FLOSS Tool for Antenna Radiation Patterns," Proceedings of the 15th Conference on Microwave Techniques, COMITE 2010, April 19-21, 2010, Brno, Czech Republic, pp. 59-62, "<http://arxiv.org/abs/1002.3072>"
- [2] Yannopoulou N.I, Zimourtopoulos P.E, "Antenna Radiation Patterns: RadPat4W – FLOSS for MS Windows or Wine Linux", FunkTechnikPlus # Journal, Issue 5, Year 2, September 2014, pp. 33-45
"www.otoiser.org/index.php/ftpj/article/view/47"
"www.otoiser.org/index.php/ftpj/issue/view/2014.09.30"
- [3] Richmond J.H., "Computer program for thin-wire structures in a homogeneous conducting medium", Publication Year: 1974, NTRS-Report/Patent Number: NASA-CR-2399, ESL-2902-12, DocumentID: 19740020595, "<http://ntrs.nasa.gov/>"
- [4] Richmond J.H., "Radiation and scattering by thin-wire structures in the complex frequency domain", Report Number: TR-2902-10, NASA-CR-2396, May 1974, NTRS 25-8-2005, "<http://ntrs.nasa.gov/>"
- [5] Yannopoulou N. and Zimourtopoulos P., "Virtual Antennas", ARG–Antennas Research Group DUTh, 1999-2000, "<http://library.wolfram.com/database/MathSource/868>"
- [6] Yannopoulou N.I, Zimourtopoulos P.E, "The Very First Ever Made 3D/4D Virtual Laboratory for Antennas", FunkTechnikPlus # Journal, Issue 3, Year 1, January 2014, pp. 7-18
"www.otoiser.org/index.php/ftpj/article/view/30"
"www.otoiser.org/index.php/ftpj/issue/view/2014.01.31"
- [7] Yannopoulou N., Zimourtopoulos P., "Mini Suite of Antenna Tools", Educational Laboratories, ARG–Antennas Research Group, 2006,
"www.antennas.gr/antsoft/minisuiteoftools/"
- [8] Yannopoulou N. and Zimourtopoulos P., "Dipole Antenna Radiation Pattern", Wolfram Demonstrations Project, 2009, "<http://demonstrations.wolfram.com/DipoleAntennaRadiationPattern/>"
- [9] wxWidgets Cross-Platform C++ GUI Library, "www.wxwidgets.org"
- [10] Code::Blocks, "www.codeblocks.org/"

- [11] Kondylis K., "Standard antenna arrays", Master Thesis #1, ARG–Antennas Research Group, DUTH, Xanthi, Greece, 2002 (in Greek)
- [12] Kondylis K., Yannopoulou N. and Zimourtopoulos P., "A Study of End-Fed Arrays with Application to Single Driving-Point Self-Standing Linear Arrays", Proceedings of the 15th Conference on Microwave Techniques, COMITE 2010, April 19-21, 2010, Brno, Czech Republic, pp. 43-46, "<http://arxiv.org/abs/1002.3871>"
- [13] Kondylis K.Th., Yannopoulou N.I, Zimourtopoulos P.E, "Self-Standing End-Fed Geometrically Uniform Linear Arrays: Analysis, Design, Construction, Measurements and FLOSS", Issue 4, Year 1, May 2014, pp. 43-52
"www.otoiser.org/index.php/ftpj/article/view/41"
"www.otoiser.org/index.php/ftpj/issue/view/2014.05.31"
- [14] Babli E., "Hentenna", Diploma Thesis #31, ARG–Antennas Research Group, DUTH, Xanthi, Greece, 2004, ch. 6 (in Greek)
- [15] Koutsos C., "Study of monopole antenna with counterpoise", Diploma Thesis #30, ARG–Antennas Research Group, DUTH, Xanthi, Greece, 2002 (in Greek)
- [16] Kesoulis M., "Simulation data for a commercial TV UHF antenna research project", Postgraduate Advanced Antenna Topics, ARG–Antennas Research Group, DUTH, Xanthi, Greece, April, 2004
- [17] Voores A., 4NEC2-4NEC2X, "NEC based antenna modeler and optimizer", "www.qsl.net/4nec2/"
- [18] Pitra K. and Raida Z., "Wideband Feeders for Millimeter-Wave Horn Antennas", Proceedings of the 15th Conference on Microwave Techniques, COMITE 2010, April 19-21, 2010, Brno, Czech Republic, pp. 39-41
- * Active Links: 03.01.2015 - Inactive Links : FTP#J Link Updates: "<http://updates.ftpj.otoiser.org/>"

Preprint Versions

"A FLOSS Visual EM Simulator for 3D Antennas"

Christos A. Koutsos, Nikolitsa I. Yannopoulou,
Petros E. Zimourtopoulos
"<http://arxiv.org/abs/1006.0031>"

Proceedings of 33rd International Conference on
Telecommunications and Signal Processing, TSP 2010,
Baden near Vienna, Austria, pp. 432-437

Follow-Up Research Paper

Not until now

Previous Publication in FUNKTECHNIKPLUS # JOURNAL

"Antenna Radiation Patterns:
RadPat4W – FLOSS for MS Windows or Wine Linux",
Issue 5, Year 2, pp. 33-45

*** About The Authors**

Christos Koutsos, was born in Kavala, Greece in 1979. He graduated in 2002 with full marks from Department of Electrical Engineering and Computer Engineering, Democritus University of Thrace, Xanthi, Greece. Since then he is a member of the Antennas Research Group. He received his MSc degree with full marks in Antennas in 2004, at Democritus University. He is currently working as IT & Communications Engineer at Ministry for Foreign Affairs, Embassy of the Hellenic Republic in Bratislava, Slovak Republic. His research interests include antenna theory and simulation, computer programming and software development.

ckoutsos@gmail.com

Nikolitsa Yannopoulou, Issue 1, Year 1, 2013, p. 15

Petros Zimourtopoulos, Issue 1, Year 1, 2013, p. 15

This paper is licensed under a Creative Commons Attribution 4.0
International License – <https://creativecommons.org/licenses/by/4.0/>

[This Page Intentionally Left Blank]

Diagnostic Techniques in Transformer Oils: Factors Affecting the Lifetime of Transformer Oil in Transformers of 150/20 kV and the Problem of Relating Diagnostics Data with their Pre-history

M.G. Danikas, S. Georghiou, I. Liapis, A.B.B.Abd. Ghani *

Department of Electrical and Computer Engineering,
Power Systems Laboratory,
Democritus University of Thrace, Xanthi, Greece [1, 2]
Public Electricity Corporation, Athens, Greece [3]
Department of Electrical Engineering,
TNB Research Sdn. Bhd., High Voltage Cable Diagnostics,
Distribution Unit, Selangor, Malaysia [4]

Abstract

The aim of this paper is the study of various parameters affecting the lifetime of transformer oil in transformers of 150/20 kV. Fifty (50) samples of oil were taken from such transformers in the major Athens area, Greece. The parameters investigated - according to international standards - were breakdown strength, oil color, humidity, interfacial tension and $\tan\delta$. Thermal and mechanical stresses have as result the oxidation of transformer oil and the deterioration of its insulating properties. Humidity and foreign particles also consist factors contributing to the lowering of the breakdown strength of transformer oil. In most examined samples the breakdown strength and $\tan\delta$ were satisfactory. It is shown that the slightest contact with the atmospheric air may affect humidity. A color index of 3 does not necessarily mean that the oil is bad. Foreign particle presence combined with humidity may decrease the interfacial tension. Generally speaking, the 50 investigated transformers were in a satisfactory state and none of them was required to have its oil replaced. A main conclusion of this work is that we should not base our judgment about the oil quality on only one or two parameters but on a combination of more parameters.

Keywords

Transformer oil, partial discharges, diagnostic tools, breakdown voltage, dielectric strength

Introduction

Transformer oil is a very important component of a transformer. It must have good thermal and insulating properties [1]. The insulating oil is used for providing insulation between the live parts of the transformer and the grounded parts as well as for carrying out the heat from the transformer to the atmosphere [2]. Faults in transformers are rare (1%-2% per year in power transmission and distribution systems), but they can be very costly in terms of economic and technical consequences. Faults can be due, among others, to lightning and switching overvoltages, insulation failure, humidity, foreign particles and bad maintenance. The latter is a significant factor for the lifetime of a transformer [3], [4]. The main factors which may accelerate the ageing of the oil are humidity, temperature variations, oxidation and foreign particles. Various factors affecting the breakdown strength of transformer oils have been discussed and analyzed [5], [6]. There is no single measurement which can deliver enough information as to the

ageing and/or deterioration of transformer oil, mainly because transformer insulation is a dynamic system, in which e.g. humidity may migrate from the oil to paper insulation and from paper insulation back to the oil [3], [7]. With this in mind, a variety of diagnostic methods were employed in order to study the state of fifty transformers of 150/20 kV. The whole work was carried out with the aid of the Public Power Corporation (PPC) Transformer Division in Athens, Greece. The fifty investigated transformers were from the major Athens area.

Diagnostic Methods

Warning signs about the state of a transformer are, among others, a big increase of partial discharges (> 2500 pC), a visible deterioration because of foreign metallic and carbon particles, the presence of humidity in the solid insulation about 3-4% and the presence of sludge. The latter is the last visible state of deterioration. Experience indicates that the breakdown behavior and breakdown voltage are determined much more from the

above mentioned factors than that of pure insulating liquids [4], [8], [9].

Several diagnostic methods were used in order to see the quality of the transformers in question. The characterization of the oil color (DIN 51517 - ASTM 155) was performed through a device (chromometer) including standard glass disks and two glass jars with lid. The control of

breakdown voltage was measured by a typical Foster test cell, according to IEC 156/95 (Fig. 1).

The control of humidity in the oil was measured by a Metrohm - 684 KF Coulometer, which consisted of a glass container with a stirrer titration in which the reagent from container storage is added.



Fig. 1: The test cell for breakdown voltage measurements

The device is fully automated and once the experimenter gives the settings, it measures the moisture content of the oil. The measurements were performed according to IEC 814. The control of interfacial tension (ASTM D971 - 91) was performed via a tensimeter, which gives the value in dynes per centimeter in a direct reading.

The device that performed measurements of $\tan\delta$ and of

resistivity, is the BAUR-DTL fully automated device for measuring dielectric losses of oils. Such a system has a fully automated process for measuring dielectric loss, relative dielectric constant and resistivity (Fig. 2). The measurements were performed according to IEC 247. The density of oil was performed according to DIN 51517, with the aid of a pipe of 250 ml, an electronic thermometer and a glass cylinder.



Fig.2: Device for measurement of $\tan\delta$ and resistivity

It is true that no single diagnostic method can give full information as to the state of the transformer oil. The aforementioned methods may give a better picture of its state.

Results

The sampling was done according to specification ASTM D 923. Sampling should take place in clean conditions (absence of humidity and pollution), suitable glass vessels

should be used and the latter should be kept clean and hermetically closed. Every sample should be kept away from light according to VDE 0370/9.61. Every sample should be taken while the oil is warm.

In Tab. 1 a classification of values of the various investigated parameters of insulating oil is given. An oil can be classified as good, acceptable or bad according to Tab. 1 [10].

Tab. 1: Classification of insulating oils

Oil Parameters	Good	Acceptable	Poor
Color	< 2	–	> 2
Breakdown Voltage (kV)	> 40	30 – 40	< 30
Humidity [ppm]	< 10	10 – 25	> 25
Interfacial Tension (mN/m)	> 28	22 – 28	< 22
tanδ	< 0.1	0.1 – 0.5	> 0.5
Resistivity (ρ) (GΩ·m)	> 3	0.2 – 3.0	< 0.2

The sampling of oil from the fifty transformers 150/20 kV was done with due care and according to the standard practice. In Figures 3-7, the results of the measurements are shown, regarding tanδ, color, humidity and interfacial

tension respectively. Green color symbolizes the good samples, yellow color the acceptable samples whereas the red color shows the bad samples. From Figs. 3 and 4, it is clear that the breakdown voltage and tanδ values of

most of the samples are very good. This is due to systematic control of the oil and the good maintenance. Figs. 3 and 4 indicate that these two factors, which are related to ageing and oxidation, are relatively stable.

In Fig. 5, humidity is in relatively acceptable levels. Only a small percentage of the transformers (4%) seems to have high humidity. Most of the samples are within the limits prescribed by the international standards. It must be emphasized that the humidity level is a parameter which changes easily, since the slightest contact of the oil with the atmosphere may change its characteristics. In Figs. 6 and 7 the results regarding the color as well as the interfacial tension are shown.

As time passes by, the oxidation products change the oil color. Most of the samples had a rather acceptable color. Even a color index of 3 does not necessarily consist an objective indication of the oil quality. For this reason, color measurements should in fact be accompanied by other parameter measurements. In fact, although 36% of the samples showed a rather dark color (Fig. 6) other parameter measurements indicated that these samples were good or acceptable. The pre-

sence of foreign particles in combination with humidity may reduce the interfacial tension of the oil. In the investigated samples, a percentage of 28% (Fig. 7) is characterized as poor. This, however, is not particularly annoying, if we take into account for these samples also the other parameter measurements.

The density of the investigated oil samples was measured in the generally acceptable values, i.e. between 0.85 and 0.92 gr/ml (with the lowest recorded being 0.85 gr/ml, whereas the highest was 0.91 gr/ml). Although the oil density does not consist per se an individual characteristic of the examined sample, its increase may imply an increase of degradation by-products. In the context of the present work the oil density was used for the calculation of the interfacial tension [11], [12].

It can be said that, in general, the state of the investigated transformer oil samples was more or less satisfactory. In a few cases, there is a need of further filtering and possibly a second sampling it should be carried out. Whereas no transformer functioned with a particularly bad oil, it is true that, with transformer ageing, the oil suffers from so-

lid impurities, free and dissolved water particles and dissolved air. Frequent sampling is necessary in order to ensure the good functioning of such transformers. The results reported here are in line with those published before [11]. Although a statistical approach of the whole subject is desirable (i.e. to try to correlate the data collected here as well as from previous published work with the pre-history of each individual transformer), it is difficult to be realized since the Greek Electricity System has transformers from a variety of manufacturers.

This inhomogeneity of suppliers certainly renders the relation between the data collected with the pre-history of transformers very difficult. It also should be noted that with the term "pre-history" we mean the detailed registration of all faults, faulty conditions, lightning strokes, switching overvoltages etc. which have occurred in a transformer. Previous work done in this direction was only partially successful since at that time, pre-history of transformers was only related to one parameter, namely that of breakdown strength [13], [14], [15].

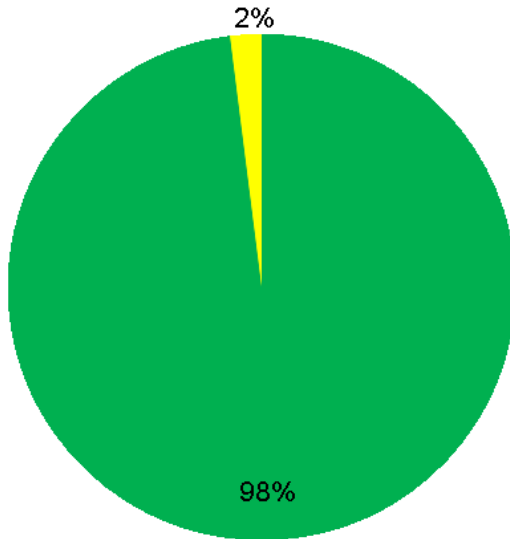


Fig.3: Graph of breakdown voltage results

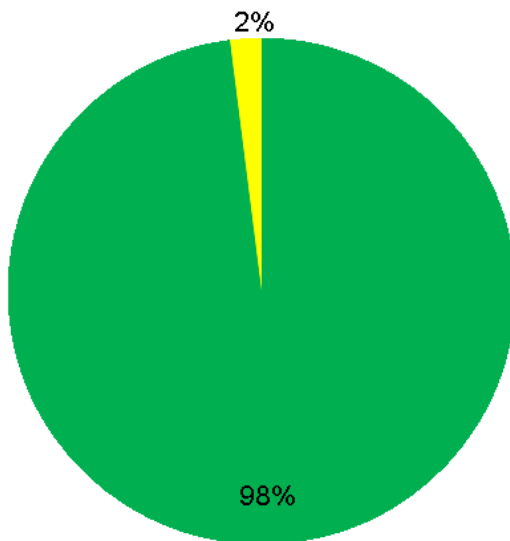


Fig.4: Graph of $\tan\delta$ results

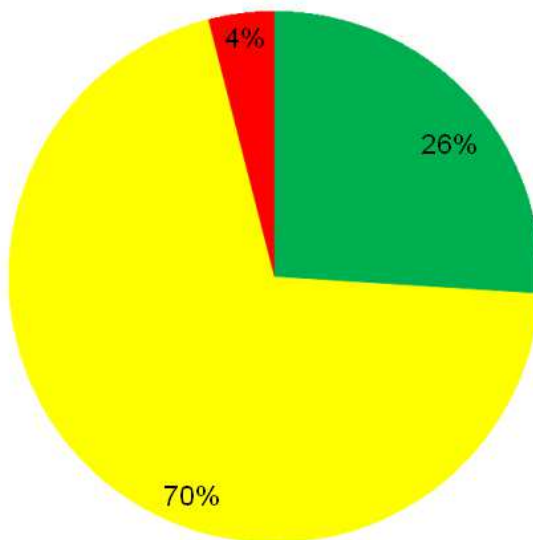


Fig.5: Graph of humidity results

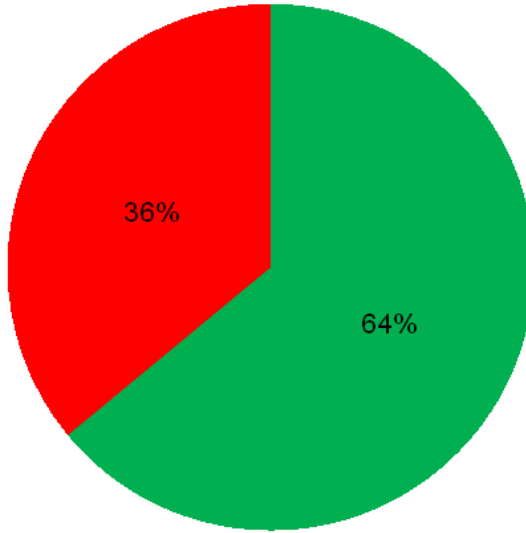


Fig.6: Graph of color results

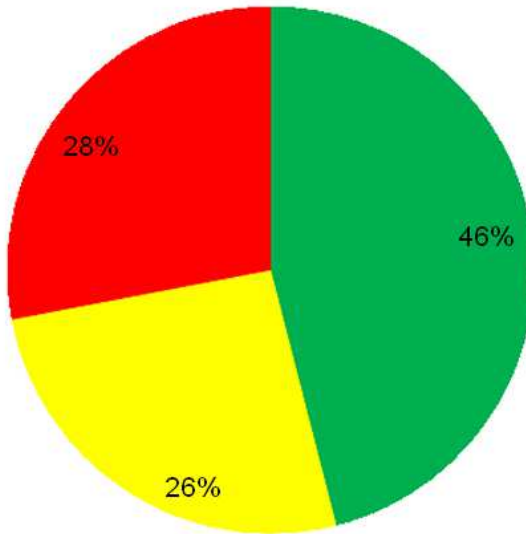


Fig.7: Graph of interfacial tension results

It can be said that this piece of work here does not consist per se an original piece of research. This paper does not claim to have explored new inroads regarding the mechanisms of breakdown of dielectric liquids, as for example in [16], or novel directions regarding new diagnostic methods, as for example in [17]. The whole purpose of this paper is, however, to show that monitoring work is necessary - not to say essential - for the correct maintenance of transformer oil in bigger transformers. An attempt to also relate the present state of transformer oil in the above mentioned transformers with their previous history will follow.

Some Further Remarks

One may ask which from the parameters investigated, are the most important. It is a difficult question to answer. However, if one has to choose between the aforementioned parameters, he would most probably select two of them, namely humidity and breakdown strength. If one looks carefully Fig. 3 (referring to breakdown voltage results) and Fig. 5 (regarding humidity results), one may see that 98% of the investigated transformers had good oil breakdown strength and 96% of

the investigated transformers had good or acceptable levels of humidity. This means that Fig. 3 and Fig. 5 are in more or less good agreement. Humidity plays a critical role, since it can contribute to a dramatic lowering of breakdown strength, as was also indicated in some older but nevertheless classical publications [18], [19], [20]. Generally speaking, inclusions of humidity more than about 10 ppm (at normal temperature) cause a lowering of breakdown strength. A low oil breakdown strength may imply that there are foreign particles and/or admixtures in the oil. On the other hand, a high breakdown strength does not necessarily mean that the oil is good. It may be possible that the quantity of foreign particles may not be sufficiently large, so that it can influence the breakdown voltage [21].

The interfacial tension, although it gives an idea of the concentration of oxidation by-products in a transformer oil, is not necessarily an indicator for definite conclusions about the oil under investigation. This is because in warmer periods of the year, the oil temperature increases and humidity may affect the oil more than in cooler periods [22].

Change of the oil color

may mean the existence of by-products or the presence of foreign particles. Although such a change may imply a certain degree of pollution of the oil under investigation, the color by itself may not be considered as a very reliable indicator of the oil quality, as was shown in this paper and was also reported in [23].

Tan δ results (Fig. 4) match very well with Fig. 3 results of breakdown strength. Tan δ changes as the oil degrades. Although tan δ measurements cannot be taken as a sole criterion of oil quality, its results match extremely well with the breakdown strength data, in the context of the present paper. The low value of tan δ depends on the nature of the oil as well as on its processing [22], [24].

A last remark should be made concerning the monitoring of both transformers of 150/20 kV and of distribution transformers (both kinds of

transformers in the major Athens area): it seems that the former have a larger percentage of good/acceptable oil than the latter [25]. To validate, however, this point, more work has to be done with transformers of both kinds from the major Athens area.

Conclusion

Insulating oil samples from transformers of 150/20 kV have been investigated. In the context of this work, several parameters - through the appropriate diagnostic techniques - affecting the state and lifetime of transformer oil have been studied. No single parameter can fully describe the state of the oil of a transformer. The variety of parameters investigated here may give a more complete picture. In the context of this work, the majority of the investigated transformer oil samples were found to be good or acceptable. This points out to the further continuing sampling at regular intervals.

References

- [1] Karsai K., Kerényi D., Kiss L., "Large Power Transformers", Eds. Elsevier, 1987
- [2] Wadhwa C.L., "High Voltage Engineering", Eds. New Age International Ltd., Publishers, New Delhi, India, 1994
- [3] Gill P., "Electric Power Transformer Engineering", Eds. CRC Press, USA, 2009

- [4] Kind D., Kaerner H., "High Voltage Insulation Technology", Eds. Friedr. Vieweg, Braunschweig Wiesbaden, Germany, 1985
- [5] Danikas M.G., "Breakdown of transformer oil", IEEE Electrical Insulation Magazine, Vol. 6, No. 5, 1990, pp. 27-34
- [6] Mitchinson P.M., Lewin P.L., Jarman P., "Oil-gap discharge in transformers", IEEE Electrical Insulation Magazine Vol. 29, No. 2, 2013, pp. 50-62
- [7] Singh S., Bandyopadhyay M.N., "Dissolved Gas Analysis technique for incipient fault diagnosis in power transformers: A bibliographic survey", IEEE Electrical Insulation Magazine, Vol. 26, No. 6, 2010, pp. 41-46
- [8] Myers S.D., Kelly J.J., Parrish R.H., "A guide to transformer maintenance", Eds. S.D. Myers Inc., ISBN 10: 0939320002, 1981
- [9] Heathcote M.J., "The J&P Transformer Book", Eds. Elsevier Ltd., Great Britain, 2007
- [10] American Society for Testing and Materials, Standard Practices for Sampling Electrical Insulating Liquids, D 923, ASTM, USA, 2004
- [11] Danikas M.G., Missas S., Liapis I., "Factors affecting the ageing of transformer oil in 150/20 kV transformers", Proceedings of the 17th International Conference on Dielectric Liquids (ICDL2011), Trondheim, Norway, Norway 26-30, June 2011, Session 06, Paper 1
- [12] Georghiou S., "Diagnostic methods in transformer oils: A study of factors affecting the lifetime of transformer oil in transformers of 150/20 kV", B.Sc. Thesis, Democritus University of Thrace, Department of Electrical and Computer Engineering, Power Systems Laboratory, Xanthi, Greece, 2012 (in Greek)
- [13] Panagiotopoulos K., "Measurements of breakdown strength in transformer oil", B.Sc. Thesis, Democritus University of Thrace, Department of Electrical and Computer Engineering, Power Systems Laboratory, Xanthi, Greece (in Greek), 1995
- [14] Zorbas M., "Measurement of dielectric strength of transformer oil", B.Sc. Thesis, Democritus University of Thrace, Department of Electrical and Computer Engineering, Power Systems Laboratory, Xanthi, Greece (in Greek), 1997

- [15] Roussos V.G., "Transformer oil: breakdown measurements", B.Sc. Thesis, Democritus University of Thrace, Department of Electrical and Computer Engineering, Power Systems Laboratory, Xanthi, Greece (in Greek), 2001
- [16] Badent R., "Modell der elektronendominanten Streame-
rentladung in Isolieroel", Ph.D. Thesis, University of
Karlsruhe, Faculty of Electrical Engineering, Institute
of Electrical Energy Systems and High Voltage Engi-
neering, 1996
- [17] Saha T.P., Purkait P., "Investigation of an expert
system for the condition assessment of transformer in-
sulation based on dielectric response measurements",
IEEE Transactions on Power Delivery, Vol. 19, No. 3,
2004, pp. 1127-1134
- [18] Nelson J.K., Salvage B., Sharpley W.A., "Electric
strength of transformer oil for large electrode areas",
Proceedings of the Institution of Electrical Engineers,
Vol. 118, No. 2, 1971, Paper 388
- [19] Zein El-Dine, Tropper H., "The electric strength of
transformer oil", Proceedings of the Institution of
Electrical Engineers, Vol. 103, 1956, pp. 35-40
- [20] Norris E.T., "High voltage power transformer insu-
lation", Proceedings of the Institution of Electrical
Engineers, Vol. 110, No. 2, 1963, pp. 428-440
- [21] Pahlavanpour B., Eklund M., Sundkvist K., "Revised IEC
standard for maintenance of in-service insulating oil",
"[http://weidmann-solutions.cn/huiyi/Seminar%202004%20Sa
cramento/PahlavanpourPaper2004.pdf](http://weidmann-solutions.cn/huiyi/Seminar%202004%20Sa
cramento/PahlavanpourPaper2004.pdf)"
- [22] Samoilis V.G., "Insulating oils", Eds. National Tech-
nical University of Athens, Athens, Greece, 1986 (in
Greek)
- [23] American Society for Testing and materials, Standard
Test Method for ASTM Color of Petroleum Products (ASTM
Color Guide), D 1500, ASTM, USA, 2004
- [24] Doudoulakis M.G., "Temperature effects on the prop-
erties and the behaviour of transformer oil", M.Sc. The-
sis, National Technical University of Athens, Athens,
Greece, 2009
- [25] Danikas M.G., Rapti E., Liapis I., Ghani A.B.B. Abd.,
"Parameters affecting the lifetime of transformer oil
in distribution transformers: Parameter monitoring of
50 transfmormers from the Athens area", FunkTechnikPlus
Journal, Issue 4, Year 1, May 2014, pp. 53-65

"www.otoiser.org/index.php/ftpj/article/view/45"

"www.otoiser.org/index.php/ftpj/issue/view/2014.05.31"

Previous Publication in FUNKTECHNIKPLUS # JOURNAL

"Electrical Machine Insulation: Traditional Insulating Materials, Nanocomposite Polymers and the Question of Electrical Trees", Issue 5, Year 2, pp. 7-32

*** About The Authors**

Michael Danikas, Issue 2, Year 1, 2013, p. 39

S. Georghiou, received his degree from Democritus University of Thrace, Department of Electrical and Computer Engineering, in 2012. He is currently employed in Cyprus.

Ioannis Liapis, Issue 4, Year 1, 2014, p. 65

Ahmad Basri Bin Abdul Ghani, Issue 4, Year 1, 2014, p. 65

[This Page Intentionally Left Blank]

[This Page Intentionally Left Blank]

[This Page Intentionally Left Blank]

In case of any doubt,
download the genuine papers from
genuine.ftpj.otoiser.org

FRONT COVER VIGNETTE

A faded synthesis of an anthemion rooted in a meandros

The thirteen-leaf is a symbol for a life tree leaf.
"Herakles and Kerberos", ca. 530–500 BC,
by Paseas, the Kerberos Painter,
Museum of Fine Arts, Boston.

www.mfa.org/collections/object/plate-153852

The simple meandros is a symbol for eternal immortality.
"Warrior with a phiale", ca. 480–460 BC,
by Berliner Maler,
Museo Archeologico Regionale "Antonio Salinas" di Palermo.

commons.wikimedia.org/wiki/File:Warrior_MAR_Palermo_NI2134.jpg

ISSN 2310-6697

toiser—open transactions on independent scientific-engineering research

FUNKTECHNIKPLUS # JOURNAL

Théorie—Expérimentation—Métrologie—Logiciel—Applications

ISSUE 7 – SUNDAY 31 MAY 2015 – YEAR 2

- 1 Contents
- 2 About
- 3 Editorial Board – Technical Support
- 4 Information for Peers – Guiding Principles
- # Electrical Engineering – Théorie
- 7 Thoughts on the Possibility of Damage of High-Voltage Electrical Insulation below the so-called Inception Voltage: The Historical Background – Part I
M.G. Danikas, Yi Yin, Jialei Hu
- # Telecommunications Engineering – Applications
- 19 A Planar Delta-Cross Shaped Loop Antenna: Analysis and Simulation – The 2 WL Case
G.A. Papadaniel, N.I. Yannopoulou, P.E. Zimourtopoulos



*This small European Journal is
In the Defense of Honesty in Science and Ethics in Engineering*

Publisher – otoiser—open transactions on independent scientific engineering research, www.otoiser.org—info@otoiser.org, Hauptstraße 52, 2831 Scheiblingkirchen, Austria

Language – We declare the origins of the Journal by using in the cover page English, German and French, as well as, a Hellenic vignette. However, since we recognize the dominance of US English in the technical literature, we adopted it as the Journal's language, although it is not our native language.

Focus – We consider Radio–FUNK, which still creates a vivid impression of the untouchable, and its Technology–TECHNIK, from an Advanced–PLUS point of view, Plus–PLUS Telecommunications Engineering, Electrical Engineering and Computer Science, that is, we dynamically focus at any related scientific-engineering research regarding Théorie, Expérimentation, Métrologie, Logiciel, ou Applications.

Scope – We emphasize this scope broadness by extending the title of the Journal with a Doppelkreuz-Zeichen # which we use as a placeholder for substitution of our Editorial Team disciplines: # Telecommunications etc. as above, or # High Voltage, # Software Engineering, # Simulation etc. as below.

Frequency – We publish 3 issues per year: on 31st of January, on 31st of May, and on 30th of September, as well as, an extra issue every 3 papers and a volume every 2 years.

Editions – We increase the edition number of an issue only when is needed to reform one or more of its papers—thus to increase their version numbers—but we keep unchanged its 1st edition date shown on its front page and we number its pages sequentially from 1. We count the editions of *About* separately.

Format – We use a fixed-space font, hyphenation, justification, unfixed word spacing, and the uncommon for Journals A5 (half A4) page size to achieve WYSIWYG printing and clear reading of 2 to 4 side-by-side pages on wide-screen displays

Printing-on-Demand – We can email gratis PDFs at 300-4000 dpi in booklet page scaling of either brochure or book type.

Copyright – We publish under a Creative Commons Attribution, CC-BY 3.0 Unported or CC-BY 4.0 International, License only.

Please download the latest *About* edition from
about.ftpj.otoiser.org

Editorial Team

Electrical Engineering

High Voltage Engineering # Insulating Materials
Professor Michael Danikas, mdanikas@ee.duth.gr
EECE, Democritus University of Thrace, Greece

Electrical Machines # Renewable Energies # Electric Vehicles
Assistant Professor Athanasios Karlis, akarlis@ee.duth.gr
EECE, Democritus University of Thrace, Greece

Computer Science

Computer Engineering # Software Engineering # Cyber Security
Professor Vasilis Katos, vkatos@bournemouth.ac.uk
Head of Computer and Informatics Dept, Bournemouth Univ, UK

Internet Engineering # Learning Management Systems
Lecturer Sotirios Kontogiannis, skontog@gmail.com
Business Administration Dept, TEI, Western Macedonia, Greece

Hypercomputation # Fuzzy Computation # Digital Typography
Dr. Apostolos Syropoulos, asyropoulos@yahoo.com
BSc-Physics, MSc-Computer Science, PhD-Computer Science
Independent Researcher, Xanthi, Greece

Telecommunications Engineering

Applied EM Electromagnetics # Applied Mathematics
Dr. Nikolaos Berketis, nberketis@gmail.com
BSc-Mathematics, MSc-Applied Maths, PhD-Applied Mathematics
Independent Researcher, Athens, Greece

Antennas # Metrology # EM Software # Simulation # Virtual Labs

Applied EM # Education # FLOSS # Amateur Radio # Electronics
Dr. Nikolitsa Yannopoulou, yin@arg.op4.eu *
Diploma Eng-EE, MEng-Telecom-EECE, PhD-Eng-Antennas-EECE
Independent Researcher, Scheiblingkirchen, Austria

Dr. Petros Zimourtopoulos, pez@arg.op4.eu *
BSc-Physics, MSc-Radio-Electronics, PhD-Antennas-EE
Independent Researcher, Scheiblingkirchen, Austria

* Copy & Layout Editing – Proof Reading – Issue & Web Management

Technical Support

Konstantinos Kondylis, kkondylis@gmail.com
Diploma Eng-EECE, MEng-EECE, Doha, Qatar

Christos Koutsos, ckoutsos@gmail.com
Diploma Eng-EECE, MEng-EECE, Bratislava, Slovakia

Information for Authors

This is a small, but independent, low profile Journal, in which we are all—Authors, Reviewers, Readers, and Editors—free at last to be Peers in Knowledge, without suffering from Journal roles or positions, Professional–Amateur–Academic statuses, or established "impact factorizations", under the following guiding principles:

Authors – We know what Work means, we respect the Work of the Independent Researcher in Science and Engineering and we want to exhibit his Work. Thus, we decided to found this Free and Open Access Journal in which to publish this Work. Furthermore, as we care indeed for the Work of the technical author—especially a young or a beginner one—we strongly support the publication of his Work, as follows:

- 0 We do not demand from the author to transfer his own copyright to us. Instead, we only consider papers resulting from original research work only, and only if the author can assure us that he owns the copyright of his own paper as well as that he submits to the Journal either an original copy or a revised version of his own paper, for possible publication after review—or even for immediate republication, if this paper has already been published after review—but, in any case under a Creative Commons Attribution, CC-BY 3 Unported or CC-BY 4 International, License, only.
- 1 We encourage the author to submit his own paper written just in Basic English plus Technical Terminology.
- 2 We encourage the author even to select a pen name, which may drop it at any time to reveal his identity.
- 3 We encourage the author to submit an accepted for publication paper, which he was forced to decline that publication because it would be based on a review with unacceptable evaluation or derogatory comments.
- 4 We encourage the author to submit any paper that was rejected after a poor, impotent, inadequate, unreasonable, irresponsible, incompetent, or "just ticking" review.
- 5 We encourage the author to submit an unreviewed paper of his own that he uploaded on some Open Access repository.
- 6 We encourage the author to upload his published papers in our Journal to a truly Free Open repository like viXra.org.
- 7 We provide the author with a decent, express, peer review process, of up to just 4 weeks, by at least 2, either anonymous or onymous, reviewers.

- 8 We provide the author with the option to choose from 2 review processes: the traditional, anonymous, close one, as well as, a contemporary, onymous, open review in our private mailing list for Peer Discussion.
- 9 Under the Clause 0 : We immediately accept for publication a research paper directly resulting from a Project Report, or a Diploma-, Master-, or PhD-thesis, which already the author has successfully defended before a committee of experts, as long as he can mention 2 members of this committee who approved his Work.
- 10 Under the Clause 0 : We immediately accept for publication any paper which is not Openly Accessible on the Internet.
- 11 We immediately publish online a paper, as soon as it is accepted for publication in the Journal.
- 12 We quickly publish an extra issue—that is in excess of the 3 issues we publish a year—as soon as the review process of 3 papers is completed.

Reviewers – Every peer may voluntarily become a reviewer of the Journal in his skillfulness for as long as he wishes. In addition, each author of the Journal must review one paper in his expertness for each one of his published papers.

Readers – Every reader is a potential post-reviewer: we welcome comments and post-reviews in our private mailing list for Peer Discussion.

Editors – Every editor owns a PhD degree—to objectively prove that he really has the working experience of passing through the dominant publishing system. An editor pre-reviews a paper in order to check its compliance to our guiding principles and to select the appropriate reviewers of it. We can accept for consideration papers only in the expertise areas currently shown in the Editorial Team page, above. However, since we are very willing to amplify and extend the Scope of the Journal, we welcome the volunteer expert, in any related subject, who wants to join the Editorial Team as long as he unreservedly accepts our guiding principles.

Electronic Publishing

We regularly use the Free Libre Open Source Software Libre Office with the Free Liberation Mono font and the Freewares PDFCreator and PDF-Xchange Viewer. We also use, with some basic html code of ours: the Free Open Source Software Open Journal System OJS by the Public Knowledge Project PKP installed in our website, and the Free Open Digital Library of

About

Internet Archive website, where we upload Issues, Paper reprints, *About* documents, and Volumes, in both portrait and landscape orientations, for exceptionally clear online reading with the Free Open Source BookReader.

Submissions

We can consider only papers submitted in a format which is fully compatible with LibreOffice—preferably in odt format.

Legal Notice – It is taken for granted that the submitter–correspondent author accepts, without any reservation, the totality of our publication conditions as they are analytically detailed here, in this *About*, as well as, that he also carries, in the case of a paper by multiple authors, the independent will of each one of his coauthors to unreservedly accept all the aforementioned conditions for their paper.

Internet Addresses

Internet Publishing Website : ftpj.otoiser.org

Internet Archive Digital Library : archive.org/details/@ftpj

Printing-on-Demand : pod@ftpj.otoiser.org

Principal Contact : principal-contact@ftpj.otoiser.org

Technical Support : technical-support@ftpj.otoiser.org

Editorial Team–Technical Support List : etts.ftpj.otoiser.org

Peer Discussion List : peers.ftpj.otoiser.org

Submissions : sub@ftpj.otoiser.org

Sample Paper Template : template.ftpj.otoiser.org

ARG NfP AoI

Antennas Research Group

Not-for-Profit Association of Individuals *

arg.op4.eu – arg@op4.eu

Hauptstraße 52, 2831 Scheiblingkirchen, Austria

* The Constitution of Greece, Article: 12(3) 2008:

www.hellenicparliament.gr/en/Vouli-ton-Ellinon/To-Politevma

* The Hellenic Supreme Court of Civil and Penal Law:

www.areiospagos.gr/en/ – Court Rulings:Civil|A1|511|2008

This document is licensed under a Creative Commons Attribution 4.0 International License – <https://creativecommons.org/licenses/by/4.0/>

Thoughts on the Possibility of Damage of High-Voltage Electrical Insulation below the so-called Inception Voltage: The Historical Background – Part I

M.G. Danikas, Yi Yin, Jialei Hu *

[1] Department of Electrical and Computer Engineering,
Power Systems Laboratory,
Democritus University of Thrace, Xanthi, Greece

[2, 3] Department of Electrical Engineering,
Shanghai Jiaotong University, Shanghai,
People's Republic of China

Abstract

Partial discharges (PD) may cause damage to high-voltage (h.-v.) electrical insulation and eventually breakdown. It is known, however, that sudden breakdowns occurred in industrial insulations after only a few months in service, although they had passed the suggested international specifications tests. In this paper, we investigate the possibility of damage of an h.-v. insulation even below the inception voltage, giving the historical background which led to certain thoughts. References to previous work are given and a differential equation is proposed regarding the possibility of having charging phenomena below the inception voltage.

Keywords

Partial discharges, high voltage insulation, cavities, inception voltage, leakage currents

Introduction

PD may cause significant damage to the h.-v. insulation [1], [2]. PD may start from asperities on the electrodes, from enclosed voids, from fissures and/or from enclosed foreign particles [3]. Numerous publications tackled the

question of the relation between PD parameters and insulation damage [4]-[7].

Although a voluminous amount of research has been performed on the questions of insulation damage and PD, no particular attention was given to possible charging

events below inception voltage. However, such events were held responsible (at least partly) for the failure of insulation equipment back in the fifties and the sixties of the last century [8]-[11]. Such incidents were reported, regarding big electrical machines as well as high voltage switches that failed abruptly, although they passed all tests the international technical committees were suggesting [8]. Which were these incidents? In the 1950's one major US manufacturer produced and sold large rotating machines with cast polymer insulation. At that time all available diagnostic techniques suggested that there should be no problem at all from low leakage currents. Surprisingly enough, these rotating machines failed while in service in a few months. Another occasion of impressive failure was registered when another US manufacturer producing 15 kV class vacuum switches, reported that, although all normal tests at that time were done, unexplained erosion of cast epoxy insulation occurred in these switches, only after a few years in service. Such were the incidents that led to the exploration of the below inception regime of charging phenomena [12]. Scientific evidence of "something" happening below inception was

provided by Filippini [13], who suggested that treeing propagation followed growth along current paths. Furthermore, Brancato [14] indicated the possibility of relating current below inception with temperature rise. In his own words, "perhaps the most exciting but speculative project is the development of techniques to determine temperature rise of void surfaces due to partial discharge. ... electrical aging may in reality be a chemical reaction in voids induced by the deposition of energy. This deposition is expended in the raising of the temperature of the walls of the void, in creation of ozone and possibly nascent oxygen which tend to oxidize the surface chemical reactions which in the presence of water components form nitric or nitrous acids which deteriorate the void surfaces and finally mechanical erosion by the resulting ion stream impinging on the void". In the same publication, Brancato also pointed out that measuring or sensing techniques may not be adequate for all classes of dielectric materials or to all aging environments and/or the inadequate sensitivity of some instruments to detect changes. Recent papers point out to the slow decline of inception voltage with time [15]. Is this also an indica-

tion of charging phenomena below the so-called inception? Would such phenomena play a role regarding the decrease/decline of inception voltage?

Hints about possible damaging events below inception voltage were discussed in a brief report by E. Brancato back in 1991 [16]. Previous work on air gaps with a non-uniform electrode arrangement suggested that such charging events were possible [17]-[20]. To the best of our knowledge, until now there are indications of possible charging effects below inception voltage but a definite proof is missing.

It is the purpose of the present paper to offer the historical background of the approach regarding charging events below the inception voltage and to explore a bit further the events below inception. An equation, which was proposed many years ago by Bruning, is discussed.

On the Problem of Inception Voltage - Historical Background

Inception voltage is called the lowest voltage under a.c. conditions, at which repetitive PD of a specified magnitude in successive cycles are observed, as the applied voltage increases [21]. Above the inception level, an

insulation may deteriorate depending on the magnitude of the imposed voltage. Things become more blurred when an insulation is subjected to an applied voltage which is lower than the extinction voltage (according to the seminal publication by Kelen [21], the extinction voltage is the voltage at which discharges of a specified magnitude will recur when an alternating voltage, which exceeds the discharge-inception voltage, is reduced).

In his important paper, Bruning and colleagues [9], pointed out that unexpected insulation failures occurred despite the fact that the insulation was operating below the inception voltage. In this doctoral thesis, Bruning [8] pointed out that there were problems in tackling and understanding the basics of current-voltage relationships for new insulating materials and/or new devices. For example, the design failure of epoxy insulators, which used the application of criteria for porcelain discharge onset, did not sufficiently characterize low current performance with contamination. On another occasion, there was a lack of fundamental current vs. voltage analytical model for the design of a new type of transformer windings. In many cases of transformer

failures, discharge testing did not indicate low level pre-discharge activities with operation. Problems also arise with underground cables, where aging effects, exacerbated by the presence of water, may give higher discharge currents which are below the level which can be satisfactorily measured. Bruning speculated that low level discharge currents cause a destructive local temperature effect. Problems related to the above questions were revealed in the USA with electrical machines, cables and high-voltage switches, which failed unexpectedly although all of them passed the required tests prescribed by the international technical committees.

All the above point to the fact that there is a need for a fresh approach for this problem, an approach which may give a possible solution to charging effects below inception. Efforts have been undertaken in Bruning's seminal publications [8], [9], where questions such as the following were put:

a) what is the insulation leakage current-voltage characteristic?

b) what is the effect of such a leakage current?

Efforts were also undertaken in some publications,

albeit with a different insulating material and a much simpler electrode arrangement [17]-[20]. In those papers, indications were presented that effects below the so-called inception level may exist. Moreover, experiments performed in polyethylene samples with enclosed cavities, indicated that at relatively low voltages sharp current waveforms were detected. This indicates sudden streamer PD mechanism in enclosed cavities. In previous years, comments regarding the relation between such sudden PD waveforms and events at or below the inception level were offered. It was speculated that there may be sudden bursts related to local rising of temperature in a cavity [22]-[26].

Possible Relation Between PD Events at Inception Voltage and Charging Events below Inception

Bruning and colleagues [8], [9], [27] proposed an equation describing the quasi-steady state for current flow

$$\nabla^2 V + \nabla V \cdot \nabla s / s = 0 \quad (1)$$

where, ∇ is the gradient and ∇^2 is the Laplace operator expressed as a function of the location, V is the local voltage and s the local conductivity of the fluid (in

our case air). They also proposed that it would be plausible to state that the local air temperature is related to the local power dissipation which is leakage current times the local voltage gradient. This being true, the local electrical conductivity is related to the local temperature. The question was as to whether such an equation was leading to a burst or sudden PD pulse even below inception. Would this be possible?

In fact the above equation was characterized as the "thermal model" in Bruning's Ph. D. Thesis [8]. It suggests a thermal model of gaseous conduction which under certain conditions of limited diffusion rate of ionized species, low radiant energy loss, and low thermal conductance, a diffuse current flow may generate a diffuse conduction process. Similar pulseless regimes were suggested in [28]. Furthermore, the same direction of research, without however being so specific, was pointed out in [29], [30], where pseudoglow regimes were observed. It may well be that the current not indicated on a conventional PD detector is a current below the detection level.

More in detail, if one assumes that in the gas there

is a dissipative current flow, using classical notation,

$$\nabla \mathbf{V} \cdot \mathbf{J} = 0 \quad (2)$$

$$\mathbf{J} = s\mathbf{E} \quad (3)$$

$$\nabla \cdot s\mathbf{E} = 0, \text{ but } \mathbf{E} = \nabla V \quad (4)$$

and consequently,

$$\nabla^2 V + \nabla \mathbf{V} \cdot \nabla s / s = 0 \quad (5)$$

The above equation, in the case of a constant conductivity s , reduces to the well known Laplace/Poisson equation. However, for a gaseous conduction process, where there is a partial variable ionization as \mathbf{J} varies with time and position, we have finally Eq. (5).

As was noted in a previous paper [27], solution of the distributed - perhaps pulseless current flow - then proceeds from ionization determined from both Saha's equation and the heat balance determining the local temperature. The complexity of the transport processes have not permitted ab initio calculations. However, approximations indicate a variation of current density and field strengths, which indicate the possibility of current below the detection level. Whether the continuous thermal conduction model arises from true continuous conduction or from

pulses too short to be detectable by conventional PD detectors, it is a question in need of an answer. It is interesting to note, however, that sudden bursts of pulses at or below the so-called inception voltage were observed recently, not only in conventional polymers but also - albeit less frequently - in nanocomposites [31], [32].

Research by Bruning and colleagues [9], [10] indicated that damage observed below inception was very similar to the damage above inception. In these papers, indications were offered that chemical changes below inception were similar to those noted above inception. Such indications gave strong ground for suggesting that "something" goes on below the inception voltage. Chemical changes that indicate chemical deterioration below inception imply the existence of charging phenomena that may render shorter the lifetime of the insulation. Charging effects below the inception voltage may imply that there is no voltage below which no deterioration takes place. More precisely, it is known that the lifetime L (time to failure) is given by the formula

$$L = c(V - V_0)^{-k} \quad (6)$$

where, V is the applied volt-

age, V_0 is the voltage below which no deterioration takes place and k is a constant. k , V_0 , and c are constants depending on the insulation material (it should be noted that original form of Eq. (6), referred to in [33], was

$$L = (A - \alpha)^k(V - \alpha A)^{-k}$$

where, L is life in minutes, A is the 1 min strength, α is a material constant, k is another material constant and V is the applied voltage). However, if one assumes that there is damage below the inception voltage, then

$$V_0 = 0 \quad (7)$$

and Eq. (6) becomes

$$L = cV^{-k} \quad (8)$$

As was noted in [9], "most equipment designers use this empirical relation without having settled the fundamental question as to whether $V_0 = 0$ or not, since empirical experiments in reasonable time periods cannot distinguish between the two forms", i.e. that of Eq. (6) from that of Eq. (8). Ambiguities regarding Eq. (6) still remain to this day, especially if one looks at insulation lifetime models [34]. The question of whether $V_0 = 0$ is also relevant to the sensitivity of PD detector as well as to the

thickness of the examined insulation, deserves to be further explored. It was reported before, that scaling laws exist, i.e. a thicker insulation requires a more sensitive PD detector [35], [36]. Needless to say that the sensitivity of a PD detector determines the inception voltage of either an insulating material or a full insulation system, or in the words of one of the most distinguished researchers of the good old generation, E. Brancato, "... electric stresses in the absence of internal discharges can cause changes in material properties. Some ascribe the changes to electrochemical reactions, while others express the suspicion that the observed changes are really caused by partial discharges but the corona detecting system is too insensitive" [37].

From the above it is indicated that, although there is not yet a universal name to it, "something" must occur below the inception voltage. Whether this "something" can be referred to as "charging phenomenon" or can be manifested as "signal", is not yet clear. Moreover, if one sees the more practical questions and if one tackles the problems of the role of antioxidants in cable insulation,

one may say that antioxidants are incorporated to prevent premature degradation during extrusion, but the role of the residual antioxidant on insulation response to aging stresses has not yet been quantified, especially in voltages below the inception level [38].

Conclusion

The present paper is an introduction to the problem of possible charging effects below the so-called inception voltage. The historical background of an approach - different from the usual approaches - is given as well as the indications that charging phenomena below inception may exist. Below inception sudden pulses were observed with an electrode arrangement of point-plane with air as insulating material. It is speculated that minute abnormalities on the cavity surface may act as emission sites and thus provoke small charging phenomena not easily detected by normal conventional PD detectors. An equation regarding the current flow in a cavity was given and commented upon. In a future publication, a solution of the said differential equation will be given together with appropriate comments.

References

- [1] Mason J.H., "Discharges", IEEE Transactions on Electrical Insulation, Vol. 13, No. 4, 1978, pp. 211-238
- [2] Devins J.C., "The physics of partial discharges in solid dielectrics", IEEE Transactions on Electrical Insulation, Vol. 19, No. 5, 1984, pp. 475-495
- [3] Danikas M.G., Karlis A.D., "Some observations on the dielectric breakdown and the importance of cavities in insulating materials used for cables and electrical machines", Advances in Electrical and Computer Engineering, Vol. 11, No. 2, 123-126, 2011
- [4] Garcia G., Fallou B., "Equipment for the energy measurement of partial discharges", Proceedings of the 1st International Conference on Conduction and Breakdown in Solid Dielectrics, Toulouse, France, 4-8 July 1983, Conf. Rec. 83CH1836-6-EI, pp. 275-281
- [5] Pearmain A.J., Danikas M.G., "A study of the behavior of a uniaxially orientted polyethylene tape/oil insulating system subjected to electrical and thermal stresses", IEEE Transactions on Electrical Insulation, Vol. 22, No. 4, 1987, pp. 373-382
- [6] Gulski E., "Digital analysis of partial discharges", IEEE Transactions on Dielectrics and Electrical Insulation, Vol. 2, No. 5, 1995, pp. 822-837
- [7] Krivda A., "Automated recognition of partial discharges", IEEE Transactions on Dielectrics and Electrical Insulation, Vol. 2, No. 5, 1995, pp. 796-821
- [8] Bruning A.M., "Design of electrical insulation systems", Ph. D. Thesis, University of Missouri-Columbia, USA, 1984
- [9] Bruning A.M., Kasture D.G., Campbell F.J., Turner N.H., "Effect of cavity current on polymer insulation life", IEEE Transactions on Electrical Insulation, Vol. 26, No. 4, 1991, pp. 826-836
- [10] Turner N.H., Campbell F.J., Bruning A.M., Kasture D.G., "Surface chemical changes of polymer cavities with currents above and below corona inception voltage", Annual Report on Conference of Electrical Insulation and Dielectric Phenomena (CEIPD), 18-21 October 1992, Victoria, B. C., Canada, pp. 687-693
- [11] Bruning A.M., Danikas M.G., "Observations on discharges above and below CIV in polymer insulation", Annual Re-

- port on Conference of Electrical Insulation and Dielectric Phenomena, 20-23 October 1991, Knoxville, Tennessee, USA, pp. 638-647
- [12] Bruning A.M., Campbell F.J., Kasture D.G., Turner N.H., "Voltage induced insulation aging - Chemical deterioration from sub-corona currents in polymer void occlusions", research Project Number: RP8007-1, July 1990, Interim-Phase 1 (Contractor: naval research Laboratory (NRL), Washington, D. C., Contractor: Lectromechanical Design Co. (LM)), Herndon, Virginia)
- [13] Filippini J.C., "Mechanical aspects of water treeing in polymers", Conference Record of the 1990 IEEE International Symposium on Electrical Insulation, Toronto, Canada, 3-6 June 1990, pp. 183-186
- [14] Brancato E.L., "Status of aging in insulating materials and systems", Conference record of the 1985 International Conference on Properties and Applications of Dielectric Materials, June 24-29, 1985, Xi'an, People's Republic of China, IEEE Paper I-7
- [15] Hossam-Eldin A.A., Dessouky S.S., El-Mekawy S.M., "Internal discharge in cavities in solid dielectric materials", Journal of Electrical Engineering, Vol. 9, No. 4, 2009 ("www.jee.ro")
- [16] Brancato E.L., "Electrical aging - A new insight", IEEE Electrical Insulation Magazine, Vol. 6, 1990, pp. 50-51
- [17] Danikas M.G., Prionistis F.K., "Detection and recording of partial discharges below the so-called inception voltage", Facta Universitatis, Series Electronics and Energetics, Vol. 17, No. 1, 2004, pp. 99-110
- [18] Danikas M.G., Vrakotsolis N., "Experimental results with small air gaps: Further thoughts and comments on the discharge (or charging phenomena) below the so-called inception voltage", Journal of Electrical Engineering, Vol. 56, No. 9-10, 2005, pp. 246-251
- [19] Danikas M.G., Pitsa D., "Detection and registration of partial discharge events below the so-called inception voltage: The case of small air gaps", Journal of Electrical Engineering, Vol. 59, No. 3, 2008, pp. 160-164
- [20] Danikas M.G., "Detection and recording of partial discharges below the inception voltage with a point-plane electrode arrangement in air: Experimental data and definitions", Journal of Electrical Engineering, Vol. 61, No. 3, 2010, pp. 177-182

- [21] Kelen A., "Studies on partial discharges on solid dielectrics: A contribution to the discharge resistance testing of insulating materials", Acta Polytechnica Scandinavica, Electrical Engineering Series, Monograph of 138 pages, 1967
- [22] Danikas M.G., "Discharge studies in solid insulation voids", 1990 Annual Report of the Conference on Electrical Insulation and Dielectric Phenomena (CEIDP), October 28-31, 1990, Pocono Manor, USA, pp. 249-254
- [23] Danikas M.G., "Some further comments on the fast measurements of partial discharges in polyethylene voids", Proceedings of the 20th Electrical and Electronics Insulation Conference, October 7-10, 1991, Boston, USA, pp. 220-224
- [24] Danikas M.G., "Fast measurements of partial discharges in polyethylene cavities with the aid of a subdivided electrode arrangement: A study of circuit parameters on the waveshape of the detected PD currents", Journal of Electrical Engineering, Vol. 51, No. 3-4, 2000, pp. 75-80
- [25] Danikas M.G., "Partial discharge behaviour of two (or more) adjacent cavities in polyethylene samples", Journal of Electrical Engineering, Vol. 52, No. 1-2, 2001, pp. 36-39
- [26] Morshuis P., "Assessment of dielectric degradation by ultrawide-band PD detection", IEEE Transactions on Dielectric and Electrical Insulation, Vol. 2, No. 5, 1995, pp. 744-760
- [27] Danikas M.G., Bruning A.M., "Comparison of several theoretical sub-corona to corona transition relations with recent experimental results", Conference Record of the 1992 IEEE International Symposium on Electrical Insulation, June 7-10, 1992, Baltimore, USA, pp. 383-388
- [28] Isa H., Sonoi Y., Hayashi M., "Breakdown process of a rod-to-plane gap in atmospheric air under DC voltage stress", IEEE Transactions on Electrical Insulation, Vol. 26, No. 2, 1991, pp. 291-299
- [29] Bartnikas R., "Some observations on the character of corona discharges in short gap spaces", IEEE Transactions on Electrical Insulation, Vol. 6, No. 2, 1971, pp. 63-75
- [30] Bartnikas R., d' Ombrain G.L., "A study of corona discharge rate and energy loss in spark gaps", IEEE Tran-

- sactions on Power Apparatus and Systems, Vol. 84, No. 9, 1965, pp. 770-778
- [31] Danikas M.G., Zhao X., Cheng Y.-H., "Experimental data on epoxy resin samples: Small partial discharges at inception voltage and some thoughts on the possibility of the existence of charging phenomena below inception voltage", Journal of Electrical Engineering, Vol. 62, No. 5, 2011, pp. 292-296
- [32] Zhang Y., Danikas M.G., Zhao X., Cheng Y.-H., "Charging phenomena below the inception voltage: Effects of nano-fillers on epoxy", Malaysian Polymer Journal, Vol. 7, No. 2, 2012, pp. 68-73
- [33] Montsinger V.M., "Breakdown curve for solid insulation", AIEE Transactions on Electrical Engineering, Vol. 54, No. 12, 1935, pp. 1300-1301
- [34] Simoni L., "Life models of insulating materials for combined thermal-electrical stresses", Colloquium on "Ageing of insulating materials under electrical and thermal stresses", 1/12/1980, Dig. No. 1980/72, pp. 1.1-1.9
- [35] Danikas M.G., "Some possible new applications of a partial discharge (PD) model and its relation to PD-detection sensitivity", European Transactions on Electrical Power, Vol. 6, No. 6, 1996, pp. 445-448
- [36] Danikas M.G., Vassiliadis G.E., "Models of partial discharges (PD) in enclosed cavities in solid dielectrics: A study of the relationship of PD magnitudes to the sensitivity of PD detectors and some further comments on insulation lifetime", Journal of Electrical Engineering, Vol. 54, No. 5-6, 2003, pp. 132-135
- [37] Brancato E.L., "Insulation aging - A historical and critical review", IEEE Transactions on Electrical Insulation, Vol. 13, No. 4, 1978, pp. 308-317
- [38] Bernstein B., Private Communication, October 2008

Previous Publication in FUNKTECHNIKPLUS # JOURNAL

"Diagnostic Techniques in Transformer Oils:
Factors Affecting the Lifetime of Transformer Oil
in Transformers of 150/20 kV and the Problem of Relating
Diagnostics Data with their Pre-history",
Issue 6, Year 2, pp. 27-40

*** About The Authors**

Michael Danikas, Issue 2, Year 1, 2013, p. 39

Yi Yin, is Professor at Shanghai Jiaotong University, Shanghai, Department of Electrical Engineering. He teaches and conducts research in the areas of high voltage engineering and of insulating materials, especially on polymer dielectric properties and applications, nanocomposite polymers and condition monitoring of electrical apparatus.

Jialei Hu, is a postgraduate student at Shanghai Jiaotong University, Department of Electrical Engineering, carrying out his Ph.D. under the supervision of Professor Yi Yin. He is doing research on polymeric materials relevant to high voltage engineering.

A Planar Delta-Cross Shaped Loop Antenna: Analysis and Simulation - The 2 WL Case

G.A. Papadaniel, N.I. Yannopoulou, P.E. Zimourtopoulos *

[1] Independent Researcher, Thessaloniki, Greece
[2, 3] Antennas Research Group, Hellas – Austria

Abstract

A planar Delta-Cross shaped loop antenna is proposed. The presentation includes results from an analytic study of the radiation pattern, as well as, from a simulation study for both the electric and radiation characteristics: input impedance, standing wave ratio, radiation pattern and directivity. The loop was initially shaped as 4 non-overlapping equilateral triangles on a plane, symmetrically oriented around a common vertex, center fed at one triangle base. In order to improve the antenna characteristics, its shape was then modified by equally changing the triangle base angle-while keeping the loop length constant and equal to 2 wavelengths WL. In this way, the final antenna loop was shaped with 4 isosceles triangles. The analytical and simulated results for the radiation pattern were found to be in good agreement. Furthermore, a comparison with antenna's dipole counterpart characteristics showed a much better performance of the proposed antenna.

Keywords

Cross loop antenna, delta elements, analysis, simulation, improvement

Introduction

The cross loop antenna consisting of four delta elements was examined as a prototype antenna during preparation of an EECE diploma thesis [1]. The main available tools for its study were the antenna theory [2], the [RadPat4W] computer program

for antenna patterns [3] the [RICHWIRE] simulation program [4] and the mini-Suite of software tools [5]. Its simple plane figure of double symmetry with respect to two axes which means easy geometrical representation for the theoretical consideration of its radiation pattern as well

as for the simulation and easy construction, was the basic reason for this proposal. The initial antenna consists of four equilateral triangles with side length $\lambda/6$ and almost coincident their four vertices. Thus, the total length of the antenna is 2λ . The feed source was at the middle of the base of one of the triangles as it is shown in Fig. 1.

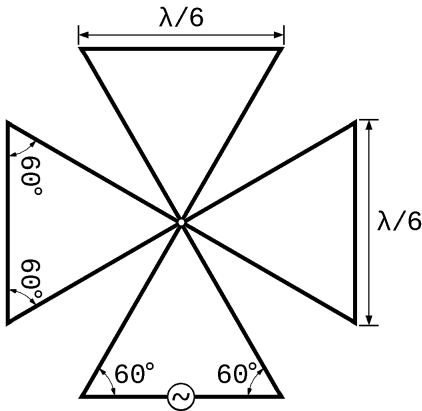


Fig. 1: Planar Delta-Cross Shaped Loop antenna

Then, the antenna was modified only with respect to the base angles of the triangles, keeping constant the triangle perimeter equal to $\lambda/2$, resulting a cross antenna of four isosceles triangles. The angle was varied between 48° and 78° , in order to improve both of its electrical and radiative characteristics and the one with

48° angle was selected as the improved Delta-Cross Shaped Loop antenna.

Analysis

The initial antenna was analytical studied considering standing waves, that is, sinusoidal, current distribution in a parallel wire transmission line. Since the perimeter of each equilateral triangle is $\lambda/2$, the total antenna length is equal to 2λ and it corresponds to a properly formed short circuited transmission line. However, the study was carried out in a $5\lambda/2$ piece of open circuited transmission line, formed properly as in Fig. 2, since the available formula of equation (1) concerns open circuited two parallel wired transmission lines

$$\dot{I}(\ell) = \dot{I} \sin(\beta(h - |\ell|)) \quad (1)$$

with

$$-h \leq \ell \leq +h \text{ where } h = \frac{5}{4}\lambda .$$

The above current distribution (1) was used to evaluate the radiation pattern of the antenna through the relations

$$\vec{E} = e^{i\beta R_{kr}} \text{PF} \begin{bmatrix} \ell_\theta \\ \ell_\varphi \end{bmatrix} \quad (2)$$

$$\text{PF} = \int_{\ell_A}^{\ell_T} \dot{I}(\ell) e^{i\beta \ell_r \ell} d\ell \quad (3)$$

According to the basic standing wave theory: i) the direction of current changes per $\lambda/2$ segment, ii) between two successive standing wave nodes the current phase remains the same and iii) if a source is between two successive standing waves the current direction does not changes. These principles were applied at the properly bended 2-wire transmission line of Fig 2, keeping in mind that the Kirchhoff laws must be simultaneously satisfied.

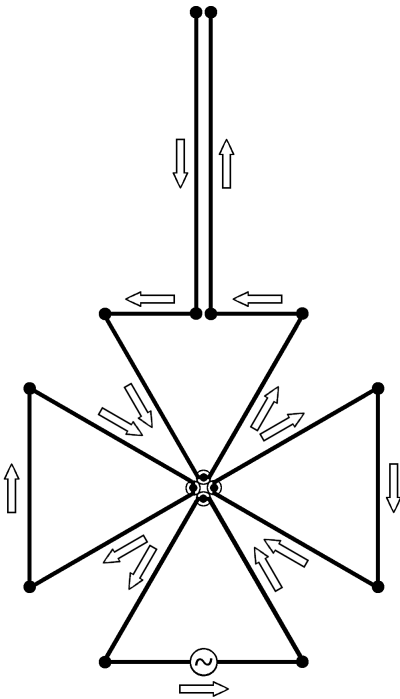


Fig. 2: $5\lambda/2$ properly bended 2-wire transmission line

The double arrows indicate the direction of $i\vec{l}$ product for every one segment, and the dotted circles at the almost coincident vertices of the four equilateral triangles correspond to a zero in the current distribution.

The two parallel $\lambda/4$ segments are almost coincident with opposite currents, so they are mutually canceled as for the radiation and they are excluded from further study. Thus, the remaining segments form the desired antenna, with total length 2λ and a current maximum at the source, as it is shown in Fig. 3.

For every one segment 0-12, of Fig. 3, we had to determine four quantities: the length of its starting point l_A , the length of its end point l_T , the position vector of its center \vec{R}_k , as if they were part of the corresponding line of 2λ length, and its unit direction vector \vec{l}'_i , with its direction to be in all segments from l_A to l_T . The planar antenna was arranged on yOz as it is shown in Fig. 4, along with all the \vec{R}_k position vectors as they were determined by the relation

$$\vec{R}_{k_v} = \vec{O}\vec{A}_v - l_{A_v} \vec{l}'_v \quad (4)$$

and Tab. 1 contains all the above mentioned geometrical quantities.

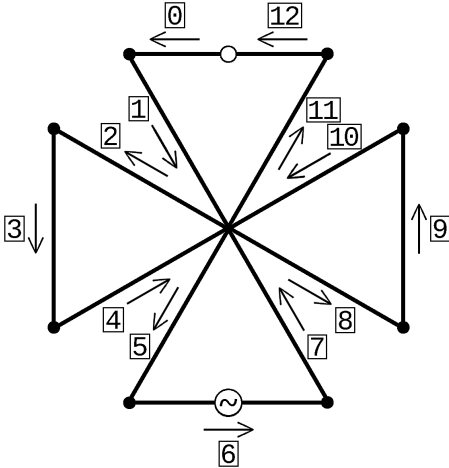


Fig. 3: 13 segments

Then through (1)-(3), that is, after the evaluation of the definite integral for the Pattern Factor PF [2], [6] the radiation pattern of all the 13 segments was formulated and according to the law of superposition the total radiation pattern is given by

$$\begin{aligned} \vec{E} &= \sum_{v=0}^{12} \begin{bmatrix} \dot{E}_{v\theta} \\ \dot{E}_{v\varphi} \end{bmatrix} = \begin{bmatrix} \dot{E}_{\theta} \\ \dot{E}_{\varphi} \end{bmatrix} = \dot{E}_{\theta} \vec{\theta}_i + \dot{E}_{\varphi} \vec{\varphi}_i = \\ &= (E_{\theta_R} + iE_{\theta_I}) \vec{\theta}_i + (E_{\varphi_R} + iE_{\varphi_I}) \vec{\varphi}_i \end{aligned} \quad (5)$$

which, after a lot of symbolic manipulation where the real parts are mutually eliminated, leads to a more simplified expression

$$\vec{E} = \begin{bmatrix} \dot{E}_{\theta} \\ \dot{E}_{\varphi} \end{bmatrix} = i (E_{\theta_I} \vec{\theta}_i + E_{\varphi_I} \vec{\varphi}_i) \quad (6)$$

and by the symmetry of the geometry radiation patterns of 0th, 12th and 6th wire are combined, as well as the five (5) couples: 1, 7 - 2, 8 - 3, 9 - 4, 10 and 5, 11 as it is obvious from Tab. 1. Thus, the total radiation pattern is

$$\begin{aligned} \vec{E} &= \vec{E}_{0,12,6} + \vec{E}_{1,7} + \vec{E}_{2,8} + \\ &+ \vec{E}_{3,9} + \vec{E}_{4,10} + \vec{E}_{5,11} \end{aligned} \quad (7)$$

Simulation

The simulation process was carried out in terms of [RICH-WIRE] program. The center frequency was 1111 [MHz] where the wavelength is $\lambda = 0.27$ [m] and the wire radius was 1 [mm]. We studied the antenna characteristics both electric and electromagnetic (SWR, Input Impedance, Directivity, Radiation Pattern) in the range [600, 1300] MHz around the center frequency with a 10 [MHz] step.

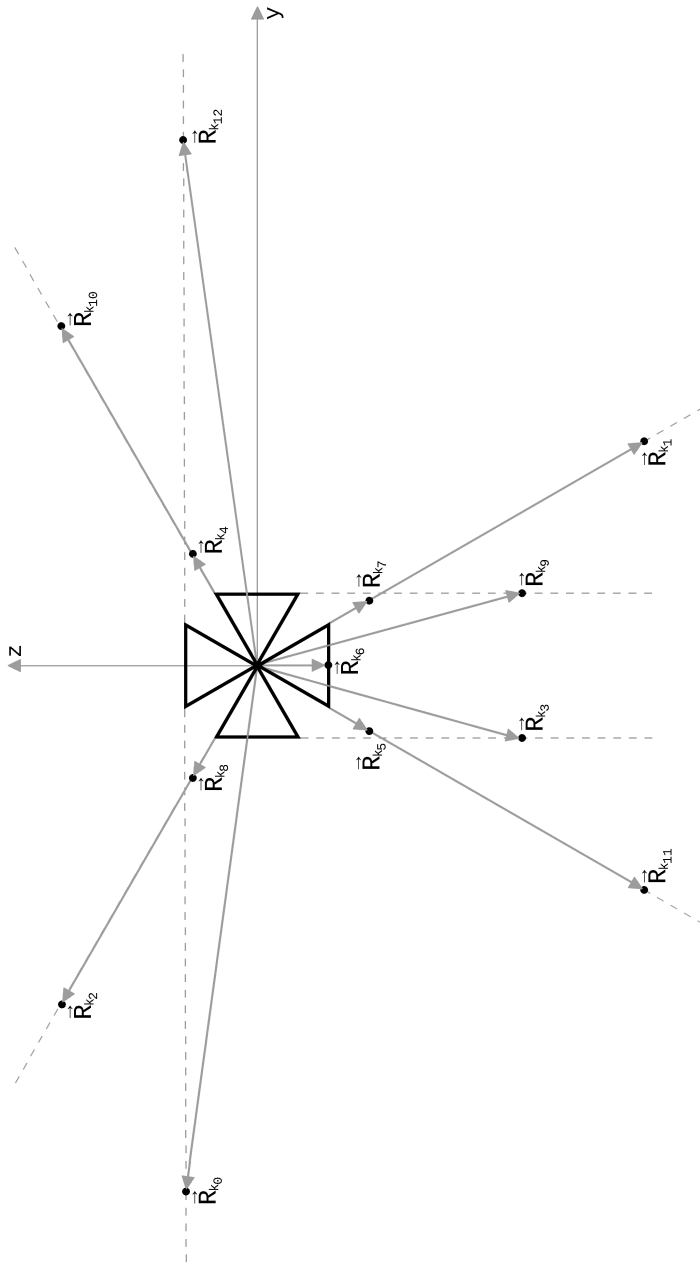


Fig. 4: 13 position vectors

Tab. 1: Geometrical Data

#	ℓ_A	ℓ_T	\vec{R}_k		βR_{k_r}
			\vec{y}_i	\vec{z}_i	
0	$-\lambda$	$-\frac{11}{12}\lambda$	$-\lambda$	$\frac{\sqrt{3}}{12}\lambda$	$-2\pi\sin\theta\sin\varphi + \frac{\sqrt{3}\pi}{6}\cos\theta$
1	$-\frac{11}{12}\lambda$	$-\frac{9}{12}\lambda$	$\frac{3}{8}\lambda$	$-\frac{3\sqrt{3}}{8}\lambda$	$\frac{3\pi}{4}\sin\theta\sin\varphi - \frac{3\sqrt{3}\pi}{4}\cos\theta$
2	$-\frac{9}{12}\lambda$	$-\frac{7}{12}\lambda$	$-\frac{3\sqrt{3}}{8}\lambda$	$\frac{3}{8}\lambda$	$-\frac{3\sqrt{3}\pi}{4}\sin\theta\sin\varphi + \frac{3\pi}{4}\cos\theta$
3	$-\frac{7}{12}\lambda$	$-\frac{5}{12}\lambda$	$-\frac{\sqrt{3}}{12}\lambda$	$-\frac{\lambda}{2}$	$-\frac{\sqrt{3}\pi}{6}\sin\theta\sin\varphi - \pi\cos\theta$
4	$-\frac{5}{12}\lambda$	$-\frac{3}{12}\lambda$	$\frac{\sqrt{3}}{8}\lambda$	$\frac{\lambda}{8}$	$\frac{\sqrt{3}\pi}{4}\sin\theta\sin\varphi + \frac{\pi}{4}\cos\theta$
5	$-\frac{3}{12}\lambda$	$-\frac{\lambda}{12}$	$-\frac{\lambda}{8}$	$-\frac{\sqrt{3}}{8}\lambda$	$-\frac{\pi}{4}\sin\theta\sin\varphi - \frac{\sqrt{3}\pi}{4}\cos\theta$
6	$-\frac{\lambda}{12}$	$\frac{\lambda}{12}$	0	$-\frac{\sqrt{3}}{12}\lambda$	$-\frac{\sqrt{3}\pi}{6}\cos\theta$
7	$\frac{\lambda}{12}$	$\frac{3}{12}\lambda$	$\frac{\lambda}{8}$	$-\frac{\sqrt{3}}{8}\lambda$	$\frac{\pi}{4}\sin\theta\sin\varphi - \frac{\sqrt{3}\pi}{4}\cos\theta$
8	$\frac{3}{12}\lambda$	$\frac{5}{12}\lambda$	$-\frac{\sqrt{3}}{8}\lambda$	$\frac{\lambda}{8}$	$-\frac{\sqrt{3}\pi}{4}\sin\theta\sin\varphi + \frac{\pi}{4}\cos\theta$
9	$\frac{5}{12}\lambda$	$\frac{7}{12}\lambda$	$\frac{\sqrt{3}}{12}\lambda$	$-\frac{\lambda}{2}$	$\frac{\sqrt{3}\pi}{6}\sin\theta\sin\varphi - \pi\cos\theta$
10	$\frac{7}{12}\lambda$	$\frac{9}{12}\lambda$	$\frac{3\sqrt{3}}{8}\lambda$	$\frac{3}{8}\lambda$	$\frac{3\sqrt{3}\pi}{4}\sin\theta\sin\varphi + \frac{3\pi}{4}\cos\theta$
11	$\frac{9}{12}\lambda$	$\frac{11}{12}\lambda$	$-\frac{3}{8}\lambda$	$-\frac{3\sqrt{3}}{8}\lambda$	$-\frac{3\pi}{4}\sin\theta\sin\varphi - \frac{3\sqrt{3}\pi}{4}\cos\theta$
12	$\frac{11}{12}\lambda$	λ	λ	$\frac{\sqrt{3}}{12}\lambda$	$2\pi\sin\theta\sin\varphi + \frac{\sqrt{3}\pi}{6}\cos\theta$

#	$\vec{\ell}_i$		ℓ_r	ℓ_θ	ℓ_ϕ
	\vec{y}_i	\vec{z}_i			
0	-1	0	$-\sin\theta\sin\varphi$	$-\cos\theta\sin\varphi$	$-\cos\varphi$
1	$\frac{1}{2}$	$-\frac{\sqrt{3}}{2}$	$\frac{1}{2}\sin\theta\sin\varphi - \frac{\sqrt{3}}{2}\cos\theta$	$\frac{1}{2}\cos\theta\sin\varphi + \frac{\sqrt{3}}{2}\sin\theta$	$\frac{1}{2}\cos\varphi$
2	$-\frac{\sqrt{3}}{2}$	$\frac{1}{2}$	$-\frac{\sqrt{3}}{2}\sin\theta\sin\varphi + \frac{1}{2}\cos\theta$	$-\frac{\sqrt{3}}{2}\cos\theta\sin\varphi - \frac{1}{2}\sin\theta$	$-\frac{\sqrt{3}}{2}\cos\varphi$
3	0	-1	$-\cos\theta$	$\sin\theta$	0
4	$\frac{\sqrt{3}}{2}$	$\frac{1}{2}$	$\frac{\sqrt{3}}{2}\sin\theta\sin\varphi + \frac{1}{2}\cos\theta$	$\frac{\sqrt{3}}{2}\cos\theta\sin\varphi - \frac{1}{2}\sin\theta$	$\frac{\sqrt{3}}{2}\cos\varphi$
5	$-\frac{1}{2}$	$-\frac{\sqrt{3}}{2}$	$-\frac{1}{2}\sin\theta\sin\varphi - \frac{\sqrt{3}}{2}\cos\theta$	$-\frac{1}{2}\cos\theta\sin\varphi + \frac{\sqrt{3}}{2}\sin\theta$	$-\frac{1}{2}\cos\varphi$
6	1	0	$\sin\theta\sin\varphi$	$\cos\theta\sin\varphi$	$\cos\varphi$
7	$-\frac{1}{2}$	$\frac{\sqrt{3}}{2}$	$-\frac{1}{2}\sin\theta\sin\varphi + \frac{\sqrt{3}}{2}\cos\theta$	$-\frac{1}{2}\cos\theta\sin\varphi - \frac{\sqrt{3}}{2}\sin\theta$	$-\frac{1}{2}\cos\varphi$
8	$\frac{\sqrt{3}}{2}$	$-\frac{1}{2}$	$\frac{\sqrt{3}}{2}\sin\theta\sin\varphi - \frac{1}{2}\cos\theta$	$\frac{\sqrt{3}}{2}\cos\theta\sin\varphi + \frac{1}{2}\sin\theta$	$\frac{\sqrt{3}}{2}\cos\varphi$
9	0	1	$\cos\theta$	$-\sin\theta$	0
10	$-\frac{\sqrt{3}}{2}$	$-\frac{1}{2}$	$-\frac{\sqrt{3}}{2}\sin\theta\sin\varphi - \frac{1}{2}\cos\theta$	$-\frac{\sqrt{3}}{2}\cos\theta\sin\varphi + \frac{1}{2}\sin\theta$	$-\frac{\sqrt{3}}{2}\cos\varphi$
11	$\frac{1}{2}$	$\frac{\sqrt{3}}{2}$	$\frac{1}{2}\sin\theta\sin\varphi + \frac{\sqrt{3}}{2}\cos\theta$	$\frac{1}{2}\cos\theta\sin\varphi - \frac{\sqrt{3}}{2}\sin\theta$	$\frac{1}{2}\cos\varphi$
12	-1	0	$-\sin\theta\sin\varphi$	$-\cos\theta\sin\varphi$	$-\cos\varphi$

The total number of 96 segments for the whole antenna, where all sides had equal number of points, was selected for the simulation, after the investigation for 13, 24, 48, 72, 96, 120, 144, 168, 192, 216, 240 segments. The above mentioned characteristics remained almost constant after this number of 96 segments. An appropriate computer program was developed in Fortran to create the input file with antenna geometry for [RICHWIRE].

A very good agreement between simulated and analyti-

cal produced radiation patterns is shown in Fig. 5 for the three main planes in 1111 [MHz], although there is a point for discussion here. A closer examination, after 7 years from the initial work [1], of what was really compared in Fig. 5, proved that the analytical patterns illustrated corresponds to rather an upper bound of the absolute radiation pattern since it results from the sum of the 13 absolute radiation patterns and not from the total absolute radiation pattern.

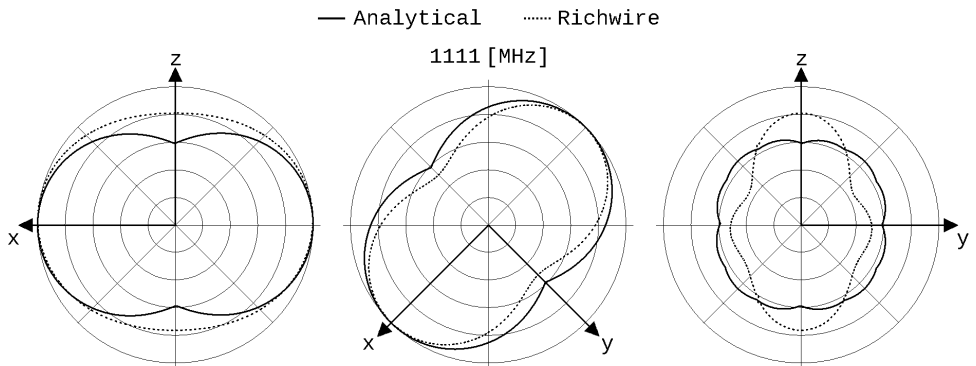


Fig. 5: Radiation patterns in 1111 [MHz]

Furthermore, the simulation model, as it is shown in Fig. 6, consists inevitable not in four equal delta elements but in four truncated ones, as care must be taken

a) to avoid the overlapping of the wires in a future construction and

b) to reduce the strong cou-

pling caused by the proximity effect.

Thus, the minimum permitted square region with side $(2a+a/10)$, where "a" is the used wire radius, was removed from the center intersection point of the four delta elements, while in the same time, in order to achieve the

connection of the neighboring sides, the base angles of every element are slightly greater than 60° , and the total length of such formed element was slightly greater than the initial $\lambda/2$.

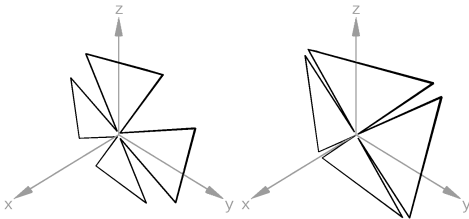


Fig. 6: Simulation models

Extremely high values of Standing Wave Ratio [SWR] in 1111 [MHz] for the three characteristic impedances 50, 75 and 300 $[\Omega]$ as it is shown

in Fig. 7, made clear the need for further research on the antenna's geometry.

The antenna was modified only with respect to the base angles for constant delta-perimeter, resulting a Delta-cross Loop antenna of four isosceles triangles. A computer program was also developed in Fortran producing the corresponding input data for [RICHWIRE].

The investigation was performed from the value of 48° for the base angles to 78° in step of 1° at the frequency of 1111 [MHz]. The best performance was noticed between 48° and 52° and the model, shown in Fig. 8, with 48° base angles was selected.

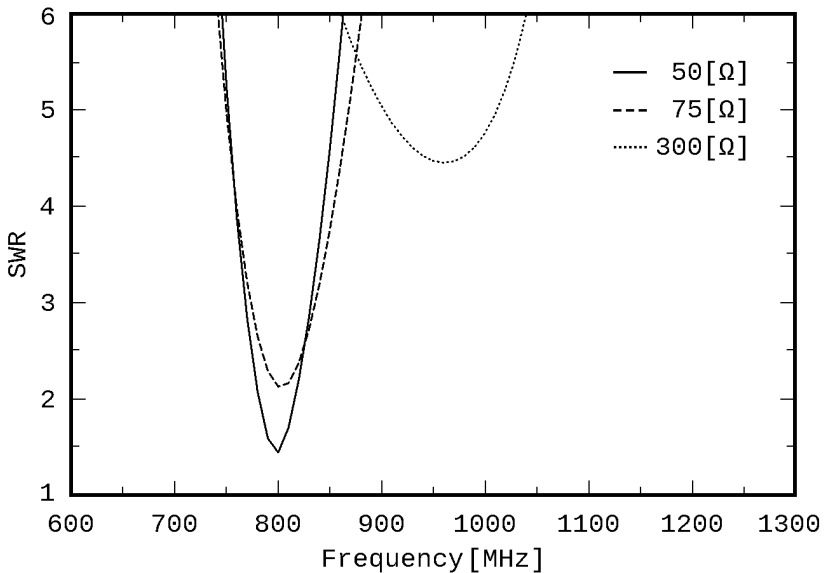


Fig. 7: Standing Wave Ratio against frequency

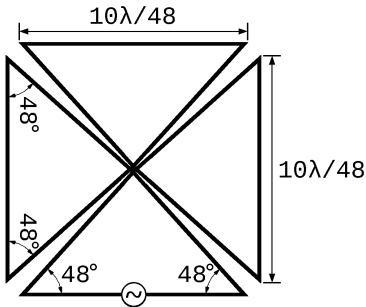


Fig. 8: Improved antenna

In Figs. 9 - 13 SWR, Input Impedance [Z_{in}] as Input Resistance R_{in} and Input Reactance X_{in} in [Ω] and Directivity D in [dB] of the improved antenna together with that of the initial one and of 2λ dipole, are shown respectively. Fig. 12 shows a properly selected window of the total frequency range for the Input Impedance in order to clarify the improvement of the modified antenna. In Figs. 14 - 15 a comparison of the radiation patterns of the three antennas is given at five frequencies in the three main planes zOx , xOy and yOz . In Fig. 16 the 3D analytical radiation pattern at 1111 [MHz] and in Fig. 17 the corresponding 3D patterns in all frequencies are shown.

Conclusion

Although, the agreement of results between simulation and analysis was very good,

the characteristics of the initial antenna were not satisfactory. An improvement process was needed and the research was here limited to the change of the base angles only to the rather small range of -12° , $+18^\circ$ around the initial 60° base angle. Thus, the improved antenna had the best performance about 100 MHz lower of the desired frequency of 1111 [MHz], as it is shown in Figs. 9 - 13. The SWR for the 50 [Ω] characteristic impedance has its best value closer to 1111 [MHz] while the initial antenna and the 2λ dipole of equivalent length had a relative small value of SWR at about 800 [MHz] (Fig. 9). It is also obvious that the Input Impedance as well as Directivity is relatively stable and slightly better for the improved antenna and much better from the initial one (Figs. 10 - 13). Corresponding values for SWR, Input Impedance and Directivity for the three antennas are given in Tab. 2.

The radiation pattern of the improved antenna is closer to that of a centered fed sinusoidal $\lambda/2$ dipole, avoiding the dispersion of radiation in multiple directions of the rather long 2λ dipole antenna (Figs. 14 - 15, 17).

Tab. 1: SWR, D, Z_{inp}

	SWR	D [dB]	Z_{inp} [Ω]
1111 [MHz]			
60°	43.7	2.49	40 - i 287
2 λ	26.1	4.09	577 - i 647
48°	6.55	3.10	70 + i 127
800 [MHz]			
60°	1.44	2.61	36 + i 5
2 λ	2.55	3.21	88 - i 52
48°	42.7	2.30	24 - i 219
1010 [MHz]			
60°	29.6	2.85	1297 + i 485
2 λ	20.4	3.74	993 + i 168
48°	1.26	2.90	40 + i 3

An extensive investigation concerning the analytical determination of the antenna radiation pattern and its normalized absolute values is in the immediate future plans of the authors in order to achieve the clarification of its relation with the one produced by simulation.

A wider range of the base angle variation or the variation of the total length of each delta element are some design ideas for a future research work. Nevertheless, the final step is, without doubt, the construction and measurement of the proposed antenna together with the comparison of the corresponding results.

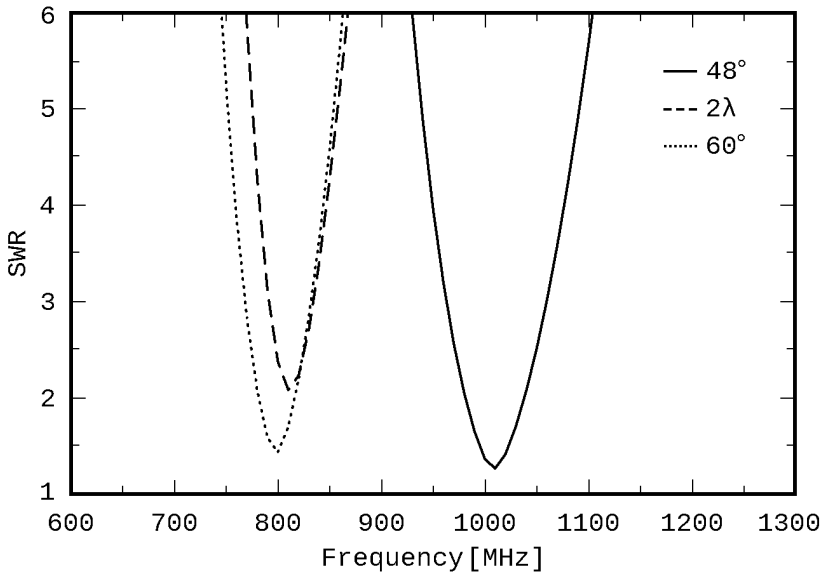


Fig. 9: SWR for improved-48°, 2 λ and initial-60° antenna

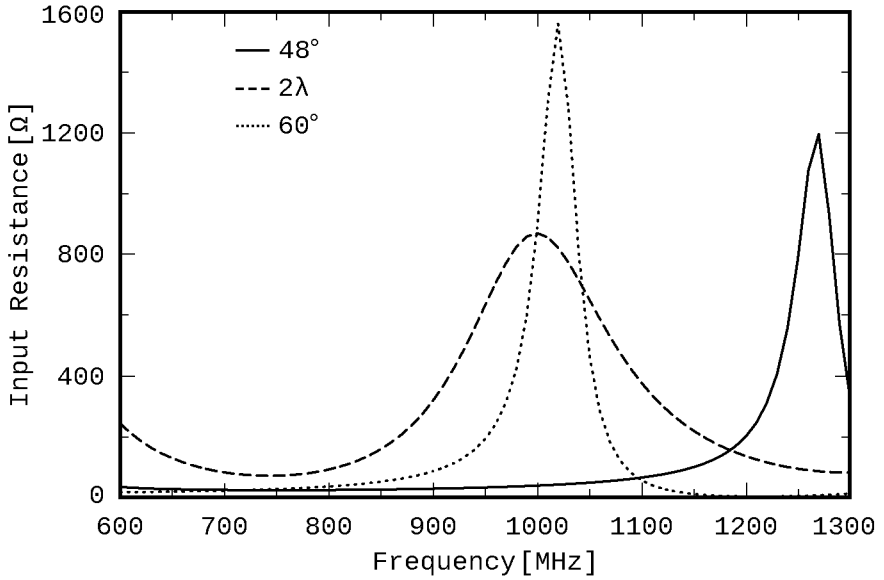


Fig. 10: R_{inp} for improved- 48° , 2λ and initial- 60° antenna

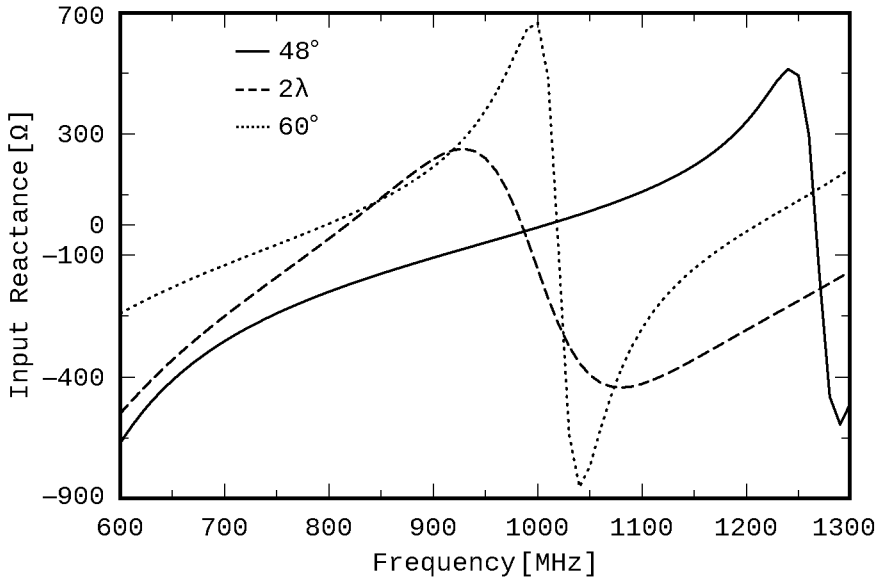


Fig. 11: X_{inp} for improved- 48° , 2λ and initial- 60° antenna

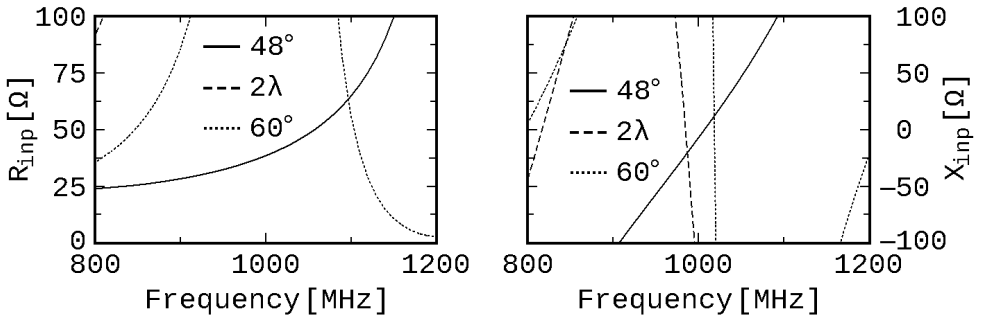


Fig. 12: R_{in} , X_{in} for the three antennas in [800, 1200] MHz

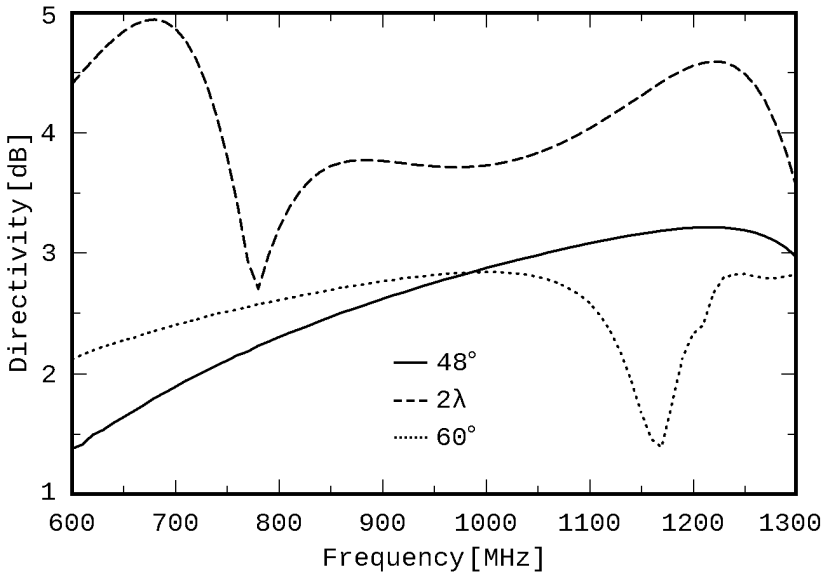


Fig. 13: Directivity of the three antennas

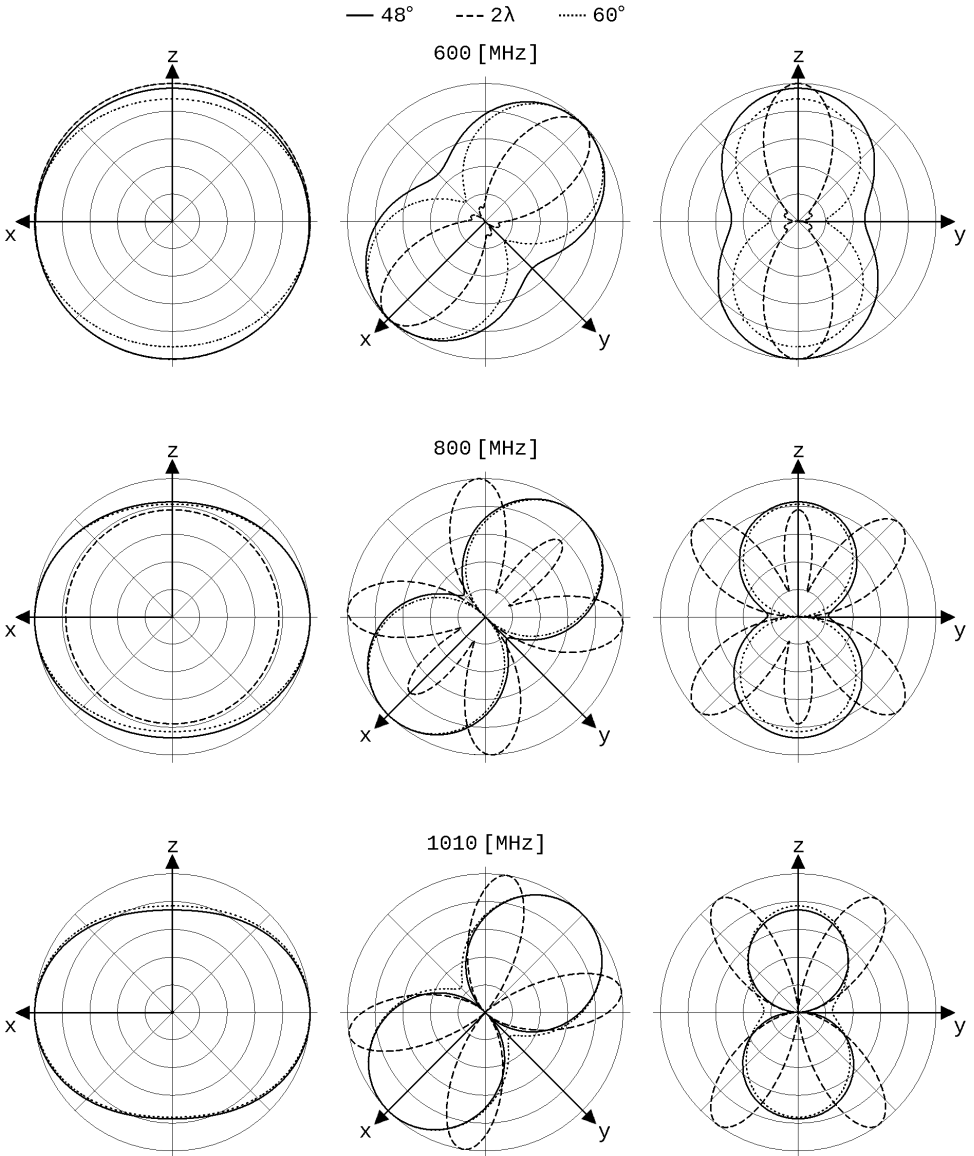


Fig. 14: Radiation patterns at 600, 800 and 1010 [MHz]

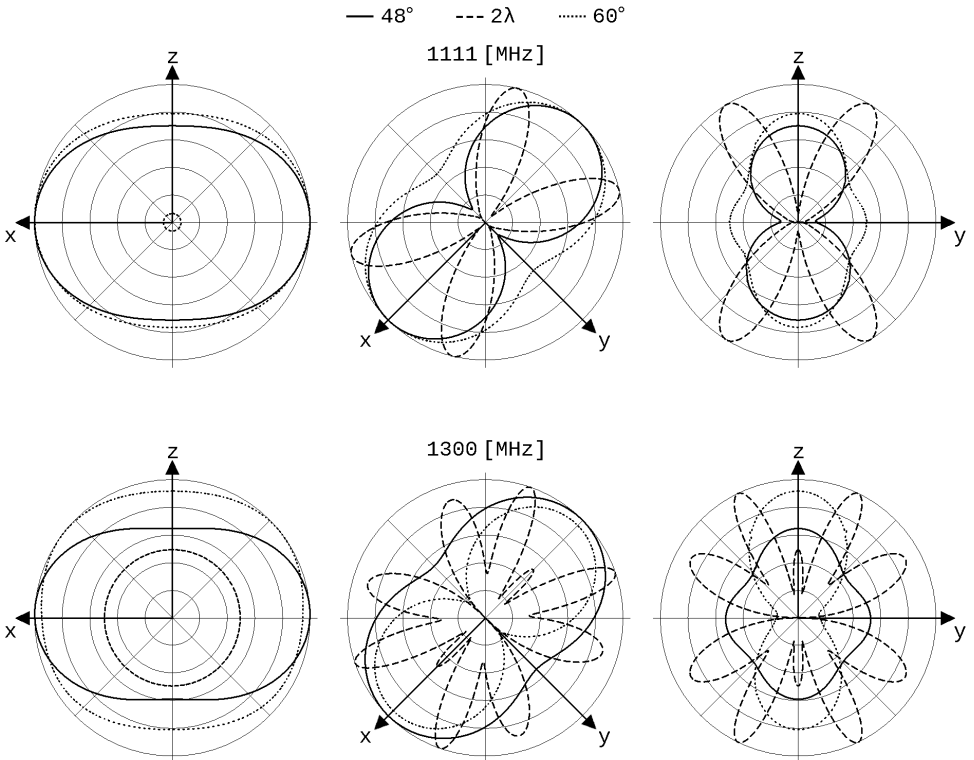


Fig. 15: Radiation patterns at 1111 and 1300 [MHz]

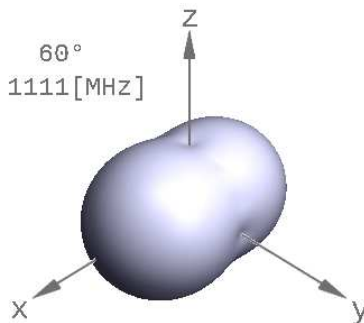


Fig. 16: 3D Analytical Radiation Pattern

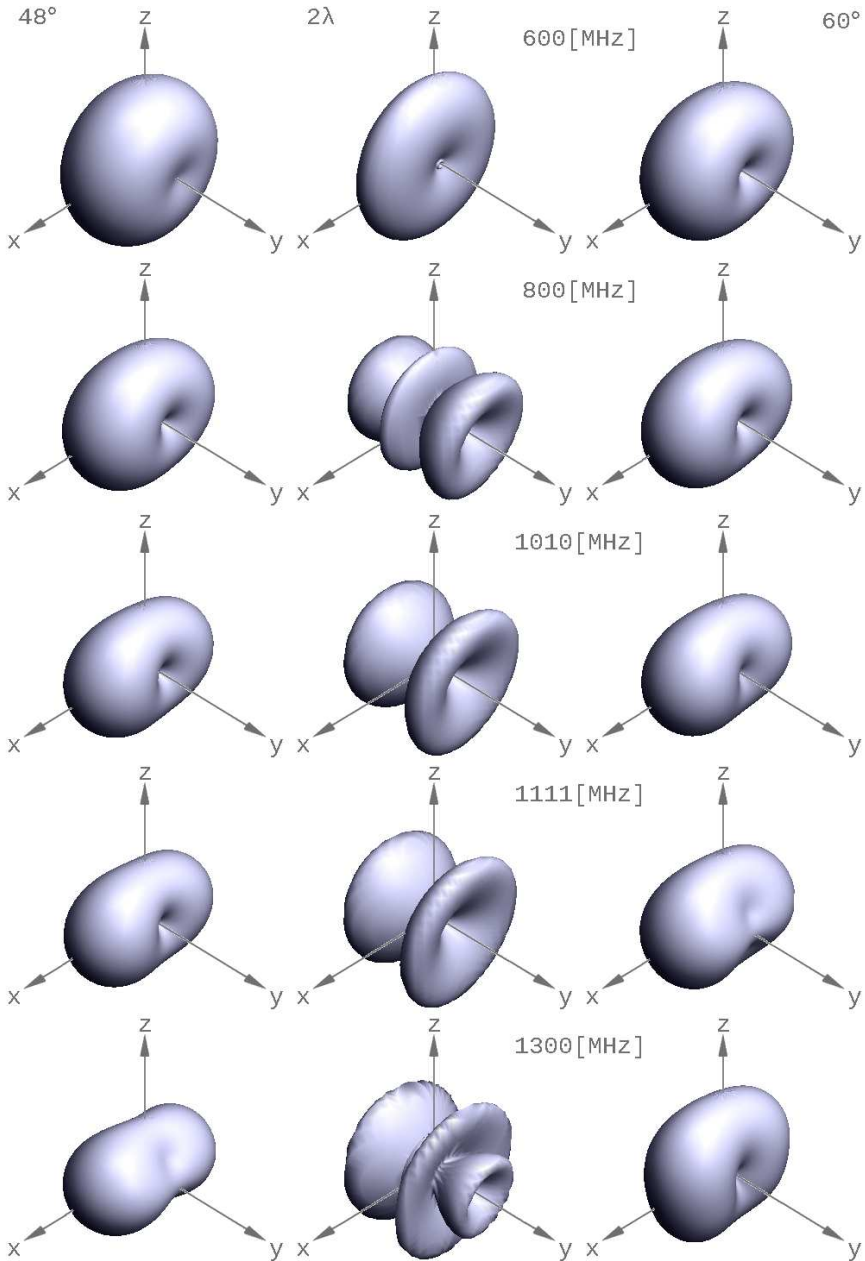


Fig. 17: 3D Simulated Radiation Patterns

References *

- [1] Papadaniel G., "The Eisernes Kreuz Antenna [Prototype ARG-06]", Diploma Thesis #40, ARG-Antennas Research Group, DUTH, 2007 (in Greek)
 - [2] Zimourtopoulos P., "Antenna Notes 1999-", Antenna Design Notes 2000-, "www.antennas.gr/antennanotes/" (in Greek)
 - [3] Yannopoulou N., Zimourtopoulos P., "A FLOSS Tool for Antenna Radiation Patterns", Proceedings of 15th Conference on Microwave Techniques, COMITE 2010, Brno, Czech Republic, pp. 59-62
 - [4] Richmond J.H., "Computer program for thin-wire structures in a homogeneous conducting medium", Publication Year: 1974, NTRS-Report/Patent Number: NASA-CR-2399, ESL-2902-12, DocumentID: 19740020595, "<http://ntrs.nasa.gov/>"
 - [5] Yannopoulou N., Zimourtopoulos P., "Mini Suite of Antenna Tools", Educational Laboratories, Antennas Research Group, 2006, "www.antennas.gr/antsoft/minisuiteoftools/"
 - [6] Yannopoulou N.I., "Study of monopole antennas over a multi-frequency decoupling cylinder", PhD Thesis, EECE, DUTH, February 2008 (in Greek), pp. (2-6)-(2-9)
- *Active Links: 27.05.2015 - Inactive Links : FTP#J Link Updates: "<http://updates.ftpj.otoiser.org/>"

Follow-Up Research Paper

Not until now

Previous Publication in FUNKTECHNIKPLUS # JOURNAL

"Visual EM Simulator for 3D Antennas: VEMSA3D – FLOSS for MS Windows", Issue 6, Year 2, pp. 7-25

* About The Authors

Nikolitsa Yannopoulou, Issue 1, Year 1, p. 15

Petros Zimourtopoulos, Issue 1, Year 1, p. 15

Papadaniel Glykeria, was born in Rodolivos-Amfipolis, Serres, Greece in 1981. She graduated from Electrical Engineering and Computer Engineering in 2007 from Democritus University of Thrace, Xanthi, Greece. Member of Antennas Research Group while she was elaborated her diploma thesis. She did practice exercise in the Hellenic Telecommunication Organisation and she worked as an Engineer in Clima, Voltampere Energy and Rodax Companies for the study/design of Photovoltaic systems, wind farms, natural gas plants and electrical installations in a thermoelectric power station. She is a certified three-dimensional graphics and computer aided Designer.

g.papadaniel@yahoo.gr

[This Page Intentionally Left Blank]

[This Page Intentionally Left Blank]

[This Page Intentionally Left Blank]

In case of any doubt,
download the genuine papers from
genuine.ftpj.otoiser.org

FRONT COVER VIGNETTE

A faded synthesis of an anthemion rooted in a meandros

The thirteen-leaf is a symbol for a life tree leaf.
"Herakles and Kerberos", ca. 530–500 BC,
by Paseas, the Kerberos Painter,
Museum of Fine Arts, Boston.

www.mfa.org/collections/object/plate-153852

The simple meandros is a symbol for eternal immortality.
"Warrior with a phiale", ca. 480–460 BC,
by Berliner Maler,
Museo Archeologico Regionale "Antonio Salinas" di Palermo.

commons.wikimedia.org/wiki/File:Warrior_MAR_Palermo_NI2134.jpg

In case of any doubt,
download the genuine papers from
www.genuine.ftpj.otoiser.org

ARG NFP AoI

Antennas Research Group

Not-for-Profit Association of Individuals [*]

www.arg.op4.eu – arg@op4.eu

Hauptstraße 52, 2831 Scheiblingkirchen, Austria

Telephone: 0 6646311483 – International: 0043 6646311483

* The Constitution of Greece, Article 12(3) – 2008:

www.hellenicparliament.gr/en/Vouli-ton-Ellinon/To-Politevma

* The Hellenic Supreme Court of Civil and Penal Law:

www.areiospagos.gr/en – Court Rulings:Civil|A1|511|2008

FRONT COVER VIGNETTE

A faded synthesis of an anthemion rooted in a meandros

The thirteen-leaf is a symbol for a life tree leaf.

"Herakles and Kerberos", ca. 530–500 BC,
by Paseas, the Kerberos Painter,
Museum of Fine Arts, Boston:
www.mfa.org/collections/object/plate-153852

The simple meandros is a symbol for eternal immortality.

"Warrior with a phiale", ca. 480–460 BC,
by Berliner Maler,
Museo Archeologico Regionale "Antonio Salinas" di Palermo:
"http://commons.wikimedia.org/wiki/File:Warrior_MAR_Palermo_NI2134.jpg"